THE UNIVERSITY *of* EDINBURGH

This thesis has been submitted in fulfilment of the requirements for a postgraduate degree (e.g. PhD, MPhil, DClinPsychol) at the University of Edinburgh. Please note the following terms and conditions of use:

- This work is protected by copyright and other intellectual property rights, which are retained by the thesis author, unless otherwise stated.
- A copy can be downloaded for personal non-commercial research or study, without prior permission or charge.
- This thesis cannot be reproduced or quoted extensively from without first obtaining permission in writing from the author.
- The content must not be changed in any way or sold commercially in any format or medium without the formal permission of the author.
- When referring to this work, full bibliographic details including the author, title, awarding institution and date of the thesis must be given.

Identification of microRNAs involved in the development and function of follicular dendritic cells

Susan Rebecca Aungier

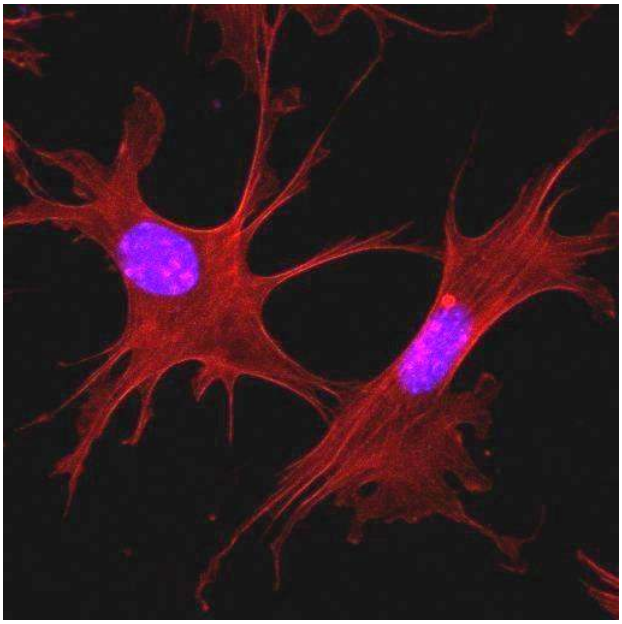

Thesis presented for the degree of Doctor of Philosophy

The University of Edinburgh

September 2013

I declare that this thesis and the work declared herein is my own, unless otherwise stated. The work described in this thesis has not been submitted for any other degree or professional qualification.

Susan Aungier

Acknowledgements

I would like to thank my supervisors Neil Mabbott and Mike Clinton, for giving me the opportunity of this PhD and for their guidance and support throughout. My thanks are extended to members of both their labs, past and present. To Karen Brown and Laura McCulloch for IHC training and advice. To Laura Bailey for guidance in miRNA techniques and Catriona Hunter for help with miRNA techniques and being there though the small RNA sequencing process. I am eternally grateful to Derek McBride for sharing his expertise in molecular biology and for his part in small RNA library preparation. I thank Sunil Nandi for always taking the time to offer help and advice. I am also grateful to Debiao Zhao and members of the Burdon lab for listening and helpful suggestions during lab meetings. I would also like to thank Fraser Lang for assisting me with the animal work and Bob Fleming for his expertise in confocal microscopy and live cell imaging. I am very grateful to Hitoshi Ohmori from Okayama University for kindly giving us the FL-YB cells.

I cannot thank my parents enough for all the support, encouragement and belief in me that has enabled me to get to this point. Thank you for always being there. My gran has been a wonderful and constant source of inspiration and encouragement (and tea and chocolate). Thank you to my sisters for their assurance and positivity (and for jelly beans and dog walks during writing). I have been lucky enough to meet and work with some wonderful friends throughout my PhD, who kept me laughing and who I know will keep me laughing for years to come.

For Mum, Dad and Gran.

Table of Contents

Abstract

Follicular dendritic cells (FDCs) are key elements of secondary lymphoid organs where they form the stromal component of B-cell follicles. FDCs possess extensive dendritic process that trap intact antigen via Fc and complement receptors on the cell surface. The antigen is displayed to B-cells, providing a basis for selection of high affinity B cells. FDC also have important roles in facilitating the clearance of apoptotic B cells by the secretion of the opsonising factor MFGE8. It is well established that lymphotoxin signalling is required for FDC maturation but the specific details of the molecular mechanisms that regulate FDC development and differentiation are not fully understood. MicroRNAs (miRNAs) are non-coding RNAs of approximately 18-25 nucleotides in length that regulate gene expression at the post-transcriptional level. MiRNAs bind to their target gene transcripts as part of the RNA induced silencing complex and repress translation of the target gene product.

The objective of this study was to identify miRNAs that play a role in the development and function of FDCs.

An *in vivo* murine model of FDC de-differentiation was used to provide material for miRNA analysis. By comparison of miRNA profiles from spleen tissue with FDC at different stages of de-differentiation, we would be able to obtain a miRNA signature for mature FDC. Spleens were collected at various time points over a 28 day period following transient blockade of lymphotoxin signalling. A variety of methods were used to profile the miRNAs expressed at different time points during the suppression and recovery of the FDC network. Comparison of the miRNA profiles of spleens containing mature, partially de-differentiated, and fully de-differentiated FDC identified a number of miRNAs that were differentially expressed during FDC de-differentiation.

To assess the role of specific miRNAs in FDC development, the mouse FDC-like cell line, FL-YB, was used as an *in vitro* model system. FL-YB cells were used to perform gain-of-function and loss-of-function studies on selected miRNAs and to assess the effects of various stimuli/conditions on miRNA expression. The effects of different treatments on cell proliferation, morphology and adhesion, and on gene expression by FL-YB, were monitored. Loss-of-function studies for one of the selected miRNA (miR-100-5p) revealed a significant effect on a number of gene transcripts involved in mediation of the germinal centre response (*Il-6, Tlr4, Ptgs1/2*). These data indicate that miR-100-5p has a role in regulating *Il-6*, *Tlr4* and *Ptgs1/2* transcripts. None of these transcripts contain predicted target sites for miR-100-5p and so the effect of miR-100-5p on these transcripts is likely to be indirect. Further studies on these miRNA: target interactions are required to elucidate the mechanisms and biological consequences of miRNA regulation in FDCs.

List of abbreviations

3'-UTR	3' untranslated region
AICD	Activation induced cell death
AID	Activation induced deaminase
ANOVA	Analysis of variance
AP	Alkaline phosphatase
APC	Antigen presenting cell
ATP	Adenosine triphosphate
BAFF	B cell activating factor
BCR	B cell receptor
BLAST	Basic Local Alignment Search Tool
Bp	Base pair
C4b	Complement component 4b
cDNA	Complementary DNA
CR1	Complement receptor 1
CR2	Complement receptor 2
D	Day
DNA	Deoxyribonucleic acid
DNase	Deoxyribonuclease
dsDNA	Double stranded DNA
E	Embryonic day
EDC	1-Ethyl-3-[3-dimethylaminopropyl]carbodiimide hydrochloride
EMSA	Electromobility shift assay
EMT	Epithelial to mesenchymal transition
FAK	Focal adhesion kinase
FBS	Foetal bovine serum
FDC	Follicular dendritic cell
fM	Femtomolar
FRC	Fibroblastic reticular cell
GC	Germinal centre
H	Hours
HIV-1	Human immunodeficiency virus 1
i.p.	Intra-peritoneal
ICAM-1	Intracellular cell adhesion molecule 1
IFN-γ	Interferon gamma
IgG	Immunoglobulin G
IgM	Immunoglobulin M

IHC	Immunohistochemistry
IKKα	IkB kinase alpha
iLF	Isolated lymphoid follicle
L	Larval stage
LFA-1	Lymphocyte function associated antigen 1
LNA	Locked nucleic acid
LPS	Lipopolysaccharide
LT	Lymphotoxin
LTi	Lymphoid tissue inducer
LTo	Lymphoid tissue organiser
LTβR	Lymphotoxin beta-receptor
LTβR-Ig	Lymphotoxin beta receptor fusion protein
mAb	Monoclonal antibody
MADCAM-1	Mucosal vascular addressin cell adhesion molecule 1
MALT	Mucosal associated lymphoid tissue
MEF	Mouse embryonic fibroblast
MFGE8	Milk fat globule-EGF factor 8 protein
Min	Minutes
miRNA	MicroRNA
mLN	Mesenteric lymph node
MRC	Marginal reticular cell
mRNA	Messenger RNA
MSC	Mesenchymal stem cell
NaAc	Sodium acetate
NFκB	Nuclear factor kappa B
NGS	Next generation sequencing
NIK	NFkB-inducing kinase
Nt	Nucleotide
PBS	Phosphate buffered saline
PCA	Principal component analysis
PCR	Polymerase chain reaction
PP	Peyer's patch
Pri-miRNA	Primary microRNA
PrP^{c}	Normal form of the host prion protein
PrP^{sc}	Scrapie-specific form of the host prion protein
qPCR	Quantitative real-time polymerase chain reaction
RA	Rheumatoid arthritis
RISC	RNA induced silencing complex
RMA	Robust multi-array analysis

RNA	Ribonucleic acid
RNAi	RNA interference
RNase	Ribonuclease
rRNA	Ribosomal RNA
RTCA	Real-time cell analysis
SDS	sodium dodecyl sulphate
SHM	Somatic hypermutation
SLE	Systemic lupus erythematosus
snRNA	Small nuclear RNA
SSC	Saline-sodium citrate
TBE	Tris/Borate/EDTA buffer
TMM	Trimmed mean of M-values
TNFR1	Tumour necrosis factor receptor superfamily, member 1
TNFR2	Tumour necrosis factor receptor superfamily, member 2
TNFα	Tumour necrosis factor alpha
UV	Ultra-violet
VCAM-1	Vascular cell adhesion molecule 1
VLA-4	Very late antigen 4

List of Figures

List of Tables

CHAPTER 1; General Introduction

Contents

1.1. Secondary lymphoid organs

1.1.1. Stromal populations of secondary lymphoid organs

Secondary lymphoid organs are highly specialised structures which allow initiation of the adaptive immune response by providing an environment in which antigen is encountered by lymphocytes. The principal secondary lymphoid organs are the spleen and lymph nodes, but there are a number of others, including the Peyer's patches and isolated lymphoid follicles (iLFs) in the gut. In addition other mucosal surfaces also contain small lymphoid organs collectively named mucosal associated lymphoid tissue (MALT). In the spleen the white pulp, comprises T cell areas which form around central arterioles. Discrete B cell follicles are situated at locations around the periphery of the T cell area. Surrounding these T and B cell compartments is the marginal zone which separates the lymphocyte-containing white pulp from the red pulp (Figure 1.1). All these different areas have specialised stromal cells which, as well as providing structural support, also support the haematopoietic cells within their relevant niches. The stromal cells in the T cell areas are termed fibroblastic reticular cells (FRC) while the stromal cells in the B cell areas are follicular dendritic cells (FDC) and those in the marginal zone are marginal reticular cells (MRC). These three stromal populations are identified by both their specific locations and by functional markers which they express. FRC express the chemokines CCL21 and CCL19 which attract CCR7 expressing T cells, whereas FDC express the Chemokine CXCL13 which attracts CXCR5 expressing B cells. FDC are also identified by their expression of complement receptor 1 (CR1 (CD35)). MRC express many of the same markers as FDC, such as CXCL13 and the adhesion molecules ICAM1 and VCAM1 but can be identified by high expression of mucosal addressin cell adhesion molecule-1 (MADCAM1) (Katakai, 2012).

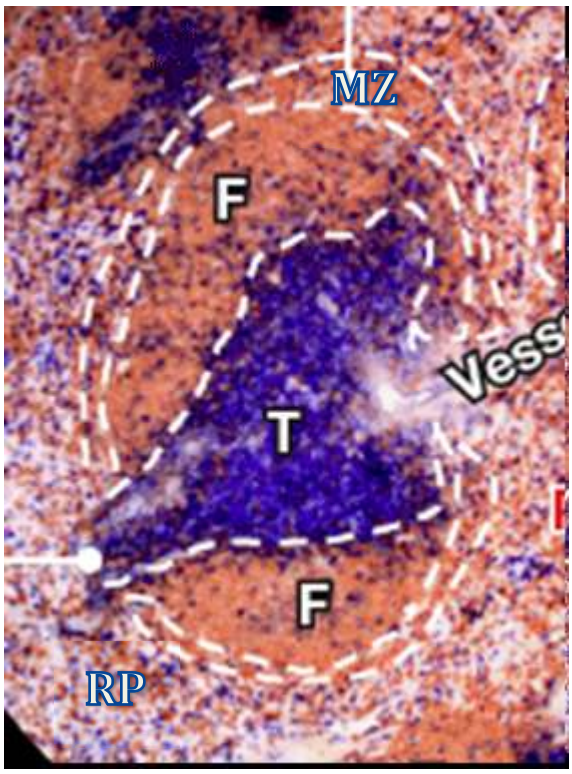

Figure 1.1 The composition of splenic white pulp. T= T cell zone F= B cell follicle, MZ= marginal zone, Vess = entrance of central arteriole, RP= red pulp. Adapted from http://www.cell.com/immunity/image_resource-spleen Wang & Cyster.

1.1.2. Antigen encounter and germinal centre reactions

When antigen is presented to T cells by professional antigen presenting cells (APC), T cells decrease expression of the chemokine receptor CCR7 which allows migration towards the B cell areas (B cell primary follicle). At the same time, B cells encounter native antigen which is displayed on the surface of FDC and increase expression of CCR7 causing migration to the periphery of the T cell area. This allows encounters between T and B cells which is important for the induction of a T cell-dependent antibody response. Interactions between the T and B cells cause T cell activation and expression of CD40 ligand and cytokines such as IL-4 and IL-2. This enables CD40:CD40L interactions and the activation of B cells to undergo proliferation and differentiation. These B cells migrate back to the follicle and through proliferation and

differentiation processes form structures termed germinal centres. B cell follicles which contain germinal centres are referred to as secondary lymphoid follicles. Germinal centres (GC) themselves contain different zones, the outer-most of which is the mantel zone that is largely made up of recirculating B cells. The apical light zone contains mainly small centrocytes whereas the basal light zone contains large centroblasts. Finally the dark zone contains centroblasts (MacLennan, 1994). B cells migrating back into GC after encountering T cells are referred to as centroblasts and they undergo proliferation (clonal expansion) in the dark zone. Centroblasts then up-regulate surface expression of immunoglobulin to become centrocytes and migrate into the light zone where the majority of FDC also reside. If the surface immunoglobulins recognise and bind to antigen that is displayed on the cell surface of FDC, they then receive survival signals from the FDC and then undergo immunoglobulin class switching (MacLennan, 1994). These centrocytes then become antibody secreting plasma cells, which migrate to areas of high antigen, or long-lived memory B cells, which stay in the follicle long after the GC has been cleared. The centrocytes that do not recognise FDC bound antigen, or do so only with low affinity, do not receive survival signals and undergo apoptosis. This is summarised in Figure 1.2.

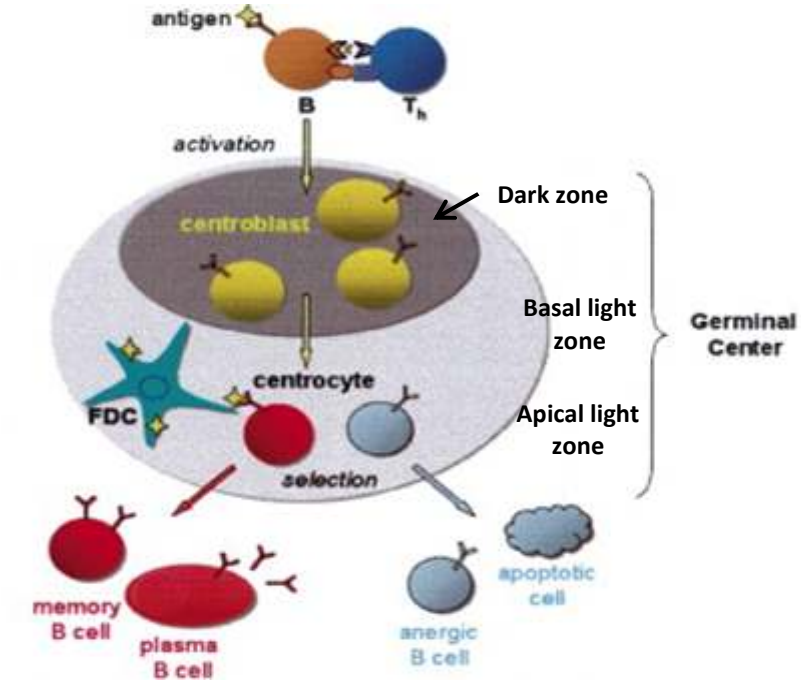

Figure 1.2 Progression of the germinal centre reaction. Adapted from (Luo et al., 2004).

1.2. Follicular dendritic cells

1.2.1. Discovery of FDC

Follicular dendritic cells were first named in 1978 (Chen et al., 1978) in a publication describing them to be present in the GC and to be stellate in shape, sending out long thin sheets of cytoplasm. FDC are large cells that in the mature state extend long, slender dendritic processes that form a network throughout the B cell follicles of secondary lymphoid tissue (Allen and Cyster, 2008; El Shikh et al., 2007a; Endres et al., 1999; Alimzhanov et al., 1997; Kuprash et al., 1999). FDCs are therefore closely associated with B cells and cross-talk between the two cell types is required by both cell types (Husson et al., 2000; Wang et al., 2011). One of the major function of FDCs is to trap immune complexes on their surface and display this to B-cells (Balogh et al., 2001; Chen et al., 1978; Sukumar et al., 2008; Allen and Cyster, 2008; Cyster, 2010),

although many other functions of FDC have been described. FDC-associated antigen is displayed to developing centrocytes, and the recognition and binding of antigen by the surface bound immunoglobulin produced by the centrocyte results in signalling from the FDC which promotes survival of the centrocyte (MacLennan, 1994). In the absence of antigen recognition and binding, these survival factors are not delivered to the centrocyte and it will then undergo apoptosis (Lindhout and Groot, 1995). FDC also have an important role in the clearance of apoptotic B cells by secreting Milk fat globule-EGF factor 8 protein (MFGE8) which binds to the apoptotic B cells opsonising them for engulfment by tingible body macrophages (Kranich et al., 2008). Another important role of FDC is in the development and organisation of secondary lymphoid organs. The production of the chemokine CXCL13 by FDC attracts CXCR5 expressing B cells towards the FDC network, thus forming B cell follicles (Amft et al., 2001). These functions of FDC will be described in greater detail in the following sections. Although there has been considerable debate regarding the lineage of FDC (Bofill et al., 2000; Imai et al., 1993; Fliedner et al., 1990; Heinemann and Peters, 2005; Mabbott et al., 2011; Szakal et al., 1995; Kapasi et al., 1998; Yoshida et al., 1995; Krautler et al., 2012; van Nierop and de Groot, 2002; Humphrey and Sundaram, 1985; Munoz-Fernandez et al., 2006) it is now widely accepted that FDC are stromal cells of mesenchymal origin (Kapasi et al., 1998; Munoz-Fernandez et al., 2006; Mabbott et al., 2011; Cho et al., 2012). FDC have been reported to arise from ubiquitous perivascular precursors which express platelet-derived growth factor receptor β (PDGFRβ) (Krautler et al., 2012). Pericytes are specialised smooth muscle cells with mesenchymal stem cell (MSC) potential (Ozen et al., 2012). Other recent publications have found that stromal cells found early in developing lymphoid tissue can arise from other MSC sources. First it has been shown that adipose derived MSC can form the early stromal component of lymph nodes (Bénézech et al., 2010, 2012) which could help explain why lymph nodes are

associated with adipose tissue *in vivo*. Early stromal components of the spleen can also be derived from mesenchymal precursors that arise from the dorsal splenopancreatic mesenchyme in the developing mouse embryo at around embryonic day 10-10.5 (Castagnaro et al., 2013). It has been suggested that FDC could differentiate from these early stromal components (Katakai et al. 2008) and thus it is possible that they can differentiate from different tissue-derived MSC dependent on their location in the body in keeping with the notion of high plasticity existing in mesenchyme tissue (Zipori, 2006).

1.2.2. FDC in the formation of lymphoid tissue

1.2.2.1. Lymphotoxin-β receptor signalling

From studies of lymphotoxin (LT)-deficient mice it is well established that LT-signalling is required for formation (De Togni et al., 1994; Rennert et al., 1996) and maintenance (Rennert et al., 1998; Kuprash et al., 1999; Wilhelm et al., 2002) of mature FDC networks. LT is a member of the tumour necrosis factor (TNF) superfamily of cytokines. Two forms of LT exist, a soluble homotrimeric form, $LT\alpha_3$, and a membrane bound heterotrimeric form ,$LT\alpha_1\beta_2$ (Browning et al., 1993). In Lymphotoxin-α (LTα)-deficient mice, which are deficient for both the soluble and membrane bound forms of LT, there are no Peyer's patches or lymph nodes and the spleen lacks GCs and FDC networks (De Togni et al., 1994; Matsumoto et al., 1997). Lymphotoxin-β (LTβ)-deficient mice lack Peyer's patches, peripheral lymph nodes, GCs in the spleen and FDC, and although these mice do develop mesenteric and cervical lymph nodes, they lack FDC networks and GC (Koni et al., 1997; Ngo et al., 1999). Early $LT\alpha_1\beta_2$ production in lymph nodes and Peyer's patches has been attributed to lymphoid tissue inducer (LTi) cells (Mebius et al., 1996; van de Pavert et al., 2009; Kim, 2008; Bénézech et al., 2010). LTi cells are hematopoietic innate lymphoid cells which are crucial for lymph node development (Lane et al., 2012). However, although LTi cells are present in

the foetal and neonatal spleen, it has been found that B cells are the main source of $LT\alpha_1\beta_2$ that leads to CXCL13 and CCL21 production by stromal cells and the infiltration of lymphocytes to the developing spleen (Vondenhoff et al., 2008; Withers et al., 2007). The stromal cells that LTi or B cells signal to, express the adhesion molecules vascular cell adhesion molecule 1 (VCAM1) and intracellular cell adhesion molecule 1 (ICAM1) at intermediate levels. LTβR signalling by these stromal cells further up-regulates VCAM1 and ICAM1 and induces expression of an additional adhesion molecule mucosal vascular addressin cell adhesion molecule 1 (MADCAM1) (Katakai et al., 2008; Bénézech et al., 2010). These $VCAM1^{hi}$, $ICAM1^{hi}$, $MADCAM1^{+}$ cells produce the chemokines CXCL13 and CCL21 and the cytokine IL-7 (Bénézech et al., 2010; Song et al., 2007) and have been described as lymphoid tissue organiser (LTo) cells as they attract further LTi cells and lymphocytes and are critical for the development of lymph node anlagen into functional lymph nodes (Bénézech et al., 2012). It has been suggested that adult splenic stromal cell populations arise from LTo cells (Katakai, 2012; Katakai et al., 2008; Roozendaal and Mebius, 2011) although the exact mechanisms of differentiation of the adult stromal cells is still unclear. LTo cells of lymph nodes have been described to arise from adipose derived stem cells upon engagement and signalling through the LTβR which activates the non-canonical form of the transcription factor NFκB (Bénézech et al., 2012). This may explain why lymph nodes are associated with a nodule of adipose tissue or 'fat-pad'. The spleen possesses a more complex structure because of the presence of the filtering red-pulp which means the lymphoid compartments are not in direct association with adipose tissue. Using a genetic lineage-tracing approach Castagnaro et al. (2013) have recently shown that FRC, FDC, MRC and mural cells of the spleen all derive from mesenchymal precursors which arise from the dorsal splenopancreatic mesenchyme from the developing embryonic liver. It was shown by artificial lymphoid organ formation experiments that these $Nkx2\text{-}5^{+}islet1^{+}$

cells are capable of initiating lymphoid organ development and contribute to the stromal component. This and the expression of markers suggest that these cells have an LTo cell-like phenotype. LTo cells of different lymphoid organs may therefore arise from different precursor cell types of the MSC lineage. Independent of the source of FDC, it is well established that LTβR-signalling is required for both maturation and maintenance of FDC networks. The membrane bound form, $LT\alpha_1\beta_2$, signals through the LTβR, whereas the soluble form, $LT\alpha_3$, signals through the TNF receptors TNFR1 and TNFR2. LTβR signalling can activate both canonical and non-canonical NFκB signalling pathways. Elegant studies have revealed that activation of the non-canonical NFκB pathway requires internalisation of the receptor while activation of the canonical pathway does not (Ganeff et al., 2011). It was shown that LTβR trimers form clusters triggering internalisation, this endocytosis was found to be dependent upon dynamin-2 GTPase activity. Once internalised the 'cytoplasmic portion' of the LTβR competes for a NFκB-inducing kinase (NIK)-inhibitory complex. This allows stabilisation of NIK, which in turn causes IκB kinase alpha (IKKα) activation and p100 processing leading to formation of the non-canonical NFκB complex p52/RelB (Ganeff et al., 2011). The differential activation of the canonical and non-canonical NFκB pathways by LTβR engagement is summarised in Figure 1.3.

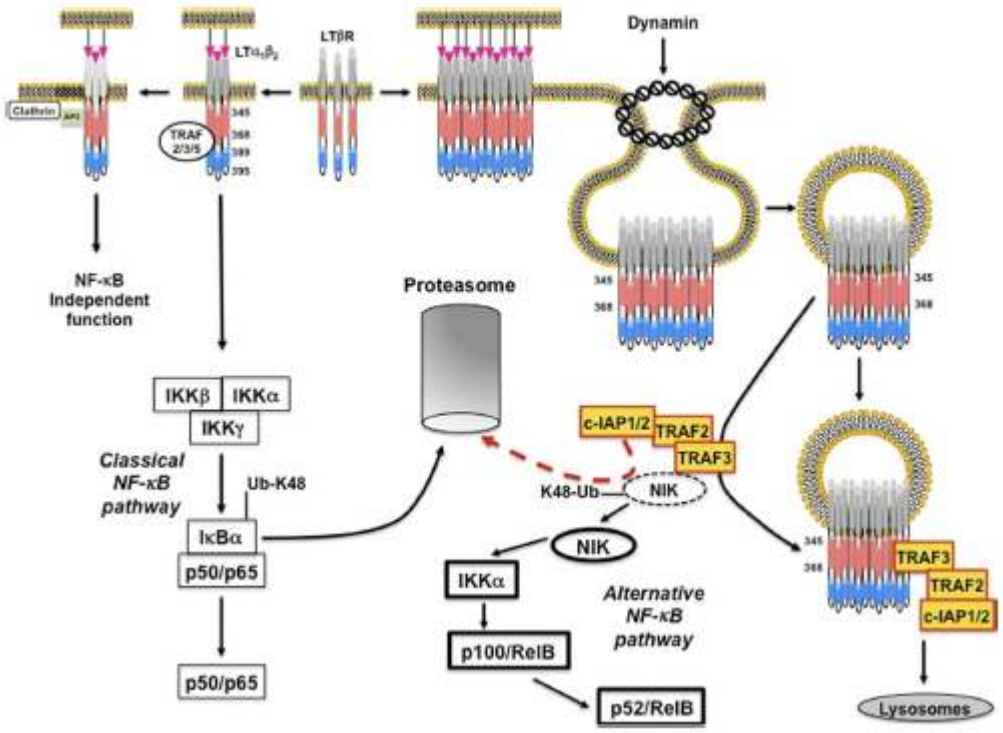

Figure 1.3 Differential mechanisms of activation of the canonical and non-canonical NFκB pathways following LTβR engagement. Taken from (Ganeff et al., 2011).

1.2.2.2. CXCL13 production

FDC secrete the chemokine CXCL13 (Förster et al., 1996; Legler et al., 1998; Cupedo et al., 2004) and generate a CXCL13 gradient around the FDC, which attracts B cells expressing the chemokine receptor CCR5 (Förster et al., 1996; Legler et al., 1998; Allen et al., 2004). Secretion of CXL13 by FDC is therefore important for the attraction of B cells into the GC enabling efficient GC reactions. CXCL13 induces increased $LT\alpha_1\beta_2$ expression on naïve B-cells which then interacts with the LTβR expressed on FDCs, promoting their maturation and hence completing a positive feed-back loop for CXCL13 (Ansel et al., 2000). However, B cell specific LTβ knockout mice only have a 30 -50% decrease in *Cxcl13* expression in the spleen, whereas full LTβR knockout mice have a complete lack of *Cxcl13* expression (Tumanov et al. 2002). This suggests that *Cxcl13* expression may also be partially dependent on a non-B-cell lymphotoxin expressing cell type. Another source of CXCL13 production in the germinal centre is germinal centre T

helper cells which deliver signals such as cytokines which help direct class switching (Ansel et al., 1999).

1.2.2.3. Formation of tertiary lymphoid tissue

The importance of FDC for optimal organisation of the microarchitecture of secondary lymphoid organs is clear. FDC also play a similar role in the formation of tertiary lymphoid tissue that can arise spontaneously during chronic inflammation (Neyt et al., 2012). Several human and experimental mouse tertiary lymphoid organs arising both as a result of autoimmunity and chronic inflammation have been found to contain FDC networks by immunohistochemical analysis (Ghosh et al. 2005; Amft et al. 2001; Drayton et al. 2003). Adipose tissue is found throughout the body and so it has been proposed that, as happens with lymph node stroma, the stromal cell population of tertiary lymphoid tissue could arise from adipose tissue-derived stem cells (Bénézech et al., 2012).

1.2.3. Functions of FDC

1.2.3.1. Immune complex trapping and B cell activation

FDC were first described in relation to the localisation of antigen (Szakal and Hanna, 1968; Nossal et al., 1968). Antigen-antibody (immune) complexes, which sometimes also include complement (Kavai, 2008) are needed to activate effector mechanisms of the immune system such as the classical complement cascade and phagocytic effector cell responses (Nimmerjahn and Ravetch, 2008). Immune complexes (IC) are held on the surface of FDC either by engagement of complement (Reynes et al., 1985; Fang et al., 1998) or Fc receptors (Qin et al., 2000). It has been shown that in primary follicles, complement receptor is sufficient for IC trapping but in secondary follicles both complement receptors and Fc receptors, that also interact with the antibody tail, are utilised (Yoshida et al., 1993; El Shikh et al., 2006). The purpose of IC trapping is to present native antigen to B cells in a form that will instigate the GC reaction (Qin et al.,

2000; Fang et al., 1998; Wu et al., 2008). Antigen in ICs are multimerised and arranged at optimal periodicity to enable efficient cross-linking of the B cell receptor (BCR) complex causing B cell activation (Sukumar et al., 2008; Wu et al., 2008). This manner of B cell activation induces cell proliferation (Li and Choi, 2002) and somatic hypermutation (SHM) (Wu et al., 2008). FDC are long-lived and thus antigen can be present on their surfaces for months allowing long-term maintenance of memory B cells (Bachmann et al., 1994; Zinkernagel et al., 1996). The immune complexes that are trapped on the surface of FDC are delivered directly to FDC by noncognate B cells (Suzuki et al., 2009; Heesters et al., 2013). Shortly after transfer to FDC, ICs are internalised by the FDC and are periodically returned to the cell surface by cycling endosomes (Heesters et al., 2013). The rapid internalisation of immune complexes helps facilitate the unidirectional transfer of antigen from B cells to FDC even though the ICs are held by complement receptor 2 by both cell types (Heesters et al., 2013).

1.2.3.2. Maintenance of germinal centre B cells

When B cells interact with FDC through antigen displayed on its cell surface, various other molecules are involved in this binding and synapse formation (Park and Choi, 2005). The adhesion molecules, VCAM-1 and ICAM-1, are expressed by FDC and up-regulated on immune-complex stimulated FDC (Victoratos et al., 2006). VCAM-1 interacts with very-late activation antigen 4 (VLA-4) on B cells and ICAM-1 interacts with lymphocyte function-associated antigen 1 (LFA-1). These interactions serve to form a stronger interaction between the B cell and FDC which lowers the threshold of B cell activation in the germinal centre (Koopman et al., 1994; Carrasco et al., 2004). Many other molecular interactions between FDCs and GC B cells take place, some of which are summarised in Figure 1.4.

The TNF family member B-cell activating factor (BAFF) is secreted by FDC in the GC and prevents apoptosis of B cells by signalling through various receptors (BCMA, TACI and BAFF-R) (Park and Choi, 2005). The most important interaction in terms of promoting B cell survival is through BAFF receptor (BAFF-R), which has been described to exert it's effects by activation of the non-canonical NFκB pathway leading to transcription of pro-survival genes (Hase et al., 2004; Zhang et al., 2005; Gardam et al., 2008). It has also been shown that interaction between the notch ligands, JAGGED 1 and Delta-like 1, expressed by FDC and the notch receptors, 1 and 2 on GC B cells, prevents GC B cell apoptosis early in the germinal centre reaction (Yoon et al., 2009). The cytokines IL-6 and IL-15 are secreted by activated FDC and they engage IL-6 and IL-15 receptors on germinal centre B cells. It has been shown that blocking IL-6 signalling in germinal centre B cells leads to reduced IgG responses and impaired SHM (Wu et al., 2009). IL-6 has also been described to be involved in tolerance in germinal centre B cells (Yan et al., 2012). IL-15 is produced by FDC and is bound by IL-15Rα on the surface of FDC. This membrane bound form of IL-15 can then be bound by signal transducing components IL-2/15βγ, expressed by germinal centre B cells, and induce B cell proliferation. Additionally, FDC produce sonic hedgehog ligand which signals through hedgehog receptors on germinal centre B cells, promoting their survival (Sacedón et al., 2005)

1.2.3.3. Toll-like receptor-4 signalling

Toll-like receptors (TLRs) are receptors that recognise structurally conserved molecular patterns, which are usually derived from microbes (PAMPs; pathogen associated molecular patterns). When TLRs bind their ligands they up-regulate various processes of the innate immune response. The classical ligand of toll-like receptor 4 (TLR4) is lipopolysaccharide (LPS) which is expressed by gram negative bacteria.

However, a number of other bacterial and host proteins can engage TLR4 (Tsan and Gao, 2004; Gay and Gangloff, 2007). Engagement of TLR4 leads to activation of various signalling pathways including the non-canonical NFκB signalling pathway(Gay and Gangloff, 2007). TLR4 expression is up-regulated on FDC in mice injected with LPS (El Shikh et al., 2007b) and TLR4 signalling up-regulates expression of Fc receptors and adhesion molecules (ICAM-1 and VCAM-1). TLR4 up-regulation can occur on FDC in germinal centres even without LPS stimulation. It has been shown that endogenous ligands of TLR4 (such as oxidised phospholipids) are produced as a consequence of B cell apoptosis within the germinal centre. There is evidence that TLR4 signalling is important for driving the maturation of FDC and, as such, strongly impacts the adaptive immune response by influencing the extent of somatic hypermutation and immunoglobulin subclass switching that takes place.

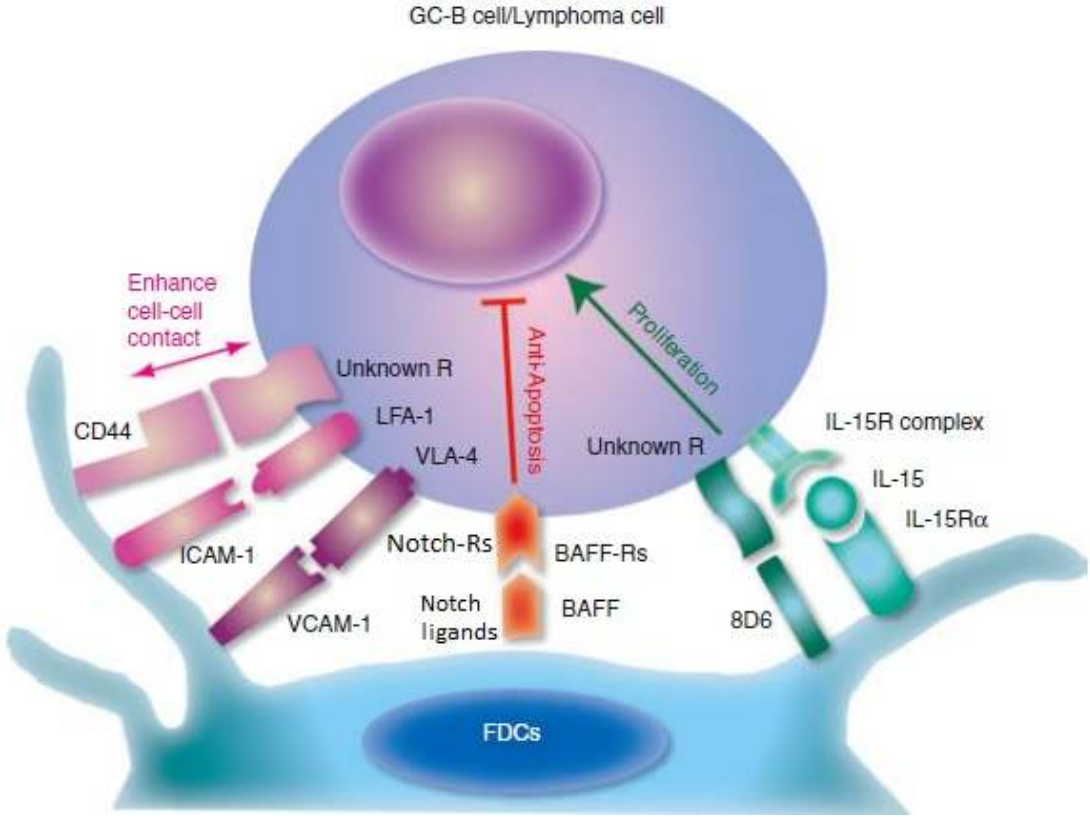

Figure 1.4 Molecular mechanisms of interaction between FDC and germinal centre B cells. Adapted from (Park and Choi, 2005).

1.2.3.4. Clearance of apoptotic B cells

Another role of FDC is mediated by the production of MFGE8. MFGE8 is secreted by FDCs in the germinal centre, and binds to exposed phosphatidylserine on the surface of apoptotic B-cells. MFGE8 on the apoptotic B cells is then bound by integrin expressed on the cell surface of tingible-body macrophages, enabling them to engulf the apoptotic B cells (Kranich et al., 2008) (Figure 1.5). FDCs therefore provide pro-survival signalling to high affinity B cells, and also control the clearance of B cells which do not receive these stimuli. Accordingly, mice deficient in MFGE8 develop spontaneous splenomegaly and glomerulonephritis and auto-reactive antibodies (Hanayama et al., 2004). When apoptotic B cells are not cleared efficiently they can undergo secondary necrosis and release components such as double stranded DNA which can then be recognised as antigen, causing auto-antibody production (Kruse et al., 2010).

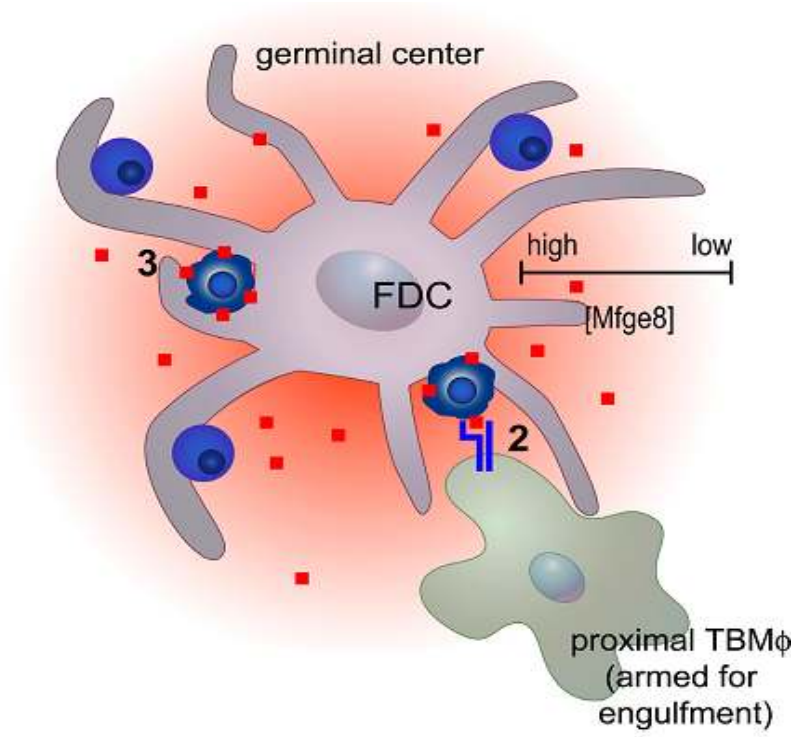

Figure 1.5 The role of Mfge8 in the clearance of apoptotic B cells. Mfge8 (red squares) produced by FDCs binding to apoptotic B-cells allowing the binding of a tingible body macrophage via integrin, thus facilitating engulfment of the apoptotic B-cell. Adapted from Kranich et al. 2008.

1.2.4. Follicular dendritic cells in disease

FDC have been associated with a number of diseases and disease processes (Rezk et al., 2013; El Shikh and Pitzalis, 2012; Smith et al., 2001; Mcculloch et al., 2011). The involvement of FDC in some of these diseases is described below.

1.2.4.1. Transmissible spongiform encephalopathy (TSE)

TSEs are fatal neurodegenerative disorders which occur in a number of mammalian species including sheep, cows and humans. They are characterised by the accumulation of amyloid plaques and eventual vacuolation of neurons in the grey matter of the brain. The amyloid plaques that form are made up of an abnormally folded, disease-associated isomer of the cellular prion protein (PrP^{c}) which is termed PrP^{sc}. The normal cellular form of the prion protein is widely expressed but is most highly expressed in the central nervous system. Within lymphoid tissues FDC also express PrP^{c} at high levels (Thielen et al. 2001). During peripherally acquired TSE disease, PrP^{sc} associates with FDC, and PrP^{c} expressing FDC are required for replication of the TSE agent within secondary lymphoid tissues and the spread of infection to the brain (Mcculloch et al., 2011).

1.2.4.2. Human immunodeficiency virus

During the early stages of human immunodeficiency virus (HIV)-1 infection, large quantities of the virus are trapped in immune complexes on the surface of FDC dendritic processes (Haase et al., 1996). Murine studies have revealed that FDCs can retain infectious virus for at least nine months after infection (Smith et al., 2001). Additionally this study also found that human FDCs in culture were able to maintain HIV infectivity for at least 25 days compared to just a few days without FDCs. $CD4^{+}$ T cells can also become infected from FDC-trapped virus while trafficking through germinal centres (Burton et al., 2002). Although HIV-1 infections can be well controlled

with drug therapy, none are available that can completely eradicate the virus. This is because the virus persists in reservoirs in the body, one of which may be FDC networks (Zhang and Perelson, 2013). The low serum titres that persist in patients between around 39-200 weeks after the start of treatment could be explained by shedding of virus from FDC reservoirs (Zhang and Perelson, 2013). FDC therefore may be a significant factor in the persistence of HIV infection even in patients receiving aggressive antiretroviral therapy.

1.2.4.3. Autoimmune diseases and chronic inflammation

As previously mentioned MFGE8-deficient mice have been found to develop autoimmune diseases as a result of the development of autoantibodies (Hanayama et al., 2004; Kruse et al., 2010). The gene, T cell immunoglobulin and mucin domain containing-4 (*Timd4*) encodes a membrane bound protein expressed by a subset of macrophages (including marginal zone macrophages). TIMD4 also binds to phosphatidylserine and supports engulfment of apoptotic cells. Mice deficient in both Mfge8 and Timd4 develop a more severe phenotype which is exacerbated by blocking of TNFα or increasing the inflammatory cytokine interferon-γ (IFN-γ) (Miyanishi et al., 2012). In some patients with systemic lupus erythematosus (SLE) it has been found that clearance of apoptotic B cells does not occur efficiently. This is possibly due to aberrant expression of MFGE8 (Yamaguchi et al., 2008). If apoptotic B cells are not cleared swiftly, they can undergo secondary necrosis, which releases auto-antigens (such as double stranded DNA) which are then trapped on the surface of FDC and presented to B cells. This allows affinity maturation of B cells producing auto-antibodies which drives autoimmune disease (Muñoz et al., 2010; Baumann et al., 2002). Additionally, FDCs produce IL-6 which is important in driving germinal centre reactions (Wu et al., 2009) and patients with SLE are known to have increased IL-6 levels (Ripley et al., 2005; Tackey et al., 2004). These studies indicate three possible

roles for FDC in the pathogenesis of SLE; aberrant Mfge8 expression, presentation of auto-antigen and aberrant expression of IL-6. These functions of FDC also have the potential to be involved in other systemic autoimmune diseases. For example, high expression of IL-6 is found in patients with Castleman's disease, which is characterised by a hyper-proliferation of B cells (Leger-Ravet et al., 1991), and may support the abnormal proliferation of B cells in this disease. Hyper-proliferation of FDC has also been described in Castleman's disease (Leger-Ravet et al., 1991).

1.2.4.4. Follicular lymphomas

Castleman's disease sometimes precedes the development of FDC sarcoma which is a very rare neoplasm (Chan et al., 1997). Follicular lymphomas arise when germinal centre B cells become neoplastic. Follicular lymphoma cells undergo spontaneous apoptosis in culture which is mediated by activation of Caspase-8 and -3 (Hengartner, 2000). Co-culture of follicular lymphoma cells with FDC reduces this spontaneous apoptosis by preventing the activation of caspase-8 and -3 (Goval et al., 2008). It was also shown that VCAM-1 and ICAM-1 interactions are important for this reduction in apoptosis indicating that direct cell-cell contact is needed. The production of the tumour suppressive signalling protein WNT5A by FDC has also been shown to reduce spontaneous apoptosis of follicular lymphoma cells by increasing CD40 expression (Kim et al., 2012b). Tumorigenic follicular lymphoma cells are attracted to FDC in culture by CXCL12/CXCR4 stimulation (Lee et al., 2012), which appears to make follicular lymphoma cells resistant to chemotherapy. Finally, drug resistance in follicular lymphoma is associated with the expression of the ATP-binding cassette, sub-family B (MDR/TAP), member 1B (MDR1), which is a transporter molecule which can actively remove therapeutic drugs from the cell. It was found that follicular lymphoma cells that express *MDR1,* are those that are in close association with FDC, and further, that a lymphoma cell line co-cultured with FDC up-regulated the expression of *MDR1*

(Yagi et al., 2013). All these studies clearly show that FDC appear to have a role in supporting and sustaining follicular lymphomas.

1.2.5. The study of FDC

FDCs were initially discovered by the examination of antigen localisation, where it was discovered that the pattern of antigen followed the cytoplasmic protrusions of dendritic reticular cells (Mitchell and Abbot, 1965; Szakal and Hanna, 1968; Chen et al., 1978). Ultrastructural studies were extended by the development of antibodies that stain FDC. The monoclonal antiboby FDC-M1 (formally 4C11) (Tew et al., 1990) was found to react with MFGE8 protein (Kranich et al., 2008). The monoclonal antibody FDC-M2 had also been used to identify FDC for many years before it was found to react with the activated complement component C4b (Taylor et al., 2002). The complement receptors CR1 and CR2 (CR35/21) have also been used widely for FDC immunostaining (Reynes et al., 1985; Yoshida et al., 1993). High expression of PrP^c has also been associated with FDC (McBride et al., 1992). The isolation of FDC is challenging because the large size and complexity of their dendritic processes means mechanical stress on the cells during isolation is often high. The strong association of B cells with FDC also means that obtaining a pure population of FDC is difficult. However, various methods of FDC isolation have been used (Schmitz et al., 1993; Usui et al., 2012; Sukumar et al., 2006; Sellheyer et al., 1989; Schriever and Freedman, 1989) to achieve almost pure populations of FDC that retain many markers and functional activity. The method to isolate FDC from human tonsils (Schriever and Freedman, 1989) was further extended by subsequent culturing and purification steps (Kim et al., 1994) and the resulting cells were termed HK. This method of isolation and subsequent culture has been widely used as a method of *in vitro* study of FDC (Choe et al., 1996; Cho et al., 2011b; Kim et al., 1995; Park et al., 2004; Kim et al., 2012a, 2006; Choe et al., 2000; Lin et al., 2011). More recently a murine FDC cell line, termed FL-Y, has been established (Nishikawa et al.,

2006) that can be cultured for extended periods of time (months). This cell line retained many markers and functional activities of FDC, such as the ability to support B cells in co-culture. FL-Y cells were subsequently transformed by expression of the murine BAFF gene, and a clone stably expressing BAFF was selected (Magari et al., 2011). The increased BAFF expression in these cells was similar to levels detected in freshly isolated FDC and the so called FL-YB cells were found to be more effective in supporting B cells than the original FL-Y cells.

The display of antigen and provision of co-stimulatory signals to B cells by FDC are critical for an efficient GC reaction. FDC also play a role in many diseases processes such as HIV-1 latency, autoimmune disorders and lymphomas. Knowledge of the development and function of FDC is increasing. However, the broader picture of how all the known functions of FDC are regulated is still unclear. A greater understanding of FDC regulation is needed, and could potentially lead to future therapeutic interventions.

1.3. MicroRNAs

1.3.1. Discovery and history of microRNAs

MicroRNAs (miRNAs) are short non-coding single-stranded RNA molecules. The first miRNA to be discovered was designated lin-4 and was found in the nematode worm *Caenorhabditis elegans* (Lee et al., 1993). Lin-4 was found to be a RNA of 22 nucleotides which supresses the production of lin-14 protein from the first larval stage. The 3'-UTR of the *lin-14* mRNA was found to contain multiple repeats copies of a sequence that is partially complementary to the lin-4 sequence. The authors proposed that lin-4 supresses lin-14 production by direct RNA:RNA binding. Later, another miRNA, let-7, was discovered in *C. elegans* and found to target both *lin-41* and *lin-42* during the later stages of larval development (Reinhart et al., 2000). Later in the same year let-7 was identified from a variety of species including human, mouse, chicken, frog, zebrafish,

sea squirt, molluscs and drosophila (Pasquinelli et al., 2000). This lead to the rapid identification of a variety of other miRNA in different species (Lee and Ambros, 2001; Lau et al., 2001; Lagos-Quintana et al., 2001). Lee & Ambros (2001) and Lau et al. (2001) identified further miRNAs in C. elegans, whereas Lagos-Quintana et al. (2001) discovered miRNAs in drosophila and Hela cells. These three studies lead to the concept that miRNAs are abundantly expressed in most species, and represent a whole level of previously unrecognised genetic control. It was acknowledged, even at this early stage of miRNA discovery that because of the partial complementarity to their miRNA targets, identification of the mRNA targets would be challenging.

1.3.2. miRNA biogenesis

The acknowledged challenges in the discovery of miRNA targets reiterated the need for an understanding of the mechanisms that regulate miRNA biogenesis and function. It had been described in the previously mentioned studies (Lee and Ambros, 2001; Lau et al., 2001; Lagos-Quintana et al., 2001) that precursor miRNAs of around 70 nucleotides were discovered for most miRNA, and that these pre-miRNA were predicted to form stem-loop structures. The enzyme Dicer, had already been discovered to be key in the biogenesis of small RNAs in the RNAi pathway (Bernstein et al., 2001) and it was found that the same enzyme was involved in the production of mature miRNA (Hutvágner et al., 2001). Primary or pri-miRNA that could include either a single or multiple precursor miRNA were described by Y. Lee et al. (2002). The same group later showed that pri-miRNAs are cleaved by the RNAse III enzyme Drosha (Lee et al., 2003b) and that pri-miRNAs are transcribed by RNA polymerase II (RNA pol II) (Lee et al., 2004). The products of Drosha cleavage, pre-miRNA, are then translocated into the cytoplasm by Exportin-5 (Yi et al., 2003). In the cytoplasm the RNAse III enzyme Dicer further cleaves the pre-miRNA (Bernstein et al., 2001; Hutvagner et al., 2002; Jakymiw et al., 2010; Knight and Bass, 2001) into a mature single stranded miRNA (Khvorova et al.,

2003; Schwarz et al., 2003). The mature miRNA is incorporated into the RNA-induced silencing complex (RISC) (Hutvagner et al., 2002). This process of miRNA biogenesis from transcription to functional miRNA in the RISC complex in summarised in figure 1.6

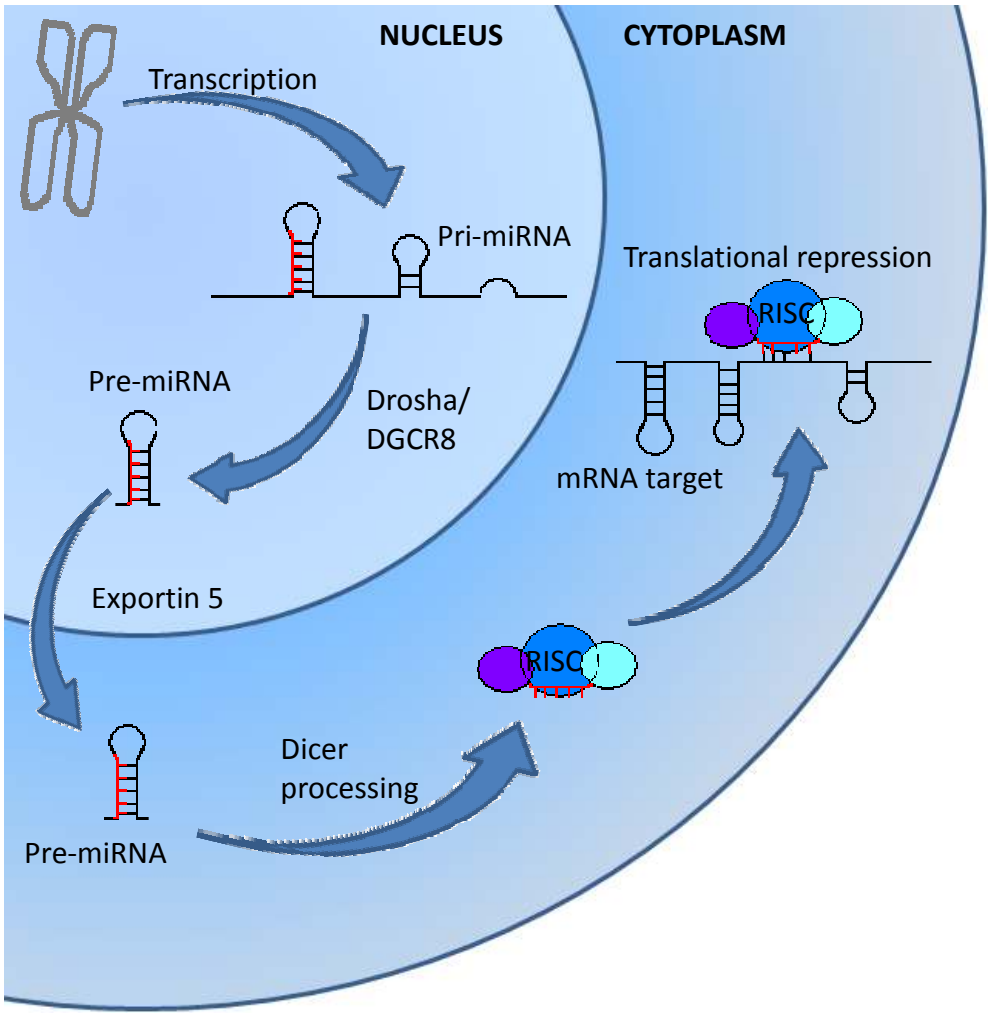

Figure 1.6 miRNA biogenesis. (a) Primary miRNA (pri-miRNA) are transcribed by RNA pol II.(b) Pri-miRNA are cleaved by the Drosha/DGCR8 complex into pre-miRNA.(c) Pre miRNA are then exported into the cytoplasm by Exportin-5. (d) In the cytoplasm the pre-miRNA is further processed by Dicer, and inserted into the RNA-induced silencing complex (RISC). (e) The miRNA-RISC complex can then bind to and repress transcription of the target mRNA.

1.3.2.1. miRNA transcription

MiRNA genes can be located within intergenic regions of the genome or within the introns of protein coding genes (Ying and Lin, 2006). Intronic miRNAs have often been found to have their own promoter sequence rather than simply being transcribed along with the host gene (Marsico et al., 2013). Some miRNAs are located adjacent to each other in the genome and can be transcribed in one pri-miRNA, this is referred to as a miRNA cluster. It is estimated that almost 50% of miRNA are transcribed with at least one other miRNA and it has been suggested that different miRNAs transcribed in the same cluster can function co-ordinately to regulate multiple members of the same signalling pathways or interaction networks (Becker et al., 2012).

1.3.2.2. The RISC complex and miRNA strand selection

In the cytoplasm, Dicer is recruited to the pre-miRNA by the transactivation response (TAR) RNA binding protein (TRBP) (Chendrimada et al., 2005). Dicer cleaves the pre-miRNA at the stem-loop and is thought to initiate unwinding of the miRNA duplex (Vermeulen et al., 2005). The argonaute protein, AGO2, is then recruited to the complex and binds the 2-nucleotide 3' overhang that is created by Dicer processing (Figure 1.7). Only one strand of the miRNA is chosen to be incorporated into the forming RISC complex, although the alternative strand may be selected in different tissues or situations (Yang et al., 2010). Nomenclature was set-up so that the more abundant miRNA that was found initially was referred to as the lead strand and the miRNA found in less abundance was referred to as the star (or passenger) strand (Griffiths-Jones et al., 2006). However because it is now known that the most abundant miRNA in one tissue can be the least abundant in another tissue of the same organism (Griffiths-Jones et al., 2011), the suffixes -5p or -3p are now used (denoting the 5' or 3' strand). Although it has previously been suggested that differences in the thermodynamic and

structural stability were crucial (Khvorova et al., 2003), it is still not known how different strands are selected in different tissues.

1.3.2.3. miRNA target recognition

Although in animals most miRNA bind with imperfect complementarity to their target mRNA, a region of conserved base pairing termed the seed region or seed sequence has been identified (Stark et al., 2003; Lewis et al., 2003). This region is located from nucleotide 2 to 7 at the 5' end of the miRNA. In addition, perfect complementarity is sometimes found to extend to nucleotide 8 and an adenine residue at position 1 is also often seen(Bartel, 2009). Although binding at the 3' end often occurs this is variable and it has been suggested that high 3' end pairing can compensate for weaker seed region pairing (e.g. only 5 nucleotides instead of 6 or 7) (Yekta et al., 2004).

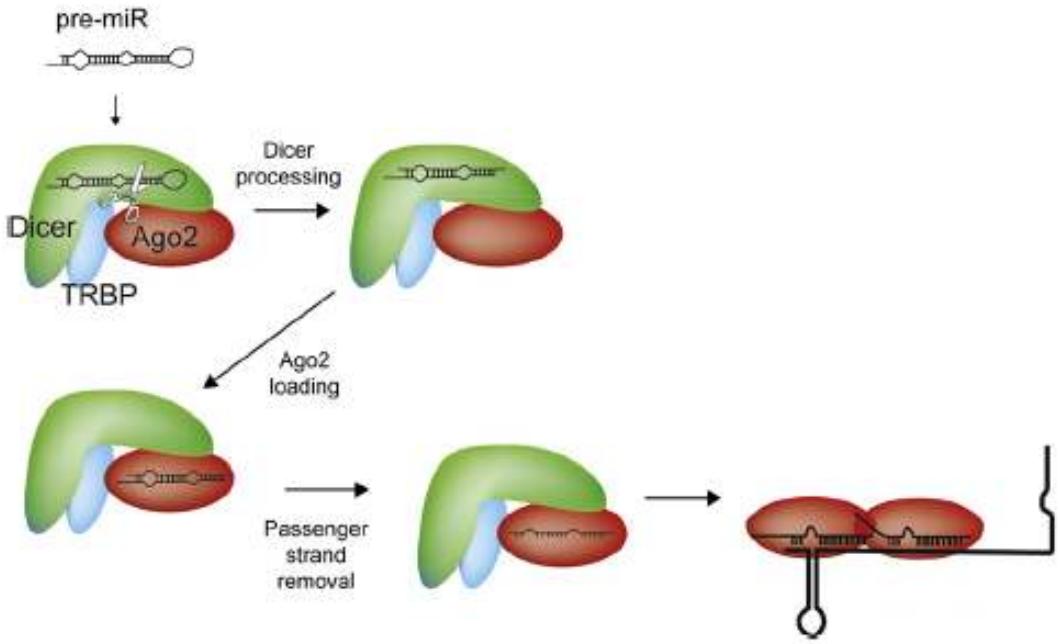

Figure 1.7 Assembly of the of the RISC-miRNA complex and mRNA targeting. Adapted from (Zhang et al., 2012)**.**

1.3.3. Mechanisms of miRNA function

In animals, miRNAs generally bind with partial complementarity to their target mRNAs and cause translational repression and, in the majority of cases, transcriptional degradation (Janas and Novina, 2012). The exact mechanisms of translational repression and transcriptional degradation are still being elucidated (Wahid et al., 2010). Several different mechanisms of translational repression have been proposed (Fabian et al., 2010) the main ones of which will be described briefly here and are summarised in figure 1.8.

1.3.3.1. Inhibiton of translation

One proposed mechanism for inhibition of translation is through miRNA-RISC–mediated interference with recognition of the 5' cap by the eiF4F complex which in turn inhibits recruitment of the 40S ribosomal subunit (Zinovyev et al., 2008). Alternatively, it has been suggested that the 60S subunit may be prevented from binding to the 40s subunit to form the functional 80S subunit (Wang et al., 2008a). The GW182 protein which forms part of the RISC complex has been reported to interact with the poly(A)-binding protein (Fabian et al., 2009). This interaction lead to the hypothesis that the miRNA-RISC complex could interfere with circularisation of the transcript (Zekri et al., 2009), thus slowing the rate of translation (Figure 1.8a).

1.3.3.2. Inhibition of translation at a post-initiation stage

Theories behind inhibition of translation at a post-initiation stage are that miRNA-RISC complex binding might cause ribosomal drop-off (Rand et al., 2005) or could increase degradation of the emerging peptide(Pasquinelli, 2012) (Figure 1. 8b).

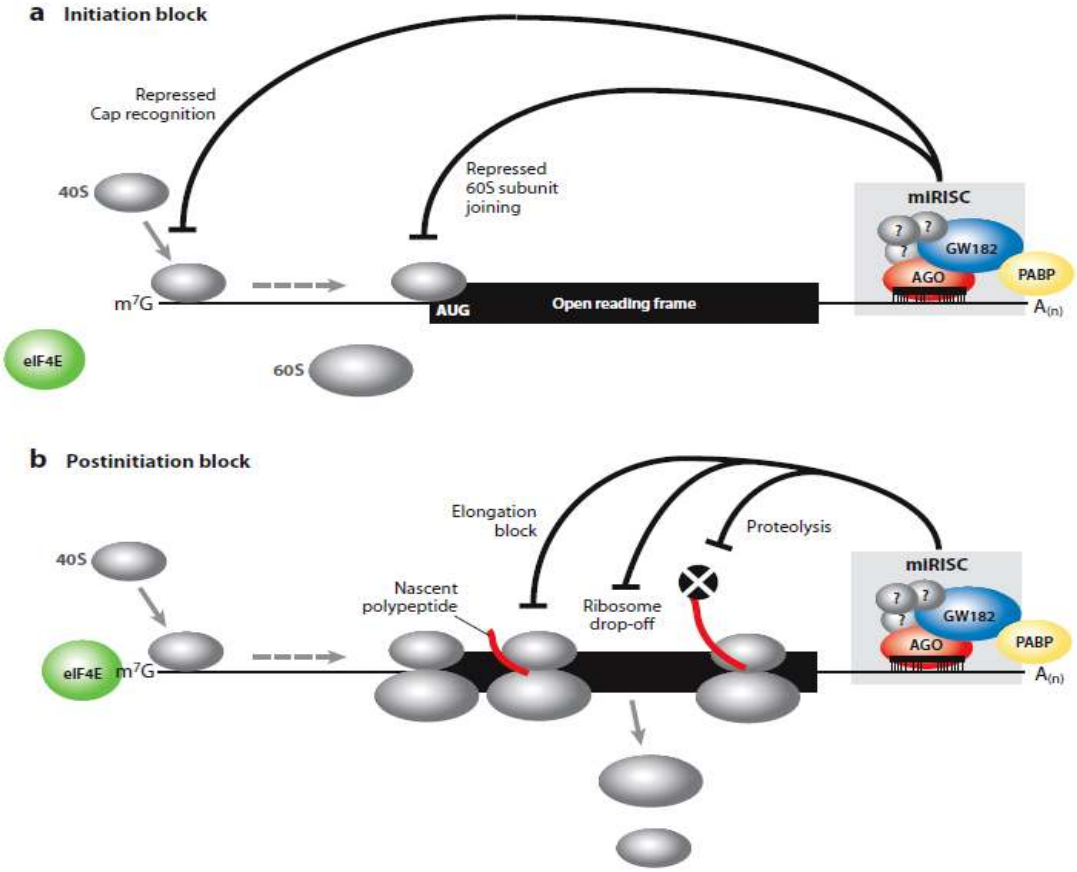

Figure 1.8 Proposed mechanisms of translational repression by the miRNA-RISC complex. (a) Inhibition of transcriptional initiation by prevention of ribosomal subunit binding. (b) Inhibition of transcriptional progression by causing ribosomal drop-off or degradation of the emerging peptide. Taken from (Fabian et al., 2010).

1.3.3.3. Transcriptional degradation

More recently it has been proposed that deadenylation and transcript degradation occurs in the majority of cases following inhibition of translational initiation (Bazzini et al., 2012; Janas and Novina, 2012). Ribosome footprinting techniques have been used in combination with RNA-Seq to show that in zebrafish embryos the natural induction of miR-430 at 2 h post fertilisation leads first to a decrease in the number of ribosomes associated with the miRNA target at 4 hours post fertilisation, followed by subsequent decrease in mRNA levels or poly(A) tail lengths of the same targets at 6 hours post

fertilisation (Bazzini et al., 2012). It is therefore proposed that miRNA transcripts undergo translational inhibition and transcriptional degradation (Figure 1.9).

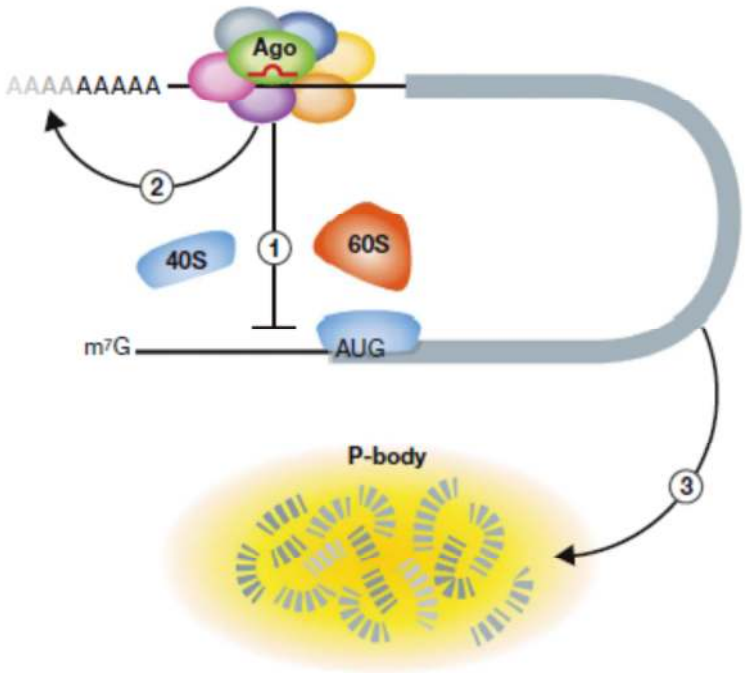

Figure 1.9 Steps of miRNA action. 1) Inhibition of transcriptional initiation 2) deadenylation of poly(A) tail followed by 3) degradation in processing-bodies (p-bodies).

1.3.3.4. Localisation of miRNA targets to processing bodies

Observed localisation of RISC proteins, miRNA and targeted mRNA transcripts to processing bodies (p-bodies) lead to the theory that targeted transcripts are sent to p-bodies either to be sequestered or to be degraded (Pillai et al., 2007). However it has also been shown that cells devoid of p-bodies have normal miRNA-mediated transcriptional silencing and thus p-bodies may be a consequence of miRNA-mediated gene silencing rather than a cause of it (Eulalio et al., 2007). Recently, it was shown that the E3 ubiquitin ligase, Malin, regulates miRNA gene silencing activity by causing the degradation of the decapping enzyme DCP1A. Loss of malin in cells resulted in altered miRNA gene silencing activity (Singh et al., 2012).

1.3.4. Biological functions of miRNAs

The first miRNAs were discovered because their loss conferred a dramatic effect upon *C. elegans* larval development (Lee et al., 1993; Reinhart et al., 2000). Subsequently other miRNA that have major roles in different processes have been discovered. For example, a single nucleotide mutation in miR-96 is associated with autosomal dominant hearing loss in humans (Mencía et al., 2009; Lewis et al., 2009). Additionally, knock-down of miR-155 has a variety of deleterious effects on the immune system including promoting T helper cell differentiation, germinal centre responses, and reduced responses to viral and bacterial challenge (Rodriguez et al., 2007; Thai et al., 2007; Worm et al., 2009; Dorsett et al., 2008). While 24,521 mature miRNA products across 206 species (www.miRBase.org (Griffiths-Jones et al., 2006)) have been identified to date, loss of the majority of these miRNAs does not cause obvious phenotypic effects (Hornstein and Shomron, 2006; Ebert and Sharp, 2012). Rather, it has been proposed that the majority of miRNAs actually confer robustness to a biological system or network rather that playing major regulatory roles on specific genes. Two main modes of action for how miRNAs add to the robustness of a biological system have been proposed (Hornstein and Shomron, 2006; Ebert and Sharp, 2012). The first scenario is a positive feed-forward loop (Tsang et al., 2007) where the miRNA target genes is being repressed at the transcriptional level, and the genes that are repressing the target, also up-regulate the miRNA (Figure 1.10a). In this way the miRNAs are 'insurance' against rogue expression of mRNA that may still get through the transcriptional repression. In this scenario the miRNA is expected to be highly expressed at the same time that the target is not expressed or expressed at very low levels. A biological example of this could be suppression of genes that are highly expressed in a sibling tissue but not in the tissue of interest. A classic example of this is in the developing drosophila embryo, where neuroectoderm progenitors give rise to

both neurons and epidermis. During development miR-124 is up-regulated in neurones whereas miR-9 is up-regulated in the developing epidermis. Neurons highly express many mRNA that contain target sites for miR-9, whereas cells in the epidermis express many genes which contain miR-124 target sites. The presence of these miRNAs 'protects' against aberrant expression of the wrong genes (Farh et al., 2005; Stark et al., 2005; Sood et al., 2006; Tsang et al., 2007).

The second scenario is where the miRNA target is being transcriptionally activated and the genes that cause this activation also cause transcription of the miRNA which then acts to fine-tune the amount of target being produced (Figure 1.10b). In this case both the miRNA and target transcript would be expected to be expressed at intermediate and steady levels simultaneously.

Figure 1.10 Proposed modes of action for miRNA conferring robustness upon a biological system. (a) The target transcript(s) are transcriptionally repressed the genes that cause this repression also up-regulate miRNA expression. The miRNA act to repress post-transcriptionally any target transcript that has been made, thus ensuring that no protein is produced. (b) The target transcript(s) are transcriptionally activated (or repressed) and the genes which cause this activation (or repression) also up-regulate miRNA expression. The miRNA then act to keep the target transcript producing protein at a steady rate. Proposed by (Hornstein and Shomron, 2006; Ebert and Sharp, 2012).

1.3.5. miRNAs in the immune response

The possibility of using miRNA therapeutics has led to considerable research focused on the roles of miRNAs in various aspects of the immune response (Lu and Liston, 2009; Navarro and Lieberman, 2010; Ha, 2011; Sonkoly et al., 2008; Asirvatham et al., 2009; Cullen, 2013; Ramiro, 2010; Bronevetsky and Ansel, 2013; Chen et al., 2013a).

Although there has been no published material looking at miRNAs in follicular dendritic cells to date, abundant miRNAs have been identified in other cells of the immune system. Of particular significance to this thesis are miRNAs that have roles in the germinal centre reaction.

1.3.5.1. FDC-mediated miRNA expression in B cell lymphoma cell lines

Two publications have described FDC-mediated induction of miRNA expression in cell lines derived from B cell lymphoma cells and in normal germinal centre B cells.

One study examined the mechanism of terminal differentiation of germinal centre B cells into plasma or memory B cells (Lin et al., 2011). This terminal differentiation is driven by the suppression of the transcription factor B cell leukemia/lymphoma 6 (BCL-6) and the increased expression of the transcription factor PR domain containing 1, with ZNF domain (PRDM1) (Crotty et al., 2010; Shaffer et al., 2002). It was shown that co-culture of the human B cell lymphoma cell line Su-4 with FDC-like HK cells, lead to a number of expression level changes in the Su-4 cells (Lin et al., 2011). As BCL-6 and PRDM1 are known to be key transcription factors that regulate terminal differentiation, the 3' UTRs of these genes were examined for miRNA target sites of miRNAs found to be regulated by HK cell-B cell co-culture. It was found that *Bcl-6* had target sites for the miR-30 family of miRNA, 3 of which were found to be up-regulated after 24 hours of co-culture. The authors showed that introduction of an anti-miR-30 oligonucleotide,

resulted in a significant reduction in the HK-induced repression of Bcl-6. In addition, let-7a and miR-9 (which were both down-regulated upon co-culture) had putative target sites in the *Prdm1* 3'UTR. Introduction of a let-7a mimic into the Su-4 cells induced similar levels of down-regulation of *Prdm1* in the absence of HK cell co-culture. These actions were shown to be dependent upon direct HK cell-B cell contact as culturing in a trans-well system did not induce changes in the expression levels of the miRNA in Su-4 cells(Lin et al., 2011).

The second study focused on miR-181a that had also been shown to be up-regulated upon HK-Su-4 cell contact (Lwin et al., 2010). miR-181a was found to target the gene encoding the pro-apoptotic protein, BCL-2-interacting mediator of cell death (BIM). miR-181a was up-regulated 24 hours after co-culture of Su-4 and HK cells, whereas *BIM* was down-regulated in B cells (Yau et al., 2013). The authors demonstrated that loss of miR-181a increased cell death of the Su-4 cell line, indicating that miR-181a is an important regulator of BIM.

These two studies provide examples of miRNAs conferring robustness in a biological system. In these situations the gene targets are transcriptionally regulated but as a robust change in gene expression is critical for these biological processes, miRNAs are also activated as 'insurance' against any transcription that is allowed to take place.

1.3.6. miRNAs in development

Differential miRNA expression in B cells through their many developmental stages has been extensively studied (Davidson-Moncada et al., 2010; Zhang et al., 2009; Yébenes, 2013; Li et al., 2013; Basso et al., 2009). This work is summarised in Figure 1.11.

1.3.6.1. miR-181a

miR-181a was the first miRNA recognised to be involved in early B cell differentiation. Overexpression of miR-181a in lymphocyte progenitor cells caused a bias towards development of B cell lineages (Chen et al., 2004). The RNA binding protein lin-28 is identified as a target of miR-181a, and it is proposed that miR-181a targeting of lin-28 disrupts the lin-28-let-7 regulatory loop, leading to up-regulation of let-7 which in turn causes differentiation (Li et al., 2013). However the exact mechanisms of miR-181a action in early B cell differentiaton remain to be fully elucidated.

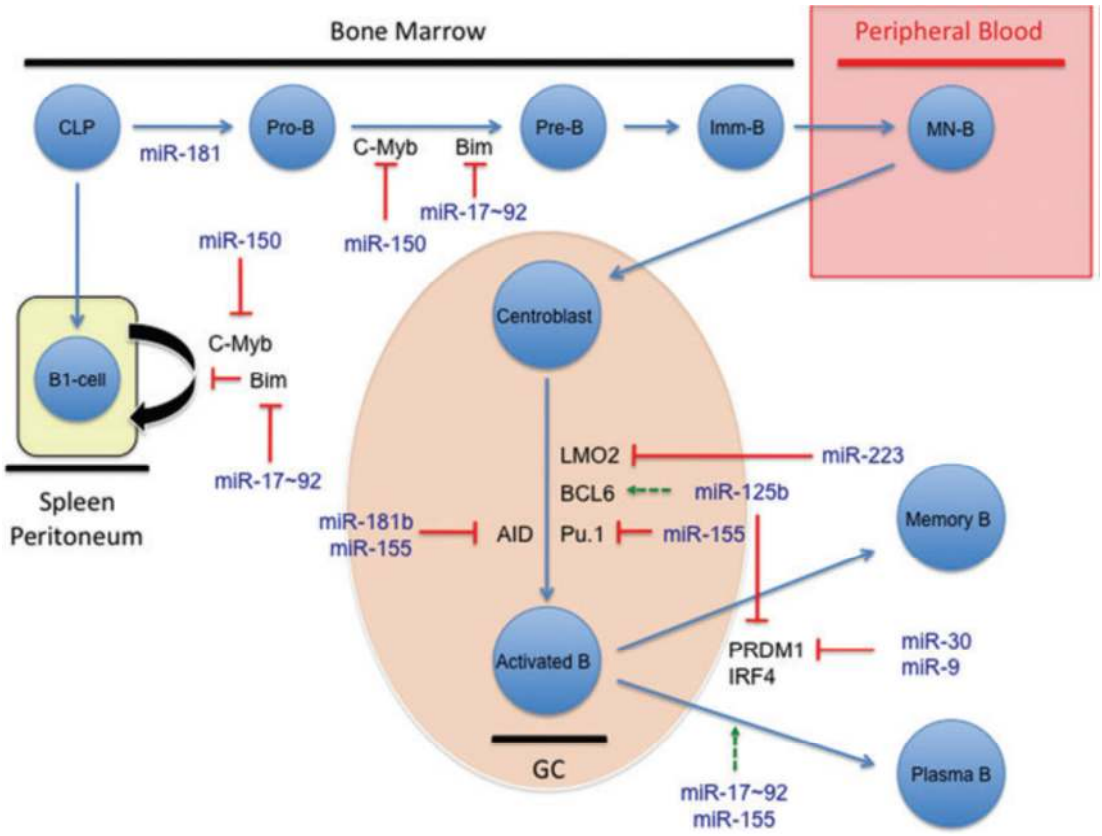

Figure 1.11 miRNA control of B-cell differentiation. Red arrows indicate down-regulation by a miRNA, green dashed arrows indicate indirect upregulation by the indicated miRNA. CLP = common lymphoid precursor, Imm-B = immature B-cell, MN-B = mature naïve B-cell. Davidson-Moncada et al. 2010.

1.3.6.2. miR-17~92 cluster

The miR-17∼92 cluster encodes six miRNAs. Deletion of this cluster in hematopoetic stem cells causes a block in subsequent B cell differentiation at the pro- to pre-B cell stage (Ventura et al., 2008). Cells deficient for miR-17∼92 also have increased levels of the pro-apoptotic protein BIM, and repression of BIM has been shown to partially rescue the phenotype (Koralov et al., 2008).

1.3.6.3. miR 34a

The overexpression of miR-34a has also been described to block B cell differntiation at the pro- to pre-B cell stage (Rao et al., 2010). This occurs by miR-34a targeting of the transcription factor FOXP1 which is required for early B cell devlopment (Rao et al., 2010).

1.3.6.4. miR-150

It has been shown that miR-150 is expressed highly in mature and resting B- and T-lymphocytes but not their progenitors (Xiao et al., 2007) indicating a role in lymphocyte development or function. The study showed that the pattern of c-Myb expression is opposite to that of miR-150 during lymphocyte development. Reporter assays revealed that miR-150 over-expression reduced reporter gene expression containing the wild-type c-Myb 3'-UTR, by seven fold. In miR-150-deficent B-cells, the induction of c-Myb protein upon IgM cross-linking was increased 2.6 fold as compared to controls. Together these results strongly suggest that miR-150 controls B-cell development by targeting the transcription factor c-Myb. These findings are consistent with a study where the authors ectopically expressed miR-150 in haematopoietic stem and progenitor cells and blocked B cell differentiation from the pro-B to pre-B cell stage (Zhou et al., 2007).

1.3.6.5. miR-155 in the germinal centre reaction

miR-155 has been found to be widely expressed in lymphoid organs but not in non-lymphoid organs (Thai et al., 2007). miR-155-deficient mice have reduced numbers and size of germinal centres compared to wild-type mice (Baltimore et al., 2008; Thai et al., 2007). miR-155 targets the transcription factor PU.1 in B cells which causes a loss of class switching to IgG1 (Vigorito et al., 2007). miR-155 has also been shown to target activation-induced cytidine deaminase (AID) (Dorsett et al., 2008; Teng et al., 2008). AID de-aminates cytosine residues and introduces U:G mismatches in DNA inducing class-switch recombination and somatic hypermutation (Hogenbirk et al., 2013). miR-155 then has a role in controlling the amount of mismatches and mutations that are introduced. Deregulated expression of AID can cause oncogenic transformation and Burkitt lymphoma which is characterised by AID-induced mutation and reciprocal translocation of the c-MYC oncogene (Borchert et al., 2011) miR-155 therefore has an important role in the prevention of lymphomas (Lawrie et al., 2007; Borchert et al., 2011; Deng et al., 2011).

1.3.7. Methods used to study miRNAs

Since the introduction of high through-put sequencing technologies, thousands of novel miRNAs have been identified in a relatively short period of time. The most widely used platform for miRNA sequencing is Illumina next generation sequencing (NGS). The illumina method uses a cluster generation approach, where for each single short RNA in the sample that is bound to the chip, a bridge amplification step is used to generate hundreds of identical copies which are then sequenced in parallel. This means that the fluorophore signal during the sequencing reaction is much greater, which allows very accurate base calling. The high accuracy of the sequencing allows for even short

sequences to be mapped to the genome. The advantage of miRNA sequencing over miRNA microarray is the ability to discover novel miRNA.

MiRNA microarray technologies are now also very widely used to identify the expression levels of known miRNAs in the samples of interest. This method is faster and simpler compared to miRNA sequencing as the sample preparation is less complicated and because the probes correspond to known miRNA the analysis of the data is simpler. However, the small size of miRNA does pose problems for this method because there is little choice in the sequence that can be used as a probe. These limited choices mean that obtaining equally optimal conditions for hybridisation for all probes is very difficult, meaning that the hybridisation of some miRNA is going to be more efficient than others.

The small size of miRNA therefore makes the challenges faced with both these high through-put technologies greater than that for mRNA. It is particularly important therefore that miRNA expression is also confirmed experimentally.

Quantitative real-time PCR (qPCR) is often used to confirm expression of miRNAs (Schmittgen et al., 2004; Chen et al., 2005; Raymond et al., 2005; Jiang et al., 2005). The same probe design problems encountered with miRNA microarray also exist for miRNA qPCR. However, because a much smaller number of miRNAs are analysed at a time, the conditions can be adjusted between experiments meaning that optimal conditions can be used for all miRNAs. This does however mean that comparisons between experiments cannot easily be made, but comparisons can be made between different samples for the same miRNA which is a common experimental goal. The advantage of qPCR is that it is a very quick and simple protocol and can be relatively inexpensive.

Northern analysis is a robust technique for the identification of miRNA. However, the small size of miRNA poses the same problems of probe design encountered by microarray and qPCR methods. The small size of the probes also means that they can only be labelled with a single fluorescent or radioactive label. This originally meant that miRNA northern analysis was a less sensitive method than standard mRNA northern analysis and as such required large amounts of starting RNA. However, the advent of locked nucleic acid (LNA) technology (Satoshi Obika, Daishu Nanbu, yoshiyuki Hari, Ken.ichiro Morio, Yasuko In, Toshimasa Ishida, 1997; Koshkin et al., 1998) has allowed vast improvements in sensitivity of miRNA northern analysis and also microarray and qPCR where LNA probes are now also used. The LNA probes bind with greater specificity because a methylene bridge between the 2'-O atom and the 4'-C atom 'locks' the oligonucleotide in a more open confirmation that is optimal for Watson-crick base pairing. Pairing is therefore more rapid and gives greater stability to the resulting duplex. A higher melting temperature also results, meaning that the specificity can be increased by carrying out more stringent washes than could otherwise be used. Further advances to the miRNA northern analysis protocol include chemical cross-linking using EDC rather than UV cross-linking (Pall and Hamilton, 2008). EDC cross-linking binds the 5'-phosphorylated miRNA to primary amine groups on the surface of the nylon membrane. While this 5'-end cross-linking is sufficient to hold the short miRNA strongly onto the nylon membrane it leaves most of the miRNA 'free' thus making binding of the labelled probe to the miRNA quicker and easier.

1.3.8. MiRNA target identification

The imperfect base pairing and diverse elements found to be involved in miRNA target recognition has meant that target identification has proved the most difficult element of miRNA research. Many bioinformatics target prediction algorithms have been devised,

however, the majority of these use seed sequence complementarity as the key element of prediction. Dependence on such a short sequence means that many false positive targets are predicted by the majority of these algorithms. Many of the algorithms take into account additional features such as secondary structure and the energy needed for the association. A number of the more commonly used algorithms along with their main features a listed in Table 1.1.

Algorithm	Features
TargetScan	Seed sequence, conservation, additonal 3' pairing, AU contributon
PITA	Seed sequence, secondary structure, GU wobble
miRDB	Based on support vector machine learning, seed sequence, location of target, duplex hybridisation energy
DIANA-microT	Seed sequence, additional 3' pairing, conservation, GU wobble
RNA22	Seed sequence, duplex binding energy, additonal 3' pairing
microRNA.org	Based on support vector regression, seed sequence, G:U wobble, seed mis-match, number of target sites

Table 1.1 Various features that some common target prediction algorithms use for ranking target predictions.

1.4. Summary

FDCs play a central role in driving and regulating germinal centre responses. The display of antigen on the surface of FDC as well as the production of various molecules to support plasma and memory B cell development is vital for driving and maintaining efficient humoral immune responses. FDC are therefore pivotal in host defence against external pathogens. The correct functioning of FDC is also essential for tolerance, and as such, dis-regulation of FDC can be a significant driver in autoimmune disorders. The development and function of FDC are likely to be regulated at a variety of transcriptional and post-transcriptional levels. MiRNAs are a small non-coding class of small RNA which function to post-transcriptionally control gene expression and have

been shown to act upon many processes of the immune system. However, to date, miRNAs have not been identified in FDC. The overall aim of this thesis was therefore to identify miRNAs that are involved in the development and function of FDC.

1.5. Aims

The overall aim of this thesis was to identify miRNAs with roles in the development and function of FDC.

An initial objective was to characterise an *in vivo* model of FDC de-differentiation and to identify differentially regulated miRNAs in this system.

To identify miRNAs, a subset of the samples with FDC at various stages of de-differentiation were used for miRNA microarray analysis. MiRNAs that correlated with the de-differentiation of FDC were identified and a subset selected for functional analysis.

To identify functional roles of these miRNA, loss- and gain- of function studies were carried out in the FL-YB cell line. Both growth and morphological characteristics were examined using a live cell monitoring system and the transcription of genes known to be important to FDC function was examined by qPCR.

CHAPTER 2: Materials and methods

Contents

Chapter 2: Materials and Methods

2.1. Mice and LTβR-Ig treatment

Age matched C57BL/6 mice were given a single intravenous (i.v.) injection of 100 μg of a fusion protein containing the soluble lymphotoxin β receptor (LTβR) domain linked to the Fc portion of human immunoglobulin G1, LTβR-Ig (Biogen, UK) (Force et al., 1995). After 1, 2, 3, 5, 7, 10, 14, 19, 21, 24 or 28 days four mice (two male and two female) were culled and spleens taken, portioned into three and snap frozen in liquid nitrogen.

LTβ$^{-/-}$ mice were obtained from B & K Universal Ltd (Hull, UK). The *Ltb* gene was rendered non-functional by insertion of a neomycin resistance cassette in reverse orientation in exon I (Wilhelm et al., 2002; Ngo et al., 1999). Mice were maintained on a C57BL/6 background.

2.2. Immunohistochemistry

Frozen sections of 8 μm were cut using a cryostat from tissue embedded in Tissue-Tek® O.C.T compound (VWR International Ltd, UK). Sections were fixed in acetone for 10 min, blocked with normal mouse serum and primary antibody was added to the sections (table 2.1). For light microscopy, if the primary antibody was not biotin conjugated a species specific biotin conjugated antibody was added. The biotin was then detected by alkaline phosphatase (AP) which was bound to the avidin-biotin complex (Vector Laboratories). Vector Red was used as the substrate (Vector Laboratories). The sections were then counter-stained with haematoxylin and cover-slipped. Light microscopy was carried out using a Nikon Eclipse E800 microscope (Nikon, UK). For fluorescent microscopy, after the primary antibody was added, a species specific secondary antibody with conjugated fluorophore was added. Slides were cover-slipped using DAKO fluorescent mounting media (Dako, Agilent technologies).

Target antigen	Primary-Antibody	Source	Secondary-Antibody	Source
CD35 (CR1)	Biotin Rat Anti-Mouse CD35	BD Pharmingen	-	-
Milk fat globule EGF factor 8	Purified Rat Anti-mouse	BD Pharmingen	Biotinylated mouse anti-rat	Jakson Laboratories
B220	Rat anti-mouse CD45R (B220)	Life technologies	goat anti rat alexa fluor® 594	Life Technologies
CD3	Hamster anti-mouse CD3-	BD Pharmingen	-	-

Table 2.1 Antibodies used for immunohistochemistry.

RNA methods

2.3. RNA Extraction

RNA-Bee (AMS biotechnology) was added to tissue samples which had been stored at -80°C. The tissue was homogenised and 0.2 volumes of chloroform was added and samples were shaken vigorously for 30 seconds. For RNA extraction from cultured cells, the cells were harvested by scraping from the culture plate with RNA-Bee and transferred into a 2 ml microcentrifuge tube before 0.2 volumes of chloroform was added. Samples were left on ice for 5 min before being centrifuged at 12,000x *g*, at 4°C for 20 min. The aqueous phase was removed and dispensed into a fresh 1.5 ml microcentrifuge tube. 0.7 volumes of isopropanol was added and samples left on ice for 15 min before being centrifuged at 12,000x *g* at 4°C for at least 20 min. The supernatant was then removed from the pellet and 85% cold ethanol was added. The samples were again centrifuged at 12,000x *g* for 10 min before the supernatant was once again removed. The samples were then put on ice for 10 min to dry. Nuclease-free water (Ambion, life technologies) was added and the sample vortexed. RNA was either stored short-term (< 4 weeks) at -80°C or long-term as an ethanol precipitate; 0.1

volumes of 3M NaAc and 2.5 volumes of 100% ethanol was added before storage at -80°C.

2.3.1. Recovery of RNA from precipitate

The samples were centrifuged at 12,000x *g*, at 4°C for at least 20 min before the supernatant was removed from the RNA pellet. Cold 85% ethanol was added to the samples before being centrifuged at 12,000x *g*, at 4°C for 10 min. The samples were then air-dried on ice for 10 min and an appropriate volume of nuclease-free water was added to the sample and vortexed.

2.3.2. Quantitative and qualitative analysis of RNA

To assess the quantity and quality, RNA was routinely assessed using a nanodrop spectrophotometer (Thermo scientific) according to the manufactures instructions. Sample pedestals were cleaned before each measurement and the spectrophotometer was blanked using a nuclease-free water sample. 1ul of each sample was pipetted onto the pedestal and absorbance read at a path-length of 0.05-1 mm. A rough assessment of quality and purity of the RNA samples was gained from the 280/260 nm and the 260/230 nm ratios. RNA quality was also assessed using an Agilent Bioanalyzer 2100 (Agilent technologies) using the Agilent RNA 6000 Nano kit, according to manufactures instructions.

2.3.3. DNase treatment of RNA

DNase treatment was carried out using DNA-free kit (Ambion, Life technologies). 0.1 volumes of 10X DNase 1 buffer and 1 µl of rDNase 1 was added to the RNA sample, mixed, and incubated at 37°C for 1 h. 0.1 volumes of inactivation reagent was then added, mixed and incubated at room-temperature for 2 min with occasional mixing. The samples were then centrifuged at 10,000x *g* for 2 min before the RNA was

transferred into a fresh microcentrifuge tube. Following DNase treatment the samples were precipitated by adding 0.1 volumes of 3M NaAc and 2.5 volumes of 100% ethanol and precipitated at -80°C for at least 1 h before recovery according to section 3.1.

2.4. Quantitative PCR analysis (qPCR) of gene expression

RNA was prepared according to section 2.3. RNA used to create cDNA for qPCR was always DNase treated (section 2.3.3). 2-5ug of RNA was used for cDNA synthesis using first-strand cDNA synthesis kit (GE healthcare) according the manufactures instructions. The resulting cDNA was aliquoted before being stored at -20°C. qPCR was carried out using Platinum® SYBR® Green qPCR SuperMix-UDG kit (Life technologies). 6-32 ng of cDNA was used per reaction in either 4.75 µl or 9.5 µl of nuclease-free water. 6.25 µl or 12.5 µl of Sybr Green mastermix, 0.625 µl or 1.25 µl of each forward and reverse primer (see table 2.2) was used at a concentration of 20 µM. The thermal profile was set according to the manufactures instructions for 40 cycles of amplification on a stratagene lightcycler 3000P QPCR machine. Mx Pro software (Agilent technologies) was used for analysis of the qPCR data and Ct (threshold cycle) values were normalised to either β-actin (cell experiments) or HPRT (hypoxanthine guanine phosphoribosyl transferase) (spleen samples).

2.4.1. Quantitative PCR analysis of miRNA expression

MiRNA qPCR was performed using the miScript PCR system (Qiagen) according to the manufactures protocol. miRNA qPCR probes for specific miRNA were also obtained from Qiagen and used according to the manufactures protocol.

Gene symbol	Column1	Primer sequence
Actb	Forward	TGACAGGATGCAGAAGGAGA
	Reverse	GTACTTGCGCTCAGGAGGAG
Hprt	Forward	GCAGTACAGCCCCAAAATGG
	Reverse	AACAAAGTCTGGCCTGTATCCAA
Cxcl13	Forward	ACAGACTCCGAGCTAAAGGTTG
	Reverse	AATGGGCTTCCAGAATACCG
Mfge8	Forward	TTCTGTGACTCCAGCCTGTG
	Reverse	GGAGCATGGTCCTCTCTCAG
Ccl19	Forward	GATCGCATCATCCGAAGACT
	Reverse	GAGGCCTGGTCCTCTCTTCT
Tnfsf13b	Forward	GGACCAGAGGAAACAGAACAAG
	Reverse	TTTCTGAGGTTCATTCCATTATCA
Tlr4	Forward	ACTCTGATCATGGCACTGTTCTT
	Reverse	GCTCAGATCTATGTTGGTTGA
Vcam-1	Forward	CCGGCATATACGAGTGTGAA
	Reverse	GGAGTTCGGGCGAAAAATAG
Il-15	Forward	CGTGCTCTACCTTGCAAACA
	Reverse	TCTCCTCCAGCTCCTCACAT
Ltbr	Forward	CAGAGAGCTGGAGGCTGAAC
	Reverse	TATGTAGATGTTGCCGGTGA
Ptgir	Forward	CTCCCTGCCTCTCATGATCC
	Reverse	GAGGAGGTCCCCCATCTCT
Il-6	Forward	CAAAGCCAGAGTCCTTCAGAG
	Reverse	GCCACTCCTTCTGTGACTCC
Ptgs1/2	Forward	TGTACAAGCAGTGGCAAAGG
	Reverse	TTCTGCAGCCATTTCCTTCT
Prnp	Forward	CTGAAGCATTCTGCCTTCCT
	Reverse	GCCGACATCAGTCCACATAG

Table 2.2 Primer sequences used for qPCR.

2.5. Illumina sequencing

Illumina sequencing libraries were prepared according to the Illumina small RNA v1.5 sample preparation guide. RNA (prepared according to section 2.3) from the spleens of two sex-matched mice from the same time-point were pooled in equal quantities. Libraries were prepared from 8 time points each with a female pool sample and a male pool sample to give a total of 16 samples. 5 ug of total RNA was used as input for the protocol. The 5' adapters, PCR primers and sequencing primers were designed and

provided by the sequencing service provider (Ark Genomics) sequences are provided in table 2.3. 15 cycles of PCR amplification was run for each sample. Following library preparation, 1 ul of each library was analysed by nanodrop spectrophotometer and Agilent Bioanlyzer using DNA 1000 series II chips (as section 2.3.2). Samples were then diluted to 10 nM and given to Ark Genomics to assess cDNA concentration using KAPA Library Quantification Kit (Kapa Biosystems, US). 5 fM of cDNA four samples were pooled, representing the samples that were to be loaded onto a single lane of the flow cell. Each of these pools was subject to the cluster generation protocol for single reads (Illumina), before diluting with Illumina hybridisation buffer HT1 to a concentration of 8 pM and being loaded onto the flow cell.

5' Adapter sequences	sequence
Index 1	GUUCAGAGUUCUACAGUCCGACGAUCGCUAG
Index 2	GUUCAGAGUUCUACAGUCCGACGAUCCAUGA
Index 3	GUUCAGAGUUCUACAGUCCGACGAUCUAGUC
Index 4	GUUCAGAGUUCUACAGUCCGACGAUCCGACU
RT primer	AGCATACGGCAGAAGACGAAC
PCR primer 1	AATGATACGGCGACCGACAGGTTCAGAGTTCTACAGTCCG
PCR primer 2	AGCATACGGCAGAAGACGAAC
Sequencing primer	CGACAGGTTCAGAGTTCTACAGTCCGACGATC

Table 3.3 Sequences for adapters and primers from Ark Genomics for Illumina sequencing.

2.5.1. Data analyis of Illumina sequencing data

Data were analysed and mapped to the mouse genome by Ark Genomics using Novoalign software (Novocraft Technologies). From the text files provided by Ark Genomics, any reads which did not map to a mature mouse miRNA were deleted (R code in appendix A) and data were 'collapsed' so that only one read value was obtained for each mature mouse miRNA (R code in appendix A). Separate data files for each sample were then merged into one (R code in appendix A) and trimmed mean of M-

value (TMM) normalisation factors were calculated using the bioconductor package 'edgeR' (Robinson and Oshlack, 2010; Robinson et al., 2010) (R code in appendix A). After, it was discovered that a single miRNA was making up the majority of the sample content in half of the samples, the normalisation factors were recalculated after deletion of this miRNA from the samples (R code in appendix A). After tag bias was seen in the data, normalisation was attempted within 'low read' tags and 'high read' tags separately to see if these data could be used in this way (R code in appendix A). The sequencing service ran a principal component analysis (PCA) on these data and it was found that the tag bias meant these data could not reliably be used.

2.6. Gene expression microarray analysis

2 µg of each RNA sample, prepared as in section 2.3, was provided to the sequencing service provider (Ark Genomics, UK). Samples were hybridised to Affymetrix Mouse 430 2.0 3'IVT Expression arrays (Affymetrix, UK). Raw data files in the .CEL format were provided after analysis. The .CEL files were read using the Bioconductor package "Affy" (Gautier et al., 2004) in R.

2.7. miRNA microarray analysis

RNA was prepared according to section 2.3 and 5 µg was sent to Exiqon (Denmark) for quality analysis and miRNA microarray analysis (Array 208400, 6th Gen). 2 µg was given to Ark Genomics (UK) for Affymetrix miRNA microarray analysis. Data obtained from both platforms were normalised by robust multi-array analysis using the bioconductor package ExiMiR (Sylvain Gubian, Alain Sewer, 2010) (R code in appendix B).

2.8. Web-based miRNA target prediction and gene enrichment analysis

Web-based miRNA target prediction was carried out using 4 different algorithms; DIANA-microT (http://diana.cslab.ece.ntua.gr/microT/, (Maragkakis et al., 2009)), RNA22 (http://cbcsrv.watson.ibm.com/rna22.html, (Miranda et al., 2006)), miRDB (http://mirdb.org/miRDB/, (Wang, 2008)), microRNA.org (http://www.microrna.org/microrna/home.do, (Johnnidis et al., 2008)(Betel et al., 2008)) the top 300 predictions from each programme were taken for each miRNA of interest (see section 4.2.4).

2.9. miRNA northern analysis

RNA prepared as previously described in section 2.3 was used. 2-5 µg of RNA was mixed with an equal amount of 2X TBE-urea sample buffer (Life technologies), denatured at 70°C for 3 min and loaded onto a 15% polyacrylamide TBE-urea gel (Criterion, Bio-rad, UK). The RNA was separated by gel electrophoresis at 125 V for 90 min. The RNA separation was visualised using Sybr®Gold nucleic acid dye (Life technologies). RNA was transferred to a nylon membrane, Amersham Hybond-NX (GE healthcare) by sandwiching the gel and 0.5 X-TBE soaked membranes between 0.5X-TBE soaked filter papers in a Bio-rad semi-dry transfer system at 220 mA for 1 h. RNA was cross-linked to the membrane using 1-Ethyl-3-[3-dimethylaminopropyl]carbodiimide hydrochloride (EDC)-cross linking solution according to the protocol described by (Pall and Hamilton, 2008). To prepare EDC cross-linking solution 245 µl of 12.5 M 1-methylimidazole was added to 9 ml nuclease-free water and the pH adjusted to pH 8.0 with 1 M HCl, 0.753 g of EDC (Thermo Scientific) was then added and the volume made up to 24 ml with nuclease-free water to give a working solution of 0.16 M EDC. Filter paper was pre-wetted in this

solution before the membrane was placed on top with the RNA facing up, the membrane and EDC soaked filter paper were wrapped in cling film and placed in a hybridisation oven at 60°C for 1 h. After this time the membrane was removed and washed with nuclease-free water.

For detection of specific miRNA molecules membranes were pre-hybridised with ULTRAhyb Oligo buffer (Ambion, Life technologies) at 42°C for a least two h and then incubated overnight at 42°C with complementary radiolabelled locked nucleic acid (LNA)-modified oligonucleotides in ULTRAhyb Oligo buffer (Ambion, Life technologies). LNA-modified oligonucleotides were obtained from Exiqon with LNA nucleotides placed approximately every 3 nucleotides (Table 2.5). Oligonucleotides were radiolabelled at the 5' end with ATP[γ-^{32}P] using mirVana probe and marker kit (Ambion, Life technologies) according to manufactures protocol. After removal of unbound oligonucleotide (2 x 15 minute washes in 2 X SSC, 0.1 % SDS at 42°C), membranes were wrapped in saran wrap, placed in an exposure cassette and exposed to autoradiograph film (Kodak, Biomax MS film) at -80°C in the presence of a maximum sensitivity intensifying screen (Kodak) for between 4 and 24 h. Autoradiographs were developed using a Konica SRX-101A X-ograph machine. If non-specific signals were observed, the membrane went through further wash steps with 0.1 X SSC, 0.1% SDS at increasing temperatures from 50°C until all non-specific signals were removed. Exposure times of up to 8 d were used to obtain optimum signal. To completely remove bound LNA-modified oligonucleotides membranes were washed in boiling 0.1 X SSC and checked for residual signal by exposure to autoradiograph film. Membranes were then re-probed as appropriate for other miRNA of interest or U6-snRNA or 5s rRNA as loading controls.

2.9.1. Phosphorimager quantification

To quantitate hybridised radiolabelled nucleic acid after miRNA northern analysis, membranes were exposed to phosphorimager screens at room temperature for the required length of time. For quantification screens were scanned using a Typhoon FLA 7000 system (GE healthcare life sciences) and quantification was performed using ImageQuant TL software (GE healthcare life sciences).

Cell Culture Techniques

2.10. FL-YB cell culture

FL-YB cells were kindly provided by Hitoshi Ohmori (Okayama University, Japan)(Nishikawa et al., 2006). Culture medium was prepared as follows; 1:1 ratio of low glucose Dulbecco's Modified Eagle Medium (Gibco, life technologies) and RPMI 1640 (Gibco, life technologies), 10 % heat-inactivated foetal bovine serum (FBS) (Gibco, life technologies), 2-Mercaptoethanol at 50 μM, 1 X penicillin:streptomycin. Cells were routinely cultured in the presence of 5 ng/ml recombinant murine TNFα (Peprotech, UK) in T75 tissue culture treated flasks (Sigma-aldrich) at a density of ~5x 10^4 to ~1x 10^5 cells/ml and passaged every 3 days at 37°C, 5% Co_2. To subculture the cells were washed 2-3 times with sterile 1 X PBS and 2 ml of 1 X TrypLE™ Express (Gibco, life technologies) was added before incubation at 37°C for 2 min. Complete culture media (8 ml)was then added, and a cell suspension created and transferred to a sterile conical centrifuge tube and centrifuged at 600x *g* for 5 min at 4°C. The cells were re-suspended in fresh culture medium as above.

2.11. Raw 264.7 cells

The macrophage cell line Raw 264.7 (Raschke et al., 1978) was cultured in RPMI 1640 (Gibco, life technologies) with 5% FBS (Gibco, life technologies) and 1 X penicillin:streptomycin in 10 cm square bacteriological plates (Sterilin, Thermo scientific). Cells were passaged every 3-4 days and detached by washing with a blunt 18 gauge needle in complete media to give a single cell suspension. 70-80% of the cell suspension was removed and replaced with fresh medium.

2.12. Cell stimulation experiments

FL-YB cells were plated at a density of 5x 10^4 cells/well in a 6-well tissue culture treated plate (Corning life sciences). To each well, one of the treatment options below was added. Cells were harvested 96 h later in RNA-Bee.

1	No supplements
2	recombinant murine TNFα (Peprotech) at 5 ng/ml
3	Recombinant murine TNFα at 5 ng/ml and agonistic LTβR MAb at 2.5 µg/ml (AbD serotec)
4	Recombinant murine TNFα at 5 ng/ml and recombinant mouse IL-4 at 5 ng/ml (R&D systems)

Table 2.4 Treatments used to stimulate FL-YB cells.

2.13. xCELLigence analysis

To perform real-time analysis of cell growth and spreading, 50 ul-100 µl of media was dispensed into each well of a 96-well E-view plate (ACEA Biosciences). A background sweep was performed on the xCELLigence SP instrument (Roche) using RTCA software (Bucher biotec) which sets this baseline value to a 'Cell Index' of 0. Cells and treatments were then added as appropriate in 100 µl of media. Cell index readings were taken every 15 min for the first ~40 h then every 30 min thereafter.

2.14. CyQUANT direct cell proliferation assay

The CyQUANT Direct Cell Proliferation Assay Kit (Life technologies) was used to assess cell viability according to the manufacturer's instructions. To measure cell viability after IL-4 treatment FL-YB cells were plated into 96-well plates at a density of 4,000 cells/well with 5ng/ml TNFα and/or 5ng/ml IL-4, the CyQUANT assays were carried out in the plates at the appropriate time-points after plating. To measure cell viability after loss or overexpression of specific miRNA, FL-YB cells were plated out at 4,000 cells/well and incubated at 37°C overnight before the medium was replaced with antibiotic-free medium containing the specific miRNA mimic or inhibitor and lipofectamine. Cells were transfected for 4 h before medium was replaced with complete media and the cyQUANT assays were again carried out directly in the plate after the appropriate length of time.

2.15. Live cell imaging

FL-YB cells were plated in a 6-well plate at a density of 6x 10^5 cells/well and treated with either TNFα at 5 ng/ml alone or in combination with IL-4 at 5 ng/ml. The plate was then placed into a plate holder in the chamber of a Zeiss live cell axio observer (Carl Zeiss) and then using Zen software, images were collected every 5 to 30 min in over a 5 d period.

2.16. miRNA gain- and loss-of-function experiments

FL-YB cells were transfected using lipofectamine 2000 (Life technologies) according to the manufactures protocol. Briefly, FL-YB cells were plated in 6-well or 96-well tissue culture plates at a density of 4x 10^5 cells/ml and incubated overnight with 5ng/ml TNFα. The media was then removed and replaced with 1 ml for (6-well) or 50 µl (for 96 well) of complete media without antibiotics or TNFα. Lipofectamine 2000 (2.5µl for

every 1μg of nucleic acid) was diluted in opti-MEM (Life technologies) and incubated at room temperature for 5 min and the nucleic acid to be transfected was diluted in opti-MEM. An equal volume of diluted Lipofectamine was added to each tube of diluted nucleic acid and incubated at room temperature for at least 30 min. An appropriate volume of transfection mixture was added to each well of cells and incubated at 37°C for 4 h before the transfection media was diluted with 2 X volumes of complete media and incubated for a further 2 h before being replaced with complete media plus 5 ng/ml TNFα as appropriate.

2.16.1. miRNA loss-of-function

miRNA expression was inhibited by transfection with LNA-modified DNA oligonucleotide (Exiqon) with complementary sequence to the miRNA being targeted (Table 2.5) at a concentration of 150nM.

miRNA target	sequence
mmu-miR-2137	CT+CCC+TGG+GGC+TCC+CGC+CGG+C
mmu-miR-138-5p	C+GGC+CTG+ATT+CAC+AAC+ACC+AGCT
mmu-miR-100-5p	C+ACA+AGT+TCG+GAT+CTA+CGG+GTT

Table 2.5 Sequences of LNA-modified oligonucleotides used for northern analysis and loss-of-function experiments.

2.16.2. miRNA gain-of-function

miRNA overexpression was achieved by transfection of mirVana miRNA mimic (Ambion, life technologies) at a concentration of 30nM. mirVana miRNA mimics consist of a stem-loop structure to mimic a natural pre-miRNA with a chemical modification to ensure incorporation of the desired mature miRNA sequence into the RNA-induced silencing complex (sequences in table 2.6 below)

Target miRNA	Mature miRNA sequence
mmu-miR-100-5p	AACCCGUAGAUCCGAACUUGUG
mmu-miR-2137	GCCGGCGGGAGCCCCAGGGAG

Table 2.6 The functional sequence of miRNA mimics used in gain-of-function experiments.

CHAPTER 3: Characterisation of a model of FDC de-differentiation

Contents

Chapter 3. Characterisation of a model of FDC de-differentiation

3.1. Introduction

A lack of genuinely specific histological markers for FDCs as well as the close association of FDCs with germinal centre B cells has meant that isolation of a pure FDC population has proven to be very difficult (Munoz-Fernandez et al. 2006; Aguzzi & Nike J Krautler 2010). This difficulty is compounded by the dependency of FDCs on signals from their microenvironment to keep them in their mature, fully functional state (Nishikawa et al. 2006; Malhotra et al. 2012). To avoid the problems associated with FDC isolation, an *in vivo* FDC de-differentiation protocol (Mackay & Jeffrey L. Browning 1998; Mabbott et al. 2000) was used to enable the identification of genes and miRNAs relevant to FDC differentiation.

LTβR-blockade by treatment with LTβR fusion proteins (LTβR-Ig) was first described by Rennert et al. (1996) to investigate the role of lymphotoxin (LT) signalling in immune system development. Introduction of LTβR-Ig into murine embryonic circulation by injection of pregnant mice abrogated the development of lymph nodes and caused disruption of splenic microarchitecture in the developing mice. Both TNF and lymphotoxin are needed for the development of a mature FDC network and constant signalling through the LTβR on FDCs is needed for the maintenance of a mature FDC network (Matsumoto et al. 1997; D. D. Chaplin & Y. Fu 1998). The introduction of LTβR-Ig blocks signalling through the LTβR on FDCs and causes rapid de-differentiation of the FDC network (Mackay & Jeffrey L. Browning 1998; Mabbott et al. 2000).

$LT\beta^{-/-}$ mice lack B cell follicles and mature follicular dendritic cells, as well as marginal zone macrophages (Koni et al. 1997). These mice also display disrupted T/ B cell boundaries in the splenic white pulp, due to reduced levels of the chemokine CXCL13

(Ngo et al. 1999). The chemokine CXCL13 is expressed by mature FDCs. Förster et al. (1996) demonstrated that CXCL13 is important for correct segregation and arrangement of CXCR5 expressing B-cells in the spleen and later Ansel et al. (2000) found this to be the same in the lymph nodes. It was found that CXCL13 induced increased $LT\alpha_1\beta_2$ expression on naïve B-cells which then interacts with the LTβR expressed on FDCs, promoting FDC maturation and hence completing a positive feed-back loop for CXCL13 (Ansel et al. 2000). Unlike $LT\alpha^{-/-}$ mice, $LT\beta^{-/-}$ mice have cervical and mesenteric lymph nodes, although these lack FDCs, suggesting a role for the soluble $LT\alpha_3$ complexes in the development of these lymph nodes (Koni et al. 1997).

Follicular dendritic cells express various surface molecules which are often used to identify the location of mature FDCs within secondary lymphoid organs. In 2008 Kranich and colleagues (Kranich et al. 2008) showed that the mAb FDC-M1 recognises Mfge8 (milk fat globule-EGF factor 8 protein) and that FDCs are the major producer of Mfge8 in the spleen. The FDC-M1 mAb has also been found to stain tingible-body macrophages (Kosco-Vilbois, 2003). FDC-derived Mfge8 binds to phosphatidylserine on apoptotic B-cells which in turn is bound by membrane bound integrin on tingible-body macrophages allowing engulfment of the apoptotic B-cells by the tingible-body macrophages (Kranich et al. 2008).

One of the primary functions of FDCs is to trap and retain intact antigen in the form of immune complexes (ICs) on the cell surface where it is displayed to germinal centre B cells aiding in the selection of B cell expressing high affinity antibodies (Fütterer et al. 1998; Li & Choi 2002). Antibodies to the complement receptors CD21 (CR2) and CD35 (CR1) recognise FDCs in both primary and secondary follicles (Allen & Jason G. Cyster 2008). Cell surface CD35 and CD21 expressed by FDCs mediates trapping of complement opsonised antigen by FDCs (Yoshida et al. 1993).

3.2. Aims

The objective here was to use LTβR-Ig treatment to de-differentiate FDCs *in vivo*. Spleen samples were taken at different time points after LTβR-Ig treatment and assessed for the extent of FDC de-differentiation as well as for changes in other cell types that could potentially be influenced by the LTβR-Ig treatment. Data from this analysis was then used to select the most appropriate spleen samples for subsequent miRNA profiling.

3.3. Results

3.3.1. *In vivo* LTβR-Ig treatment causes rapid FDC de-differentiation in the spleen

LTβR signalling blockade leads to rapid de-differentiation of FDCs in secondary lymphoid organs including the spleen. In order to generate material containing FDCs at various stages of de-differentiation, age and sex-matched C57BL/6 mice were given a single intraperitoneal injection of 100 μg of LTβR-Ig (Force et al. 1995). Spleen tissue from four treated mice (two male and two female) was collected at 1, 2, 3, 5, 7, 10, 14, 19, 21, 24 and 28 days following injection, and from four untreated control mice. For comparison, spleens were also collected from four $LT\beta^{-/-}$ mice which lack mature FDCs (Koni et al. 1997; Ngo et al. 1999). In order to assess the degree of FDC de-differentiation, a third of each spleen was snap frozen and processed for histology. Sections of spleens were prepared and immunostained for the expression of typical FDC markers (CD35 and MFGE8) (Kranich et al. 2008). Immunostained sections were examined by light microscopy, and representative images were collected (summarised in Table 3.1). Immunohistochemical (IHC) analysis revealed the presence of extensive $CD35^{+}$ FDC networks and MFGE8 staining in the sections prepared from spleens of control mice (Figure 3.1). As early as two days following LTβR-Ig treatment there was a clear reduction in CD35 and MFGE8 staining. Analysis of spleen sections from other time points in this experiment revealed that by day three following LTβR-Ig treatment, CD35 and Mfge8 immunostaining was either completely absent or greatly reduced. There was no evidence of $CD35^{+}$ FDC networks or MFGE8 immunostaining in the spleens collected from mice between 3 days and 21 days after treatment, (the spleens collected 21 days following treatment showed wide variance). There was evidence of low levels of CD35 from 21 days following LTβR-Ig treatment, but even after 28 days only minimal CD35 staining is seen. From the later time points, Mfge8 staining was only

observed in two animals at 21 days after treatment. As expected, no CD35 or MFGE8 was observed in the LTβ$^{-/-}$ mice in line with previous findings (Kranich et al. 2008).

Group	No. of CD35 positive spleens	No. of MFGE8 positive spleens
Untreated	4/4	4/4
Day 1	4/4	4/4
Day 2	4/4	3/4
Day 3	2/4	0/4
Day 5	0/4	0/4
Day 7	0/4	0/4
Day 10	1/4	1/4
Day 14	0/4	0/4
Day 19	0/4	0/4
Day 21	2/4	2/4
Day 24	2/4	0/4
Day 28	2/4	0/4
LTβ$^{\Delta/\Delta}$	0/4	0/4

Table 3.1 Summary of immunostaining for mature FDC markers in untreated, LTβR-Ig treated and LTβ$^{\Delta/\Delta}$ mice. In order to assess the degree of de-differentiation at different time points following LTβR-Ig treatment, a portion of each spleen was fixed and processed for histology. Sections were immunostained for the expression of the typical FDC markers CD35 and MFGE8. Immunostained sections were examined by light microscopy, and representative images were collected. The table shows a summary of the number of spleens (out of four at each time point) that were positive for CD35 or Mfge8 staining.

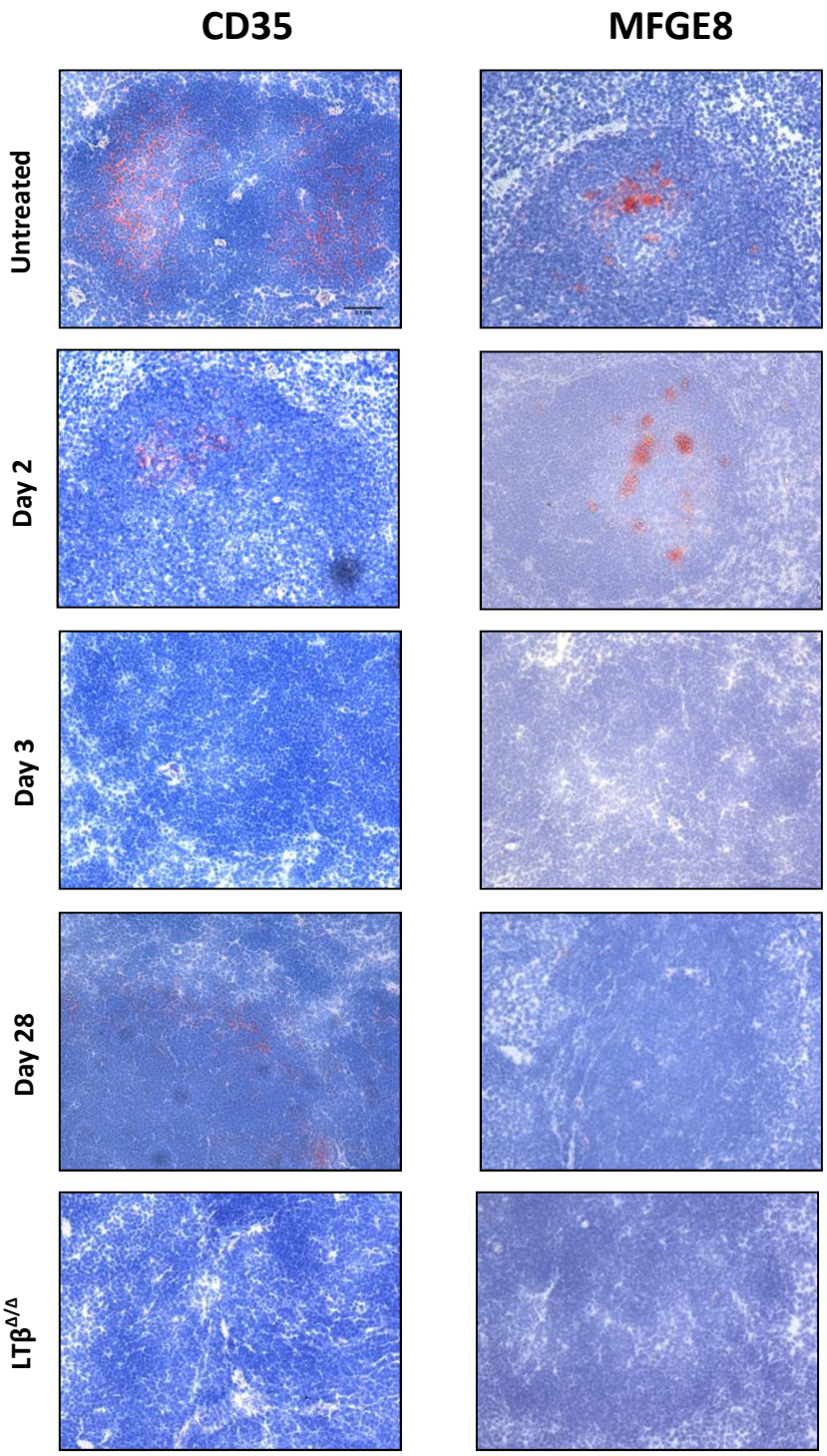

Figure 3.1 Loss of follicular dendritic cell markers following LTβR-Ig treatment. IHC analysis of CD35 and Mfge8 expressed by FDCs (red). The untreated spleen shows extensive follicular dendritic cell networks and MFGE8 immunostaining. CD35 staining reveals a dramatic reduction in the FDC network by day 2 and a complete loss of $CD35^{+}$ FDCs by day 3. MFGE8 is also lost between day 2 and 3. A small amount of CD35 staining is seen between day 21 and 28 but no MFGE8 staining is observed. $LT\beta^{-/-}$ mice lacked CD35 and Mfge8 positive FDCs. Sections counterstained by haematoxylin (blue). Scale bar is 100μm.

3.3.2 Disruption of splenic microarchitecture following de-differentiation of follicular dendritic cells

FDCs play an important role in the maintenance of splenic microarchitecture through expression of the chemokine CXCL13 (Alimzhanov et al. 1997; Ettinger et al. 1996). To determine the extent and timing of microarchitecture disruption seen after LTβR-Ig treatment in this experiment, the distribution of T and B cells was compared by IHC. Cryosections were co-stained with MAb for B220 (CD45R) to detect B cells and anti-CD3 to detect T cells. Sections were analysed by confocal microscopy and representative images were collected. Spleens from untreated mice showed the expected distinct B cell follicles around the T cell area (Figure 3.2a). In the sections prepared from the spleens collected two days after LTβR-Ig treatment it is evident that some B cells (arrows) were beginning to migrate out of the B cell follicles and encroach on the T cell area. This migration of B cells out of the follicles appears to progress over time following LTβR-Ig treatment. In spleen sections collected fourteen days following LTβR-Ig treatment the B cells appear to entirely surround the T cell area in a ring rather than in discrete follicles. The disruption of the B cell follicles continues to progress right up to the final time point at 28 days after LTβR-Ig treatment, where there is little segregation of B cells from T cells. As seen in Figure 3.2f the $LT\beta^{-/-}$ mice clearly lack proper segregation of B cells and T cells. These observations suggest that although the return of some CD35 staining is observed from 21 days after treatment, these $CD35^{+}$ FDCs are unlikely to secrete sufficient quantities of CXCL13 to have an attractive effect on the B-cells.

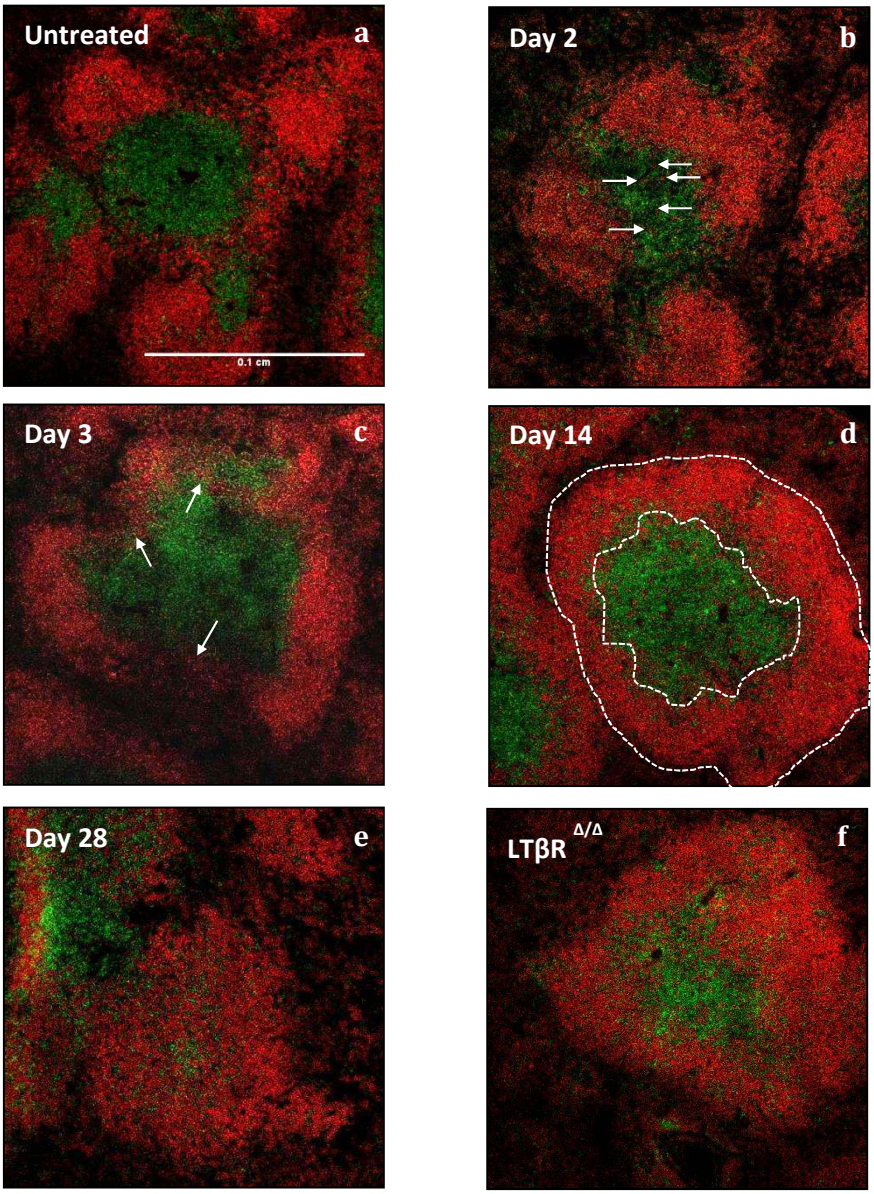

Figure 3.2 Splenic microarchitecture is disrupted following LTβR-Ig treatment. IHC for B cells (B220 positive cells, red) and CD3 marking T cells (Green). The untreated spleen shows the B cells in distinct follicular areas at points around the T cell zone. B cells appear to progressively disperse from the B cell follicles (arrows) to surround (dashed lines) and eventually invade the T cell area (day 28). In $LT\beta^{-/-}$ mice there again seems to be only modest segregation of the B and T cells. Scale bar is 100µm.

3.3.3 The effect of LTβR-blockade on gene expression in the spleen

To gain a more global picture of the changes that occur in the spleen following LTβR-Ig treatment, gene expression was monitored by microarray analysis (Affymetrix mouse genome MOE430 2.0 expression arrays). Immunohistochemistry data (Figure 3.1) was used to select time points for microarray analysis. 1.) Spleens collected from mice two days after the LTβR-Ig treatment. At this time point the immunostaining revealed that the mice still had CD35 positive FDC networks but they were much reduced in size and minimal Mfge8 staining was seen indicating the FDCs are considerably less mature than in the untreated spleen samples. 2.) Spleen samples collected fourteen days after LTβR-Ig treatment were also chosen as no CD35 or MFGE8 staining was seen in any of these spleen sections indicating there are no mature FDCs present in these spleen samples. 3.) For comparison, spleens from $LT\beta^{-/-}$ mice which lack mature FDCs were also included. 4.) Spleen tissue from untreated control mice which were seen to contain large, mature FDC networks. RNA was prepared from a portion of the spleens from 4 mice from each of the four selected groups and pooled so that there were two sex matched pools of two from each group. These pooled RNA samples were profiled for gene expression using Affymetrix Mouse 430 2.0 3'IVT Expression arrays. The resulting data sets were normalised using robust microarray analysis, or RMA (Irizarry 2003) and the expression values averaged within each group. To identify transcripts with expression profiles that correlated with a loss of FDCs, the fold-change in expression value was calculated between the untreated group and the other three groups for each gene. Genes showing the largest fold-changes between the spleens collected 14 days after LTβR-Ig treatment and the untreated spleens are shown in Table 3.2. Many of the genes showing decreased levels as a result of the LTβR-Ig treatment have previously been described to be highly expressed in FDCs as indicated in the references column of Table 3.2. To assess the potential biological consequences of these gene expression

changes *in silico* gene enrichment analysis was undertaken. The 50 genes that show the largest increase and the largest decrease in the day 14 post treatment spleens compared to the untreated spleens were used as input for the functional analysis that was carried out using the web-based software ToppFun (Chen et al. 2009). This analysis showed that the genes with decreased expression upon LTβR-Ig treatment were enriched for genes involved in immune and inflammatory responses as well as those involved in cell adhesion and motility. The genes found to have increased expression levels following LTβR-Ig treatment were enriched for genes involved in erythrocyte development and homeostasis as well as general homeostatic processes. Comparing expression in untreated and $LT\beta^{\Delta/\Delta}$ mice revealed 27 genes that were in the top 50 decreased, and 14 genes that were in the top 50 increased 14 days following LTβR-Ig treatment (Table 3.3). The 27 genes showing a decrease in expression again were enriched for genes that have functions in the immune response and cell movement. This indicates that the LTβR-Ig treatment is having an negative effect on the white pulp functions within the spleen, but the functions of the red pulp are largely unaffected.

		Fold change in gene expression vs.			
	Gene	Day 2	Day 14	$LT\beta^{\Delta/\Delta}$	Reference
Genes decreased following LTβR-Ig treatment	***Mfge8***	0.504	0.212	0.172	
	Ttn	0.393	0.240	0.168	(Kranich et al. 2008)
	Ryr3	0.390	0.258	0.218	
	Bst1	0.497	0.260	0.180	
	Cxcl13	0.664	0.269	0.105	(Ngo et al. 1999)
	Dsc3	0.552	0.290	0.226	(Gunn et al. 1998)
	Clec4g	0.352	0.297	0.207	(Huber et al. 2005)
	Bex6	0.822	0.299	0.418	
	Il22ra2	0.318	0.302	0.308	
	Sulf1	0.563	0.307	0.178	(Ota et al. 2011)
	S1pr3	0.571	0.308	0.204	
	Dsc2	0.517	0.311	0.296	(Zindl et al. 2009)
	Clu	0.636	0.316	0.184	(Malhotra et al. 2012)
	Prg3	0.678	0.327	0.287	(Huber et al. 2005)
	Cilp	0.693	0.354	0.155	
	Pla2g2d	0.609	0.355	0.078	(Wilke et al. 2010)
	Timd4	0.680	0.357	0.179	Similar role to Mfge8
	Gpm6b	0.649	0.363	0.321	
	Enpp2	0.698	0.366	0.158	(Huber et al. 2005)
	Dclk1	0.651	0.378	0.238	(Wilke et al. 2010; Huber et al.
Genes increased following LTβR-Ig treatment	***Tmem56***	2.01	3.08	2.57	
	AI661323	1.29	2.78	1.59	
	Car1	1.76	2.68	2.76	
	Rhd	1.28	2.64	1.52	
	Asns	1.70	2.64	2.02	
	Cldn13	1.37	2.62	1.66	
	Epb4.2	1.08	2.61	1.35	
	Apol8	1.29	2.60	1.60	
	Klf1	1.54	2.57	1.74	
	Kel	1.18	2.56	1.73	
	Gypa	1.22	2.53	1.16	
	Pdia2	1.86	2.51	1.58	
	Rhag	1.22	2.51	1.72	
	Ypel4	0.97	2.49	1.41	
	Ccl8	1.02	2.48	2.09	
	Ermap	1.39	2.47	1.81	
	Slc38a5	1.38	2.46	1.94	
	Sox6	1.17	2.46	1.55	
	Tal1	1.36	2.45	1.84	
	Fam132a	1.73	2.45	2.13	

Table 3.2 Top 20 differentially regulated genes at Day 14 following LTβR-Ig treatment. Gene expression microarray data from LTβR-Ig treated and $LT\beta^{-/-}$ mouse spleen tissue. The fold change from untreated mice for the 20 genes with expression levels that were most decreased 14 days following LTβR-Ig treatment are shown at the top of the table. The 20 genes with expression levels that were most increased 14 days following LTβR-Ig treatment compared to untreated samples are shown at the bottom of the table. References indicate those genes that have previously been described to be expressed by FDCs.

3.3.4 Confirmation of microarray predicted gene expression changes

To confirm the reliability of the microarray data set, quantitative real-time PCR (qPCR) was carried out for some of the genes that showed altered expression levels as a result of FDC depletion. Two genes known to be highly expressed by FDCs, *Mfge8* and *Cxcl13*, were selected for measurment by qPCR. RNA prepared from the same tissues used for microarray analysis was also used to generate cDNA for qPCR analysis. In addition, qPCR was also performed on cDNA generated from spleens selected at all other time points following LTβR-Ig treatment. As can be seen in Figure 3.4 the relative levels of gene expression between the groups agree very well for both *Cxcl13* and *Mfge8* when comparing the microarray and qPCR data. Furthermore, the time points after LTβR-Ig treatment that were not analysed by microarray showed a trend that fitted very well with the gene expression levels seen at the day 2 and day 14 time points. The only exception to the general trend of down regulation of both *Cxcl13* and *Mfge8* was seen for two of the spleens collected 21 days following LTβR-Ig treatment. The spleens from this day 21 time point were seen to have a wide variation in the expression levels of *Mfge8* and *Cxcl13* mRNA for measurements by qPCR and protein levels by IHC for Mfge8, as well as in the disruption of splenic B cell follicles. This data suggests a large variation in the levels of CXCL13 between the animals at that time point.

Gene symbol	Fold change D2	Fold change D14	Fold change LTb$^{-/-}$
Mfge8	-1.99	-4.71	-5.82
Ttn	-2.55	-4.17	-5.96
Ryr3	-2.56	-3.89	-4.59
S1pr3	-1.88	-3.87	-6.63
Bst1	-2.01	-3.84	-5.54
Cxcl13	-1.5	-3.72	-9.7
Dsc2	-2.05	-3.59	-3.82
Dsc3	-1.81	-3.45	-4.42
Clec4g	-2.84	-3.37	-4.84
Il22ra2	-3.14	-3.31	-3.25
Sulf1	-1.76	-3.25	-5.72
Clu	-1.56	-3.14	-5.39
Prg3	-1.47	-3.06	-3.48
Pla2g2d	-1.64	-2.87	-12.83
Cilp	-1.44	-2.82	-6.43
Timd4	-1.47	-2.8	-5.6
Gpm6b	-1.56	-2.77	-3.14
Enpp2	-1.43	-2.73	-6.33
Dclk1	-1.54	-2.64	-4.18
Synpo2	-1.65	-2.44	-2.8
Ube2e2	-1.38	-2.35	-2.83
Madcam1	-1.46	-2.14	-2.75
Gpr126	-1.42	-2.13	-2.78
Parm1	-1.43	-2.11	-2.87
Slc36a2	-1.27	-2.03	-2.89
C2	-1.51	-2	-2.84
Cfb	-1.51	-2	-2.84
Fam59a	1.5	2.13	1.92
Gata1	1.36	2.17	1.84
Abcg4	1.69	2.24	1.93
Trfr2	1.64	2.24	2.21
Add2	1.22	2.28	1.8
Tal1	1.36	2.45	1.84
Slc38a5	1.39	2.46	1.94
Ermap	1.39	2.47	1.81
Ccl8	1.03	2.5	2.1
Klf1	1.54	2.57	1.74
Fam132a	1.76	2.58	2.26
Car1	1.76	2.68	2.76
Asns	1.72	2.78	2.06
Tmem56	2.02	3.12	2.6

Table 3.3 Genes regulated in LTβR-Ig treated and LTβ$^{-/-}$ mice. The table shows gene expression microarray data from which the fold change in expression value is calculated by dividing the LTβR-Ig treated or LTβ$^{-/-}$ expression value by the untreated expression value. 27 genes that were in the top 50 decreased upon LTβR-Ig treatment and in LTβ$^{-/-}$ mice are shown at the top of the table marked in red. Those genes that were identified to be in the top 50 increased in the LTβR-Ig treated and LTβ$^{-/-}$ spleens compared to the untreated spleens are shown at the bottom of the table marked in blue.

Fibroblastic reticular cells (FRC) are the main stromal cell population situated within the T cell area and it has previously been reported that these cells also express the LTβR (Ngo et al. 1999). To evaluate whether the FRC were also de-differentiated following LTβR-Ig treatment we looked at the expression of *Ccl19*. This chemokine is expressed by FRC and attracts CCR7 expressing T cells into the parafollicular areas. The microarray data suggests that the expression levels of *Ccl19* dropped to ~70% in the spleens collected 14 days following LTβR-Ig treatment compared to untreated spleens. qPCR analysis of *Ccl19* expression levels (Figure 3.4) suggested a slight increase immediately following LTβR-Ig treatment followed by a return to levels similar to those seen in the untreated mice by day 5. The *Ccl19* gene expression levels seen in the spleens collected from the $LT\beta^{-/-}$ mice were seen to be half that seen in the untreated mice as measured by microarray and the qPCR data suggested a similar if not slightly more severe decrease in the $LT\beta^{-/-}$ mice. Taken together it is likely that mature FRC are not affected as much as that of the FDC following LTβR-Ig treatment.

3.3.5 The effect of the LTβR-Ig treatment on B and T lymphocytes

The major cell types in the splenic white pulp are the B and T lymphocytes which, as illustrated in Figure 3.2, have a disrupted localisation in LTβR-Ig treated mice. However, gene expression microarray data reveals expression levels for typical B and T cell markers was unchanged in the spleens of LTβR-Ig treated mice compared to untreated mice (Figure 3.5). This indicates that the segregation but not the proportion of B and T cells have been significantly affected by LTβR-Ig treatment. Further, slight changes in the $LT\beta^{-/-}$ mice compared to the untreated mice suggests that the lack of LTβR signalling through development causes some more severe changes to other immunological cell types compared to the transient blockade.

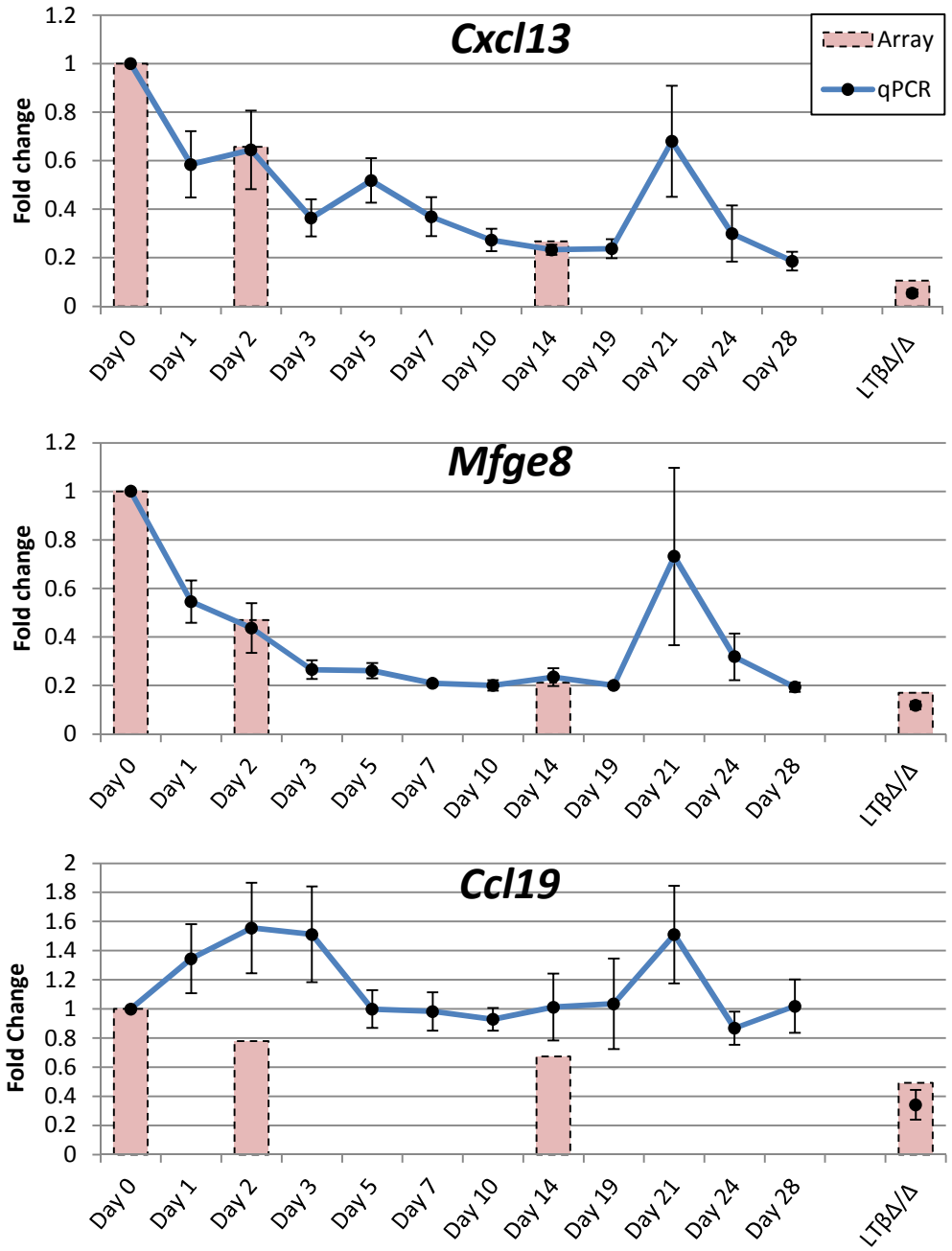

Figure 3.3 Microarray data for FDC and FRC genes is confirmed by qPCR. RNA extracted from spleen tissue from each of the four animals at each time point following LTβR-Ig treatment and from the LTβ$^{-/-}$ mice, was used to generate cDNA for qPCR analysis of FDC genes *Cxcl13* and *Mfge8* and FRC gene *Ccl19*. The expression levels from the microarray data from the same samples is shown by light red bars in the background. n=4 for each time point.

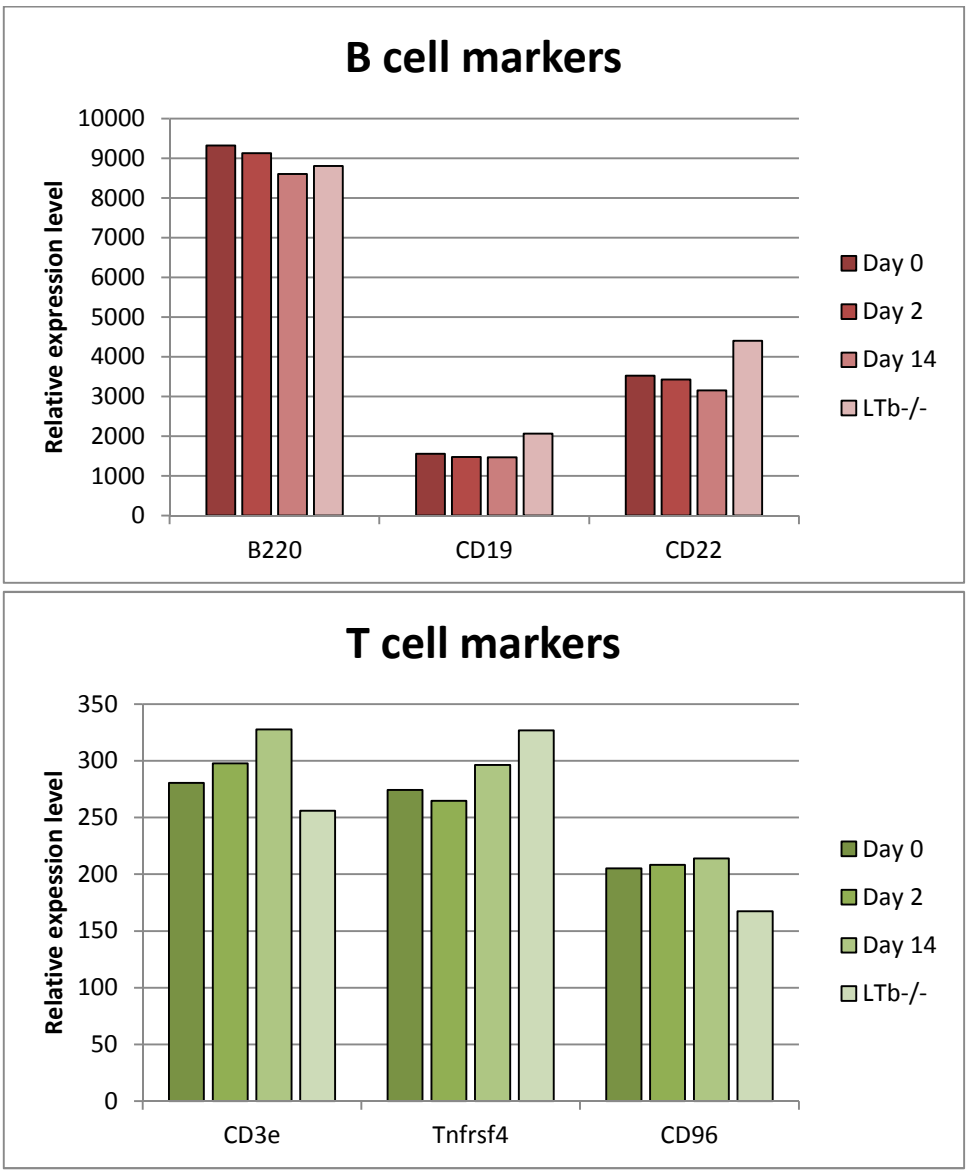

Figure 3.4 Expression levels of typical B cell and T cell marker genes are largely unchanged after LTβR-Ig treatment. Gene expression microarray data from untreated (Day 0) spleens, spleens from mice 2 days and 14 days after LTβR-Ig treatment and spleens from $LT\beta^{-/-}$ mice. Although it was shown that B cells migrate out of their normal follicles following LTβR-Ig treatment (figure 3.2), the spread seen between the groups for these typical marker genes of B and T cells suggest the actual numbers of T and B cells do not change following LTβR-Ig treatment. n=4

3.4 Discussion

Treatment of mice with LTβR-Ig blocks LTβR-signalling and causes rapid de-differentiation of FDCs. Data presented in this chapter characterised the effect of this treatment on FDCs up to 28 days following injection. This characterisation enabled the identification of spleen tissue with FDC networks at different stages of de-differentiation. Gene expression microarray data from these spleen samples with full, small or absent FDC networks indicated that gene transcripts that are known to be highly expressed in FDCs could readily be identified. This method of identification of FDC transcripts is important as it gives us the opportunity to study FDCs without isolation which has proven to be difficult and sometimes inaccurate because of the high dependency of FDCs on signalling from their microenvironment.

The spleens collected from mice 21 days after LTβR-Ig injection showed wide diversity as indicated in Figure 3.3. It is not clear why such diversity in terms of the FDC network was seen between the animals. It could have been due to a number of factors including variation in the efficiency of LTβR-Ig injection, an unusually rapid clearance of the LTβR-Ig injected.

The CD35 staining (figure 3.1) for mature FDC networks showed a small amount of staining returning at the two latest time points looked at, day 24 and 28. The pattern of staining in most of the sections is not typical of fully mature FDC networks. It is likely that it is the case that fully mature FDC networks have not formed at these time points. From the B and T cell staining it is also seen that the microarchitecture of the white pulp in the spleen is still disrupted which would account for the more spread out appearance of the CD35 staining seen in some of the sections at these later time points. It has been proposed that FDCs arise from perivascular precursors (Krautler et al., 2012), which within the white pulp of the spleen are largely located within the

marginal zone. It is possible that the CD35 staining that is seen at these later time points is from premature FDCs that could be located in the re-forming marginal zone. However without staining for marginal zone markers it is impossible to tell if the CD35 staining is in this area, or if the microarchitecture is still too disrupted to define the different area.

A comparison of the gene expression array data from the untreated spleen tissue and the spleen tissue collected 14 days after LTβR-Ig treatment, or spleen tissue from LTβR$^{-/-}$ mice enabled the identification of many genes that have been previously described to be highly expressed in FDCs (Table 3.2). It is to be noted that some genes identified in this way have not previously been described to be highly expressed in FDCs. Some of these genes have roles in the immune response such as proteoglycan 3 which is highly expressed by eosinophils (Tang et al., 2009) , and phospholipase A2 which is an effector molecule of T-reg cells (Von Allmen et al., 2009). However, the majority of these genes are fairly ubiquitously expressed genes such as titin (involved in muscle elasticity (Minajeva et al., 2001)) and Sulf1 (involved in signalling transduction (Dhoot et al., 2001)), and are therefore unlikely to be closely related to the effect on the follicular dendritic cells.

Although the B and T cell staining showed extensive disruption of the microarchitecture and these two cell types. Microarray data showed that the gene expression levels for general markers of B and T cells were changed very little between the four groups. This implies no significant change in the numbers of B and T cells present in the untreated, LTβR-Ig treated, or LTβ$^{-/-}$ spleen tissue.

Overall data in this chapter show the efficacy of using spleen tissue from LTβR-Ig treated animals to identify LTβR-dependent transcripts expressed by FDCs. Data from

this chapter will be used in the next chapter to select LTβR-Ig-treated samples for miRNA profiling to identify miRNAs likely to be expressed by FDCs.

CHAPTER 4: The effect of LTβR blockade on microRNA expression in the murine spleen

Contents

Chapter 4: The effect of LTβR blockade on microRNA expression in the murine spleen

4.1. Introduction

MiRNAs regulate many aspects of the immune system and development. To date there are no published data describing miRNAs expressed by FDCs. Two papers however have described how miRNA expression in B-cells isolated from non-Hodgkin's lymphomas can be influenced by direct cell contact with FDCs. The first of these papers (Lwin et al., 2010) showed that co-culture of non-Hodgkin's B-cell lymphoma cells with human FDC cells induced miR-181a expression in the B cells which targeted Bim, causing increased cell survival. This fits with data showing (Ramkissoon et al., 2006) that miR-181 is expressed at higher levels in leukaemia B cell lines when compared to normal B cell lines. The second paper (Lin et al., 2011) showed that in similar experiments FDC-B cell contact induced the expression of the miR-30 family in B cells causing a decrease in Bcl6 expression, and a decrease in the expression of the miRNA let-7a causing an increase in Prdm1 expression. These papers clearly show that miRNAs play an important role in finite regulation of the humoral immune response. Differential expression of miRNAs controlling the development and maturation of different B cell lineages have also been described (reviewed by Davidson-Moncada et al. 2010).

The identification of miRNAs that play a role in the differentiation or functioning of FDCs could lead us to the identification of the genes and pathways that regulate those processes. As they are under miRNA regulation these pathways are presumably very important to the normal functioning of FDCs.

The small size of miRNAs along with the close sequence similarity that two different miRNAs may have makes precise identification of miRNAs in biological samples

challenging. Many methods however have been developed to achieve this and each method has different merits and limitations.

The first method for identification of miRNAs that is used in this chapter is small RNA Illumina deep sequencing (Bentley et al., 2008). This method was chosen initially because it allows identification of potentially novel miRNAs as well as all known miRNAs. Illumina sequencing of small RNAs involves ligation of adaptors on to both the 5' and 3' ends of small RNA. Both the adapters are needed for the reverse transcription of the small RNA prior to PCR amplification and the 3' adapter is additionally needed for attachment to the flow cell via the amplification primer. The 5' adaptors used here additionally had a unique 5 nucleotide sequence at the 3' end of the adaptor that was used as a 'barcode' for multiplexing the samples on the flow cell. After reverse transcription, 12 cycles of PCR amplification are carried out before gel purification of the product. Matched quantities of the cDNA libraries are then attached to the flow cell and amplified to form clusters. A sequencing-by-synthesis approach is then used where each of the cDNA molecules serves as a template for the generation of a complement with fluorescently labelled nucleotides. At each addition of a nucleotide an image is created and the nucleotide that was added identified from the fluorescent wavelength emitted. The next nucleotide is added, and the cycle is repeated. All the sequences generated from a single cluster are used to identify the most likely sequence of the original cDNA, thus reducing the error rate. The adaptor sequences are 'trimmed' from the small RNA sequences and the 5 nucleotide 'barcode' is used to assign the sequence to its appropriate library. The small RNA sequences are then compared against the annotated sequences in miRBase. Any novel small RNAs that are not identified to be 'contaminating' RNA (rRNA, primer dimer etc.) are aligned to the mouse genome and assessed for features of miRNAs such as the ability to form a hairpin structure (Wang et al., 2005).

The other high through-put method of miRNA identification used in this chapter is miRNA microarray. There are several platforms for miRNA microarray produced by different companies. The most commonly used of these are Affymetrix, Agilent, Exiqon and Invitrogen. In this chapter both the Affymetrix and Exiqon platforms were used because each has different strengths. Exiqon miRCURY LNA miRNA Arrays use locked nucleic acid probes (LNAs) which improve specificity and sensitivity compared to DNA probes (Rajwanshi et al., 2000). Exiqon recommends two colour arrays for single experiment samples, these arrays use a common reference sample that is hybridised to each array slide along with the sample, this reference is then used for intra- and inter-slide normalisation. Affymetrix is one of the most widely used array platforms and the miRNA arrays offer high specificity and sensitivity combined with affordability.

Quantitative real-time PCR for miRNAs has increasingly become a standard method for the quantitation of miRNAs in biological samples. There are however various limitations of miRNA qPCR compared to mRNA qPCR which should be recognised. The short nature of miRNAs means that there is very limited primer choice to amplify the miRNA. Additionally only one primer is specific for the miRNA, the other primer is a universal primer that is directed against a sequence that is added to the small RNA sequence during the reverse transcription reaction via the reverse transcription primer. This increases the chances of amplification of another small RNA that has a similar sequence to the miRNA of interest. This is a particular concern when discriminating against related miRNAs that may only have one nucleotide difference in their sequences. For these reasons miRNA northern analysis will be used where possible.

miRNA Northern analysis is a fairly slow and expensive method for miRNA identification. However, with the advent of LNAs it has become very specific, with a

good level of sensitivity. Northern analysis allows you to visualise the product band and additional washing steps can be performed to reduce the amount of probe that is bound weakly, leaving only very strong, specific signal.

4.2. Aims

The main aim of this chapter was to use spleen samples from animals with FDCs at various stages of de-differentiation to identify miRNAs that are associated with FDC differentiation and maturation. This required accurate profiling of the miRNAs in the spleen tissues. Profiling of the miRNAs was first carried out using a high through-put method, and then the differential expression of a number of these were confirmed using the more specific and sensitive methods of miRNA northern analysis and miRNA qPCR.

4.3. Results

4.3.1. Profiling of miRNAs from LTβR-Ig treated and LTβ$^{-/-}$ spleen tissue by illumina next-generation sequencing

In order to identify miRNAs that may play a role in FDC differentiation we compared untreated control spleen samples with spleens from mice treated with LTβR-Ig chosen on the basis of the immunohistochemistry data (see section 3.2.1). RNA from the spleens of control and LTβR-Ig treated animals collected 1, 3, 5, 14, 21 and 28 days following treatment, and LTβ$^{-/-}$ spleen tissue were selected to give the best comparisons of mature (untreated mice), de-differentiating (day 1 and 3 post treatment), de-differentiated (day 5 and 14 post treatment), and re-differentiating (day 21 and 28) FDCs. RNA was pooled into two groups of two mice for each time point, with one male group and one female group. Small RNA libraries were prepared using the alternative v1.5 sample preparation guide from illumina. Library preparation (see materials and methods section 2.5) involves ligation of adapters on to either end of the small RNA, followed by reverse transcription and PCR amplification to generate the cDNA library. A 'tagging' approach was used where by the 5' adapter has a unique 5 nucleotide tag at the 3' end, thus giving each small RNA a tag to identify the library from which it came. Four different tags (sequences in Table 4.1) were used to allow sequencing of four different samples in the same lane of a sequencing flow cell. Libraries for 4 samples with the same 5' adapter tag were prepared simultaneously. To reduce the risk of user bias four of the samples were prepared by an independent researcher (Derek McBride). Table 4.1 illustrates the group, tag and lane of the flow cell for each sample. After preparation and purification of the libraries, 1ug of each library was assessed for concentration and quality by Nanodrop 1000 (Thermo scientific) measurements and Agilent Bioanalyser RNA 6000 nano assay. Illumina next generation sequencing was carried out on the 16 small RNA libraries.

Pool	Samples	Tag	Lane	Library prepared by
Untreated F	B59400 and B59401	4 (CGACU)	1	S. Aungier
Untreated M	B60778 and B59403	2 (CAUGA)	4	S. Aungier
Day 1 F	B58907 and B58908	3 (UAGUC)	1	S. Aungier
Day 1 M	B58909 and B58910	1 (GCUAG)	4	D. McBride
Day 3 F	B58966 and B58967	2 (CAUGA)	1	S. Aungier
Day 3 M	B58968 and B58969	4 (CGACU)	4	S. Aungier
Day 5 F	B58981 and B58982	1 (GCUAG)	1	D. McBride
Day 5 M	B58983 and B58984	3 (UAGUC)	4	S. Aungier
Day 14 F	B59098 and B59099	3 (UAGUC)	2	S. Aungier
Day 14 M	B59100 and B59101	1 (GCUAG)	3	D. McBride
Day 21 F	B59180 and B59181	2 (CAUGA)	2	S. Aungier
Day 21 M	B59184 and B59185	4 (CGACU)	3	S. Aungier
Day 28 F	B59287 and B59289	1 (GCUAG)	2	D. McBride
Day 28 M	B59184 and B59291	3 (UAGUC)	3	S. Aungier
$LT\beta^{-/-}$ F	B59292 and B59293	4 (CGACU)	2	S. Aungier
$LT\beta^{-/-}$ M	B59294 and B59295	2 (CAUGA)	3	S. Aungier

Table 4.1 Small RNA library preparation for Illumina sequencing. RNA from the indicated samples was combined in equal quantities into the indicated pools before library preparation using 5' adaptors with the indicated tag. Four libraries were pooled before being loaded onto the indicated lane of the flow cell for illumina sequencing.

The data files received from the array service provider (Ark Genomics) included the mature mouse miRNA name, the count for that sequence, and the coverage including the isomiRs (sequences which have small variations compared to the reference sequence). To analyse these data, first the miRNAs deemed 'dead' by miRBase or ambiguous small RNAs were deleted; the remaining data were then collapsed so the read counts for each mature miRNA were merged with any other counts for that mature miRNA (R scripts in appendix A). To allow normalisation of the sixteen samples with each other, the files from the sixteen different libraries were merged into one data table with only the mature miRNA name and read counts for each miRNA in each library. To normalise for differences in sequencing depth between the samples the read counts were normalised by dividing by the library size for the sample to be normalised, then multiplying by the average library size. The two most highly expressed miRNAs in the untreated spleen samples were miR-142-3p and miR-143 which have both been described to be highly expressed in murine spleen tissue (Lagos-Quintana et al., 2003;

Landgraf et al., 2007). However, it was observed that the profiles of these two miRNAs (Figure 4.1a and b), had an unusual pattern. MiR-142-3p had a much higher expression level (~20-fold) in the untreated, day 3, day 21, and LTβ$^{-/-}$ samples, compared to the day 1, 5, 14 and 28 samples. MiR-143 had the opposite expression pattern to that of miR-142-3p. In the samples in which miR-142-3p was high, this single miRNA comprised 47-81% of the total libraries. This raised the concern that the coverage of the other miRNAs may be skewed against these samples due to miR-142-3p comprising the majority of the coverage of these libraries. Robinson & Oshlack (2010) describe a normalisation method, termed trimmed mean of M-values (TMM), which attempts to address this kind of problem where transcripts that are highly expressed in limited samples potentially lead to reduced sequencing coverage available for other transcripts. The normalisation factors for this trimmed mean of M-values (TMM) normalisation method were calculated using the R Bioconductor software package edgeR (Robinson et al., 2010) (R scripts in appendix A). Figure 4.1c and d show the expression profiles for miR-142-3p and miR-143, after TMM normalisation. The bias of miR-143 against the samples in which miR-142-3p is very high looks as though it has been evened out by the TMM normalisation so that the expression levels of miR-143 at 1,3,14 and 28 day time points are not so low compared to the other time points. Figure 4.2 shows the expression profiles for two other miRNAs that were expressed at fairly high levels in the female untreated sample having been normalised to library size (a and b) or with the TMM normalisation (c and d). Following normalisation by library size(a and b) the expression profile for miR-29a showed a clear bias towards the untreated female (f), day 3 male (m), day 21 m, and LTβ f samples. It was noted that those samples were prepared with the 5' adapter with tag 4 (CGACU); Table 4.1. The expression profile of miR-30a showed no clear bias towards any sample. Application of TMM normalisation did not compensate for the clear bias seen in the expression profile

of miR-29a, and in the case of miR-30a, actually seemed to bias the expression profile towards those samples that were miR-142-3p high, perhaps suggesting an over compensation for the expected reduction in coverage in these samples. Additionally, it was noted that those samples that had high miR-142-3p expression levels were prepared using 5' adapters with tags 2 and 4. Together these data strongly suggested sequencing bias due to the 5 nucleotide tags introduced at the 3' end of the miRNA via the 5' adapter.

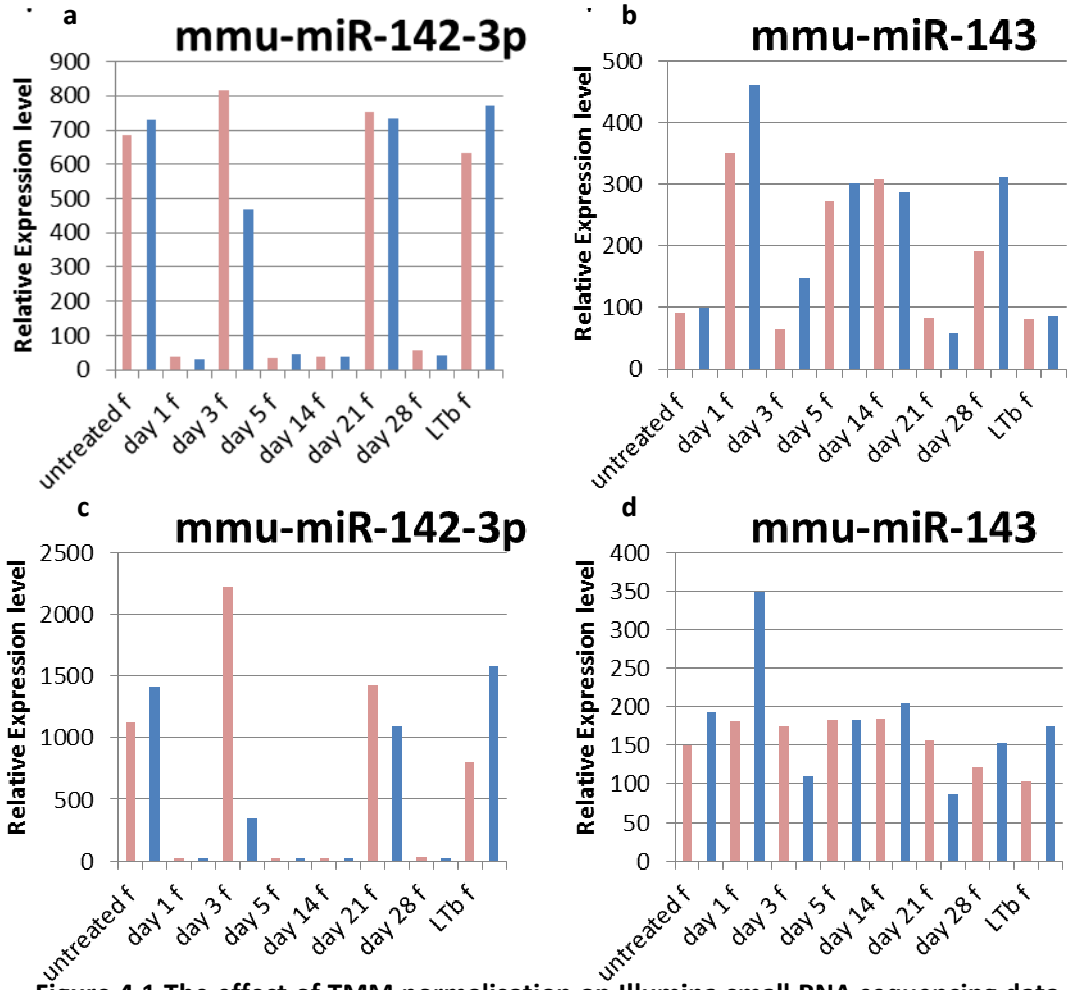

Figure 4.1 The effect of TMM normalisation on Illumina small RNA sequencing data. The figure shows that TMM normalisation corrects for the apparent bias caused by the high incidence of miR-142-3p in some samples. The high incidence of miR-142-3p in the untreated, day 3, day 21 and LTβ$^{-/-}$ samples can be seen (a), and a converse pattern is seen in the next most abundant miRNA, miR-143 (b). After TMM normalisation the bias seen with miR-142-3p (c) is still largely the same but the distribution of miR-143 appears to be more even (d). Each bar represents a sequencing sample (n=2), there are two samples for each time point with the female pool represented in pink and the male pool represented in blue.

Where this apparent bias was introduced was unknown. To check whether this pattern of expression was seen in the RNA that the libraries were prepared from, the patterns were analysed by miRNA northern analysis. Figure 4.3b shows miRNA northern analysis of miR-142-3p expression compared with the sequencing data (Figure 4.3a). The expression profile for miR-142-3p obtained by Illumina sequencing appeared to be different to the miRNA northern data obtained from the same samples. This was also true for miR-29a. The sequencing service was notified of this apparent tag bias and they carried out a principal component analysis (PCA) on the data. The PCA plot can be seen in Figure 4.4 and it shows that the data points cluster (indicating similarity) by tag rather than biological similarity. This analysis clearly indicates that the sequencing data could not be used to give a reliable measure of miRNA expression levels between the samples studied.

It was noted that although northern analysis data and sequencing data indicated different patterns of miR-142-3p expression between spleen samples, in both data sets the levels of miR-142-3p were widely disparate between samples. This could indicate that the differential expression of miR-142-3p is a biological phenomenon rather than an artifact. Later, Exiqon miRNA microarray data from a subset of the spleen samples did not show any differences between the levels of miR-142-3p expression in the treated and untreated spleen samples and a relatively modest 32% reduction in the lymphotoxin beta knock-out mice (Appendix C, page 224). Interestingly, although the Exiqon miRNA microarray showed very high levels of miR-142-3p, the Affymetrix miRNA microarrays performed on the same samples did not detect miR-142-3p at levels above that used for the threshold cut-off. This perhaps indicates that miR-142-3p is very sensitive to small differences in processing of the samples in preparation for miRNA arrays or sequencing. It is unclear why this would be so, however relatively frequent mutation of even the seed region of miR-142-3p has been reported in B-cell

lymphoma (Kwanhian et al. 2012). If miR-142-3p is more prone to mutation it could be a source of the variation seen, particularly using methods of miRNA profiling that are regarded to be more sensitive and specific.

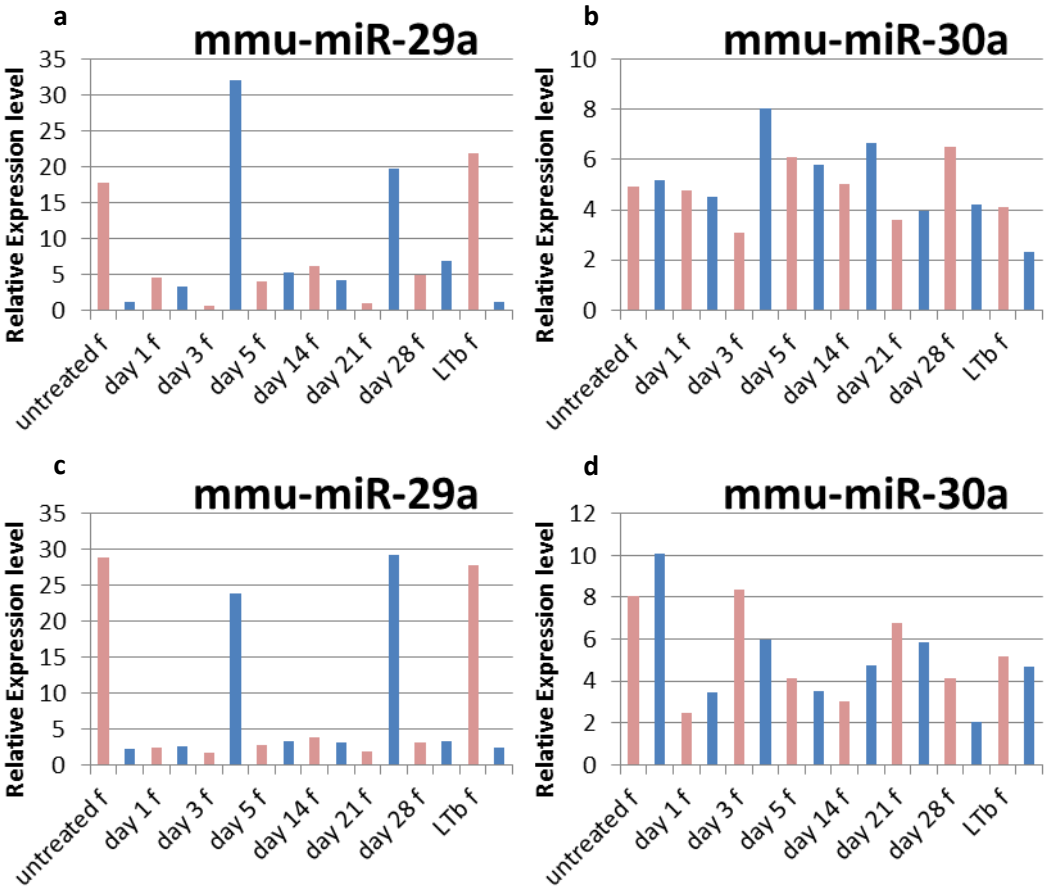

Figure 4.2 The effect of TMM normalisation on small RNA sequencing data. The figure shows that TMM normalisation does not help large biases in data (a and c), and in some cases apparently causes bias (b and d). The top two graphs show the expression profile of miR-29a and miR-30a from the sequencing data normalised to the library sizes, miR-29a shows a clear bias for those samples with tag1, whereas miR-30a shows no obvious bias. The bottom panel shows the same data which has been TMM normalised. miR-29a still shows the same bias, whereas miR-30a now appears to be biased towards samples with tag 2 and 4 suggesting that the TMM normalisation may be over compensating for the reduced coverage in these samples. Again each bar represents a sequencing sample (n=2), there are two samples for each time point with the female pool represented in pink and the male pool represented in blue.

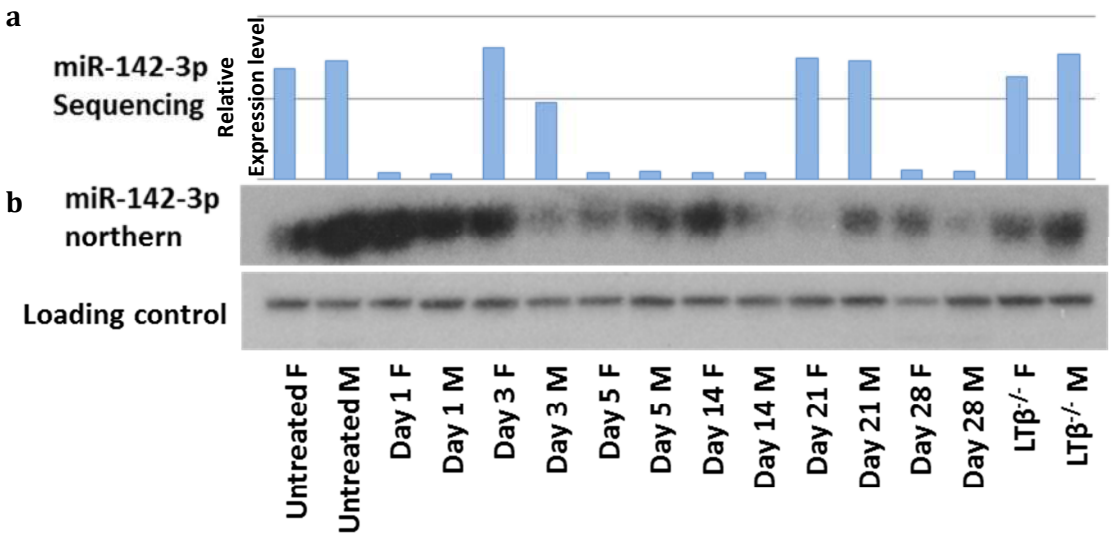

Figure 4.3 Comparison of sequencing data with miRNA northern analysis. MiRNA northern analysis was carried out to confirm the pattern of expression seen in the sequencing data was caused by tag bias rather than true expression from the samples. The same RNA samples that the sequencing libraries were prepared from were used to run a miRNA northern analysis, and the membrane was probed for miR-142-3p. As can be seen, the pattern of expression seen from the sequencing data bears no resemblance to the expression seen with miRNA northern analysis from the same samples.

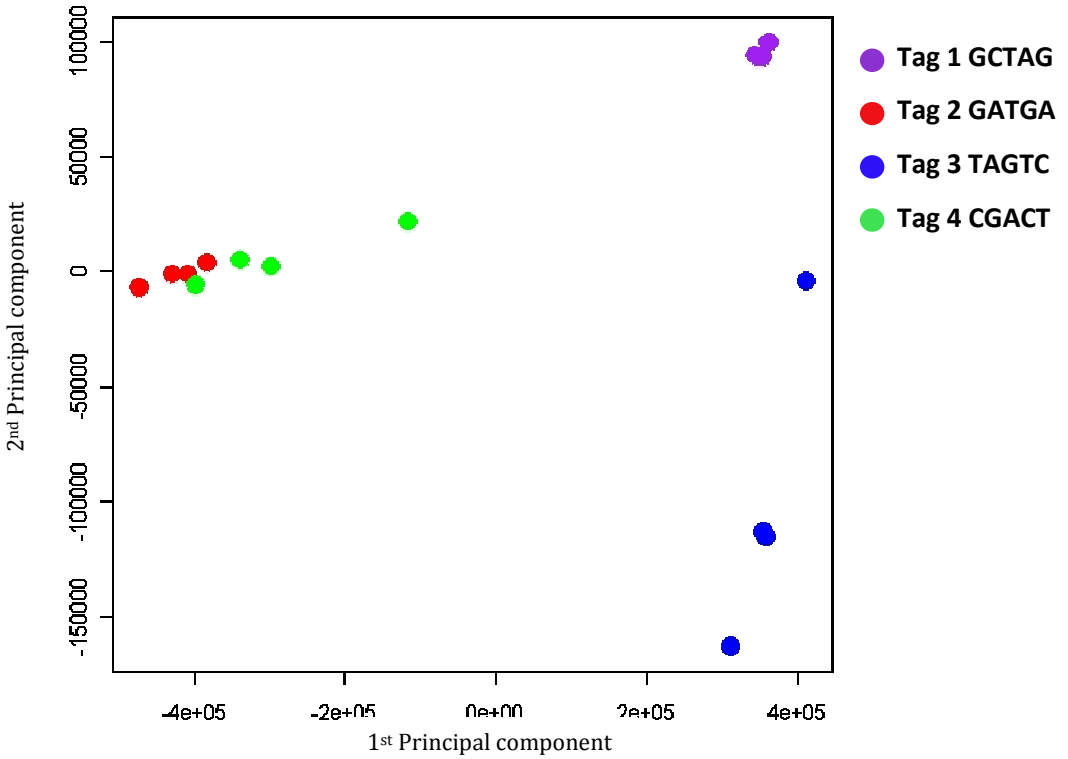

Figure 4.4 The miRNA sequencing data clusters by Tag rather than biological similarity. Principal component analysis was carried out on the miRNA sequencing data. As can be seen the samples with the same tags cluster together showing that the tags have caused a bias in sequencing.

4.3.2. Profiling of miRNA expression in spleens from LTβR-Ig treated and LTβ$^{-/-}$ mice by microarray

As the miRNA sequencing data could not be reliably used Affymetrix miRNA microarrays (GeneChip Mouse Genome 430 2.0 Array**)** were used. The samples selected for this analysis were the same as those used for gene expression microarrays, see section 3.3.3, (untreated, day 2 and 14 after LTβR-Ig treatment and LTβ$^{-/-}$). Considerable variation is seen between different miRNA microarray platforms (Sato et al., 2009; Git et al., 2010). It was therefore decided to also analyse the same samples by Exiqon miRNA microarray (miRCURY LNA miRNA Array 6th GEN) to reduce the risk of false positives. RNA samples from untreated control spleens, day 2 and day 14 after LTβR-Ig treatment and spleens from LTβ$^{-/-}$ mice were again pooled in two samples of two for each group. 5ug of RNA was sent to Exiqon for QC analysis and microarrays (miRCURY LNA miRNA Array 6th GEN) whereas 2ug of the same RNA pools were given to Ark genomics to carry out Affymetrix microarrays (GeneChip Mouse Genome 430 2.0 Array**)**.

4.3.3. Analysis of miRNA microarray profiling

The Exiqon microarrays were analysed by the company using global lowess regression normalisation(Milan et al., 2011). The raw affymetrix CEL files received from Ark Genomics were analysed in R using the bioconductor package EximiR (Sylvain Gubian et al. 2010) to perform robust multi-array analysis (RMA) (Irizarry, 2003). Previous data suggest that the use of different normalisation methods can result in fairly large differences between data sets. The background subtracted Exiqon results were therefore also normalised in R using the EximiR package to perform RMA

normalisation (R scripts in appendix B). In each of these datasets the two samples from each group were averaged unless a very large disparity was seen between the samples (Appendix C). The fold-change from the Day 0 sample was calculated for each of the treated time points and the LTβ$^{-/-}$ sample (Appendix C). Those miRNAs with a 2-fold or greater difference in expression between Day 0 and LTb$^{-/-}$ samples, with a change in the same direction at day 2 and day 14 were considered for further analysis. Only one up-regulated miRNA fitted these criteria in the Affymetrix data set (although with low expression levels), and while 12 up-regulated miRNA from the Exiqon data set did fit these criteria, the vast majority were up-regulated less than 0.2-fold in the day 2 and day 14 treated samples (Appendix C). It was therefore decided to focus on the miRNAs that were seen to be down-regulated in line with decreased numbers of mature FDC, indicating that these miRNAs could be high in mature FDC and decrease in de-differentiated FDC.

Taking the twenty miRNAs that showed the biggest reduction in the LTβ$^{-/-}$ samples compared to the untreated samples in the RMA normalised Exiqon data it was found that 14 of these miRNAs were also present in the lowess normalised data. Of the twenty miRNAs that were most reduced in the LTβ$^{-/-}$ spleens compared to the untreated spleens in the RMA normalised Exiqon dataset, six were also in this top twenty in the Affymetrix dataset. Four of those six were also present in the lowess normalised Exiqon data. Table 4.2 shows the 20 miRNAs that had the largest reduction in expression levels in the LTβ$^{-/-}$ samples compared to the untreated samples from each array platform. Looking at the most down regulated miRNAs in the day 14 samples, again 6 miRNAs were in the top 20 down-regulated lists for both platforms, 5 of which are the same miRNAs identified in the untreated versus LTβ$^{-/-}$ comparison (Table 4.3).

	Fold-change in expression levels			
Exiqon	**Day 0**	**Day 2**	**Day14**	**LTb$^{-/-}$**
mmu-miR-100	1.00	0.82	0.68	0.27
mmu-miR-592*	1.00	0.66	0.56	0.29
mmu-miR-2137	1.00	0.91	0.62	0.34
mmu-miR-3102*	1.00	0.82	0.70	0.34
mmu-miR-762	1.00	0.72	0.65	0.35
mmu-miR-33	1.00	1.57	0.86	0.36
mmu-miR-138	1.00	0.97	0.59	0.38
mmu-miR-3090*	1.00	0.86	0.75	0.40
mmu-miR-487b	1.00	1.10	1.12	0.41
mmu-miR-2861	1.00	0.81	0.63	0.42
mmu-miR-1894-3p	1.00	0.73	0.68	0.43
mmu-miR-25*	1.00	0.69	0.65	0.44
mmu-miR-32	1.00	1.18	0.93	0.46
mmu-miR-187	1.00	0.83	0.54	0.47
mmu-miR-99a	1.00	0.83	0.76	0.47
mmu-miR-10b	1.00	0.78	0.77	0.47
mmu-miR-101b	1.00	1.00	0.93	0.48
mmu-miR-711	1.00	0.94	0.76	0.48
mmu-miR-28	1.00	0.67	0.76	0.50
mmu-miR-151-5p	1.00	0.78	0.76	0.51

	Fold-change in expression levels			
Affymetrix	**Day 0**	**Day 2**	**Day14**	**LTb$^{-/-}$**
mmu-miR-708	1.00	0.78	0.64	0.20
mmu-miR-138	1.00	0.98	0.48	0.36
mmu-miR-2137	1.00	0.85	0.57	0.41
mmu-miR-187	1.00	0.93	0.52	0.46
mmu-miR-466h	1.00	1.02	1.43	0.49
mmu-miR-1893	1.00	0.80	0.66	0.50
mmu-miR-762	1.00	0.76	0.59	0.50
mmu-miR-100	1.00	0.78	0.72	0.53
mmu-miR-1224	1.00	0.62	0.61	0.54
mmu-miR-1937a	1.00	0.92	0.79	0.56
mmu-miR-139-3p	1.00	1.20	0.77	0.56
mmu-miR-1894-3p	1.00	0.66	0.69	0.57
mmu-miR-1937b	1.00	0.84	0.82	0.58
mmu-miR-2133	1.00	0.99	0.63	0.60
mmu-miR-151-3p	1.00	0.84	0.73	0.61
mmu-miR-193b	1.00	1.10	0.66	0.62
mmu-miR-1959	1.00	0.59	0.68	0.63
mmu-miR-466f	1.00	1.20	1.12	0.66
mmu-miR-455	1.00	0.97	0.94	0.67
mmu-miR-19a	1.00	1.30	1.45	0.67

Table 4.2 Top 20 down-regulated miRNAs from Exiqon and Affymetrix microarray data. Exiqon and Affymetrix miRNA microarray were carried out on the same samples. Data were normalised to the untreated sample and fold-change from untreated calculated for the day2, day 14 and LTβ$^{-/-}$ samples. The tables show the top 20 down regulated miRNAs in the LTβ$^{-/-}$ samples compared to the untreated (Day 0) samples. Highlighted in red are those miRNAs that appear in this category in the data from both platforms.

Day 2/ Untreated	**Day 14/ Untreated**	**LTβ$^{-/-}$ / Untreated**
miR-100	miR-100	miR-100
-	miR-2137	miR-2137
miR-762	-	miR-762
miR-2861	miR-2861	-
miR-1894-3p	miR-1894-3p	miR-1894-3p
-	miR-138	miR-138
-	miR-187	miR-187
miR-339-5p	-	-

Table 4.3 miRNAs consistently down regulated with de-differentiation of FDCs. The miRNAs listed in the table are those that appeared in the top 20 down-regulated in both the Exiqon and Affymetrix at the noted time points. Highlighted in red are those that appeared down-regulated at all three time points and in blue those that were down-regulated 14 days post LTβR-Ig treatment and in the LTβ$^{-/-}$ where no FDCs were seen.

MiRNAs function as part of the RNA induced silencing complex (RISC) to post-transcriptionally repress expression of their target genes. Identification of the genes targeted by miRNAs is central to understanding their biological roles. The diversity of targets that a single miRNA can have has made identification of miRNA targets problematic (Barbato et al., 2009; Liu et al., 2010; Kast, 2011). However, many computational algorithms and approaches have been developed to identify the likely target genes of either a single or group of miRNAs of interest. Several web-based packages that integrate a number of these algorithms to identify fewer, more likely miRNA target genes also exist (Liu et al., 2010; Tsang et al., 2010; Lu et al., 2012). We used one of the most recent of these, miRsystem (Lu et al., 2012), which also integrates function and pathway analyses. The eight miRNAs listed in Table 4.3 which are in the top 20 down regulated genes for both microarray platforms in LTβR-Ig treated and $LT\beta^{-/-}$ spleen tissue were entered into miRsystem for target prediction. This analysis failed to come up with any predicted target genes for three of the miRNAs, miR-2861, miR-1894-3p and miR-2137. This is likely to be due to the fact that these are newly described miRNAs and the databases have not been updated to include them. Four target prediction algorithms were found that did supply target predictions for these newer miRNAs. The predicted targets for these miRNAs were therefore taken from DIANA micro-T (Maragkakis et al., 2009), miRNA.org (Betel et al., 2008), miRDB (Wang, 2008) and RNA22 (Loher and Rigoutsos, 2012). If the programmes gave over 300 predictions only the top 250 predictions were used. The lists of predicted gene targets were cross referenced and those genes that were predicted to be miRNA targets by three or more of the target prediction programmes were selected. Similarly for the miRNAs that miRSystem suggested genes that were predicted to be targeted by the same miRNA by three or more target prediction programmes were selected. These gene target lists for each miRNA were then cross referenced and those that three or

more of the miRNAs were predicted to target were selected. In this way a list of eight genes that are predicted to be targeted by three or more of the eight miRNAs, by three or more target prediction programmes was produced. These eight genes and the miRNAs they are predicted to be targeted by are set out in Table 4.4. Some of these genes could have roles in the biological functions affected by LTβR-Ig, particularly Gnai2 which has been described to be involved in the organisation of secondary lymphoid organs (Hwang et al., 2010). It has been described that target genes of miRNAs often change at the transcript level if the repression is strong (Ruike et al., 2008; Guo et al., 2009). The expression of these eight genes was viewed over the de-differentiation from the gene expression array data (Chapter 3, section 3.3.3). It was found that while the level of expression of six of the genes (including Gnai2) did not change at all, the expression of Arrdc3 was down by around 22% at day 2 after LTβR treatment but higher at day14 and in the $LT\beta^{-/-}$ spleens. The expression of Dnmt3a was unchanged 2 days after LTβR-Ig treatment but was decreased by around 23% after 14 days but was not significantly changed in the $LT\beta^{-/-}$ spleens. As previously mentioned miRNA target prediction algorithms tend to make many false positive predictions, and because the mRNA levels of these genes were not changed it was decided to narrow-down the miRNA selection rather than immediately follow up any of these genes.

4.3.4. Confirmation of miRNA profiling by miRNA northern analysis and miRNA quantitative PCR.

In order to validate the miRNA microarrays, miRNA northern analysis was carried out for some of the miRNAs that were seen to be down-regulated upon LTβR-Ig treatment and also in the $LT\beta^{-/-}$ spleen tissue (Table 4.3). The five miRNAs selected to follow-up initially were miR-100-5p, miR-2137, miR-138-5p, miR-592* and miR-3102*. These miRNAs were selected because they were down-regulated in at least two of the three

Gene symbol	Gene name	miRNAs predicted to target the gene
Arrdc3	arrestin domain containing 3	miR-138-5p, miR-187-3p, miR-339-5p
Gnai2	guanine nucleotide binding protein (G protein), alpha inhibiting 2	miR-138-5p, miR-339-5p, miR-762
Lphn1	latrophilin 1	miR-138-5p, miR-339-5p, miR-762
Pik3r1	phosphatidylinositol 3-kinase, regulatory subunit, polypeptide 1 (p85 alpha)	miR-138-5p, miR-339-5p, miR-762
Znrf1	zinc and ring finger 1	miR-138-5p, miR-339-5p, miR-762, miR-2137
Dnmt3a	DNA methyltransferase 3A	miR-138-5p, miR-762, miR-2137
Sox12	SRY-box containing gene 12	miR-138-5p, miR-762, miR-2137
Setd5	SET domain containing 5	miR-339-5p, miR-762, miR-1894-3p

Table 4.4 Genes predicted to be targets of three or more miRNAs. Target prediction was carried out using at least four different target prediction programmes for the eight miRNAs that are listed in Table 4.3. The eight genes shown in the table were predicted by at least three of the prediction programmes to be targeted by three or more of the miRNAs (indicated).

treatment/ transgenic groups compared to untreated controls. These miRNAs were also selected because they had higher expression levels in the untreated spleens as measured by both array platforms than other miRNAs with the same pattern of expression. The two star strand miRNAs, were only included in the Exiqon dataset, but were both measured to have relatively high expression levels in the untreated spleens. Figure 4.5 shows miRNA northern analysis for the three lead strand miRNAs that were down-regulated with FDC de-differentiation as measured by the microarrays. The miRNA northern analysis shows a general pattern of down regulation of the miRNAs in the LTβR-Ig treated and the $LT\beta^{-/-}$ tissue. MiR-2137 was found to be at the limits of detection by northern analysis. This was unexpected because miR-2137 expression was approximately 6 times higher than miR-100-5p according to Exiqon array data, and around 10 times higher according to Affymetrix array data. These discrepancies could

be due to a number of reasons related to both the array and the northern analysis. miR-2137 has a very G/C rich (86%) sequence, meaning that it is more likely that the LNA probes directed against the miRNA will form secondary structures which could prevent efficient end labelling of the probe. The northern analysis (Figure 4.5) shows that the expression level of one of the miRNAs, miR-138-5p, drops between the day 2 and day 3 time points and stays at this lower level of expression up to the final 28 day time point after LTβR-Ig treatment. This is a very similar pattern of expression as the FDC marker Mfge8 as assessed both by immunohistochemistry and qPCR (Figure 3.1 and 3.3). Two of the miRNAs miR-100-5p and miR-2137, show a decrease in expression following LTβR-Ig treatment, with an increase in expression at day 21 echoing the immunohistochemistry data for the FDC marker CD35 (Figure 3.1). It can be seen that, as measured by northern analysis, miR-2137 had a peak in expression level at day 10. A relatively small amount of CD35 expression was observed by IHC at day 10 (Figure 3.1), indicating that there is a biological difference in some of the day 10 sections. Additionally, this day 10 increase may be artificially exaggerated because miR-2137 was found to be close to the limits of detection by northern analysis in the spleen tissue.

Northern analysis was also carried out for the two star strand miRNAs, miR-592* and miR-3102*. However a signal from these miRNAs could not be detected. The expression of these star strand miRNAs in the spleen was therefore measured by quantitative PCR. The high Ct values obtained from the qPCR strongly suggest that these miRNAs are only expressed at very low levels in these spleen tissues contrary to what was suggested by the microarray results. However, miR-592* did have a pattern of down-regulation upon LTβR-Ig treatment and in the $LT\beta^{-/-}$ spleen tissue as suggested by the microarray results (Figure 4.6).

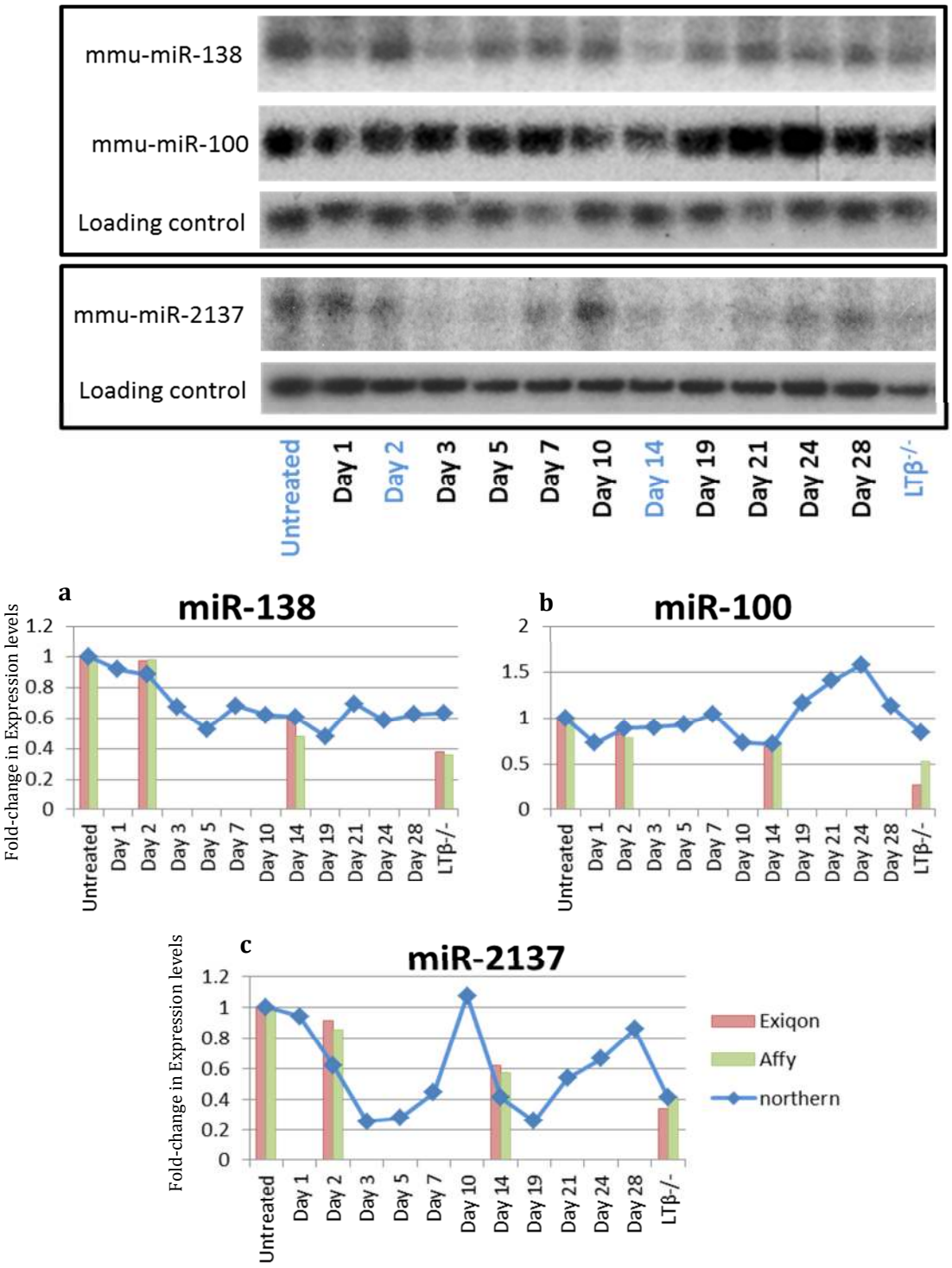

Figure 4.5 miRNA northern confirmation of miRNA microarray data. RNA samples that the microarrays were carried out on were used for miRNA northern analysis. Top panel shows a northern membrane probed for miR-2137 and bottom panel shows a membrane that was prepared in parallel and probed for miR-100 and miR-138. Bar graphs show the phosphoimager quantification of the signal from the northern membranes (blue line) along with the two sets of microarray data (red and green bars). This shows that the northern and microarray data generally correspond very well.

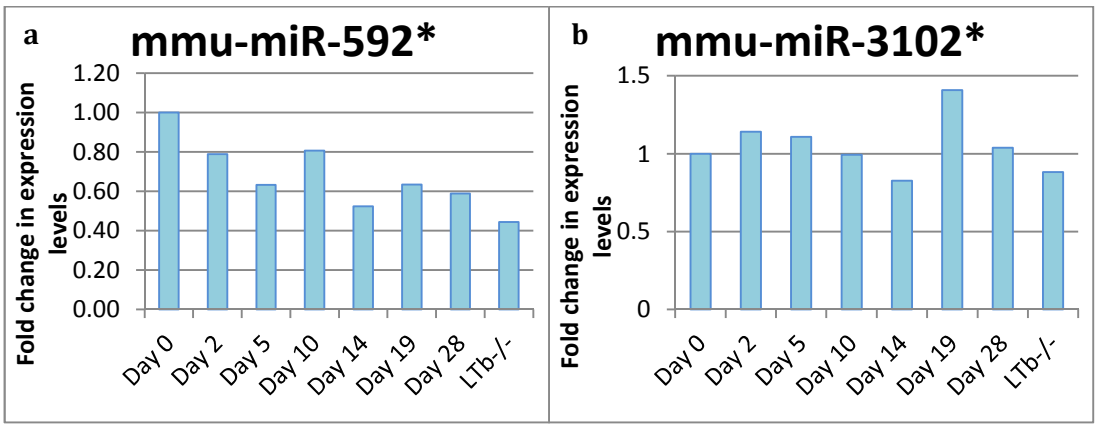

Figure 4.6 miRNA qPCR confirmation of microarray data. The same RNA samples that were used for miRNA microarray were used to carry out miScript reverse transcription and quantitative real-time PCR for the star strand miRNAs miR-592* and miR-3102*. n=2

4.3.5. Expression analysis of genes containing differentially represented miRNAs

Three of the five miRNAs that were selected for further study were found to be located within the introns of protein coding genes. The two star strand miRNAs, miR-592* and miR-3102*, are located within the genes *Grm8* and *Arbgef17* respectively (Kozomara and Griffiths-Jones, 2011). Both miR-100-5p and miR-138-5p are located within intergenic regions of the genome (Kozomara and Griffiths-Jones, 2011). miR-2137 is located within intron1 of *Zfp185* (Kozomara and Griffiths-Jones, 2011), a protein that associates directly with F-actin (Wang et al. 2008a) and has been shown to have roles in the development and activation of T lymphocytes (Wang et al. 2008b). ARHGEF17 is also implicated in actin cytoskeleton organisation (Rümenapp et al., 2002). To ascertain if these miRNAs were being transcribed as part of the gene that they are located within, gene expression microarray data for these genes was assessed. Both *Grm8* and *Zfp185* had very low levels of expression, whereas *Arhgef17* had relatively high levels of expression. All three genes were found to have stable levels of expression between the untreated, LTβR-Ig treated, and the $LT\beta^{-/-}$ samples, suggesting that the miRNAs, at least in the case of miR-2137, could be transcribed independently of the genes that they are contained within.

4.4 Discussion

Data in this chapter show that during Illumina small RNA sequencing the 5 nucleotide tag introduced at the 3' end of the 5' adaptor that was added to the RNA samples during library preparation unfortunately caused considerable sequencing bias. This sequencing bias was identified first of all through the variable expression of miR-142-3p across the samples. Although miR-142-3p has been identified previously to be highly expressed in spleen tissue (Landgraf et al., 2007), this study found that by far the most abundant miRNA in murine spleen tissue was miR-143. miR-143 was found to be the second overall most abundant miRNA in our sequencing data. However, miR-142-3p was over 12 times more abundant than miR-143 in some samples but over 15 times less abundant in other samples. It was noticed that those samples in which miR-142-3p was very abundant either had tag 2 or tag 4 in the 5' adaptor. A bias based on the tag was confirmed by principal component analysis. Due to these reasons, it was decided to analyse miRNA expression in a subset of the samples by miRNA microarray.

Previous data show that there is a significant amount of variation in data obtained from different miRNA array platforms (Sato et al., 2009; Git et al., 2010). Here two different miRNA microarray platforms, Affymetrix and Exiqon, were used to analyse the same samples to attempt to reduce the frequency of false positives. There was a fairly large discrepancy between data obtained from the Affymetrix and Exiqon arrays. Looking at the 50 miRNAs that were decreased the most between the untreated samples and the samples collected 14 days after LTβR-Ig treatment, only 11 were identified by both platforms, and from the top 20 only 3 agreed between the platforms. When the two datasets were normalised using the same method, a small increase in agreement was seen. Again looking at the 50 miRNAs that were most decreased in the samples collected 14 days after the LTβR-Ig compared to the untreated samples, 14 miRNAs

appeared in this list for both platforms and when looking at the top 20 miRNAs, 6 appeared in the lists from both platforms. The fairly large differences seen between the two platforms were not unexpected because the two platforms use very different methods and probes. However, agreement that was observed between the two different methods gave a good basis for selection of miRNAs, with a much reduced chance of false positives.

A list of 8 miRNAs which were in the top 20 most decreased miRNAs in at least two of the LTβR-Ig treated spleen samples or the transgenic samples when compared to the untreated samples was created. This list of miRNAs was used as input for computational target prediction using online software. Unfortunately, many of these data bases do not include some of the more newly discovered miRNA. Therefore, four databases that were found to have predictions for all of the 8 miRNAs were selected to be used for target prediction (DIANA micro-T (Maragkakis et al., 2009), miRNA.org (Betel et al., 2008), miRDB (Wang, 2008) and RNA22 (Loher and Rigoutsos, 2012)). Some of these databases included hundreds of predicted target genes for a single miRNA. This is because of the diversity that has been seen in miRNA:mRNA target pairings, specificity of the generated predicted targets is often sacrificed in order to gain a good sensitivity from the algorithm (Zhang and Verbeek, 2010; Witkos et al., 2011). When hundreds of predictions are made, the algorithms often also rank the predictions so that the user can decide to increase the specificity as wanted. An arbitrary cut-off of 250 predictions was used for when there was more than this number of predictions for a single miRNA.

Some studies show that miRNAs that have similar expression patterns in a particular tissues or cell types can act in concert to regulate different genes of the same pathway (Hornstein and Shomron, 2006; Ooi et al., 2011; Cloonan et al., 2011; Shirdel et al.,

2011), or even the same gene (Doench and Sharp, 2004; Lim et al., 2005; Saetrom et al., 2007). For this reason, the target gene predictions for all 8 of the selected miRNAs were combined. Eight genes were found that were predicted to be targeted by three or more of the miRNAs, at least three of the four target prediction programmes. However, because none of these genes were either found to be closely related in terms of function, or have obvious roles in the typical functions of FDCs, it was decided to carry out some more validation of the miRNAs before following up potential gene targets (see chapter 5).

To confirm the expression of the miRNAs in the untreated, treated and transgenic spleen tissue miRNA northern analysis was performed. The log ratios of the LTβR-Ig treated and transgenic samples compared to the untreated samples were generally seen to correspond very well for the samples looked at by both methods. For one of the miRNAs, miR-2137 the correspondence between the array and northern data was generally poorer. It was noted that this miRNA has a very high GC content (86%) which could cause an artificially high intensity values from the arrays if other small RNA with a high GC content binds to the probes for miR-2137. This could also potentially cause difficulties in labelling of the probe for miRNA northern analysis because secondary structures would be more likely to form because of the high GC content, which could prevent end labelling if there is not a free-end. This, coupled with the fact that the signal from the northern analysis was close to the limits of detection for this miRNA could explain the discrepancies.

A signal for miR-592* (miR-592-3p), or miR-3102* (miR-3102-5p) could not be obtained by northern analysis. qPCR was carried out for these two miRNAs because it is a more sensitive method than northern analysis. The Ct values obtained from the qPCR analysis were around 31-34 indicating very low expression levels in the spleen

samples. These data are in agreement with Illumina sequencing data on B cells isolated from murine spleen (Yamane et al., 2011), where both these miRNAs were found to be expressed, but only at very low levels.

The aim of this chapter was to identify miRNAs that were likely to be expressed by FDC and to be important for the development or function of FDC. Profiling of miRNAs was performed on spleen samples that had previously been identified by immunostaining to contain FDC at different stages of maturation following LTβR-Ig treatment. Due to technical difficulties, data from Illumina small RNA sequencing could not be used for these purposes. However, miRNA microarray analysis was successfully used to identify miRNAs that had a pattern of down-regulation similar to that seen by immunohistochemistry for FDC (Figure 3.1). The expression pattern of some of these miRNAs in the spleen samples were confirmed by miRNA northern analysis. In the following chapters functional studies for some of these miRNAs will be carried out to begin to identify their roles within FDCs.

CHAPTER 5: Characterisation of an *in vitro* murine FDC model

Contents

Chapter 5: Characterisation of an *in vitro* murine FDC model

5.1. Introduction

Isolation of FDC in a fully mature and functional state is problematic (Sukumar et al., 2006; Myers et al., 2013) and isolation of sufficient numbers of FDC to carry out functional studies of miRNA will be challenging. The primary aim of this chapter is to assess the suitability of a murine FDC cell line, termed FL-Y and FL-YB, that has previously been established(Nishikawa et al., 2006; Magari et al., 2011).

FL-Y cells are a rapidly growing clone selected from a cell line that was established using 3D culture of lymph nodes from immunised mice (Nishikawa et al., 2006). FL-Y cells were found to retain many phenotypic features of FDC, including expression of *Mfge8, Ltβr, Vcam-1, FcγRII/III, Cd21*, and *Baff*. However the authors found the expression levels of BAFF in the original cell line to be significantly higher than in the FL-Y cell line. The authors therefore created the FL-YB cell line which has levels of BAFF expression similar to the original cell line. FL-YB cells were generated by retroviral transfer of the murine *Baff* gene into FL-Y cells followed by selection of a clone stably expressing BAFF (Magari et al., 2011). The FL-YB cell line was found to have superior ability to support B cells compared to the FL-Y cell line.

In this chapter the xCELLigence system (Ke et al., 2011) is used to phenotypically compare the FL-YB cells under different conditions. Once the FL-YB cell phenotype has been characterised under different conditions, these phenotypes can then be used as a measureable output for loss and gain of function experiments for the selected miRNAs. The xCELLigence system is based on real-time cell electronic sensing (RT-CES) technology (Solly et al., 2004) developed by ACEA Biosciences and Roche Applied Science (Ke et al., 2011). Micro-electrodes in the bottom of a specially designed 96-well plate (E-plate) are used to monitor impedance in electrical current. Impedance occurs

when cells are adhered to the electrodes on the bottom of the well. This means that when more cells are adhered, the impedance is higher which the RTCA software translates into a higher cell index value. The impedance is also higher if the cells are more spread-out or are adhered with greater strength to the plate. This means that the cell index provides an indication of cell proliferation, cell spreading, adherence and morphological changes.

A number of different stimuli are used in this chapter to measure the response of FL-YB cells. FL-YB cells are usually grown in the presence of recombinant murine TNFα at a concentration of 5ng/ml. The group who established the cell line also sometimes culture in the presence of an agonistic LTβR MAb which causes signalling through the receptor, which was reported to increase proliferation of the FL-Y cell line (Nishikawa et al., 2006). It is possible that the identified miRNAs would be involved in this signalling pathway, because they were identified by the *in vivo* blockade of this pathway. IL-4 was one of the cytokines added in the initial cultures when the original cell line was being isolated (Nishikawa et al., 2006). IL-4 is produced mainly by Th2 cells and stimulates isotype switching to IgE by activated B-cells (Coffman et al., 1986). It also plays a role in the selection and expansion of memory B cells during the GC reaction. Pre-treatment of human FDC-like cells, HK, with IL-4 can repress cycloxygenase2 (COX2) which abrogates prostaglandin production by the cells (Lee et al., 2008; Cho et al., 2013, 2011a). Lipopolysaccharide (LPS) has also been used as a treatment to stimulate FL-YB cells in some experiments in this chapter. The LPS receptor TLR4 has been shown to be expressed on murine FDCs *in vivo,* and LPS treatment *in vivo* confers an activated FDC phenotype (El Shikh et al., 2007b). The production of IL-6 has been reported to be induced in immune complex-activated FDCs, which both promotes GC reactions, IgG responses and somatic hypermutation (Wu et al., 2009). Isolated FDC have been found to up-regulate IL-6 following TNFα and

LTα1β2 treatment (Husson et al., 2000) and FL-Y cells have been shown to express IL-6 and up-regulate the transcript upon TNFα stimulation (Nishikawa et al., 2006). The intergrin VCAM-1 is expressed on the surface of FDCs and is important for the formation of synapses between FDCs and B cells, which are important for B cell activation (Kosco et al., 1992; Maeda et al., 1995). Again VCAM-1 has been shown to be up-regulated in immune complex-activated FDCs (El Shikh et al., 2006). Cultured human FDC-like cells have also been described to up-regulate VCAM-1 upon TNFα, LTα1β2 and IL-4 stimulation (Husson et al., 2000). IL-15 is secreted by FDC *in vivo* and in the HK cell line, it has been shown to enhance germinal centre B cell proliferation (Park et al., 2004). IL-15 has also been shown to enhance the proliferation of and chemokine secretion from FDC (Gil et al., 2010).

5.2. Aims

The main aim of this chapter was to assess whether FL-YB cells would be a suitable *in vitro* model for functional analysis of the miRNAs identified in Chapter 4. It was first established that all three miRNAs that were confirmed to be expressed in spleen samples in chapter 4 were expressed at detectable levels in FL-YB cells. Further characterisation studies of the FL-YB cells confirmed that they highly expressed many typical markers of FDC, and responded to TNFα stimulation. Treatment of the cells with different stimuli and real-time monitoring of the cells using the xCELLigence system allowed measurement of the cellular response to these stimuli. Quantitative real-time PCR analysis revealed some gene transcript changes in FL-YB cells upon treatment with different stimuli. These parameters will be used in chapter 6 to determine whether any of the miRNAs identified in chapter 4 have roles in any of these differentially activated phenotypes.

5.3. Results

5.3.1. Expression of miRNAs by FL-YB cells

To assess if FL-YB cells were an appropriate model to carry out functional analysis of the selected miRNAs, it was first important to know whether the cells expressed the selected miRNAs. To this end miRNA northern analysis was carried out using RNA extracted from FL-YB cells. Following 4 days of culture without TNFα supplementation FL-YB cells were plated out in complete media supplemented with 5ng/ml recombinant murine TNFα. RNA was isolated from the cells 48, 72, and 96 hours later. 3μg of the extracted RNA was used for miRNA northern analysis. The miRNA northern membranes were probed with radiolabelled anti-sense LNA oligonucleotides to miR-100-5p, miR-138-5p, and miR-2137. All three of these miRNAs were found to be expressed by the FL-YB cells under these conditions (Figure 5.1). These data imply that the decrease in expression of those miRNA *in vivo* following LTβR-blockade may be due to loss of mature FDC. These data also suggest that FL-YB cells are a useful model to study the function of these miRNAs in a FDC-like cell.

5.3.2. Expression of typical FDC related genes by FL-YB cells

Next, the expression of characteristic FDC related genes by FL-YB cells was characterised by quantitative real-time PCR (qPCR). For comparison the expression levels of the same transcripts were also measured in Raw264.7 cells, which are a virus transformed murine macrophage cell line (Raschke et al., 1978). Raw 264.7 cells were chosen for comparison here because many of the functions of FDCs are immunological so it was logical to compare the gene expression levels of FL-YB to another immune cell type. One of the most typical markers of FDCs, MFGE8, has also been described to be expressed by macrophages under certain conditions (Aziz et al., 2008; Miksa et al., 2007).

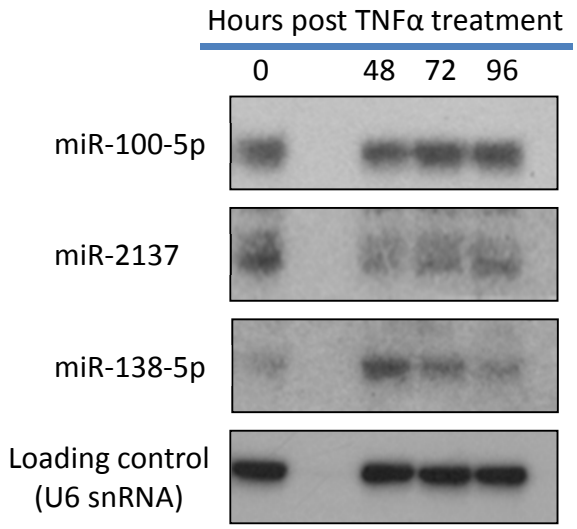

Figure 5.1 Expression of miRNAs identified from *in vivo* analysis by FL-YB cells. FL-YB cells were cultured for 4 days without TNFα before being harvested and plated out in a 6-well plate with 5ng/ml of TNFα. Cells were harvested 48, 72, or 96 hours later for RNA. 3µg of the resulting RNA was used for miRNA northern analysis. LNA/DNA probes against the full length miRNAs were radiolabelled before being hybridised to the membrane. The loading control is the snRNA U6.

FL-YB and Raw 264.7 cells were grown in 6-well plates in the appropriate complete media (see materials and methods section 2.11). The cells were harvested 48 hours later and RNA extracted. After purification 5ug of RNA was used to synthesise cDNA. This cDNA was used in qPCR assays with primers designed to amplify *Mfge8, Prnp, Vcam-1* and *Ltβr* (Figure 5.2)which are all typical markers of FDCs (Kranich et al., 2008; Brown et al., 1999; van Dinther-Janssen et al., 1991; Murphy et al., 1998). MFGE8 is secreted by FDCs and opsonises apoptotic cells for engulfment by macrophages (Kranich et al., 2008). The prion protein, PrP^c (encoded by *Prnp*), has an unknown function but it has been shown that expression of PrP^c by FDCs is obligatory in FDC for prion infection (McCulloch et al., 2013).

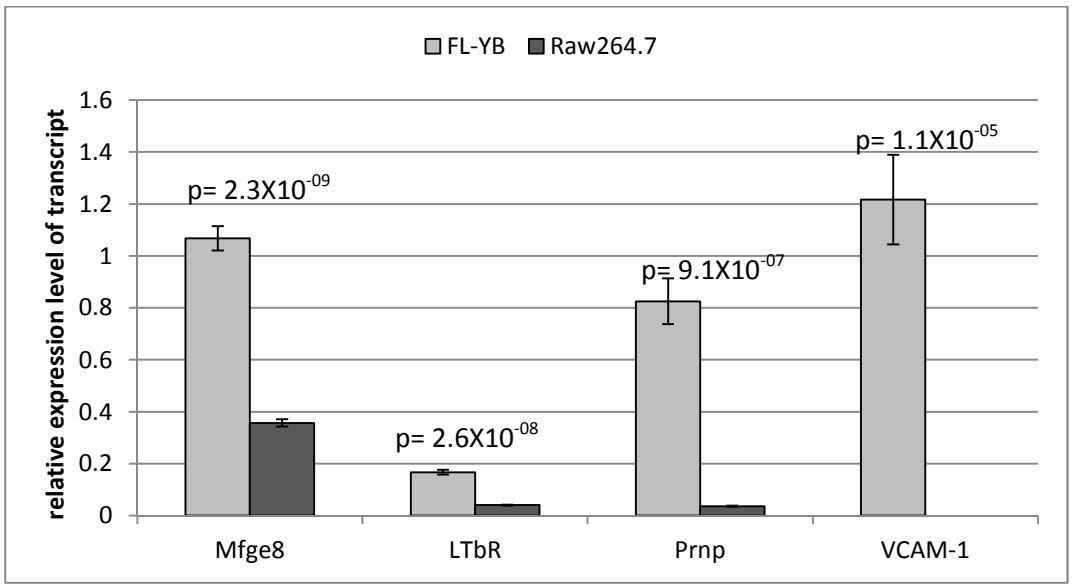

Figure 5.2 Expression of typical FDC markers in FL-YB and Raw264.7 cells. Quantitative real-time PCR was carried out on cDNA created from RNA extracted from FL-YB and Raw264.7 cells. Light grey bars = FL-YB cells, Dark grey bars = Raw264.7 cells. Ct values were normalised against HPRT levels in the same samples and are displayed relative to the normalised Ct value for *Mfge8* in one of the four independent experiments carried out. P values were calculated by independent student's t-tests. The transcripts were seen to be expressed at statistically significantly higher levels in FL-YB cells compared to Raw 264.7 cells.

Vascular cell adhesion molecule 1 (encoded by *Vcam-1*) is an adhesion molecule expressed on the surface of FDC that is bound by the VLA-4 intergrin on B-cells, preventing the apoptosis of the B-cells (Koopman et al., 1994). LTβR signalling as previously described is needed for maintenance of mature FDC networks. The expression levels of these four typical mature FDC markers were as expected shown by t-test to be significantly higher in FL-YB cells when compared to Raw 264.7 cells (Figure 5.2). In the case of *Vcam-1*, expression was undetectable in the Raw264.7 cells. These data show that FL-YB express abundant levels of typical FDC-related genes *Mfge8*, *Prnp*, *Vcam-1* and *LTβR*.

5.3.3. The effect of different activation stimuli on gene expression

To assess the effect of different stimuli on FL-YB cells the expression levels of genes that are known to be up-regulated in activated FDC was measured. Treatments were

carried out in 6-well tissue culture plates. Individual wells were either not supplemented, or supplemented with 5ng/ml TNFα, both 5ng/ml TNFα and 5ng/ml IL-4, or both 5ng/ml TNFα and 2.5μg/ml anti-LTβR. Cells were cultured with these treatments for 96 hours before being harvested for RNA. 2μg of RNA was used to create 15ul of cDNA for qPCR analysis. Each treatment was carried out twice independently of the other. This meant that statistical analysis was not possible however the results from the two independent experiments were seen to correlate well indicating a biological trend with each treatment.

IL-6 has been described to be produced by immune complex activated FDCs (Wu et al., 2009) and plays a role in IgG responses and somatic hypermutation (SHM). In line with previous findings in FL-Y cells (Nishikawa et al., 2006), the level of expression of the *Il-6* transcript was seen to be enhanced ~3-fold in the FL-YB cells by TNFα treatment (Figure 5.3a). The addition of IL-4 to FL-YB cells cultured in the presence of TNFα further increases the expression of *Il-6*, whereas addition of agonistic LTβR MAb causes no enhancement of *Il-6* expression.

IL-15 is another cytokine that is produced by FDC and acts to up-regulate proliferation of germinal centre B cells (Park et al., 2004). It also acts in a positive feedback loop to enhance both proliferation and chemokine secretion of FDC (Gil et al., 2010). TNFα treatment of FL-YB cells caused no change in the expression level of *Il-15* however the addition of IL-4 caused a moderate increase in expression of *Il-15* (Figure 5.3b). Additional LTβR signalling had no substantial effect on *Il-15* expression levels.

The integrin VCAM-1 has been described to be up-regulated on FDCs upon germinal centre formation (Balogh et al., 2002) and immune complex-mediated activation (Wu et al., 2009). In FL-YB cells it was found that *Vcam-1* expression was slightly increased

upon treatment of cells with TNFα and further up-regulated upon additional treatment of the cells with agonistic antibody to LTβR (Figure 5.3c).

Cyclooxygenase 2 (encoded by *Ptgs2*) is an enzyme that converts arachidonic acid to PGH2 which is then converted into prostaglandis or prostacyclin, a process which has been described in human FDCs (Lee et al., 2007, 2008; Cho et al., 2011a). Prostacyclin is involved in various roles including control of T cell numbers (Lee et al., 2005) and enhancement of B cell antigen presenting capability (Kim et al., 2012a). Here, the expression of Ptgs transcripts (1 and 2) were assessed by qPCR and it was found that expression increases two-fold in FL-YB cells treated with TNFα compared to cells given no supplements. Again it was also seen that the addition of IL-4 to the cultures further increases the expression levels of Cox transcript (Figure 5.3d). Expression levels of the prostacyclin receptor (*PtgiR*) in FL-YB cells were seen to increase (> 2-fold) in cultures treated with TNFα. Once more the addition of IL-4 to the cultures was seen to further enhance *PtgiR* expression levels, while LTβR signalling had no further effect (Figure 5.3e).

Toll-like receptor 4 (*TLR4*), the receptor for the endotoxin lipopolysaccharide, has been described to be expressed by FDCs *in vivo*(El Shikh et al., 2007b; Garin et al., 2010; Milićević et al., 2011) and TLR4 signalling has been shown to up-regulate various markers of FDC activation (El Shikh et al., 2007b). Here, it was found that although there was no substantial increase in *Tlr4* transcription by FL-YB cells treated with TNFα, the addition of IL-4 to the cultures increased *Tlr4* transcription ~3-fold. The addition of TNFα and LTβR MAb had no further effect on *Tlr4* levels compared to TNFα alone (Figure 5.3f). Overall this data suggests that culture of FL-YB cells in the presence of TNFα increases the expression of several genes that are related to FDC activation. For many of these transcripts, the addition of IL-4 to cultures further increased

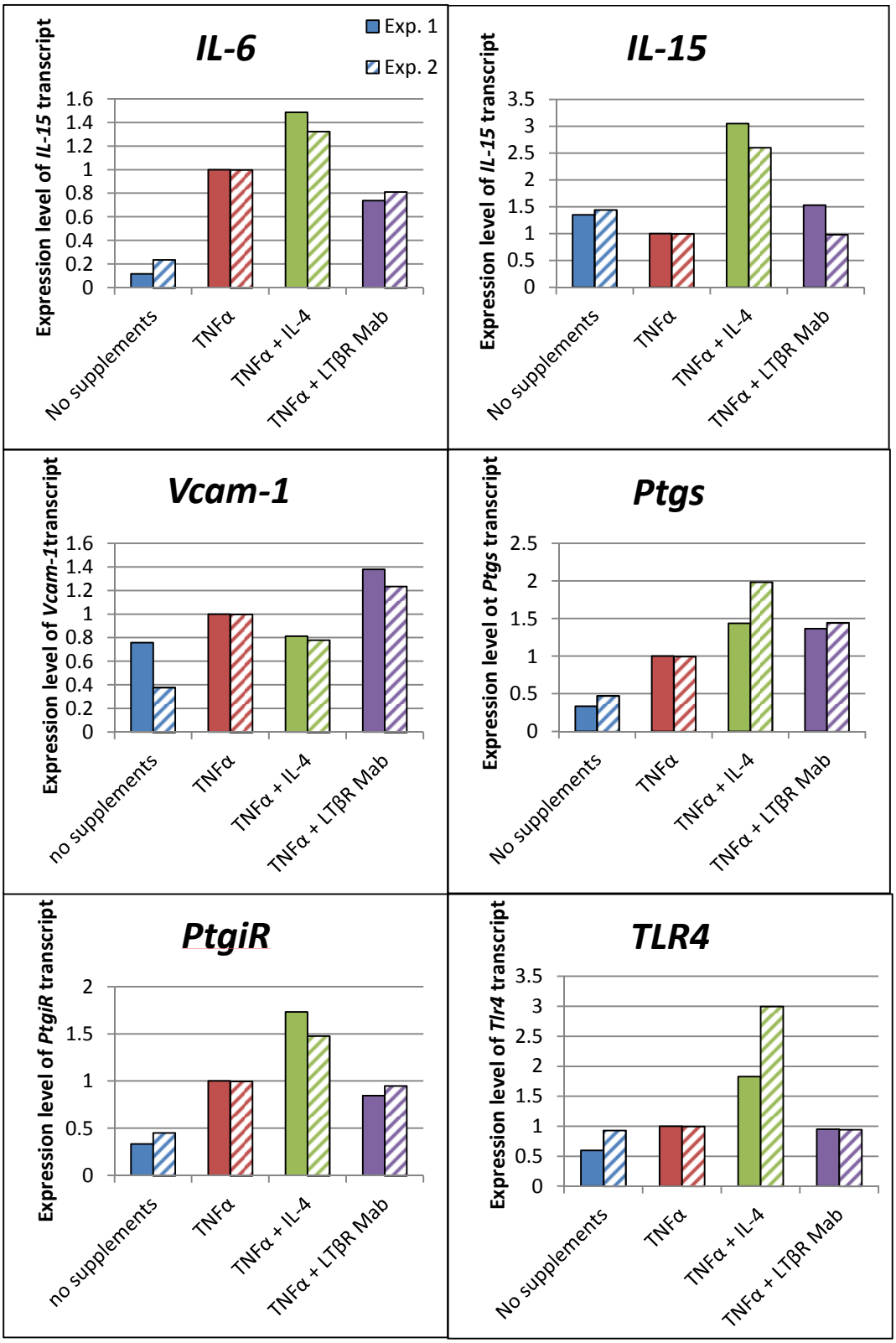

Figure 5.3 The effect of various external stimuli on the expression level of typical FDC transcripts in FL-YB cells. FL-YB cells were grown in 6-well plates in complete media alone, or supplemented with TNFα at 5ng/ml, TNFα and IL-4 both at 5ng/ml, or TNFα at 5ng/ml and agonistic anti-LTβR at 2.5µg/ml. Cells were cultured under these conditions for 96 hours before being harvested for RNA. cDNA was synthesised from 2µg RNA, and qPCR was carried out on the cDNA using primers specific for the indicated transcripts. Bars indicate the mean of three technical replicates in each of the two experiments shown. Once Ct values were normalised to the housekeeping gene beta-actin, the levels of each transcript are shown relative to the level of the transcript in TNFα treated cells within each experiment.

expression levels, suggesting further activation of the FL-YB cells. Additional signalling through the LTβR caused more subtle effects on most of the genes examined, perhaps because there is some redundancy between TNFR1 and LTβR signalling.

5.3.4. Growth and morphological characteristics of FL-YB cells

Next, normal growth and morphology characteristics of the FL-YB cell line were investigated under steady-state conditions. To gain real time measurement of FL-YB cell growth and morphology, the Roche xCELLigence system was used. FL-YB cells were plated out into a 96-well xCELLigence E-plate at a density of 4,000 cells/well. Cells were grown in complete media and half the wells were supplemented with 5ng/ml TNFα. Cells were analysed for approx. 8 d. Figure 5.4 shows the cell index plot from this experiment. It can be seen that the cell index measurement is enhanced with the addition of TNFα to the FL-YB cell cultures, indicating that TNFα enhances FL-YB cell survival, proliferation or adhesion.

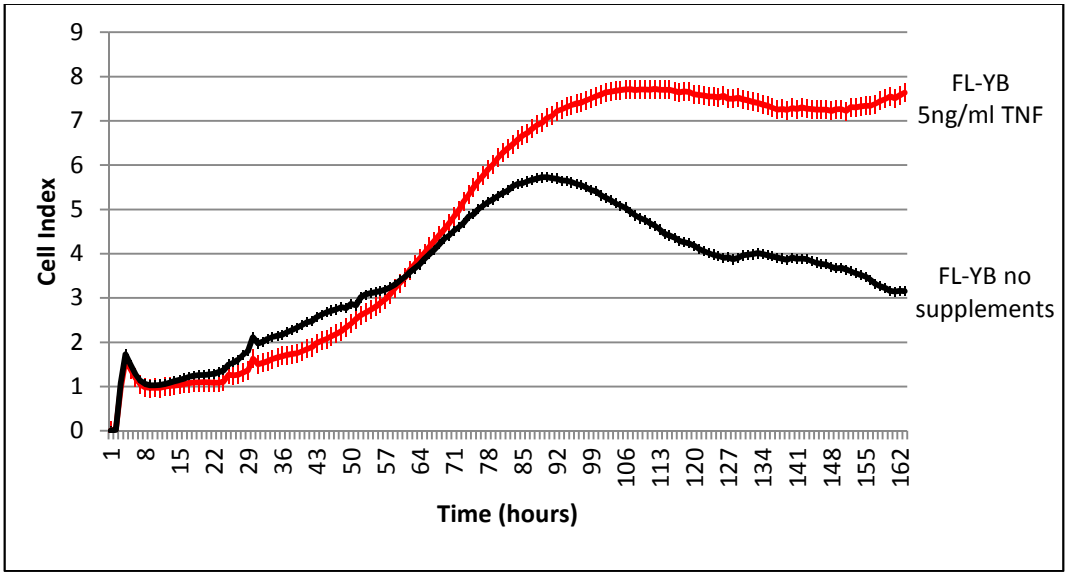

Figure 5.4 The growth and morphology profiles of FL-YB cells measured by the xCELLigence system. Cells were grown with or without TNFα supplementation in a 96-well E-plate and monitored using the xCELLigence system**.** The addition of TNF to FL-YB cell cultures was seen to facilitate a sustained higher cell index measurement. This indicates greater growth, survival, adhesion or spreading of the cells in the presence of TNFα. The lines indicate the mean of 8 replicates on the same plate with standard deviation indicated.

To assess whether the effect of TNFα treatment is a general effect which would occur with other stromal cell types, the xCELLigence profiles of FL-YB cells were compared to those of NIH 3T3 cells, an embryonic fibroblast cell line (Todaro and Green, 1963). Cells were plated out into a 96-well xCELLigence E-plate at a density of 4,000 cells/well. The wells for the NIH 3T3 cells were coated with fibronectin (section 2.11) as in its absence a very low cell index was observed. Cells were grown in the recommended media and parallel wells for each cell type were supplemented with 5ng/ml TNFα. Figure 5.5 shows the cell index plot from this experiment. Unlike in FL-YB cells (Figure 5.5a), the 3T3 cells do not respond with a positive increase in cell index measurement when supplemented with TNFα (Figure 5.5b). Further, when supplemented with TNFα, the FL-YB cells reach a much higher cell index than the 3T3 cells (Figure 3.4a). The higher cell index value seen with the FL-YB cells in response to TNFα is likely to be due to these cells being a larger, more adherent cell type than 3T3s. Overall, these data indicate that the FL-YB cells are responding in a positive manner to TNFα as expected for FDCs. Furthermore, this response was specific to the FL-YB cells suggesting they are a useful model to study FDC *in vitro*.

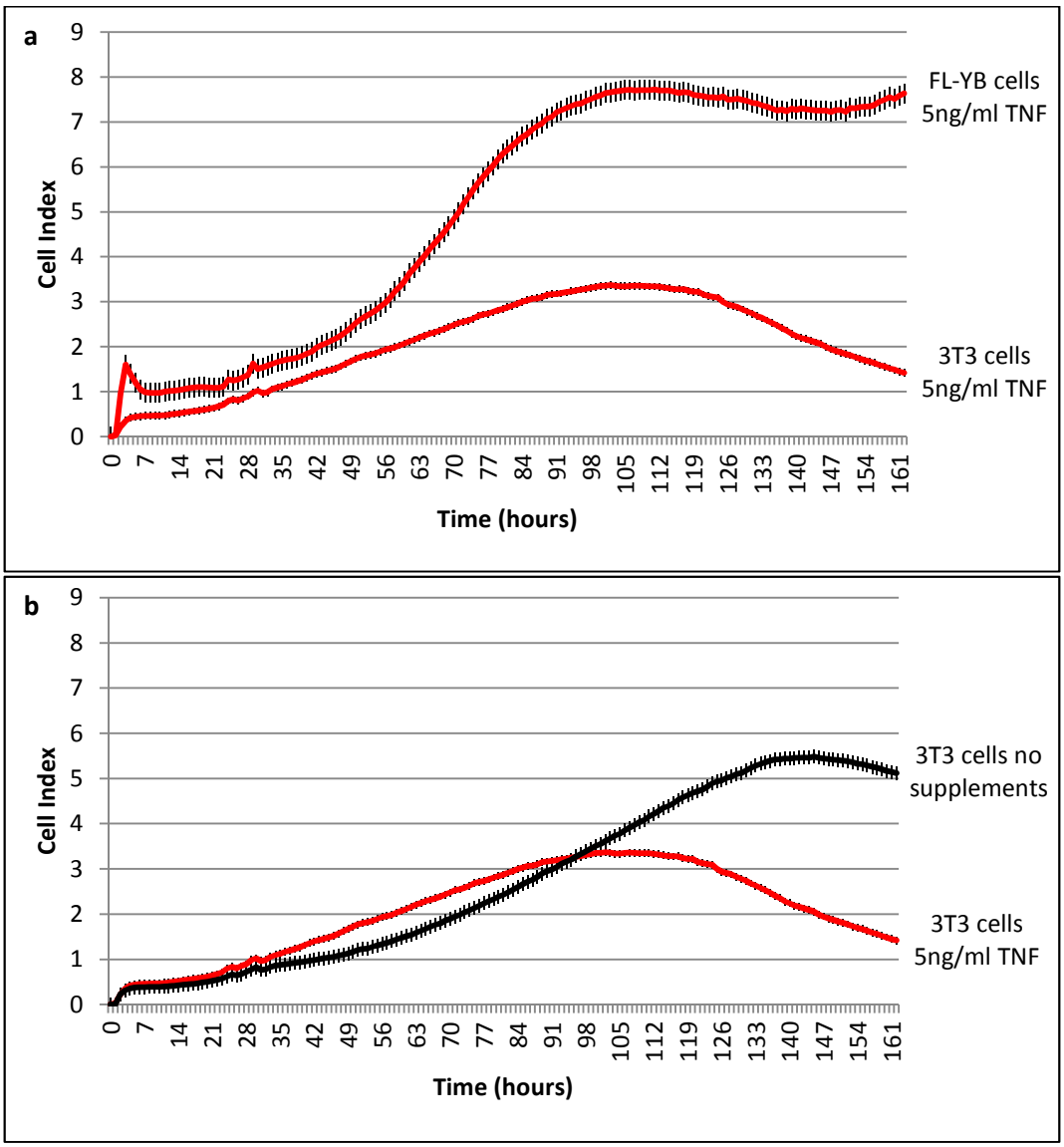

Figure 5.5 Comparison of the growth and morphology of FL-YB cells and NIH3T3 cells. Cells were grown with (top graph) or without (bottom graph) TNFα supplementation in a 96-well E-plate and monitored using the xCELLigence system**.** FL-YB cells are seen to have a much higher cell index compared to 3T3 cells, indicating a larger/ more adherent cell type. The addition of TNF to 3T3 cell cultures resulted in a lower cell index with an earlier decrease which is the opposite effect to that seen on the FL-YB cells. This indicates that FL-YB cells thrive in the presence of TNF, but that this is not a general effect of TNF on all cell types. Lines shown indicate the mean of 4 replicates from the same plate with standard deviation indicated.

5.3.5. Response of FL-YB cells to different activation stimuli

The obvious response of the FL-YB cells to TNFα treatment seen from the cell index measurement opened up the possibility of being able to use this as a way to measure cell response to other treatments that have previously been described to affect FDCs. Experiments were set up as before (section 5.2.4). Cells were grown in complete media, supplemented with 5ng/ml TNF, 2.5μg/ml agonistic LTβR MAb, 5ng/ml TNFα and 2.5μg/ml LTβR MAb, 5ng/ml TNF and 5ng/ml IL-4 or 5ng/ml TNF and 100ng/ml LPS (8 replicate wells with each treatment). The experiment was repeated three times, the curves in Figure 5.6 represent the mean and standard error of these three experiments.

The cell index measurements from the differentially treated FL-YB cells reveals that the agonistic anti-LTβR in these experiments does not have the same sustaining effect on the cell index measurement as TNFα treatment does (Figure 5.6a). Furthermore, cells treated with both TNFα and anti-LTβR do not show the same sustained cell index profile that cells treated with TNFα alone, indicating that although the TNFα and anti-LTβR both ultimately result in NFκB activation, the different modulation of this through the two receptors also affects the ultimate cellular response.

LPS has been shown to enhance accessory activity of FDCs *in vivo* (El Shikh et al., 2007b). TNFα and LPS have also been described to similarly up-regulate the expression of prostaglandins by HK cells *in vitro* whereas IL-4 abrogates this up-regulation of prostaglandins (Lee et al., 2008). LPS treatment (Figure 5.6b) does not afford any further effect on the cell index measurement when the cells are treated with TNFα and LPS than when treated with TNFα alone.

The IL-4 treatment has a dramatic effect upon the cell index measurement at later stages of monitoring. As seen in Figure 5.5c after approx. 90 hours of culture a sharp decrease in cell index occurs in the TNFα and IL-4 treated cells compared to those

treated with TNFα alone. IL-4 has previously been described to enhance the proliferation of the human FDC-like cell line HK (Lee et al., 2003a). It is not clear from this experiment if this dramatic decrease in cell index is due to cell death, or change in cell morphology or adherence (see section 5.2.6).

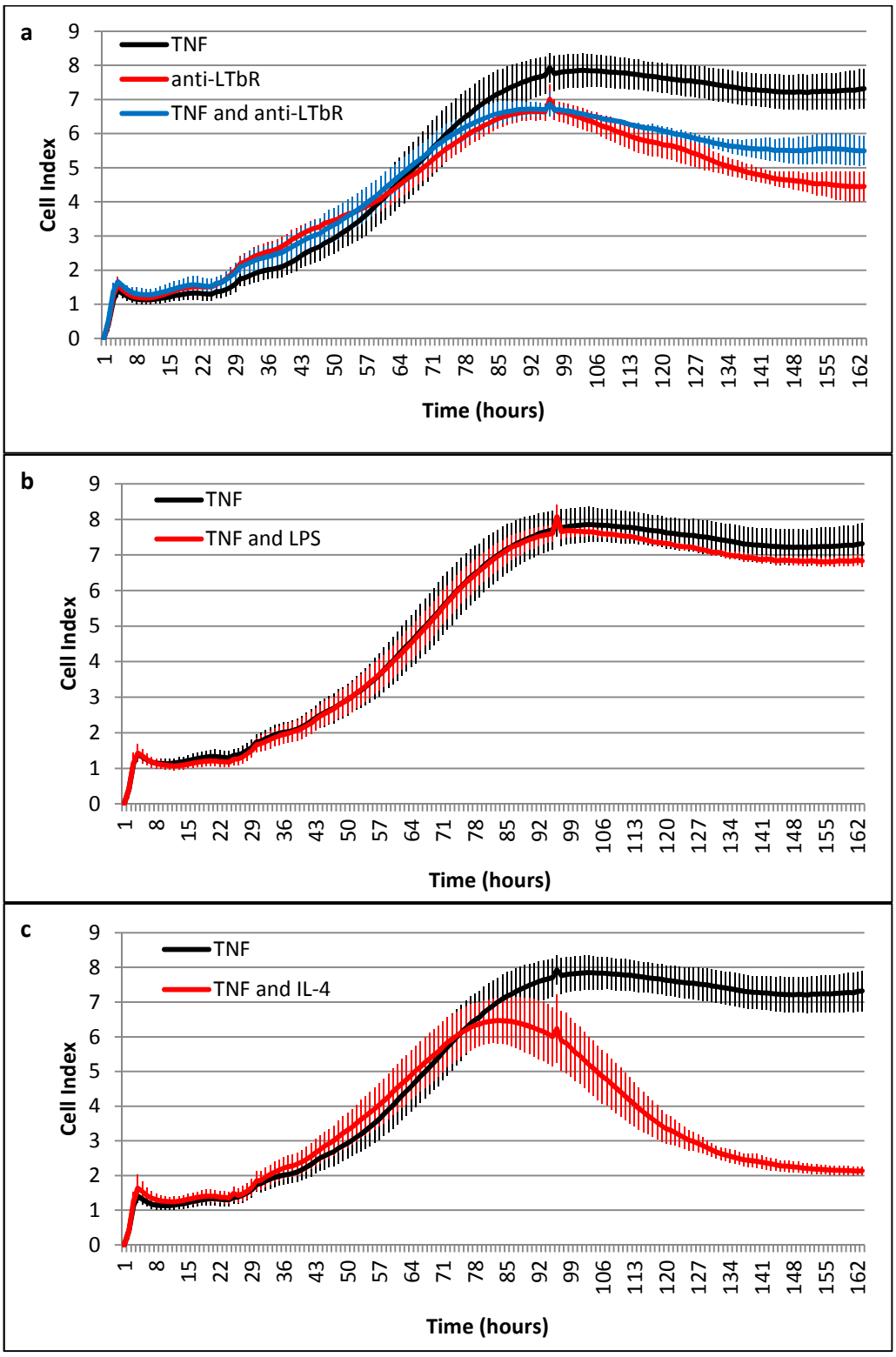

Figure 5.6 The response of FL-YB cells to various external stimuli. FL-YB cells were grown in a 96-well E-plate and monitored on the xCELLigence system. Cells were treated as indicated and any difference in cell index measurement from the normal growth conditions (5ng/ml TNFα) was noted. Curves represent the mean of three independent experiments (each with 6 replicates) with error bars showing standard error of the mean.

5.3.6. The effect of IL-4 treatment on FL-YB cells

To investigate the possibility of the sudden decrease in cell index seen in the FL-YB cells treated with IL-4 being due to cell death or decreased proliferation, the cell viability was measured using the CyQUANT® direct cell proliferation assay (Life Technologies). FL-YB cells were either grown in complete media with no supplements, with 5ng/ml TNFα, with 5ng/ml of IL-4, or with both TNFα and IL-4. Measurements were taken every 24 hours for 6 days. Each treatment was performed in quadruplicate for each time point. Figure 5.7 shows the average fluorescent reading from three independent experiments. A two-factor analysis of variance indicated that there is no difference in the fluorescent intensity (and therefore live cell number) between any of the treatments at the respective time points. This reveals that the sudden drop in cell index value seen at later time points in the TNF and IL-4 treated cells was not due to death or a loss of proliferation of the cells.

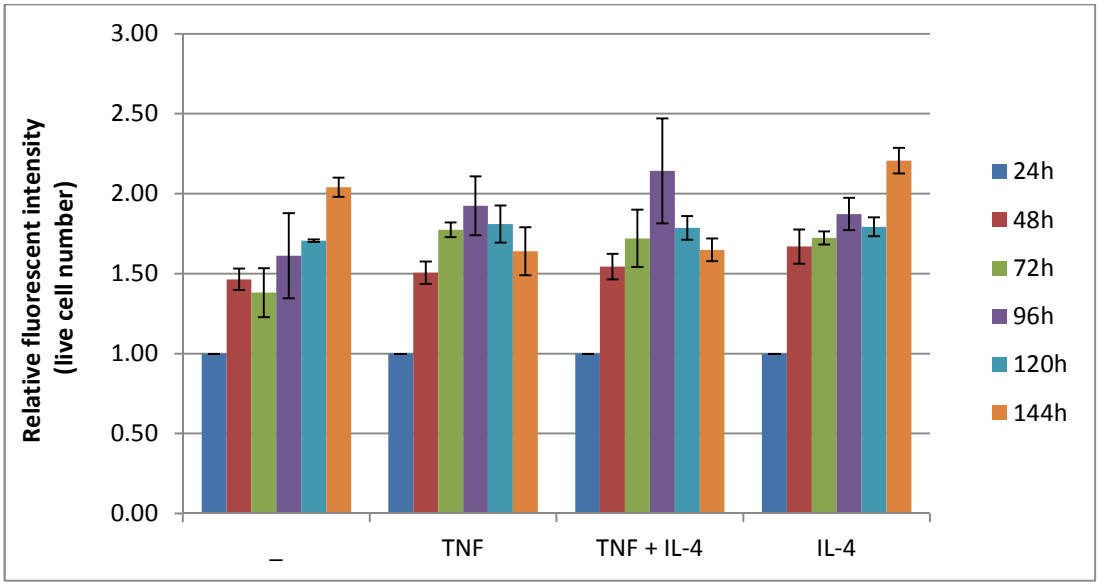

Figure 5.7 Measurement of live cell numbers after treatment of FL-YB cells with TNF and/ or IL-4. Cells were grown in 96-well plates under the indicated conditions before a cyQUANT cell proliferation assay was carried out. No statistical significance was found by paired student's t-test in the measured fluorescent intensity between any of the treatment groups at 72, 96 or 120 hours. A drop in cell index is generally seen between 60 and 80 hours in the TNF and IL-4 treated group as measured on the xCELLigence system. This shows that the drop in cell index seen is not caused by a decrease in live cell number.

To investigate whether this effect of IL-4 is cell density dependent, cells at two different densities were monitored by the xCELLigence system. Figure 5.8 shows that the effect that IL-4 confers on cell index value at later stages is cell density dependent, with cells plated at a higher density displaying the phenotype sooner than those plated at lower densities.

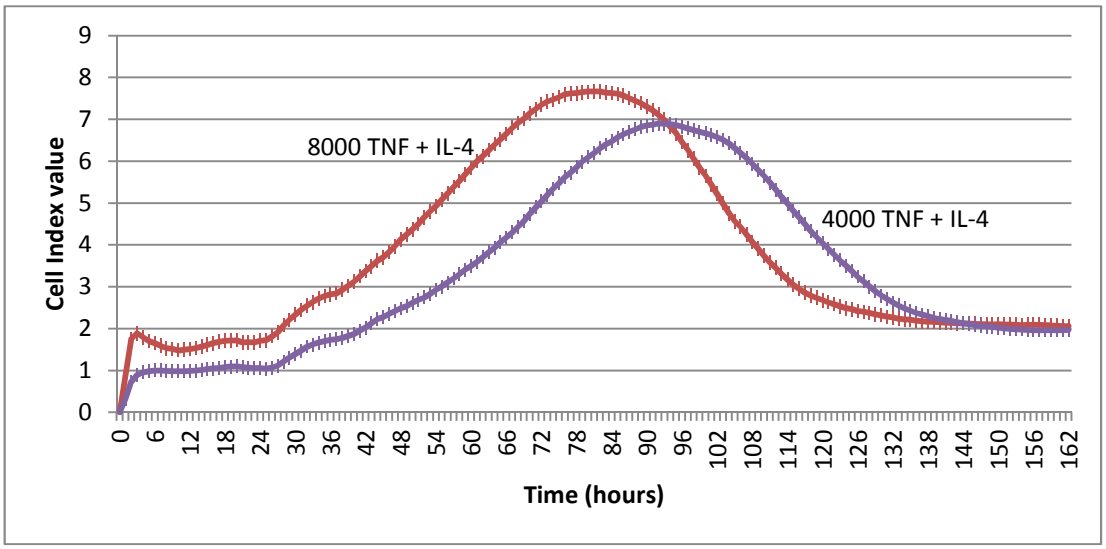

Figure 5.8 The effect of cell density during IL-4 treatment of FL-YB cells. Cells were plated at either 4,000 or 8,000 cells per well and treated with 5ng/ml TNFα and IL-4. Cells were monitored over 7 days. Cells plated at a lower density (purple curve) underwent the sudden drop in cell index at a later time point than the cells plated at a higher density (red curve) indicating that this effect is cell density –dependent. Lines indicate the mean of 8 replicates, from the same plate, with standard error of the mean shown.

Similar experiments were conducted to look into the effect of different doses of IL-4. Figure 5.9a clearly shows that the effect of IL-4 treatment on FL-YB cells is dose-dependent. Figure 5.9b shows that the maximal effective dose is between 20 and 40ng/ml. Figure 5.9c shows that the addition of IL-4 to FL-YB cells that were grown without TNFα has no substantial effect on the cell index measurement. This indicates that TNFα creates a phenotype in the FL-YB cells that IL-4 changes.

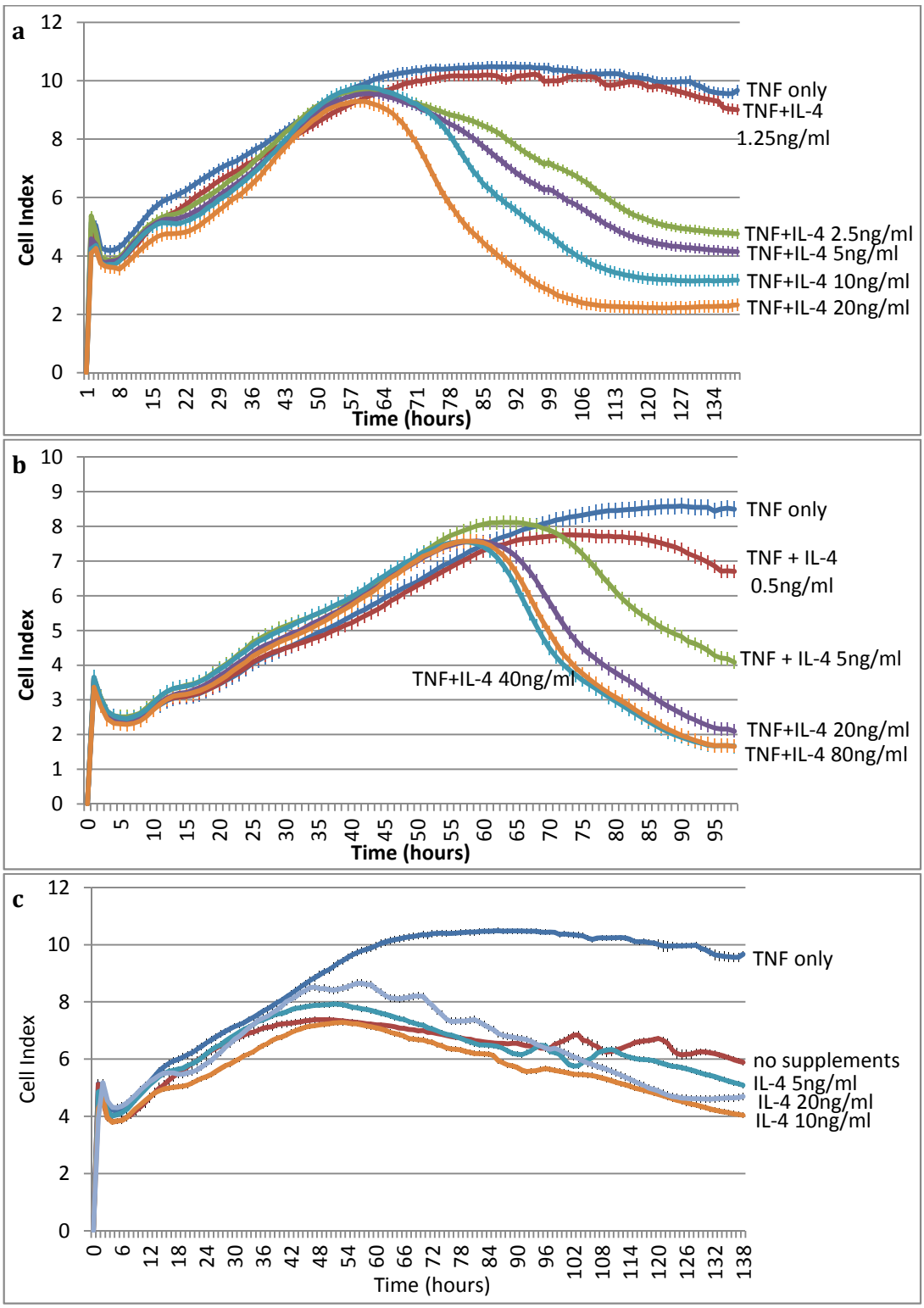

Figure 5.9 FL-YB cells respond in a dose dependent manner to IL-4 treatment and the response is TNFα-dependent. Cells were grown in 96-well E-plates and monitored using the xCELLigence system. Increasing doses of IL-4 caused a correspondingly sharper decrease in the cell index measurement from around 60-65 hours (a). The maximal effect of IL-4 is seen between 20 and 40ng/ml (b). The response to IL-4 is dependent on TNFα (c). Lines represent the mean of 8 replicates from the same plate, with standard error of the mean indicated.

Live cell imaging was carried out to try and see if there were any changes in cell morphology that could explain the drop in cell index seen. Cells were plated out at high density, one well was supplemented with 5ng/ml TNFα and the other with 5ng/ml TNFα and IL-4. Images were taken at the same point of both wells every 5min, 10 min or 30 min, in a series of movies captured over a period of 5 days. No obvious difference in morphology was seen between the cells with the two different treatments. Images taken from 74.5 hours to 92.5 hours suggest that the cells treated with TNFα and IL-4 do not have such a flat morphology compared to those treated with TNFα only. Cells treated with TNFα and IL-4 also looked to be more granular than those treated with TNFα alone.

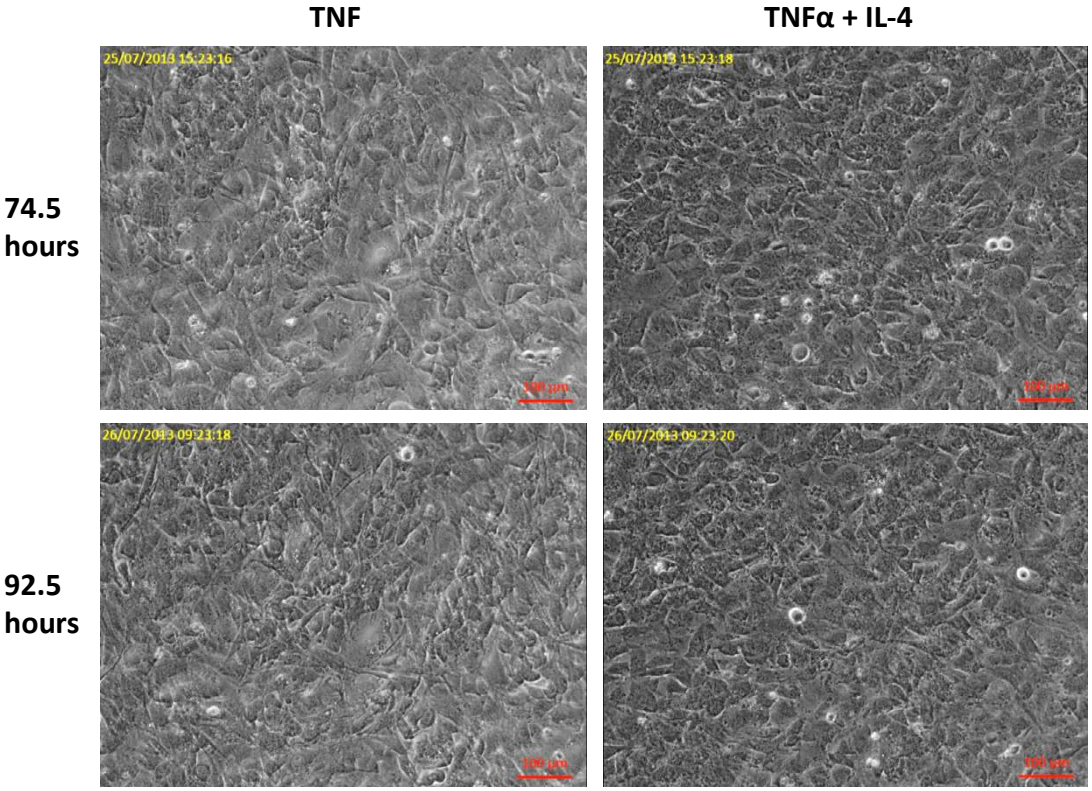

Figure 5.10 The effect of IL-4 on FL-YB cell morphology. A slightly flatter morphology of cells treated with TNFα only was observed. Additionally a slightly more granular appearance was apparent for cells treated with TNFα and IL-4 compared to those treated with TNFα only.

5.4. Discussion

In this chapter it was shown that the miRNAs selected for further study were expressed at easily detectable levels in the FL-YB cells. These miRNAs were identified from the *in vivo* model of FDC de-differentiation and confirmation of their expression in FL-YB cells indicated that the model successfully identified miRNAs that were expressed in FDCs. The observations that FL-YB cells expressed typical markers of FDC, including *Mfge8, Prnp and Vcam-1*, at considerably higher levels than Raw 264.7 cells , and the xCELLigence data that showed a positive response of the FL-YB cells, but not NIH-3T3 cells, to TNFα indicated that the FL-YB cells were a good *in vitro* model for FDCs.

Gene enrichment analysis on genes predicted to be targeted by at least one of the three miRNAs, revealed enrichment for genes involved in cell migration, locomotion, regulation of proliferation and cell to cell communication. For this reason it was decided to use the Roche xCELLigence system in loss- and gain-of-function of miRNA experiments. By measuring electrical impedance caused by cellular attachment to electrodes on the bottom of the wells of a specialised tissue culture plate, the system gives a measure of the cell number, size, any changes in morphology and adherence of cells. xCELLigence measurements under normal conditions were first characterised and then the response to some further activation stimuli was also assessed using the system. These measurement will provide a basis for miRNA gain- and loss-of-function studies.

An obvious signalling/ activation pathway that the miRNAs would be likely to play a role in is LTβR signalling, as they were identified *in vivo* following blockade of this pathway. Supplementing the cells with 2.5μg/ml of an agonistic LTβR MAb (as used in (Magari et al., 2011)) resulted in a slightly lower cell index value at later time points than that seen from cells supplemented with TNFα. This was not expected as it was

previously reported that TNFα and LTβR signalling synergistically increased FL-YB cell proliferation (Nishikawa et al., 2006). However because the xCELLigence cell index value is a measurement of a combination of different growth characteristics, the slightly lower cell index values seen with LTβR signalling could well indicate that the proliferation of LTβR MAb treated cells is enhanced, but this means that they will generally be slightly smaller and more rounded up with decreased adhesion to the plate. As the xCELLigence system is combining all these things in one measurement it could be that the cell index value is actually lower for cells that are proliferating more quickly.

LPS treatment did not alter the cell index value of FL-YB cells, LPS has previously been described to increase number and size of FDC *in vivo* (Milićević et al., 2011). This was in an *in vivo* situation and it is likely that the increase in number of mature FDC described could be due to maturation of immature cells, rather than proliferation of the existing cells.

IL-4 treatment had the most dramatic effect on cell index values, at later time points a significant decrease in cell index value was seen. It was found that this decrease in cell index was cell density dependent as when plated at higher densities the decrease occurred at an earlier time point. The effect was also IL-4 dose-dependent with a more pronounced decrease seen at higher doses of IL-4. IL-4 did not affect the cell index when the cells were not also treated with TNFα indicating that TNFα induces changes in the cells that are disturbed by IL-4. Cell proliferation assays revealed that the decrease in cell index was not due to a decrease in proliforation. This phenotype only occurred once cells were confluent making it difficult to assess cell morphology. Live cell imaging did suggest that TNFα and IL-4 treated cells were more granular and had a less flattened morphology than cells treated with TNFα alone. However because live

cell imaging was only performed once for one field of view, it is not possible to tell if this really is an effect of IL-4 treatment.

In order to look at the response to these activation stimuli at a molecular level, quantitative PCR was performed for a number of gene transcripts that have previously been reported to change in activated FDCs. Treatment of FL-YB cells with TNFα caused up-regulation of *IL-6*, *PtgiR* and Cox (*Ptgs2*). IL-6 is known to be important in regulation IgG responses (Deng et al., 2002) as it induces T-cells to produce cytokines such as IL-4 and IFN-γ which then induces isotype switching to IgG (Wu et al., 2009). Both PTGIR and PTGS are involved in the prostaglandin system, PTGIR is the receptor for prostacyclin while, cyclooxygenases (Ptgs1/2) are involved in the synthesis of prostaglandins. Prostaglandins can have wide ranging effects depending on the cytokine milieu. They can promote both survival and apoptosis of germinal centre B cells depending on other signals received by the B cells.

Addition of TNFα and IL-4 to cultures caused further up-regulation of *Il-6, Tlr4, PtgiR, Cox* and *Il-15*. IL-6 and IL-15 have previously been described to be up-regulated in immune complex activated FDC (Wu et al., 2009; Gil et al., 2010) and in HK cells treated with TNFα and LTα1β2 (Husson et al., 2000). The up-regulation of both of these cytokines in TNFα and IL-4 treated cells suggests that IL-4 is activating the FL-YB cells. In agreement with this is the up-regulation of *Cox, PtgiR* and *Tlr4* with TNFα and IL-4 treatment of FL-YB cells. The up-regulation of *Tlr4* following IL-4 stimulation is an interesting result because IL-4 decreases the expression of TLR4 on macrophages and PBMCs but it has been found that IL-4 causes up-regulation of TLR4 on B cells (Mita et al., 2002; Ganley-Leal et al., 2010). As FDCs are so closely associated with B cells it could be that the increase of TLR4 that is promoted by IL-4 has a role in the humoral immune response. Additionally the up-regulation of many genes at the transcript level

that indicate activation could also be a reason why cells treated with TNFα and IL-4 appeared more granular.

Only *Vcam-1* showed any increase in expression in FL-YB cells cultured with TNFα and agonistic LTβR MAb compared to cells cultured with TNFα alone. The cell adhesion molecule VCAM-1 is important for FDC-B cell synapse formation and prevention of GC-B cell apoptosis (Koopman et al., 1994) and up-regulation of VCAM-1 is often used as a marker of FDC activation (Balogh et al., 2002; El Shikh et al., 2007b).

The data in this chapter has shown that the FL-YB cell line will be a good model for functional analysis of the miRNAs identified from the *in vivo* model. FL-YB cells express miRNAs of interest at easily detectable levels, they also express many typical markers of FDC and respond positively to TNFα stimulation. Gene expression analysis has indicated that they are activated by TNFα, and further activated by the addition of recombinant IL-4. The phenotype induced in the FL-YB cells by TNFα is modified by IL-4 once the cells reach confluence. The FL-YB cells will be used in the next chapter for functional analysis of the selected miRNAs, using the phenotypes characterised in this chapter as base-line measurements.

CHAPTER 6: Identifying the potential role of selected microRNAs in follicular dendritic cell biology

Contents

Chapter 6: Identifying the potential role of selected microRNAs in follicular dendritic cell biology

6.1. Introduction

One method widely used for functional analysis of miRNAs is the analysis of a biological system after loss-of-function of the miRNA(s) of interest, and conversely after overexpression of the miRNA(s) of interest (Martinez-Sanchez and Murphy, 2013).

The nature of loss and gain of function studies means that phenotypic studies can be carried out to determine what biological processes the miRNA(s) of interest might be involved in (Wang et al., 2008b; Elia et al., 2009; Akhtar et al., 2010). In chapter 5 a number of cellular phenotype signatures for the FL-YB cells were established using the xCELLigence system as a measure of these (section 5.2.5). In this chapter any deviation from these signature phenotypes will be assessed following knock down or overexpression of the miRNAs identified to be expressed in the FL-YB cell line (section 5.2.1). The aim was to give a broad indication of the types of cellular processes that the miRNAs may help regulate.

More specific analyses after gain-or loss-of-function studies involve analysis of effects on gene and protein expression levels. The targeting of a gene transcript by miRNA(s) may also cause changes in expression level of the transcript (Lim et al., 2005; Valencia-Sanchez et al., 2006). This means the expression level of mRNA after miRNA knockdown or overexpression can often reveal miRNA regulated genes. Often the gene targets identified in this manner are relatively strongly suppressed by the miRNA of interest (Baek et al., 2008; Selbach et al., 2008). Analysis of the transcriptome is often quicker and relatively inexpensive, making this a widely used method.

6.2. Aims

Using FL-YB cells as an *in vitro* model, the aim of this chapter was to identify the potential roles that the miRNAs identified in previous chapters have in FDC biology. To achieve this both miRNA loss- and gain-of-function studies were undertaken. The cell proliferation, morphology and adhesion were measured in cells with loss or overexpression of specific miRNAs using real-time cell analysis. The transcript levels of genes important to FDC function were also measured following specific miRNA loss or overexpression.

6.2. Results

6.2.1. Assessment of cytotoxicity of different transfection reagents on FL-YB cells

First, experiments were undertaken to determine how the FL-YB cells would respond to treatment with transfection reagents. The xCELLigence system was used to assess the effect of three different transfection reagents on the FL-YB cells; lipofectamine 2000, lipofectamine LTX and Fugene HD. FL-YB cells were plated out in a 96-well xCELLigence plate at a density of 4,000 cells/well. The cell index was measured overnight as the cells were left to adhere. Four replicate wells were then treated with either an anti-miR-294 LNA, or a transfection mix of Lipofectamine 2000 and the anti-miR-294 LNA, Lipofectamine LTX and the anti-miR-294 LNA or Fugene HD and the anti-miR-294 LNA. An anti-miR-294 LNA was used as this miRNA was not found to be expressed in the spleen samples. The cell index values were once again measured, after four hours before the transfection media was replaced with complete media supplemented with 5ng/ml TNFα. The plate was then monitored for another five days to assess any potential toxic effects of the transfection reagents on the cells. An uneven loss of cells was seen to occur during the two media replacements before and after the transfection. The cell index values were therefore normalised to the first cell index measurement after replacement of the transfection media. Figure 6.1 shows that there is no substantial difference in the cell index curves between any of the transfection reagents or the cells treated only with the LNA. These data suggest there is little toxic effect of any of the transfection reagents on the FL-YB cells. For all subsequent transfection experiments Lipofectamine 2000 was used.

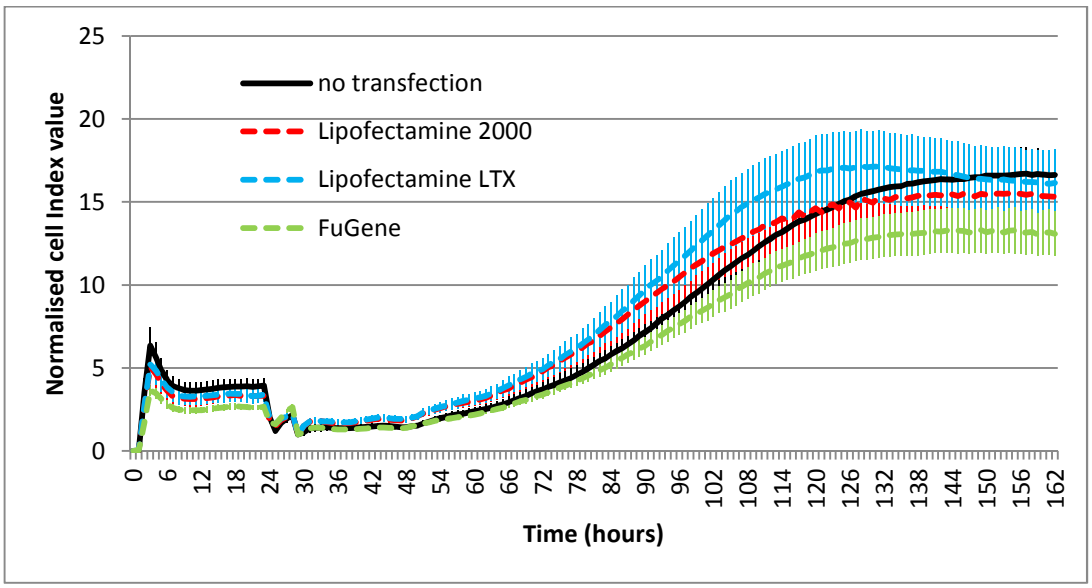

Figure 6.1 Transfection reagents are well tolerated by FL-YB cells. FL-YB cells were plated out at 4,000 cells per well in a 96-well xCELLigence plate after 24 hours the cells were transfected in quadruplicate with an anti-miR-294 LNA using the transfection reagents indicated for four hours before replacement of the media with complete media. The cells were monitored on the xCELLigence system for another five days. It can be seen that there was very little difference in the cell index curves indicating minimal cytotoxicity from any of the transfection reagents. Lines indicate the mean of 8 replicates from a single plate with the standard deviation indicated.

6.2.2. Assessment of the efficiency of miRNA knock down and over expression in FL-YB cells

To assess the efficiency of knock down and overexpression of the miRNAs, northern analyses were carried out on RNA collected from FL-YB cells that had been transfected with LNAs directed against miR-100-5p, miR-138-5p and miR-2137, or miRNA mimics for miR-100-5p and miR-2137. Cells were transfected for four hours before dilution of the transfection reagents with complete media and incubation for a further 24 hours. RNA was then harvested from the cells and 2µg used for miRNA northern analysis. Images of autoradiography films exposed to hybridised membranes and phosphoimager quantification data are shown in Figure 6.2. All miRNAs were found to be decreased by at least 80% when the specific anti-sense LNA was transfected. In contrast, the miRNA mimics caused at least a 5-fold increase in the amount of the specific mature miRNA detected by northern analysis.

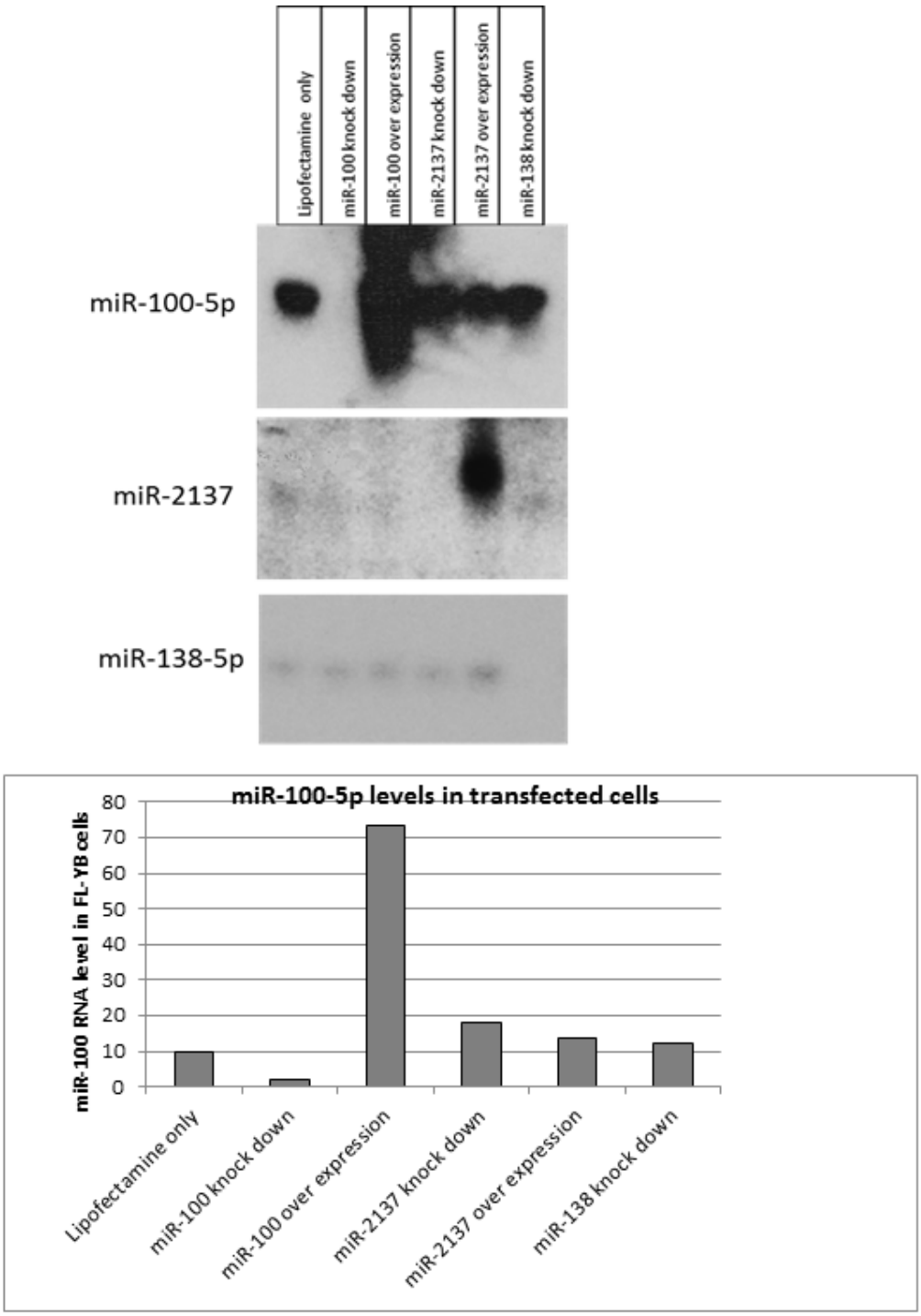

Figure 6.2 miRNAs are efficiently and specifically knocked down or overexpressed in FL-YB cells using anti-sense LNA oligonucleotides and miRNA mimics. Cells were transfected with either anti-sense LNA oligonucleotides for the miRNAs indicated to knockdown the miRNAs or double stranded RNA mimics to overexpress the indicated miRNAs. Cells were harvested 24 hours following transfection and 2ug of RNA from each sample was run on the gel for northern analysis. The LNAs caused efficient and specific knockdown of all the miRNAs whereas the mimics caused at least a 5-fold increase in the amount of mature miRNA detected. The graph represents phosphorimager quantitation of the miR-100-5p knock down and over expression, normalised to the lipofectamine control, indicating a 5-fold decrease in miR-100 upon following transfection of a specific LNA and a 7-fold increase in miR-100 following transfection of a specific mimic. No significant change in miR-100 levels were seen with other miRNA mimic or inhibitor transfection.

6.2.3. The effect of miRNA knockdown or overexpression on cell viability

After miRNA knockdown or overexpression in FL-YB cells, live cell numbers were assessed to determine whether the specific LNAs or mimics adversely affected cell proliferation or viability. FL-YB cells were plated out at 4,000 cells per well in a 96-well tissue culture plate and incubated at 37°C for 18 hours. The media was then replaced with transfection media: 100µl optiMEM with 15ρmol anti-sense LNA, or 2ρmol miRNA mimic and 1µl of lipofectamine 2000. Cells were incubated at 37°C for four hours before the transfection media was replaced with complete media. Live cell numbers were estimated using the Invitrogen CyQuant direct cell proliferation assay immediately or after 18 or 24 hours further incubation. This data is represented in Figure 6.3. Student's independent t-tests showed that only cells treated with miR-100 mimics or miR-2137 inhibitors had significantly different levels of fluorescence at the 24 hour time point ($p=0.0001$ and $p=0.017$ respectively). Overall, these data indicate that in general, transfection with LNA oligos or miRNA mimics is well tolerated by FL-YB cells. These results also indicate that miR-100-5p and miR-2137 may have an effect on cell viability and/or proliferation; further experiments were used to examine this over an extended time frame (section 6.2.5).

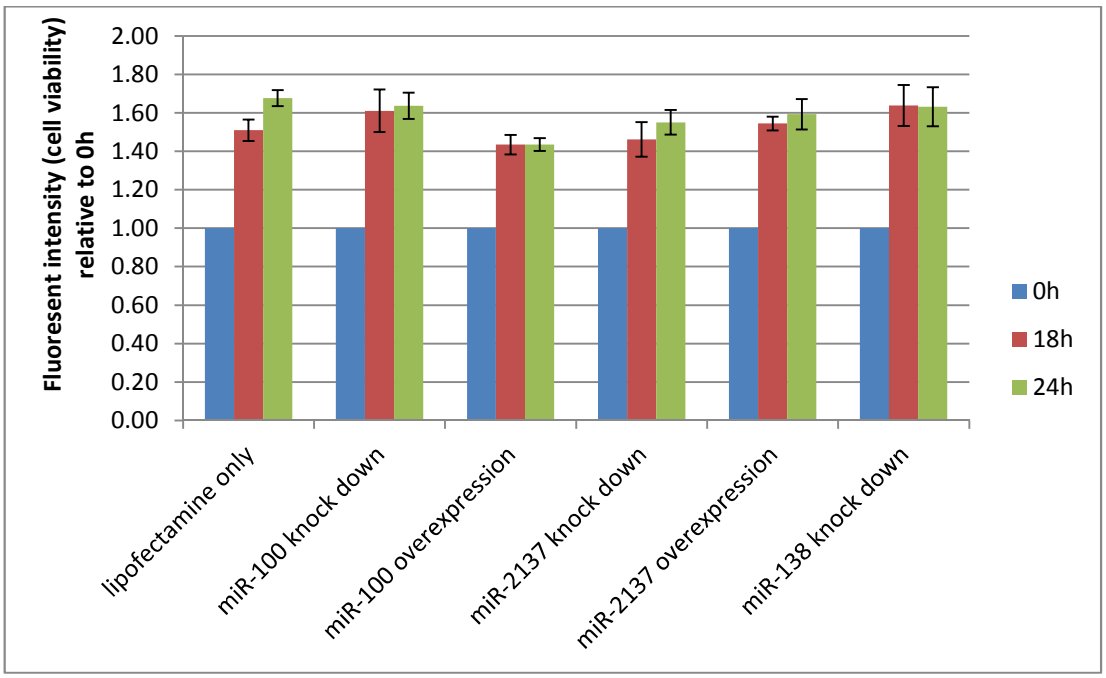

Figure 6.3 Knock-down or overexpression of miRNAs causes no significant change in cell proliferation or death. FL-YB cells were transfected with miRNA mimics or inhibitors as indicated. CyQuant direct cell proliferation assay was performed in quadruplicate for each treatment immediately following transfection and at 18 hours and 24 hours following transfection. The measured fluorescent intensity was normalised to that at the 0h time point for each transfection. The bars represent the mean of the four replicates with error bars indicating standard deviation. Student's independent t-test showed that miR-100-5p overexpression (P=0.0001) and miR-2137 knockdown (p=0.017) showed statistically significant difference from the lipofectamine control at 24 hours.

6.2.4. miRNA target prediction using web based algorithms

The three miRNAs that were selected for their pattern of decreased expression levels following the loss or absence of FDCs in LTβR-Ig treated or $LT\beta^{\Delta/\Delta}$ mice (miR-100-5p, miR-2137 and miR-138-5p) were all found to be expressed in FL-YB cells (Figure 5.1). Furthermore, it was shown that expression levels of these miRNAs could be successfully manipulated in FL-YB cells (Figure6.2). For these reasons, these three miRNAs were selected to carry out functional analysis using the FL-YB cells as a model system. To gain a more focused prediction of targets for just these three miRNAs, the data obtained from the web based algorithm predictions (section 4.2.4) for just these

three miRNAs was re-analysed. Those genes that were predicted to be targeted by one of the miRNAs by at least two of the four algorithms used were listed. This list of 319 genes was used as input for the gene enrichment software ToppFun (Chen et al., 2009). This analysis revealed that the top 20 biological processes that the genes were enriched for could be grouped into seven categories according to biological function 1) Chromatin functions, 2) Response to oxygen, 3) Axon and synapse regulation, 4) Cell motility, 5) Cell communication and signalling, and 7) protein modification (see table 6.1, genes in appendix C). As these three miRNAs showed a very similar pattern of expression in response to LTβR-Ig treatment and in the $LT\beta^{\Delta/\Delta}$ mice, it is plausible that they target the same pathways or the same genes. These gene lists were therefore cross referenced with each other to find any genes that were predicted to be targeted by more than one of these miRNAs. Five genes that were predicted to be targeted by two of the three miRNAs were found, and are set out in table 6.2. Four of the five genes in table 6.2 were either not expressed or expressed at very low levels in the gene expression array data from the untreated, LTβR-Ig treated and $LT\beta^{\Delta/\Delta}$ spleens (*Ace, Nox4, Rara, Shroom1*). One of the genes found not to be expressed was retinoic acid receptor alpha (*Rara*). This gene has previously been reported to be expressed in enriched populations of lymph node (LN) and Peyer's patch (PP) FDC (Suzuki et al., 2010). However, because of the lack of expression of this gene in any of the spleen samples, miRNA targeting of this gene in this system was unlikely. One, *Obfc2a* was expressed at moderate levels, the gene encodes for a protein that is a nucleic acid binding protein that forms part of a complex involved in DNA repair at the G2/M phase checkpoint (Richard et al., 2008). This is therefore unlikely to be something that is involved in FDC specific functions. It was therefore decided to try some broader functional studies using the Roche xCELLigence system. As mentioned many of the predicted targets of these miRNAs have roles in locomotion or cell proliferation,

changes in either of these should result is a different cell index profile when monitored on the xCELLigence system. It was therefore decided to carry out overexpression and knock down studies for the miRNAs in FL-YB cells and to monitor the cells using the xCELLigence system.

Go: Biological process	P-value	Hit	Total
chromatin modification	3.06E-06	24	435
response to decreased oxygen levels	6.71E-06	17	252
response to oxygen levels	1.43E-05	17	267
axon guidance	1.89E-05	20	360
regulation of synapse organization	2.36E-05	7	46
chromatin organization	3.01E-05	25	532
locomotion	5.02E-05	44	1253
regulation of synapse structure and activity	5.36E-05	7	52
positive regulation of cell communication	8.29E-05	33	854
regulation of cell proliferation	1.39E-04	41	1189
histone methylation	1.51E-04	7	61
cell migration	1.62E-04	32	847
chromosome organization	1.71E-04	28	701
protein alkylation	1.77E-04	8	83
protein methylation	1.77E-04	8	83
axonogenesis	1.89E-04	23	527
positive regulation of intrinsic apoptotic signaling pathway	1.94E-04	4	16
regulation of mitochondrial membrane permeability	1.94E-04	4	16
positive regulation of protein oligomerization	1.94E-04	4	16
regulation of synapse assembly	2.31E-04	5	30

Table 6.1 The top 20 biological processes which genes predicted to be targeted by miR-100-5p, miR-138-5p or miR-2137 are most highly enriched for as analysed by the ToppFun software. The processes fit into seven main catagories 1) Chromatin functions, 2) Response to oxygen, 3) Axon and synapse regulation, 4) Cell motility, 5) Cell communication and signalling, and 7) protein modification.

mmu-miR-100-5p	mmu-miR-138-5p	mmu-miR-2137
	Ace (angiotensin I converting enzyme)	*Ace* (angiotensin I converting enzyme)
Nox4 (NADPH oxidase 4)		*Nox4* (NADPH oxidase 4)
Obfc2a (nucleic acid binding protein 1)	*Obfc2a* (nucleic acid binding protein 1)	
	Rara (retinoic acid receptor, alpha)	*Rara* (retinoic acid receptor, alpha)
Shroom1 (shroom family member 1)		*Shroom1* (shroom family member 1)

Table 6.2 Genes predicted to be targeted by two of the miRNAs confirmed to be expressed in FL-YB cells. Four target prediction programmes were used to predict gene targets for miR-100-5p, miR-138-5p and miR-2137. Listed are five genes that are predicted targets of two of the miRNAs, predicted by at least two of the four prediction programmes.

6.2.5. The selected miRNAs do not have any significant effect on growth, morphology or adhesion of FL-YB cells

CyQuant assays had previously indicated that miR-100-5p and miR-2137 may have an effect on cell viability and/or proliferation (Figure 6.3). It was therefore decided to monitor cell behaviour following knock down and overexpression of these miRNAs in FL-YB cells using the xCELLigence system. Since disproportionate cell loss occurred when the transfection media was changed it was decided to perform the transfections in 6-well plates and then subsequently transfer the transfected cells into the 96-well xCELLigence E-plates for monitoring. 8,000 FL-YB cells/well were plated into an xCELLigence E-view plate and grown in complete media in the presence of 5ng/ml TNFα. Cells were monitored over a five day period. Figure 6.4 shows the resulting cell index curves, from one representative experiment of four (at least 6 replicate wells in each experiment). The cell index values for each condition were normalised to the lipofectamine control and the mean value across the four experiments was taken for

each condition at time intervals of 6 hours. A two-way analysis of variance indicated no difference between any of the conditions over the four experiments (p=0.76).

Although the curves and cell index values were seen to be slightly different in each separate experiment, the values within each single experiment were very similar. This variation most likely reflects slight differences in the state of the cells at the time of analysis and small differences in the composition of the media used.

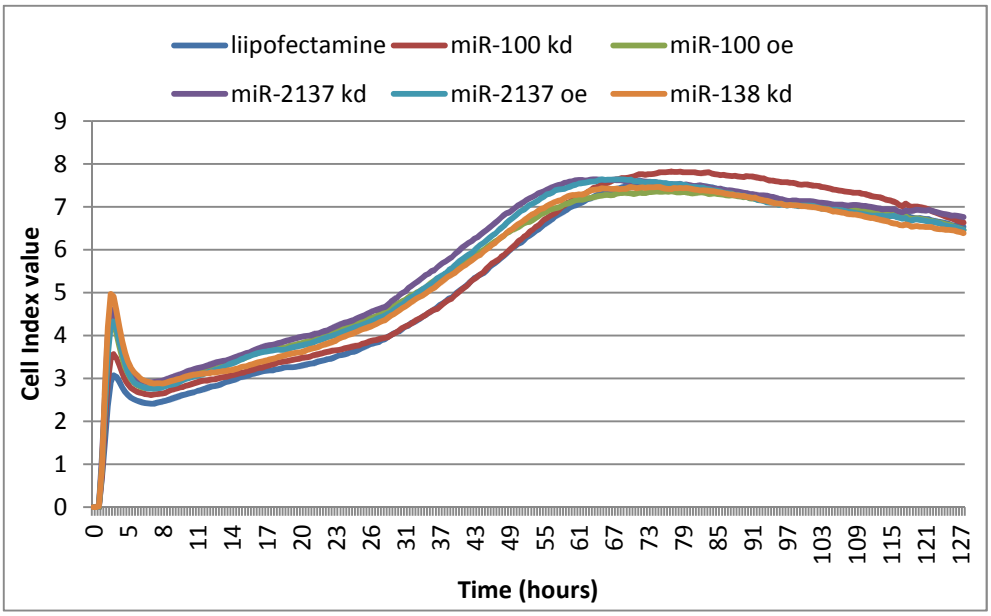

Figure 6.4 The effect on miRNA knock-down or over expression in FL-YB cells. Cells were transfected either with miRNA inhibitors or miRNA mimics, transfection media was diluted out after four hours of transfection. Cells were rested overnight before being plated out in complete media with 5ng/ml TNFα at a density of 8,000 cells per well in a xCELLigence 96-well E-view plate, which was placed on the xCELLigence system with a measurement taken every 30 minutes for approximately five days. This experiment was repeated 4 times with at least 6 technical replicates for every condition in every experiment. 2-factor ANOVA revealed no statistical significant differences between the any of the conditions (p=0.76).

6.2.6. The effect of miRNA knockdown and overexpression in FL-YB cells treated with IL-4

It has recently been proposed that the majority of miRNAs confer robustness of biological networks (Ebert and Sharp, 2012). This makes the identification of miRNAs

under steady state conditions difficult and many researchers have found that the role of miRNAs only become

apparent when the biological system of study is put under stress (Kagias et al., 2012; Sánchez-Jiménez et al., 2013). Although it is not clear what phenotype IL-4 is conferring upon the FL-YB cells, a dramatic and reproducible signature that was consistently observed (Figure 5.6). For this reason the knockdown and overexpression experiments were repeated using cells treated with both TNFα and IL-4 after transfection. Data from one representative experiment of four are shown in Figure 6.5. The data for the four experiments was analysed at 6 hour time intervals by two-factor ANOVA as before but overall no statistically significant difference was seen between any of the conditions (p=0.37).

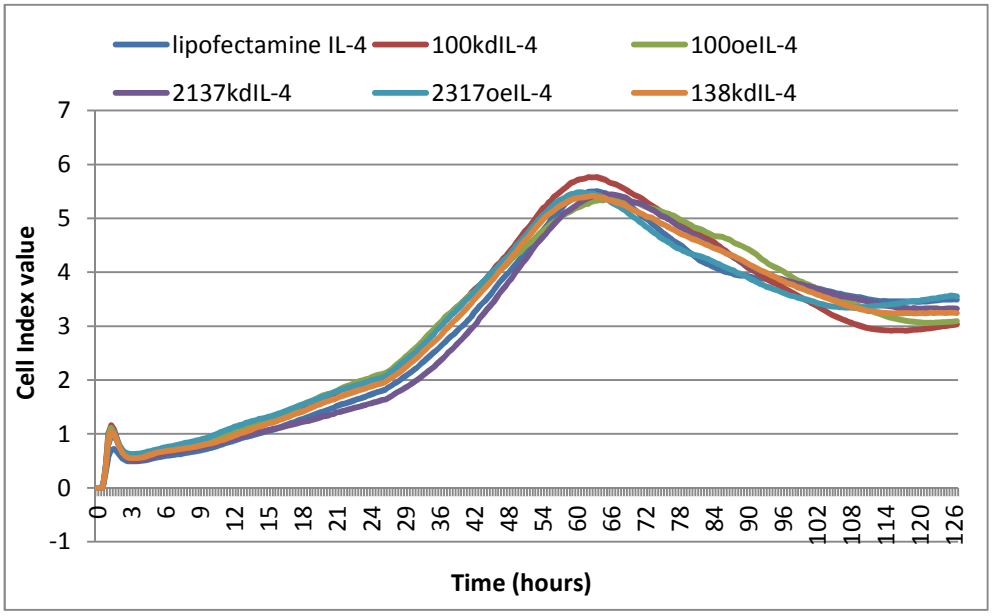

Figure 6.5 The effect of miRNA knock-down or over expression on the IL-4 treatment phenotype in FL-YB cells. Cells were transfected either with miRNA inhibitors or miRNA mimics, transfection media was diluted out after four hours of transfection. Cells were rested overnight before being plated out at a density of 8,000 cells per well in a xCELLigence 96-well E-view plate, with 5ng/ml of recombinant TNFα and IL-4. Measurements were taken every 30 minutes for approximately five days. This experiment was repeated 4 times with at least 6 technical replicates for every condition in every experiment. 2-factor ANOVA revealed no statistical significant differences between the any of the conditions (p=0.37).

6.2.7. Assessment of the effect of miRNA knockdown and overexpression on gene expression in FL-YB cells.

The effect of miRNA knock down or overexpression on gene expression in FL-YB cells was compared. Transient transfections of miRNA inhibitors or mimics were carried out as described previously (section 6.2.5). Following the four hour transfection, the media was changed to complete media with 5ng/ml TNFα and the cells were incubated at 37°C for a further 24 hours. The expression levels of Cyclooxygenases 1 and 2 (*Ptgs1/2*), toll-like receptor 4 (*Tlr4*), interleukin-6 (*Il-6*) and prostacyclin receptor (*PtgiR*) were compared by qPCR. Over three experiments it was found that there was a significant increase in the levels of *Tlr4*, *Ptgs1/2*, and *Il-6* transcripts in the cells that had miR-100-5p knocked down (Figure 6.6). For all three of these transcripts the knockdown of miR-100-5p resulted in statistically significantly higher expression levels compared to those cells where miR-2137 expression was knocked down. *Tlr4* p=0.05, *Ptgs1/2* p=0.04, *Il-6* p=0.01. The *Il-6* transcript also showed an increase in expression in the cells in which miR-138-5p was knocked down however this was not statistically significant (p=0.26). Despite *PtgiR* being predicted to be a miR-100-5p target by three of the four target prediction programmes used (DIANA micro-T, microRNA.org and RNA22)(section6.2.4) no statistically signififcant differences were seen in any of the cells with miRNA knockdown or overexpression.

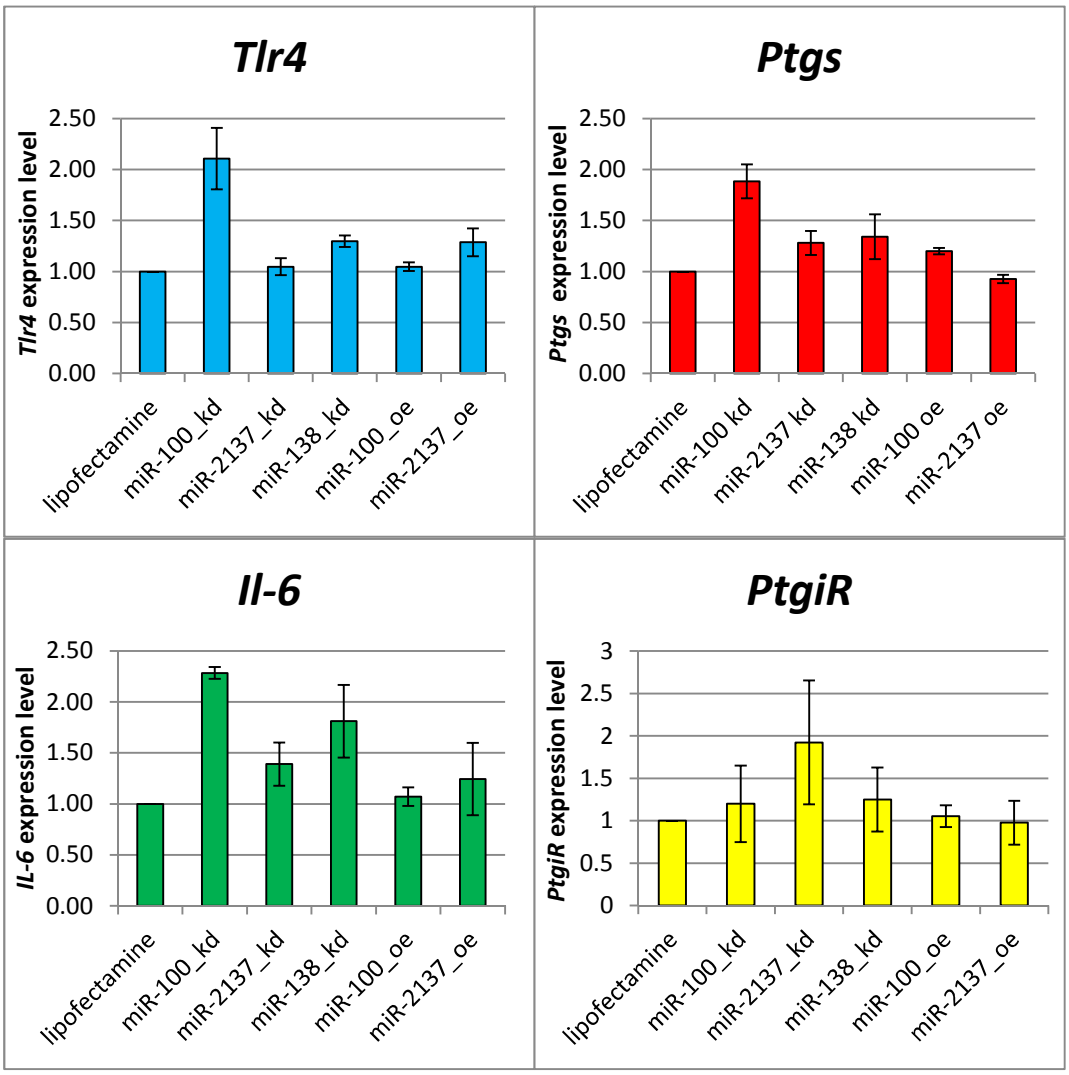

Figure 6.6 Knockdown of miR-100-5p causes increased expression of *Tlr4*, *Ptgs1/2* and *Il-6*. RNA extracted from FL-YB cells were transfected with miRNA inhibitors or mimics was used to synthesise cDNA for qPCR analysis. Gene transcripts known to be important to normal FDC function were measured by qPCR analysis following transfection and a subsequent 24 h incubation in complete media supplemented with 5µg/ml TNFα. Transcripts were normalised to the housekeeping transcript β-actin, and are shown relative to the levels seen in non-transfected, lipofectamine treated control cells. Student's independent t-test revealed that miR-100 knockdown causes an increase in expression of *Tlr4 (p=0.05)*, *Ptgs1/2 (p=0.04)*, and *Il-6* (p=0.01) transcripts compared to miR-2137 knockdown. There were no statistically significant changes in *PtgiR* expression with any miRNA knockdown or overexpression. The data shown is the mean and standard error across three independent experiments.

6.3. Discussion

Data presented in this Chapter show that miR-100-5p appears to exert some level of control over pro-inflammatory gene expression in FL-YB cells. The genes that have been identified to be affected are all down-stream genes of the NFκB pathway (Libermann and Baltimore, 1990; Schmedtje et al., 1997; Yan, 2006). The LTβR signals through both the canonical and non-canonical NFκB pathways (Dejardin et al., 2002). Since LTβR blockade was the method used to identify miR-100-5p *in vivo* it is plausible that miR-100-5p targets genes in the LTβR/NFκB signalling pathway.

Prostacyclin receptor was included in the study because three of the four target prediction algorithms used predicted this gene to be a target of miR-100-5p. No effect of either miR-100-5p knockdown or overexpression was seen on the expression levels of *PtgiR* in the FL-YB cells. It could be however that PTGIR is affected at the protein level, or as previously mentioned target prediction algorithms have been found to give many false positive results (Barbato et al., 2009; Zheng et al., 2013), of which *PtgiR* could be one.

It has been found that FDC are the main cell type in the germinal centre (GC) that produce IL-6 (Kopf et al., 1998) and that IL-6 production is up-regulated by immune complex activated FDC (Wu et al., 2009). IL-6 is known to be important in terminal differentiation of B cells (Morse et al., 1997; Kopf et al., 1994) and SHM (Wu et al., 2009; Yan et al., 2012). This indicates that miR-100-5p potentially plays an important role in control of the germinal centre response by regulation of IL-6 production by FDC.

IL-6 is also implicated in a number of autoimmune diseases including rheumatoid arthritis (RA)(Nawata et al., 1989) and systemic lupus erythematosus (SLE) (Ripley et al., 2005). An anti-IL6 receptor antibody (Tocilizumab) is in clinical use for the

treatment of RA (Smolen et al., 2013) and for Castleman's disease in Japan (Nishimoto et al., 2008).

TLR4 is the receptor for lipopolysaccharide (LPS) and signalling through the receptor results in NFκB activation (Pålsson-McDermott and O'Neill, 2004). Recently it has been discovered that FDC express TLR4 (El Shikh et al., 2007b) and that LPS causes FDC activation conferring an up-regulation of adhesion molecules and Fc receptors. It was later discovered that immunisation with a non-TLR4 agonist causes a similar co-ordinated up-regulation of TLR4, VCAM-1, ICAM-1 and Fc receptors indicating that TLR4 is generally up-regulated upon activation (Garin et al., 2010). Oxidised phospholipids which are generated during apoptosis can also act as ligands for TLR4 and it has been shown that these are present in germinal centres and are engaged by TLR4 on FDC showing that external pathogens are not needed to directly signal through TLR4 to drive activation of FDC (Garin et al., 2010). The same study also showed that TLR4 signalling by FDC is needed for high affinity Ig responses and SHM, indicating a critical role for TLR4 on FDC which impacts germinal centre reactions and the humoral immune response *in vivo* (Garin et al. 2010; N. M. Milićević et al. 2011; El Shikh et al. 2007).

Cyclooxygenase 2 (encoded by *Ptgs2*) converts arachidonic acid to prostaglandin H2 (*PGH2*) which can then be converted into different prostaglandins and prostacyclin. It has been shown that in the human FDC cell line, HK, that PTGS2 is responsible for the production of PGE2 and PGI2 by not prostacyclin (Cho et al., 2011a; Lee et al., 2007). It has recently be shown that prostaglandins produced by FDC promotes germinal centre B cell survival (Kim et al., 2013). It is well established in both macrophages and epithelium that LPS signalling through TLR4 results in up-regulation of PTGS2 (Fukata et al., 2006).

It is therefore clear that the genes that have been found to increase upon miR-100-5p knockdown in FDC all have key roles in the modulation of germinal centre responses by FDC, indicating miR-100-5p to have a critical role in control of FDC activity.

Even though knock-down of miR-100-5p caused an increase in *Il-6*, *Tlr4* and *Ptgs1/2* transcripts, overexpression of the same miRNA had no effect on the level of these transcripts. The levels of miR-100-5p appear to be relatively high in FL-YB cells based on the signal that was obtained from northern analysis. This along with the robust levels of knockdown needed to see the effect on the transcripts suggests that the miR-100-5p is already in excess of what is functionally active in terms of regulation of this system. It would therefore not be expected that addition of more miR-100-5p would have any biological effect on this system. It should also be noted that overexpression indicated by northern analysis does not necessarily correspond to functional miRNA activity, as the miRNA may be free rather than interacting with miRNA machinery. A possible method of measuring functionality of the miRNA would be to look at expression levels of known targets. This was not carried out here because miRNA targeting has often shown to be cell specific and thus known targets of miR-100 in other cell types may not be targets of miR-100 in FDC. This meant that several known targets would have to be screened which would have been difficult due to time constraints.

High levels of miR-100-5p in mature FDC and the down-regulation of pro-inflammatory genes by miR-100-5p could indicate that miR-100-5p acts as a mechanism for suppression of the FDC-driven immune reaction. This would be important for resolution of the immune response following clearance of the pathogen or trigger. This would mean that miR-100-5p plays an important role in avoidance of an inappropriate immune response.

Alternatively, miR-100-5p may be at relatively high levels in FDC to "fine-tune" the expression of pro-inflammatory genes. Again, this could be important to prevent FDC from driving inappropriate levels of immune responses. This could also explain why the levels of miR-100-5p are high in the mature FDC as these will be activated by trapped immune complex, whereas de-differentiating FDC would not be activated. Activated FDC would need higher levels of miR-100-5p to regulate pro-inflammatory genes because the expression levels of the pro-inflammatory genes would be higher.

Overall, the data presented in this chapter show that miR-100-5p plays a role in regulation of genes that are key in the regulation of GC response by FDC. The genes that have found to be regulated by miR-100-5p in FDC, *TLR4*, *IL-6* and *Ptgs2* are all induced by NFκB. miR-100-5p was identified *in vivo* following LTβR blockade, because LTβR signalling activates both canonical and non-canonical NFκB it is plausible that miR-100-5p regulates this pathway at some level

CHAPTER 7: General Discussion

Contents

Chapter 7: General Discussion

7.1. Introduction

Follicular dendritic cells (FDCs) are key elements of secondary lymphoid organs where they form the stromal component of B-cell follicles (Guettier et al., 1986). FDCs possess extensive dendritic process that trap immune complexes which they then display to B-cells to stimulate the production of high affinity antibodies (Radoux et al., 1984; Tew et al., 1990; Kosco and Gray, 1992; Fütterer et al., 1998; Wang et al., 2000). FDC also produce Mfge8 which is important for efficient clearance of low affinity B cells which have undergone apoptosis (Kranich et al., 2008). FDCs have been implicated in various disease processes, including prion diseases (Mabbott et al., 1998; Mcculloch et al., 2011), HIV latency (Sprenger et al., 1995; Burton et al., 2002), and autoimmune diseases (Luzina et al., 2001; Vinuesa et al., 2009; Yau et al., 2013). The identity of the FDC precursor cell type has been a source of considerable debate, although evidence was recently put forward that indicates that they arise from perivascular precursors (Krautler et al., 2012). It is well established that lymphotoxin, produced by LTi cells and B-cells, is required for FDC differentiation and mature function (Alimzhanov et al., 1997; Gonzalez et al., 1998; Mackay and Browning, 1998; Mabbott et al., 2003). These processes can ordinarily be regulated at a variety of different transcriptional and post-transcriptional levels.

The specific aim of this current study was to define the role that miRNAs play in the development and function of FDCs. MiRNAs are short non-coding RNAs that post-transcriptionally control expression of a wide variety of genes by binding to mRNA, blocking translation into protein (Lagos-Quintana et al., 2003; Ambros, 2004). Identifying the miRNAs and target transcripts involved in FDC development and function will aid in understanding the pathways and mechanisms that are under tight control during FDC development and function.

7.2. Characterising the effect of *in vivo* LTβR-Ig treatment on the murine spleen

7.2.1. Immunostaining for markers of FDC function

We wished to use an *in vivo* model of FDC de-differentiation to identify miRNAs associated with the development and function of FDCs. Previous studies have shown that a single *in vivo* injection with LTβR-Ig causes rapid, temporary de-differentiation of FDCs (Mackay and Browning, 1998; Mabbott et al., 2000). This approach was used in the present study (section 3.2.1) and spleens were collected from treated mice at various time points following LTβR-Ig treatment. Sections from each individual spleen were analysed by immunohistochemistry for the presence of the FDC markers, CD35 and MFGE8, to determine the exact timing of FDC de-differentiation. No MFGE8 staining was seen in any of the spleens by 3 days following LTβR-Ig treatment, whereas CD35 staining was seen in some of the day 3 spleens, but by day 5 no CD35 staining was detected in the spleens. Correspondingly, CD35 staining was observed to return from 21 days after treatment but no MFGE8 staining was seen to return, even by d 28. This indicates that CD35 is retained for longer than MFGE8 in the de-differentiating FDC, and is expressed before MFGE8 in the re-differentiating FDC. As FDC precursors have been described to express MFGE8 (Krautler et al., 2012), data presented here suggest that following LTβR-Ig treatment, FDC are not completely lost and replaced by new precursor cells but rather de-differentiate to a less functional state. Previous observations using electron microscopy after TNFR signalling-blockade, which has a similar effect on FDC status to LTβR-blockade, shows that immuature FDC are still present but their dendrites have regressed (Mabbott et al., 2002). This suggests that following LTβR-Ig treatment, FDC de-differentiate to a minimally functional state. As MFGE8 is a secreted factor involved in clearance of apoptotic B cells it is possible that MFGE8 production is restricted to fully mature FDC, as it will only be required during a germinal centre reaction. CD35 is more likely to be expressed by FDC over more stages

of maturation as it is required for initial immune complex capture before a germinal centre reaction (Fang et al., 1998).

7.2.2. The effect of LTβR-Ig on FDC-associated gene expression in the spleen

To identify gene expression changes resulting from LTβR-Ig treatment, RNA from (a) untreated spleens with full FDC networks, (b) spleens collected 2 days after LTβR-Ig treatment with partially de-differentiated FDC, (c) spleens collected 14 days after LTβR-Ig treatment with fully de-differentiated FDC, and (d) spleens from $LT\beta^{-/-}$ mice which never develop mature FDC, was used in a gene expression microarray analysis experiment. This approach enabled the identification of genes that were either up-regulated or down-regulated as a result of FDC de-differentiation (Table 3.2). These data were compared with data from an independent study previously carried out using mesenteric lymph node (mLN) tissue (Huber et al., 2005). In the Huber et al. study, gene expression was assessed by microarray from mLN tissue 1, 2, 3, 27 and 35 days after LTβR-Ig treatment. In general, known FDC genes down-regulated in the mLN study correlated very well with the genes that were found to be decreased as a result of LTβR-Ig treatment in the spleen samples analysed here. Exceptions include glycosylation-dependent cell adhesion molecule 1 (*Glycam-1*), which, like MFGE8, has also been shown to be responsive to prolactin. In the present study *Glycam-1* expression was unchanged in the LTβR-Ig treated spleen (section 3.2.3) while the Huber study found it to be greatly down-regulated in the LTβR-Ig treated mesenteric lymph nodes (Huber et al., 2005). The same study also identified transcripts that were highly expressed in FDC enriched samples compared to FDC-depleted samples. The list of genes that were found to be down-regulated in LTβR-Ig treated and $LT\beta^{-/-}$ spleens (section 3.2.4) correlated better with the FDC enriched genes from the Huber study over those identified from LTβR-Ig treated mesenteric lymph nodes in the same study.

One possible reason for this could be the less severe effect that loss of LTβR signalling in LTβ$^{-/-}$ mice has on mesenteric and cervical lymph nodes, as these tissues develop in LTβ$^{-/-}$ mice whereas other lymph nodes and Peyer's patches do not (Koni et al., 1997). The authors also found no disruption of B cell location in mLN from LTβ$^{-/-}$ mice, whereas extensive disruption of B cells localisation was seen in the LTβR-Ig treated spleens (section 3.2.1) suggesting a more severe effect on splenic white pulp than on mesenteric lymph nodes.

It has recently been proposed that FDC arise from perivascular precursors that express platelet derived growth factor receptor, beta polypeptide (PDGFRβ) (Krautler et al., 2012). As these pericyte precursors differentiate into FDC they lose the pericyte-associated genes PDGFRβ and chondroitin sulfate proteoglycan 4 (CSPG4). Because of these findings, the expression of *Pdgfrβ* and *Cspg4* in the spleens collected following LTβR-Ig treatment were analysed. *Pdgfrβ* was seen to be highly expressed in the spleen samples but no real change was seen in the expression levels in the LTβR-Ig treated spleens, or the expression levels of *Cspg4*. This is in agreement with the hypothesis that LTβR-Ig treatment causes 'de-activation' of FDC rather than complete loss followed by replacement from precursors.

It was seen in the spleens collected from two of the four mice 21 days following LTβR-Ig treatment that expression levels of FDC-associated genes were considerably higher than in the spleens collected 19 or 24 days following LTβR-Ig treatment (Figure 3.3). A portion of the same spleens were analysed for FDC markers by IHC, and it was seen that two of the four spleens from this time point showed both CD35 and MFGE8 immunostaining. This indicates that the spleens from these two mice contained mature FDC and so could be eliminated from further study.

7.2.3. The effect of LTβR-Ig treatment on lymphocyte and macrophage gene expression

Although LTβ$^{-/-}$ mice do not develop peripheral lymph nodes, they do develop mesenteric and cervical lymph nodes (Ngo et al., 1999). In our study the localisation of B cells was severely disrupted and this correlates with a decrease in expression of *Cxcl13*. The Huber study found no evidence of differential localisation of B cells in the mLN despite gene expression data showing a strong down regulation of chemokines including *Cxcl13* and *Ccl19*. The difference in B cell localisation between the present study and the Huber study may be accounted for by the fact that no time points between 3 days and 27 days after LTβR blockade was studied by Huber et al. (2005), which was when the largest disruption in the microarchitecture was evident in the spleen (Figure 3.2). Only limited disruption was evident at earlier time points. Data from the gene expression microarray data (section 3.2.3) showed that expression levels for general markers of B and T cells such as B220 (encoded by *Ptprc*) and CD3 were unchanged in the LTβR-Ig treated or LTβ$^{-/-}$ spleens (Figure 3.4). This suggests that LTβR signalling does not affect overall cell number in the short term but is necessary for localisation of B cells (Figure 3.2).

Other cell types in the spleen could have been directly or in-directly affected by the LTβR blockade. For example expression levels of the lysozyme genes, *Lyz1* and *Lyz2*, were found to be lower in the LTβR-Ig treated and LTβR$^{-/-}$ spleens compared to untreated spleens. This indicates a possible decrease in macrophage activity or numbers. The Huber study also identified a decrease in expression of lysozyme after LTβR-Ig treatment (Huber et al., 2005). It is possible that the reduction in *Mfge8* that is seen causes a decrease in macrophage phagocytic activity and decreases the requirement for lysozyme production.

Overall, genes identified in the present study as showing decreased expression levels in LTβR-Ig treated and LTβ$^{-/-}$ spleens correlated well with those previously described to be highly expressed by mature FDC. This indicated that LTβR-Ig treatment was an effective method to identify FDC-associated genes and was likely to be a useful approach to identify FDC-associated miRNAs.

7.3. Identification of LTβR-signalling dependent miRNAs in the spleen

Illumina deep sequencing was first used to identify FDC-associated miRNAs in the spleen tissue collected from LTβR-Ig, LTβ$^{-/-}$ and untreated mice (chapter 4). Total RNA was extracted from selected spleens, checked for sufficient quality and pooled (see section 2.6). Multiplexed libraries were generated using adaptors designed by, and sourced directly from, the sequence service provider. It transpired that the use of this particular adaptor design resulted in severe sequencing bias. Around the same time that the sequencing bias was discovered (section 4.2.1) two independent studies were published describing bias caused by the same method. The first study (Alon et al., 2011) found that introduction of a barcode sequence at the adapter ligation stage caused bias which they suggested to be bias in ligation of the modified adapters to the small RNAs (Alon et al., 2011). This study put forward an alternative barcoding method which introduced the 5 nucleotide sequence during the PCR amplification step which dramatically reduced bias. The second study (Van Nieuwerburgh et al., 2011) suggested that the bias was introduced during the PCR amplification step and developed a method to ligate the barcode sequences to the small RNA libraries after this step.

At this point it was decided to carry out identification of miRNAs by miRNA microarray. Intra-platform microarray variability has previously been described (Sato et al., 2009; Git et al., 2010) and so to reduce the potential for false positive results two different

array platforms, Exiqon and Affymetrix were used. 16 miRNA were identified from the Exiqon data as having an expression level of 50% or less in LTβ$^{-/-}$ spleens compared to untreated spleens and also a decreased expression level in the day 14 LTβR-Ig treated spleens. By the same criteria, 6 miRNA were identified as decreased in the Affymetrix data set. 7 miRNA from the Exiqon data were identified to have increased expression levels by at least 50% in the LTβ$^{-/-}$ spleens and also to have increased expression levels in the day 14 spleens. Again by the same criteria the 10 miRNAs were identified as decreased from the Affymetrix data. MiRNAs were chosen for further study on the basis of decreased expression levels in both the LTβR-Ig treated and LTβ$^{-/-}$ spleens. Three miRNAs (miR-100-5p, miR-2137 and miR-138-5p) were chosen because of decreased expression levels in the LTβR-Ig treated and LTβ$^{-/-}$ spleens on both platforms. The expression levels of these miRNA were analysed by northern analysis of RNA from spleens from untreated, LTβR-Ig treated and LTβ$^{-/-}$ mice. This analysis confirmed the changes in expression levels associated with de-differentiation of FDC. The expression of two star strand miRNAs that were identified to have decreased expression levels in treated and transgenic spleen compared to untreated spleen from the Exiqon data alone were also analysed by miRNA northern analysis. The expression of these star strand miRNA could not be confirmed by miRNA northern analysis. MiRNA qPCR suggested that these sequences were present only at very low expression levels and unchanged as a result of treatment (section 4.2.4). This supports the contention that the use of two different platforms can help avoid selection of false positive results, from systemic noise, for further study.

Results from Chapter 4 show that while the levels of the majority of splenic miRNAs were not affected, a small number of miRNAs were differentially expressed following LTβR-Ig treatment. The effects on differentially expressed miRNAs were more pronounced in the spleens collected 14 days after LTβR-Ig treatment than those

collected 2 days after treatment correlating well with loss of FDC function. In contrast to the effects of LTβR-Ig treatment, a larger number of miRNAs were differentially expressed between the spleens of $LT\beta^{-/-}$ transgenic and wild-type mice. This suggests that the permanent lack of mature FDC in the $LT\beta^{-/-}$ mice may have had impacts on other cell types such as B cells and tingible body macrophages. Because the use of LTβR-Ig only temporarily de-differentiated FDC it means that other cell types were only minimally affected. The use of LTβR-Ig treatment therefore allowed the selection of genes and miRNAs that are more likely to be FDC-associated. The gene expression array data showed that some of the transcripts that are most affected are from FDC-associated genes, this suggests that FDC-associated miRNAs would also be some of the most affected. The finding that the three miRNAs that were selected for further study were all found to be expressed in FL-YB cells supports this contention. Given similar probe labelling efficiencies, northern analysis suggested that miR-100-5p was the most highly expressed of the three miRNAs examined in FL-YB cells.

Although no data on miRNA expression by FDCs has been published to-date, two studies have been published describing changes in the expression level of miRNAs in B cell lymphoma cell lines when co-cultured with FDC. One of these studies examined the mechanism of terminal differentiation of B cells (Lin et al., 2011). Terminal differentiation of B cells into plasma cells or memory B cells is driven by suppression of the transcription factor Bcl-6 and the expression of the transcription factor Prdm1 (Crotty et al., 2010; Shaffer et al., 2002). Lin et al. (2010) found that expression of the miR-30 family is up-regulated and expression of let-7a and miR-9 are down-regulated in human B cell lymphoma cells when co-cultured with a human FDC cell line. Targeting of *Bcl6* by the miR-30a family and targeting of *Prdm1* by let-7a and miR-9 was found to play a role in the terminal differentiation of B cells. These miRNA and genes were found to be largely stable in the LTβR-Ig treated spleen samples. Moderate changes in

expression of miR-30 family members were seen in the LTβ$^{-/-}$ mice but these changes were inconsistent between family members. This indicates that terminal differentiation of B cells is not hugely effected in the LTβR-Ig treated or LTβ$^{-/-}$ mice, which is consistent with reports that IgM and sometimes IgG responses are largely normal in LTβ$^{-/-}$ mice (Alimzhanov et al., 1997; Junt et al., 2006).

The second study had also identified differentially expressed miRNA in B cell after co-culture with the FDC cell line HK. In this study FDC co-culture was found to induce the expression of miR-181a which targeted the pro-apoptotic protein, BCL-2-interacting mediator of cell death (BIM) thus reducing apoptosis of the B cells (Lwin et al., 2010). In our analysis it was found that the expression levels of BIM (*BCL2L11*) were unchanged in the LTβR-Ig treated and the LTβ$^{-/-}$ mice. It was also seen that the LTβR-Ig treatment did not have any effect on the level of miR-181a expression in the spleen. This suggests that there is little change in the occurrence of BIM-mediated apoptosis in either LTβ$^{-/-}$ mice or LTβR-Ig treated mice.

7.4. Characterisation of a murine FDC cell line

Following the identification of miRNAs and confirmation of their expression in the spleen, it was necessary to perform functional analyses of those specific miRNA. As there are difficulties in the isolation of FDC (Munoz-Fernandez et al., 2006; Aguzzi and Krautler, 2010) it would be impractical to isolate sufficient FDCs to carry out loss-of-function and gain-of-function studies. For this reason the murine FL-YB cell line was used as an *in vitro* model of FDC (Magari et al., 2011). The FL-YB cell line is derived from murine FDC and is dependent on TNFα signalling to remain in a mature and functional state. All three of the miRNAs selected for further study were shown to be expressed in the FL-YB cell line by miRNA northern analysis (Figure 6.1).

To assess whether FL-YB cells respond in a similar manner to *in vivo* FDC activation, the gene expression levels for *Il-6, Il-15, Vcam-1, Ptgs1/2, PtgiR* and *Tlr4* were measured 48 hours after addition of different stimuli. These 'marker' transcripts were selected on the following basis: IL-6 produced by FDC has been shown to promote germinal centre reactions and somatic hyper mutation (Wu et al., 2009); IL-15 produced by FDC causes increased proliferation of germinal centre B cells (Park et al., 2004); Expression of VCAM-1 by FDC promotes interaction with germinal centre B cells through VCAM-1/VLA-4 binding which enables FDC-mediated prevention of B cell apoptosis (Koopman et al., 1994). It has been reported that FDC production of prostaglandins is supressed via reduction of Cyclooxygenase2 (*Ptgs2*)(Cho et al., 2011b, 2013). Expression of prostacyclin receptor (*PtgiR*) has been previously reported on FL-Y cells (Nishikawa et al., 2006) and was predicted by 3 miRNA target prediction algorithms to be a target of miR-100-5p (DIANA micro-T, microRNA.org and RNA22); and TLR4 has been shown to be up-regulated on activated FDC and TLR4 signalling by FDC has been found to be a key for initiation of the germinal centre response (Garin et al., 2010; El Shikh et al., 2007b).

To maintain a mature FDC-like state, FL-YB cells are routinely cultured in the presence of recombinant TNFα (Nishikawa et al., 2006). We found that the addition of TNFα leads to an increase in the expression of *Il-6*, *Vcam-1*, *PtgiR* and cyclooxygenase (*Ptgs*) by the FL-YB cells. TNFα signalling activates canonical NFκB and leads to up-regulation of *Il-6* transcription in a variety of cell types (Husson et al., 2000; Tseng et al., 2010). Cyclooxygenase2 is also known to be transcribed by NFκB (Tridon et al., 2005; Tak and Firestein, 2001) and cyclooxygenase 2 activates the prostacyclin receptor (PtgiR) through increased synthesis of prostacyclin. TNFα has also been shown to induce VCAM-1 expression in FDC and other cell types (Husson et al., 2000; Lee et al., 2006).

The transcriptional response of the FL-YB cells to TNFα treatment therefore correlates well with the current literature and understanding.

Treatment with a monoclonal antibody against LTβR initiates signalling through the LTβR and activates both the canonical and non-canonical pathway of NFκB activation. In general, the addition of agonistic LTβR MAb to FL-YB cells cultured in the presence of TNFα, had only limited additional effects on the expression of genes assessed to be upregulated by TNFα alone. This suggests that the activation of NFκB through TNFα signalling is already high. Addition of agonistic LTβR MAb did however increase the expression level of *Vcam-1*, and this effect has previously been described in a variety of stromal cells (Matsumoto et al., 1999; Dejardin et al., 2002).

Interestingly it was found in the present study that addition of IL-4 to the FL-YB cultures increased expression of many genes including *Il-6*, *Il-15, Tlr4, PtgiR* and cycloxygenase (*Ptgs1/2*). Zamorano et al. (2001) found that IL-4 enhances TNFα-induced NFκB activation in the 32D myeloid cell line and a similar mechanism may also occur in the FL-YB cell line under these conditions to further increase expression of the above genes. However, as LTβR signalling, which induces activation of NFκB did not result in transcriptional increases of these genes (Figure 5.3), IL-4 may be mediating these effects through different pathways. It has previously been found that IL-4 inhibits the production of cycloxygenase 2 in the human cell line HK (Cho et al., 2011b, 2013; Lee et al., 2008, 2005). However this was upon pre-treatment of the FDC with IL-4, whereas in the experiments described in section 5.2.3, the cells were routinely cultured with TNFα and IL-4 was added in addition to TNFα. The functions of IL-4 are known to be dependent on cell type, on other signalling pathways and on factors in the microenvironment (Nelms et al., 1999). For example, IL-4 down-regulates TLR4 expression by monocytic cells (Mita et al., 2002, 2001) but increases expression of

TLR4 by B cells (Ganley-Leal et al., 2010). The results in section 5.2.3 also indicate that IL-4 up-regulates *Tlr4* on FDC, perhaps indicating that this effect is associated with the germinal centre microenvironment.

The effects of IL-4 on FL-YB cells were also monitored using the xCELLigence system. This equipment generates a resistance signature representing a combination of cellular characteristics; proliferation, adhesion, morphology and viability. Having established a basic cell-index signature for cells grown in the presence of TNFα, the present study showed that IL-4 stimulation had a dramatic effect on this signature. This effect was shown to be dependent on the presence of TNFα, on cell density and on the dose of IL-4 (Figure 5.8 and 5.9). Analysis of cell number suggested that this effect was not due to a difference in proliferation or viability of the cells, and more likely a result of changes in adhesion and/or morphology (Figure 5.7). However, no morphological differences between cells cultured in the presence or absence of IL-4 cells were obvious by light microscopy. Live cell imaging of IL-4 treated cells showed a possible increase in granularity and a slightly more rounded-up cells shape (Figure 5.10). This could indicate a more activated phenotype in the TNFα and IL-4 treated cells than the cells treated with TNFα alone. Future work to reveal the phenotype modifying the cell-index signature of IL-4 treated FL-YB cells, would include further imaging of the cells to confirm if there is an increase in granularity and roundness of the cells treated with IL-4. As the effect could be a difference in cell adhesion, immunostaining of adhesion molecules such as focal adhesion kinase (FAK) or cell adhesion assays could be used to assess this.

7.5. Functional analysis of miRNAs in FDC

MiRNA northern analysis confirmed expression of miR-100-5p, miR-138-5p and miR-2137 in FL-YB cells (Figure 6.1).

7.5.1 Known functions of miR-100-5p

Previously established targets of miR-100-5p include the mammalian target of rapamysin (mTOR) gene transcript. This gene contributes to the regulation of neovascularisation in endothelial vascular smooth muscle cells (Grundmann et al., 2011). Expression of miR-100 also leads to increased vascularisation of tumours and thus is associated with tumour progression and unfavourable prognosis of many types of cancer (Chen et al., 2013b; Wang et al., 2013) leading to miR-100-5p being described as an oncomiR (Leite et al., 2013; Petrelli et al., 2012; Zheng et al., 2012) . It has also been described that miR-100 and α_v integrins play a role in regulation of neovascularisation during graft-versus-host disease (Leonhardt et al., 2013). In the present study expression of *Mtor* was unchanged in the LTβR-Ig treated and LTβ$^{-/-}$ spleens compared to untreated samples, and *Mtor* expression could not be detected in FL-YB cells by qPCR. This suggests that, at least in FL-YB cells, miR-100-5p targeting of Mtor is unlikely. Another reported target of miR-100-5p is the bone morphogenetic protein receptor, type II (*Bmpr2*), which regulates osteogenic differentiation of human adipose-derived mesenchymal stem cells. Again *Bmpr2* expression levels were similar in the untreated, LTβR-Ig treated and LTβ$^{-/-}$ spleens. Lymphoid tissue organiser (LTo) cells can be derived from adipose derived mesenchymal stem cells (Bénézech et al., 2012). LTo cells are the original stromal cell population in developing lymph nodes and share functions such as maturation through LTβR signalling and the production of Cxcl13 in common with FDC (Bénézech et al., 2010). It may be that the association of miR-100-5p with mature FDC seen here (section 4.2.2) could indicate a wider role for

miR-100-5p in MSC differentiation. miR-100-5p has also been implicated in epithelial to mesenchymal transition (EMT) and increases the motility of cells (Shimamura et al., 2011). EMT involves a loss of cell-cell contact and mobilisation of the cells, one of the defining features of FDC is direct cell-cell contact with B cells and their long-live immobile state. The role of miR-100-5p in EMT indicates a possible role in cell-cell contact or mobilisation of cells. miR-100-5p has also been found to be significantly up-regulated in the blood of patients with multiple sclerosis (Keller et al., 2013) indicating association with an inflammatory phenotype.

7.5.2 Known functions of miR-138-5p

Like miR-100-5p, miR-138-5p has also been implicated in EMT, although in a suppressive role (Liu et al., 2011). In addition, miR-138-5p has also been described to attenuate bone formation by negative-regulation of osteogenic differentiation of human mesenchymal stem cells (MSC) (Eskildsen et al., 2011), and has also been described to inhibit MSC differentiation into adipocytes (Yang et al., 2011). FDC are stromal cells that have been reported to differentiate from pericytes (Krautler et al., 2012) that could be MSC (Uccelli et al., 2006) and so the decreased miR-138-5p expression seen with FDC de-differentiation (Table 4.2) could indicate a role for miR-138-5p in FDC differentiation. Inhibition of miR-138-5p in oesophageal squamous cell carcinoma causes sustained NFκB activation by targeting lipid-raft components (Gong et al., 2013), as FDC function relies heavily on NFκB activation through LTβR signalling a similar role in FDC could be possible.

7.5.3 Known functions of miR-2137

miR-2137 is a recently described miRNA (Chiang and Schoenfeld, 2010), and to date expression of miR-2137 has only been reported in mouse, not other species. The expression levels of miR-2137 were found to be increased in mouse embryonic fibroblasts (MEF) following induction of endoplasmic reticulum (ER) stress (Behrman et al., 2011). In addition, a study of miRNAs in different B cell lineages and stages identified miR-2137 to only be expressed in the B1 B cell lineage and not the B2 lineage at any stage (Spierings et al., 2011).

7.6. miR-100-5p regulates pro-inflammatory genes in FDC

The levels of miR-100-5p, miR-138-5p and miR-2137 were manipulated in FL-YB cells by the use of either complementary LNA-modified oligonucleotide sequences or miRNA mimics. The effect of miRNA over-expression or depletion on the expression of selected FDC-associated transcripts was assessed by qPCR analysis. Functional analysis of miR-100-5p, miR-138-5p and miR-2137 in FL-YB cells revealed that the loss of miR-100-5p resulted in an approximately 2-fold increase in the transcript levels of three pro-inflammatory genes 24 hours later (section 6.2.7). Expression levels remained at this elevated level for a further 24 hours. These genes were *Il-6* (encodes interlukin-6), *Ptgs1/2* (encodes Cyclooxygenase 1 and 2) and *Tlr4* (encodes toll-like receptor 4).

IL-6 is a cytokine that is involved in many different processes. IL-6 plays a central role in the induction of acute phase protein synthesis (Castell et al., 1989; Heath et al., 1993). It is also involved in breakdown of bone and cartilage (Le Goff et al., 2010) and as such is involved in osteoporosis (Manolagas et al., 1995). IL-6 is an important cytokine for progression of the germinal centre reaction (Wu et al., 2009; Eto et al., 2011; Deng et al., 2002). The main source of IL-6 in the germinal centre is FDC (Kopf et

al., 1998). Mice deficient in IL-6 do not develop full size germinal centres and IgG2 and IgG3 responses are considerably impaired (Kopf et al., 1998). IL-6 or IL-21, the production of which is induced by IL-6, are required for optimal follicular T cell differentiation (Eto et al., 2011). T follicular helper cells interact with naïve B cells and secrete cytokines that promote their differentiation into antibody secreting plasma cells. Increased IL-6 expression is found in tissues of patients with a variety of autoimmune diseases including systemic lupus erythematous (Ripley et al., 2005), rheumatoid arthritis (Nawata et al., 1989) and Sjogren syndrome (Hulkkonen et al., 2001). However, it has also been proposed that IL-6 has a role in a checkpoint of immune tolerance (Yan et al., 2012). IL-6 plays such a large role in autoimmune diseases that a neutralising antibody to IL-6 receptor (Tocilizumab) has been developed as a therapy and is now widely used in the treatment of RA patients (Smolen et al., 2013; Assier et al., 2010).

Blocking the function of miR-100-5p in FL-YB cells caused an increase in levels of the *Il-6* transcript. This suggests that the high levels of miR-100-5p usually found in FL-YB cells could have a role in preventing excessive IL-6 production by FDC. This could have important implications in the prevention of autoimmunity. In future work it will be important to confirm that the increase of IL-6 with miR-100-5p knockdown is seen at the protein as well as the transcript level in FL-YB cells.

It is possible that the increased *Il-6* levels seen in FL-YB cells depleted of miR-100-5p could be a result of increased *Tlr4* levels. It was recently shown that FDCs express toll-like receptor 4 (*Tlr4*) (El Shikh et al., 2007b) and that injection of mice with LPS caused up-regulation of activation markers, such as FcγRIIb, VCAM-1 and ICAM-1 on FDC *in vivo.* Increased expression of these markers was also seen on FDC treated with LPS *in vitro* (El Shikh et al., 2007b) and this observation indicated the importance of TLR4

signalling in FDC which is a key driver for the germinal centre response (Garin et al., 2010). Loss of TLR4 on FDCs leads to a decrease in both the number and size of germinal centres (GC), reduced IgM titres from GC B cells and a decrease in the proportion of germinal centre B cells in the GC. Experiments generating bone marrow chimeras revealed that it is the stromal cells in the germinal centre that express TLR4. Without TLR4 expression, minimal ICAM-1 was expressed on the FDC which reduces the frequency of FDC-GC B cell interactions and which in turn markedly reduces the selection of high affinity plasma cells. High affinity IgG1, IgG2a and IgG2b responses were substantially impaired in mice deficient for TLR4 on FDC and the rate of SHM was decreased. FDCs that did not express TLR4 showed a reduction in the expression levels of a number of other genes. These included *LTβR*, the cytokines *IL-1b*, *IL-6*, *IL-10*, *IL-15* and the chemokines CCL19, CCL21, and CXCL12. These deficiencies go some way to explaining the reduced number and size of GCs (LTβR and chemokines), the reduced isotype switching (IL-6) and the reduction in GC B cell numbers (IL-10 and IL-15). The increase in *Tlr4* expression upon loss of miR-100-5p (section 6.2.7) in FL-YB cells indicates that miR-100-5p causes down-regulation of *Tlr4* expression. As TLR4 signalling in FDC has been found to be important for driving the germinal centre reaction the modulation of *Tlr4* by miR-100-5p could have an important role in regulation of the germinal centre reaction to avoid inappropriate, autoimmune or over-active immune responses. TLR4 signalling up-regulates IL-6 and aberrant expression of both of these genes has been implicated in autoimmune disease (Hwang et al., 2009; Assier et al., 2010). miR-100-5p may therefore have an important role in fine tuning the expression of these and other genes that drive and mediate germinal centre reactions to prevent the occurrence of autoimmune reactions.

The final gene that was, shown to have increased expression levels after depletion of mir-100-5p in FL-YB cells was cyclooxygenase1/2 (*Ptgs1/2*). Cyclooxygenase enzymes

are responsible for converting arachidonic acid into prostaglandin H (PGH) which can then be converted into a variety of other prostaglandins. Arachidonic acid is released from membrane phospholipids by phospholipase A_2 in response to inflammatory stimuli (Harris et al., 2002). Prostaglandins have many complex and often opposing roles depending on the situation and microenvironment of target cells. It has been shown in HK cells that whereas cyclooxygenase 1 is constitutively expressed as in many other tissue and cell types, cyclooxygenase 2 (Ptgs2) is up-regulated upon stimulation by TNFα, TGF-β or LPS (Lee et al., 2008). This indicates that cyclooxygenase 2 can be up-regulated by TLR4 signalling in FDCs, again providing the possibility that, like *Il-6*, the up-regulation of *Ptgs2* upon miR-100-5p knockdown in FL-YB cells may also be secondary to the up-regulation of *Tlr4*. The increase in *PTGS2* causes increased expression of prostaglandin E_2 and I_2 (PGE_2 and PGI_2) in HK cells (Lee et al., 2008). PGE_2 is known to inhibit the proliferation of T cells and also to protect T cells from TCR-mediated activation-induced cell death (AICD) (Harris et al., 2002). It has been shown that prostaglandins produced by HK cells can carry out both of these functions on follicular T cells (Lee et al., 2008). PGE_2 can also induce regulatory T cell function which in turn supress immune responses and maintain tolerance (Baratelli et al., 2005). Future work would be needed to determine if the increase in *Ptgs* transcript after mir-100-5p knockdown correlates with an increase in the secretion of prostaglandins by the FL-YB cells and if so which prostaglandins.

The gene expression microarray data (chapter 4) revealed that the expression levels of *Il-6* and *Ptgs2* transcripts were not above the threshold level that was set for the data set. Because the mice were not immunised this is not unexpected and could support the hypothesis of miR-100-5p acting to post-transcriptionally supress any transcript which is being made despite transcriptional suppression. *Tlr4* expression levels were high in

all spleens but significantly reduced in the d14 and LTβ$^{-/-}$ mice, which is probably due to reduced FDC and the resulting reduce immune response.

These results therefore indicate that miR-100-5p plays a role in regulating pro-inflammatory genes in FDC. As previously mentioned miRNA often act to "fine-tune" the levels of their target gene. In this case, miR-100-5p is likely to have a role in maintaining the specific amounts of pro-inflammatory genes produced by FDC. These genes produced by FDC go on to play important roles in determining the level and efficiency of the humoral immune response generated within a germinal centre highlighting the potential importance of the role miR-100-5p plays in FDC.

7.7. Future studies

The proposed role of miR-100-5p in FDC development and/or function would be further supported by identification the miRNA expression in FDCs *in vivo.* One method that could be used for this is miRNA *in situ* hybridisation (Pena et al., 2009). In future studies it would also be interesting to compare the miR-100-5p levels in FDC in primary and secondary follicles, as the FDC within secondary follicles are more activated than those from primary follicles (Allen and Cyster, 2008). As miR-100-5p is highly conserved and the human miR-100-5p has exactly the same sequence as the mouse it would be interesting to evaluate the human FDC cell line HK for expression of miR-100-5p. If hsa-miR-100-5p was found to be expressed in this cell line it would be interesting to see if knockdown had similar effects on the *Il-6*, *Tlr4* and *Ptgs* transcripts. The HK cell line could also potentially be a useful further model. For example, when *Vcam-1* and *Icam-1* expression levels were evaluated in FL-YB cells in the present study some increases were seen upon loss of miR-100-5p. However, these observations were not consistent, possibly because the expression levels of *Vcam-1* and *Icam-1* were very low in the FL-YB cells. As HK cells have been reported to express these two adhesion

molecules at functional levels (Kim et al., 1994) they may be a superior model to measure the effect of miR-100-5p on these transcripts. It should be noted however that although miR-100-5p sequence is highly conserved the targets in human and mouse cells may not be the same because of sequence and/or structural differences in the target transcripts. As the actual target transcripts of miR-100-5p are unknown it is impossible, at this stage, to determine whether the function will be conserved between species (Friedman et al., 2009).

As mentioned before the increase in *Il-6* and *Ptgs* could be a down-stream consequence of the increase in *Tlr4* expression and signalling. To investigate this, an inhibitor of TLR4 signalling such as a neutralising antibody or LPS-RS (invivoGen, UK) could be used in culture of the cells following miR-100-5p knockdown. It would also be interesting to measure whether addition of LPS to the cultures would cause further increased expression of *Il-6* or *Ptgs* by FL-YB cells.

The expression of *TLR-4*, *Ptgs1/2* and *IL-6* have all been described to be up-regulated upon NFκB activation (Libermann and Baltimore, 1990; Schmedtje et al., 1997; Yan, 2006). To assess the possible involvement of NFκB in the up-regulation of the transcripts NFκB luciferase reporter assays or electrophoretic mobility shift assays (EMSA) could be carried out. The advantage of EMSA is that it would also allow the identification of the specific NFκB subunits that are being activated which would reveal if canonical, non-canonical or both signalling pathways were playing a role.

No traditional (6-mer seed sequence or greater in the 3'UTR of the transcript) miR-100-5p target sites have been identified in any of the transcripts that have been found to increase upon miR-100-5p knockdown (RNAhybrid, Targetscan). However, increasingly miRNA targets which do not fit these traditional criteria are being identified (Shin et al., 2010; Lal et al., 2009; Betel et al., 2010). The ~2-fold increase

which is seen in the expression level of the transcripts 24 h following miR-100-5p knockdown does however suggest that miR-100-5p is not directly targeting these transcripts as most miRNAs only cause a fairly modest repression of their target transcripts. This coupled with the possibility of all these transcripts being under the control of the same pathway or even *Il-6* and *Ptgs* expression being controlled by TLR4 suggests that the transcripts are indirect targets of miR-100-5p.

This raises the question of what transcript(s) miR-100-5p is targeting. Additional indirect targets as well as possible direct targets may be identified by proteome or transcriptome analysis of FL-YB cells following miR-100-5p knockdown. The identification of additional transcriptional changes in FL-YB cells upon miR-100-5p knockdown would also help to infer the functional consequences of this miRNA. To identify direct targets of miR-100-5p comparison of cells with and without miR-100-5p knockdown could be carried out by a method such as Ago HITS-CLIP (high throughput sequencing by crosslinking and immunoprecipitation) which involves cross-linking of the RISC protein Ago with any bound RNA i.e. miRNA and their target sequences.

To further investigate the impact of miR-100-5p knockdown on the function of FL-YB cells, it would be useful to look at the impact on B cell co-culture in experiments similar to those previously carried out between FL-YB and B cells (Nishikawa et al., 2006).

The other miRNAs identified to be differentially regulated upon FDC de-differentiation are also likely to have important roles in FDC function. Functional effects of the other two miRNAs identified to be expressed in FL-YB cells (miR-2137 and miR-138-5p) were not discovered in this thesis. However the functional analysis carried out to date is limited and further analysis would have to be carried out on different aspects of FDC function to determine the role of these miRNA. Target identification could also be carried out with the aid of the computational target prediction carried out in this thesis.

Target prediction was carried out both for individual miRNAs and for the group of eight miRNAs which were all identified to have decreased expression levels with FDC de-differentiation. MiRNAs often function in networks, with many miRNAs regulating gene expression at different levels or expression of related genes in a way that tightly regulates a certain biological process. It would therefore be interesting to develop that work, as several miRNAs that display the same pattern of expression upon de-diffentiation of FDC were identified in this thesis. One way of looking at the co-ordinated effect of several miRNAs would be to transfect cells with pools of several miRNA inhibitors to knock-down several miRNAs at once. This work was started, where miR-100-5p, miR-138-5p and miR2137 antisense LNAs were transfected into cells which were then monitored by the xCELLigence system, early results did not indicate any significant effect on the cell index measurements and the work was not continued due to time constraints. It would be valuable to study knock-down of more of the miRNAs and also monitoring more specific and functions (such as proliferation) and outputs (such as the genes already looked at following individual miRNA inhibition) of the cells.

7.8. Conclusions

In conclusion, the data presented in this thesis suggests that the miRNA, miR-100-5p, plays a role in the regulation of pro-inflammatory gene expression in murine FDC.

The *in vivo* blockade of LTβR signalling caused rapid de-differentiation of FDC and comparisons of spleen samples with FDC at different stages of de-differentiation allowed the identification of a number of miRNA associated with FDC maturation and/or function.

Three of these miRNA were selected on the basis of their expression pattern, and shown to be expressed in the murine FDC cell line FL-YB.

The FL-YB cell line was found to respond to TNFα by up-regulating the expression of a number of genes associated with FDC activation and IL-4 treatment was found to increase the expression levels of many of the activation-associated transcripts.

Functional analysis of the identified miRNAs in the FL-YB cells revealed that depletion of miR-100-5p resulted in an increase in expression of a number of gene transcripts of pro-inflammatory genes. Increased expression of these genes, *Il-6*, *Tlr4* and *Ptgs,* has been implicated in autoimmune diseases. These genes are all also down-stream genes of the transcription factor NFκB, raising the possibility of miR-100-5p having a role in the regulation of the TNFR/LTβR-NFκB pathway at some level.

Together these data suggest that miR-100-5p has a role in the regulation of pro-inflammatory genes in FDC, which may have important implications in the progression of some autoimmune reactions.

Bibliography

Aguzzi, A. and Krautler, N.J. (2010) Characterizing follicular dendritic cells: A progress report. **European journal of immunology**, 40 (8): 2134–8

Akhtar, N., Rasheed, Z., Ramamurthy, S., et al. (2010) MicroRNA-27b regulates the expression of matrix metalloproteinase 13 in human osteoarthritis chondrocytes. **Arthritis and rheumatism**, 62 (5): 1361–71

Alimzhanov, M.B., Kuprash, D. V, Kosco-Vilbois, M.H., et al. (1997) Abnormal development of secondary lymphoid tissues in lymphotoxin beta-deficient mice. **Proceedings of the National Academy of Sciences of the United States of America**, 94 (17): 9302–7

Allen, C.D.C., Ansel, K.M., Low, C., et al. (2004) Germinal center dark and light zone organization is mediated by CXCR4 and CXCR5. **Nature immunology**, 5 (9): 943–52

Allen, C.D.C. and Cyster, J.G. (2008) Follicular dendritic cell networks of primary follicles and germinal centers: Phenotype and function. **Seminars in Immunology**, 20 (1): 14–25

Von Allmen, C.E., Schmitz, N., Bauer, M., et al. (2009) Secretory phospholipase A2-IID is an effector molecule of CD4+CD25+ regulatory T cells. **Proceedings of the National Academy of Sciences of the United States of America**, 106 (28): 11673–8

Alon, S., Vigneault, F., Eminaga, S., et al. (2011) Barcoding bias in high-throughput multiplex sequencing of miRNA. **Genome research**, 21 (9): 1506–11

Ambros, V. (2004) The functions of animal microRNAs. **Nature**, 431 (7006): 350–5

Amft, N., Curnow, S.J., Scheel-toellner, D., et al. (2001) Ectopic expression of the B cell-attracting chemokine BCA-1 (CXCL13) on endothelial cells and within lymphoid follicles contributes to the establishment of germinal center-like structures in Sjögren's syndrome. **Arthritis and rheumatism**, 44 (11): 2633–41

Ansel, K.M., McHeyzer-Williams, L.J., Ngo, V.N., et al. (1999) In vivo-activated CD4 T cells upregulate CXC chemokine receptor 5 and reprogram their response to lymphoid chemokines. **The Journal of experimental medicine**, 190 (8): 1123–34

Ansel, K.M., Ngo, V.N., Hyman, P.L., et al. (2000) A chemokine-driven positive feedback loop organizes lymphoid follicles. **Nature**, 406 (6793): 309–14

Asirvatham, A.J., Magner, W.J. and Tomasi, T.B. (2009) miRNA regulation of cytokine genes. **Cytokine**, 45 (2): 58–69

Assier, E., Boissier, M.-C. and Dayer, J.-M. (2010) Interleukin-6: from identification of the cytokine to development of targeted treatments. **Joint, bone, spine : revue du rhumatisme**, 77 (6): 532–6

Aziz, M.M., Ishihara, S., Rumi, M.A.K., et al. (2008) Prolactin induces MFG-E8 production in macrophages via transcription factor C/EBPbeta-dependent pathway. **Apoptosis : an international journal on programmed cell death**, 13 (5): 609–20

Bachmann, M.F., Kündig, T.M., Hengartner, H., et al. (1994) Regulation of IgG antibody titers by the amount persisting of immune-complexed antigen. **European journal of immunology**, 24 (10): 2567–70

Baek, D., Villén, J., Shin, C., et al. (2008) The impact of microRNAs on protein output. **Nature**, 455 (7209): 64–71

Balogh, P., Aydar, Y., Tew, J.G., et al. (2001) Ontogeny of the follicular dendritic cell phenotype and function in the postnatal murine spleen. **Cellular immunology**, 214 (1): 45–53

Balogh, P., Aydar, Y., Tew, J.G., et al. (2002) Appearance and phenotype of murine follicular dendritic cells expressing VCAM-1. **The Anatomical record**, 268 (2): 160–8

Baltimore, D., Boldin, M.P., O'Connell, R.M., et al. (2008) MicroRNAs: new regulators of immune cell development and function. **Nature immunology**, 9 (8): 839–45

Baratelli, F., Lin, Y., Zhu, L., et al. (2005) Prostaglandin E2 induces FOXP3 gene expression and T regulatory cell function in human CD4+ T cells. **Journal of immunology**, 175 (3): 1483–90

Barbato, C., Arisi, I., Frizzo, M.E., et al. (2009) Computational challenges in miRNA target predictions: to be or not to be a true target? **Journal of biomedicine & biotechnology**, 2009: 803069

Bartel, D.P. (2009) MicroRNAs: Target Recognition and Regulatory Functions. **Cell**, 136 (2): 215–233

Basso, K., Sumazin, P., Morozov, P., et al. (2009) Identification of the Human Mature B Cell miRNome. **Immunity**, 30 (5): 744–752

Baumann, I., Kolowos, W., Voll, R.E., et al. (2002) Impaired uptake of apoptotic cells into tingible body macrophages in germinal centers of patients with systemic lupus erythematosus. **Arthritis and rheumatism**, 46 (1): 191–201

Bazzini, A.A., Lee, M.T. and Giraldez, A.J. (2012) Ribosome profiling shows that miR-430 reduces translation before causing mRNA decay in zebrafish. **Science**, 336 (6078): 233–7

Becker, L.E., Lu, Z., Chen, W., et al. (2012) A systematic screen reveals MicroRNA clusters that significantly regulate four major signaling pathways. **PloS one**, 7 (11): e48474

Behrman, S., Acosta-Alvear, D. and Walter, P. (2011) A CHOP-regulated microRNA controls rhodopsin expression. **The Journal of cell biology**, 192 (6): 919–27

Bénézech, C., Mader, E., Desanti, G., et al. (2012) Lymphotoxin-β Receptor Signaling through NF-κB2-RelB Pathway Reprograms Adipocyte Precursors as Lymph Node Stromal Cells. **Immunity**, 37 (4): 721–34

Bénézech, C., White, A., Mader, E., et al. (2010) Ontogeny of stromal organizer cells during lymph node development. **Journal of immunology**, 184 (8): 4521–30

Bentley, D.R., Balasubramanian, S., Swerdlow, H.P., et al. (2008) Accurate whole human genome sequencing using reversible terminator chemistry. **Nature**, 456 (7218): 53–9

Bernstein, E., Caudy, a a, Hammond, S.M., et al. (2001) Role for a bidentate ribonuclease in the initiation step of RNA interference. **Nature**, 409 (6818): 363–6

Betel, D., Koppal, A., Agius, P., et al. (2010) Comprehensive modeling of microRNA targets predicts functional non-conserved and non-canonical sites. **Genome biology**, 11 (8): R90

Betel, D., Wilson, M., Gabow, A., et al. (2008) The microRNA.org resource: targets and expression. **Nucleic acids research**, 36 (Database issue): D149–53

Bofill, M., Akbar, a N. and Amlot, P.L. (2000) Follicular dendritic cells share a membrane-bound protein with fibroblasts. **The Journal of pathology**, 191 (2): 217–26

Borchert, G.M., Holton, N.W. and Larson, E.D. (2011) Repression of human activation induced cytidine deaminase by miR-93 and miR-155. **BMC cancer**, 11 (1): 347

Bronevetsky, Y. and Ansel, K.M. (2013) Regulation of miRNA biogenesis and turnover in the immune system. **Immunological reviews**, 253 (1): 304–16

Brown, K.L., Stewart, K., Ritchie, D.L., et al. (1999) Scrapie replication in lymphoid tissues depends on prion protein-expressing follicular dendritic cells. **Nature medicine**, 5 (11): 1308–12

Browning, J.L., Ngam-ek, A., Lawton, P., et al. (1993) Lymphotoxin [beta], a novel member of the TNF family that forms a heteromeric complex with lymphotoxin on the cell surface. **Cell**, 72 (6): 847–856

Burton, G.F., Keele, B.F., Estes, J.D., et al. (2002) Follicular dendritic cell contributions to HIV pathogenesis. **Seminars in Immunology**, 14 (4): 275–284

Carrasco, Y.R., Fleire, S.J., Cameron, T., et al. (2004) LFA-1/ICAM-1 Interaction Lowers the Threshold of B Cell Activation by Facilitating B Cell Adhesion and Synapse Formation. **Immunity**, 20 (5): 589–599

Castagnaro, L., Lenti, E., Maruzzelli, S., et al. (2013) Nkx2-5+Islet1+ Mesenchymal Precursors Generate Distinct Spleen Stromal Cell Subsets and Participate in Restoring Stromal Network Integrity. **Immunity**, 38 (4): 782–791

Castell, J. V, Gómez-Lechón, M.J., David, M., et al. (1989) Interleukin-6 is the major regulator of acute phase protein synthesis in adult human hepatocytes. **FEBS letters**, 242 (2): 237–9

Chan, J.K., Fletcher, C.D., Nayler, S.J., et al. (1997) Follicular dendritic cell sarcoma. Clinicopathologic analysis of 17 cases suggesting a malignant potential higher than currently recognized. **Cancer**, 79 (2): 294–313

Chen, C., Ridzon, D. a, Broomer, A.J., et al. (2005) Real-time quantification of microRNAs by stem-loop RT-PCR. **Nucleic acids research**, 33 (20): e179

Chen, C.-Z., Li, L., Lodish, H.F., et al. (2004) MicroRNAs modulate hematopoietic lineage differentiation. **Science**, 303 (5654): 83–6

Chen, C.-Z., Schaffert, S., Fragoso, R., et al. (2013a) Regulation of immune responses and tolerance: the microRNA perspective. **Immunological reviews**, 253 (1): 112–28

Chen, J., Bardes, E.E., Aronow, B.J., et al. (2009) ToppGene Suite for gene list enrichment analysis and candidate gene prioritization. **Nucleic acids research**, 37 (1): W305–11

Chen, L., Adams, J. and Steinman, R. (1978) Anatomy of germinal centers in mouse spleen, with special reference to “follicular dendritic cells”. **The Journal of Cell Biology**, 77 (1): 148–164

Chen, P., Zhao, X. and Ma, L. (2013b) Downregulation of microRNA-100 correlates with tumor progression and poor prognosis in hepatocellular carcinoma. **Molecular and cellular biochemistry**, (ahead of print)

Chendrimada, T.P., Gregory, R.I., Kumaraswamy, E., et al. (2005) TRBP recruits the Dicer complex to Ago2 for microRNA processing and gene silencing. **Nature**, 436 (7051): 740–4

Chiang, H. and Schoenfeld, L. (2010) Mammalian microRNAs: experimental evaluation of novel and previously annotated genes. **Genes & Development**, pp. 992–1009

Cho, K.-A., Kim, J.-Y., Kim, H.S., et al. (2012) Tonsil-derived mesenchymal progenitor cells acquire a follicular dendritic cell phenotype under cytokine stimulation. **Cytokine**, 59 (2): 211–4

Cho, W., Hong, S.H. and Choe, J. (2013) IL-4 and HDAC Inhibitors Suppress Cyclooxygenase-2 Expression in Human Follicular Dendritic Cells. **Immune network**, 13 (2): 75–9

Cho, W., Kim, J., Cho, K.-B., et al. (2011a) Production of prostaglandin e(2) and i(2) is coupled with cyclooxygenase-2 in human follicular dendritic cells. **Immune network**, 11 (6): 364–7

Cho, W., Kim, Y., Jeoung, D.-I., et al. (2011b) IL-4 and IL-13 suppress prostaglandins production in human follicular dendritic cells by repressing COX-2 and mPGES-1 expression through JAK1 and STAT6. **Molecular immunology**, 48 (6-7): 966–72

Choe, J., Kim, H.S., Zhang, X., et al. (1996) Cellular and molecular factors that regulate the differentiation and apoptosis of germinal center B cells. Anti-Ig down-regulates Fas expression of CD40 ligand-stimulated germinal center B cells and inhibits Fas-mediated apoptosis. **Journal of immunology**, 157 (3): 1006–16

Choe, J., Li, L., Zhang, X., et al. (2000) Distinct role of follicular dendritic cells and T cells in the proliferation, differentiation, and apoptosis of a centroblast cell line, L3055. **Journal of immunology**, 164 (1): 56–63

Cloonan, N., Wani, S., Xu, Q., et al. (2011) MicroRNAs and their isomiRs function cooperatively to target common biological pathways. **Genome Biology**, 12 (12): R126

Coffman, R.L., Ohara, J., Bond, M.W., et al. (1986) B cell stimulatory factor-1 enhances the IgE response of lipopolysaccharide-activated B cells. **Journal of immunology**, 136 (12): 4538–41

Crotty, S., Johnston, R.J. and Schoenberger, S.P. (2010) Effectors and memories: Bcl-6 and Blimp-1 in T and B lymphocyte differentiation. **Nature immunology**, 11 (2): 114–20

Cullen, B.R. (2013) MicroRNAs as mediators of viral evasion of the immune system. **Nature Immunology**, 14 (3): 205–210

Cupedo, T., Lund, F.E., Ngo, V.N., et al. (2004) Initiation of cellular organization in lymph nodes is regulated by non-B cell-derived signals and is not dependent on CXC chemokine ligand 13. **Journal of immunology**, 173 (8): 4889–96

Cyster, J.G. (2010) B cell follicles and antigen encounters of the third kind. **Nature immunology**, 11 (11): 989–96

Davidson-Moncada, J., Papavasiliou, F.N. and Tam, W. (2010) MicroRNAs of the immune system: roles in inflammation and cancer. **Annals of the New York Academy of Sciences**, 1183 (1): 183–94

Dejardin, E., Droin, N.M., Delhase, M., et al. (2002) The lymphotoxin-beta receptor induces different patterns of gene expression via two NF-kappaB pathways. **Immunity**, 17 (4): 525–35

Deng, C., Goluszko, E., Tüzün, E., et al. (2002) Resistance to experimental autoimmune myasthenia gravis in IL-6-deficient mice is associated with reduced germinal center formation and C3 production. **Journal of immunology**, 169 (2): 1077–83

Deng, N., Puetter, A., Zhang, K., et al. (2011) Isoform-level microRNA-155 target prediction using RNA-seq. **Nucleic acids research**, 39 (9): e61

Dhoot, G.K., Gustafsson, M.K., Ai, X., et al. (2001) Regulation of Wnt signaling and embryo patterning by an extracellular sulfatase. **Science**, 293 (5535): 1663–6

Van Dinther-Janssen, A.C., Horst, E., Koopman, G., et al. (1991) The VLA-4/VCAM-1 pathway is involved in lymphocyte adhesion to endothelium in rheumatoid synovium. **Journal of immunology**, 147 (12): 4207–10

Doench, J. and Sharp, P. (2004) Specificity of microRNA target selection in translational repression. **Genes & development**, pp. 504–511

Dorsett, Y., McBride, K.K.M., Jankovic, M., et al. (2008) MicroRNA-155 Suppresses Activation-Induced Cytidine Deaminase-Mediated Myc-Igh Translocation. **Immunity**, 28 (5): 630–638

Ebert, M. and Sharp, P. (2012) Roles for microRNAs in conferring robustness to biological processes. **Cell**, 149 (3): 515–524

Elia, L., Quintavalle, M., Zhang, J., et al. (2009) The knockout of miR-143 and -145 alters smooth muscle cell maintenance and vascular homeostasis in mice: correlates with human disease. **Cell death and differentiation**, 16 (12): 1590–8

Endres, R., Alimzhanov, M.B., Plitz, T., et al. (1999) Mature follicular dendritic cell networks depend on expression of lymphotoxin beta receptor by radioresistant stromal cells and of lymphotoxin beta and tumor necrosis factor by B cells. **The Journal of experimental medicine**, 189 (1): 159–68

Eskildsen, T., Taipaleenmäki, H., Stenvang, J., et al. (2011) MicroRNA-138 regulates osteogenic differentiation of human stromal (mesenchymal) stem cells in vivo. **Proceedings of the National Academy of Sciences of the United States of America**, 108 (15): 6139–44

Eto, D., Lao, C., DiToro, D., et al. (2011) IL-21 and IL-6 are critical for different aspects of B cell immunity and redundantly induce optimal follicular helper CD4 T cell (Tfh) differentiation. **PloS one**, 6 (3): e17739

Eulalio, A., Behm-Ansmant, I., Schweizer, D., et al. (2007) P-body formation is a consequence, not the cause, of RNA-mediated gene silencing. **Molecular and cellular biology**, 27 (11): 3970–81

Fabian, M.R., Mathonnet, G., Sundermeier, T., et al. (2009) Mammalian miRNA RISC recruits CAF1 and PABP to affect PABP-dependent deadenylation. **Molecular cell**, 35 (6): 868–80

Fabian, M.R., Sonenberg, N. and Filipowicz, W. (2010) Regulation of mRNA translation and stability by microRNAs. **Annual Review of Biochemistry**, 79 (1): 351–379

Fang, Y., Xu, C., Fu, Y.-X.X., et al. (1998) Expression of complement receptors 1 and 2 on follicular dendritic cells is necessary for the generation of a strong antigen-specific IgG response. **Journal of immunology**, 160 (11): 5273–9

Farh, K.K.-H., Grimson, A., Jan, C., et al. (2005) The widespread impact of mammalian MicroRNAs on mRNA repression and evolution. **Science**, 310 (5755): 1817–21

Fliedner, A., Parwaresch, M.R. and Feller, A.C. (1990) Induction of antigen expression of follicular dendritic cells in a monoblastic cell line. A contribution to its cellular origin. **The Journal of pathology**, 161 (1): 71–77

Force, W.R., Walter, B.N., Hession, C., et al. (1995) Mouse lymphotoxin-beta receptor. Molecular genetics, ligand binding, and expression. **Journal of immunology**, 155 (11): 5280–8

Förster, R., Mattis, a E., Kremmer, E., et al. (1996) A putative chemokine receptor, BLR1, directs B cell migration to defined lymphoid organs and specific anatomic compartments of the spleen. **Cell**, 87 (6): 1037–47

Friedman, R.C., Farh, K.K., Burge, C.B., et al. (2009) Most mammalian mRNAs are conserved targets of microRNAs. **Genome research**, 19 (1): 92–105

Fukata, M., Chen, A., Klepper, A., et al. (2006) Cox-2 is regulated by Toll-like receptor-4 (TLR4) signaling: Role in proliferation and apoptosis in the intestine. **Gastroenterology**, 131 (3): 862–77

Fütterer, a, Mink, K., Luz, a, et al. (1998) The lymphotoxin beta receptor controls organogenesis and affinity maturation in peripheral lymphoid tissues. **Immunity**, 9 (1): 59–70

Ganeff, C., Remouchamps, C., Boutaffala, L., et al. (2011) Induction of the alternative NF-κB pathway by lymphotoxin αβ (LTαβ) relies on internalization of LTβ receptor. **Molecular and cellular biology**, 31 (21): 4319–34

Ganley-Leal, L.M., Liang, Y., Jagannathan-Bogdan, M., et al. (2010) Differential regulation of TLR4 expression in human B cells and monocytes. **Molecular immunology**, 48 (1-3): 82–8

Gardam, S., Sierro, F., Basten, A., et al. (2008) TRAF2 and TRAF3 signal adapters act cooperatively to control the maturation and survival signals delivered to B cells by the BAFF receptor. **Immunity**, 28 (3): 391–401

Garin, A., Meyer-Hermann, M., Contie, M., et al. (2010) Toll-like Receptor 4 Signaling by Follicular Dendritic Cells Is Pivotal for Germinal Center Onset and Affinity Maturation. **Immunity**, 33 (1): 84–95

Gautier, L., Cope, L., Bolstad, B.M., et al. (2004) affy--analysis of Affymetrix GeneChip data at the probe level. **Bioinformatics**, 20 (3): 307–15

Gay, N.J. and Gangloff, M. (2007) Structure and function of Toll receptors and their ligands. **Annual review of biochemistry**, 76: 141–65

Gil, M., Park, S.-J., Chung, Y.-S., et al. (2010) Interleukin-15 enhances proliferation and chemokine secretion of human follicular dendritic cells. **Immunology**, 130 (4): 536–44

Git, A., Dvinge, H., Salmon-Divon, M., et al. (2010) Systematic comparison of microarray profiling, real-time PCR, and next-generation sequencing technologies for measuring differential microRNA expression. **RNA**, 16 (5): 991–1006

Le Goff, B., Blanchard, F., Berthelot, J.-M., et al. (2010) Role for interleukin-6 in structural joint damage and systemic bone loss in rheumatoid arthritis. **Joint, bone, spine : revue du rhumatisme**, 77 (3): 201–5

Gong, H., Song, L., Lin, C., et al. (2013) Downregulation of miR-138 sustains NF-κB activation and promotes lipid raft formation in esophageal squamous cell carcinoma. **Clinical cancer research : an official journal of the American Association for Cancer Research**, 19 (5): 1083–93

Gonzalez, M., Mackay, F., Browning, J.L., et al. (1998) The Sequential Role of Lymphotoxin and B Cells in the Development of Splenic Follicles. **J. Exp. Med.**, 187 (7): 997–1007

Goval, J.-J., Thielen, C., Bourguignon, C., et al. (2008) The prevention of spontaneous apoptosis of follicular lymphoma B cells by a follicular dendritic cell line: involvement of caspase-3, caspase-8 and c-FLIP. **Haematologica**, 93 (8): 1169–77

Griffiths-Jones, S., Grocock, R.J., Van Dongen, S., et al. (2006) miRBase: microRNA sequences, targets and gene nomenclature. **Nucleic Acids Research**, 34 (Database issue): D140–D144

Griffiths-Jones, S., Hui, J.H.L., Marco, A., et al. (2011) MicroRNA evolution by arm switching. **EMBO reports**, 12 (2): 172–7

Grundmann, S., Hans, F.P., Kinniry, S., et al. (2011) MicroRNA-100 regulates neovascularization by suppression of mammalian target of rapamycin in endothelial and vascular smooth muscle cells. **Circulation**, 123 (9): 999–1009

Guettier, C., GATTER, K.C., HERYET, A., et al. (1986) Dendritic reticulum cells in reactive lymph nodes and tonsils: an immunohistological study. **Histopathology**, 10 (1): 15–24

Guo, Y., Niu, C., Breslin, P., et al. (2009) c-Myc-mediated control of cell fate in megakaryocyte-erythrocyte progenitors. **Blood**, 114 (10): 2097–2106

Ha, T.-Y. (2011) The Role of MicroRNAs in Regulatory T Cells and in the Immune Response. **Immune network**, 11 (1): 11–41

Haase, a T., Henry, K., Zupancic, M., et al. (1996) Quantitative image analysis of HIV-1 infection in lymphoid tissue. **Science**, 274 (5289): 985–9

Hanayama, R., Tanaka, M., Miyasaka, K., et al. (2004) Autoimmune disease and impaired uptake of apoptotic cells in MFG-E8-deficient mice. **Science**, 304 (5674): 1147–50

Harris, S.G., Padilla, J., Koumas, L., et al. (2002) Prostaglandins as modulators of immunity. **Trends in immunology**, 23 (3): 144–50

Hase, H., Kanno, Y., Kojima, M., et al. (2004) BAFF/BLyS can potentiate B-cell selection with the B-cell coreceptor complex. **Blood**, 103 (6): 2257–65

Heath, D.I., Cruickshank, a, Gudgeon, M., et al. (1993) Role of interleukin-6 in mediating the acute phase protein response and potential as an early means of severity assessment in acute pancreatitis. **Gut**, 34 (1): 41–5

Heesters, B.A., Chatterjee, P., Kim, Y.-A., et al. (2013) Endocytosis and recycling of immune complexes by follicular dendritic cells enhances B cell antigen binding and activation. **Immunity**, 38 (6): 1164–75

Heinemann, D.E. and Peters, J.H. (2005) Follicular dendritic-like cells derived from human monocytes. **BMC Immunology**, 6 (23): 23

Hengartner, M.O. (2000) The biochemistry of apoptosis. **Nature**, 407 (6805): 770–6

Hogenbirk, M. a, Heideman, M.R., Velds, A., et al. (2013) Differential Programming of B Cells in AID Deficient Mice. **PloS one**, 8 (7): e69815

Hornstein, E. and Shomron, N. (2006) Canalization of development by microRNAs. **Nature genetics**, 38 Suppl (June): S20–4

Huber, C., Thielen, C., Seeger, H., et al. (2005) Lymphotoxin-beta receptor-dependent genes in lymph node and follicular dendritic cell transcriptomes. **Journal of immunology**, 174 (9): 5526–36

Hulkkonen, J., Pertovaara, M., Antonen, J., et al. (2001) Elevated interleukin-6 plasma levels are regulated by the promoter region polymorphism of the IL6 gene in primary Sjögren's syndrome and correlate with the clinical manifestations of the disease. **Rheumatology**, 40 (6): 656–61

Humphrey, J.H. and Sundaram, V. (1985) Origin and turnover of follicular dendritic cells and marginal zone macrophages in the mouse spleen. **Advances in experimental medicine and biology**, 186: 167–70

Husson, H., Lugli, S.M., Ghia, P., et al. (2000) Functional effects of TNF and lymphotoxin alpha1beta2 on FDC-like cells. **Cellular immunology**, 203 (2): 134–43

Hutvágner, G., McLachlan, J., Pasquinelli, a E., et al. (2001) A cellular function for the RNA-interference enzyme Dicer in the maturation of the let-7 small temporal RNA. **Science**, 293 (5531): 834–8

Hutvagner, G., Zamore, P.D. and Hutvágner, G. (2002) A microRNA in a multiple-turnover RNAi enzyme complex. **Science**, 297 (5589): 2056–60

Hwang, I.Y., Park, C., Harrision, K.A., et al. (2010) Variations in Gnai2 and Rgs1 expression affect chemokine receptor signaling and the organization of secondary lymphoid organs. **Genes and immunity**, 11 (5): 384–96

Hwang, I.-Y., Park, C., Harrison, K., et al. (2009) TLR4 signaling augments B lymphocyte migration and overcomes the restriction that limits access to germinal center dark zones. **The Journal of experimental medicine**, 206 (12): 2641–57

Imai, Y., Maeda, K., Yamakawa, M., et al. (1993) Heterogeneity and cellular origin of follicular dendritic cells. **Advances in experimental medicine and biology**, 329: 339–44

Irizarry, R. a. (2003) Summaries of Affymetrix GeneChip probe level data. **Nucleic Acids Research**, 31 (4): 15e–15

Jakymiw, A., Patel, R.S., Deming, N., et al. (2010) Overexpression of dicer as a result of reduced let-7 MicroRNA levels contributes to increased cell proliferation of oral cancer cells. **Genes, chromosomes & cancer**, 49 (6): 549–59

Janas, M.M. and Novina, C.D. (2012) Not lost in translation: stepwise regulation of microRNA targets. **The EMBO journal**, 31 (11): 2446–7

Jiang, J., Lee, E.J., Gusev, Y., et al. (2005) Real-time expression profiling of microRNA precursors in human cancer cell lines. **Nucleic acids research**, 33 (17): 5394–403

Johnnidis, J.B., Harris, M.H., Wheeler, R.T., et al. (2008) Regulation of progenitor cell proliferation and granulocyte function by microRNA-223. **Nature**, 451 (7182): 1125–1129

Junt, T., Tumanov, A. V, Harris, N., et al. (2006) Expression of lymphotoxin beta governs immunity at two distinct levels. **European journal of immunology**, 36 (8): 2061–75

Kagias, K., Nehammer, C. and Pocock, R. (2012) Neuronal responses to physiological stress. **Frontiers in genetics**, 3 (October): 222

Kapasi, Z.F., Qin, D., Kerr, W.G., et al. (1998) Follicular Dendritic Cell (FDC) Precursors in Primary Lymphoid Tissues. **J Immunol**, 160 (3): 1078–1084

Kast, J. (2011) A quick reality check for microRNA target prediction. **Expert review of proteomics**, 8 (2): 149–52

Katakai, T. (2012) Marginal reticular cells: a stromal subset directly descended from the lymphoid tissue organizer. **Frontiers in immunology**, 3 (July): 200

Katakai, T., Suto, H., Sugai, M., et al. (2008) Organizer-Like Reticular Stromal Cell Layer Common to Adult Secondary Lymphoid Organs. **J Immunol**, 181 (9): 6189–6200

Kavai, M. (2008) Immune complex clearance by complement receptor type 1 in SLE. **Autoimmunity reviews**, 8 (2): 160–4

Ke, N., Wang, X., Xu, X., et al. (2011) "The xCELLigence System for Real-Time and Label-Free Monitoring of Cell Viability." In Stoddart, M.J. (ed.) **Mammalian cell viability: methods and protocols**. Totowa, NJ: Humana Press. pp. 33–43

Keller, A., Leidinger, P., Steinmeyer, F., et al. (2013) Comprehensive analysis of microRNA profiles in multiple sclerosis including next-generation sequencing. **Multiple sclerosis**, (epub ahead of print)

Khvorova, A., Reynolds, A. and Jayasena, S.D. (2003) Functional siRNAs and miRNAs exhibit strand bias. **Cell**, 115 (2): 209–16

Kim, H.S., Zhang, X. and Choi, Y.S. (1994) Activation and proliferation of follicular dendritic cell-like cells by activated T lymphocytes. **Journal of immunology**, 153 (7): 2951–61

Kim, H.S., Zhang, X., Klyushnenkova, E., et al. (1995) Stimulation of germinal center B lymphocyte proliferation by an FDC-like cell line, HK. **Journal of immunology**, 155 (3): 1101–9

Kim, J., Kim, Y.-M., Jeoung, D.-I., et al. (2012a) Human follicular dendritic cells promote the APC capability of B cells by enhancing CD86 expression levels. **Cellular immunology**, 273 (2): 109–14

Kim, J., Lee, S., Kim, Y.-M., et al. (2013) Human follicular dendritic cells promote germinal center B cell survival by providing prostaglandins. **Molecular immunology**, 55 (3-4): 418–23

Kim, J.J., Kim, D.W., Chang, W., et al. (2012b) Wnt5a is secreted by follicular dendritic cells to protect germinal center B cells via Wnt/Ca2+/NFAT/NF-κB-B cell lymphoma 6 signaling. **Journal of immunology**, 188 (1): 182–9

Kim, M.-Y. (2008) Roles of Embryonic and Adult Lymphoid Tissue Inducer Cells in Primary and Secondary Lymphoid Tissues. **Yonsei Medical Journal**, 49 (3): 352–356

Kim, Y., Kim, J., Park, J., et al. (2006) TC1(C8orf4) is upregulated by IL-1beta/TNF-alpha and enhances proliferation of human follicular dendritic cells. **FEBS letters**, 580 (14): 3519–24

Knight, S.W. and Bass, B.L. (2001) A role for the RNase III enzyme DCR-1 in RNA interference and germ line development in Caenorhabditis elegans. **Science**, 293 (5538): 2269–71

Koni, P.A., Sacca, R., Lawton, P., et al. (1997) Distinct Roles in Lymphoid Organogenesis for Lymphotoxins [alpha] and [beta] Revealed in Lymphotoxin [beta]-Deficient Mice. **Immunity**, 6 (4): 491–500

Koopman, G., Keehnen, R.M., Lindhout, E., et al. (1994) Adhesion through the LFA-1 (CD11a/CD18)-ICAM-1 (CD54) and the VLA-4 (CD49d)-VCAM-1 (CD106) pathways prevents apoptosis of germinal center B cells. **Journal of immunology**, 152 (8): 3760–7

Kopf, M., Baumann, H., Freer, G., et al. (1994) Impaired immune and acute-phase responses in interleukin-6-deficient mice. **Nature**, 368 (6469): 339–42

Kopf, M., Herren, S. and Wiles, M. (1998) Interleukin 6 influences germinal center development and antibody production via a contribution of C3 complement component. **The Journal of Experimental medicine**, 188 (10): 1895–1906

Koralov, S.B., Muljo, S.A., Galler, G.R., et al. (2008) Dicer Ablation Affects Antibody Diversity and Cell Survival in the B Lymphocyte Lineage. **Cell**, 132 (5): 860–874

Kosco, M., Pflugfelder, E. and Gray, D. (1992) Follicular dendritic cell-dependent adhesion and proliferation of B cells in vitro. **J Immunol**, 148 (8): 2331–2339

Kosco, M.H. and Gray, D. (1992) Signals involved in germinal center reactions. **Immunological Reviews**, 126: 63–76

Kosco-Vilbois, M.H. (2003) Are follicular dendritic cells really good for nothing? **Nat Rev Immunol**, 3 (9): 764–769

Koshkin, A., Singh, S. and Nielsen, P. (1998) Nucleic Acids): Synthesis of the adenine, cytosine, guanine, 5-methylcytosine, thymine and uracil bicyclonucleoside monomers, oligomerisation, and unprecedented. **Tetrahedron**, 54: 3607–3630

Kozomara, A. and Griffiths-Jones, S. (2011) miRBase: integrating microRNA annotation and deep-sequencing data. **Nucleic acids research**, 39 (Database issue): D152–7

Kranich, J., Krautler, N.J., Heinen, E., et al. (2008) Follicular dendritic cells control engulfment of apoptotic bodies by secreting Mfge8. **J. Exp. Med.**, 205 (6): 1293–1302

Krautler, N.J., Kana, V., Kranich, J., et al. (2012) Follicular dendritic cells emerge from ubiquitous perivascular precursors. **Cell**, 150 (1): 194–206

Kruse, K., Janko, C., Urbonaviciute, V., et al. (2010) Inefficient clearance of dying cells in patients with SLE: anti-dsDNA autoantibodies, MFG-E8, HMGB-1 and other players. **Apoptosis : an international journal on programmed cell death**, 15 (9): 1098–113

Kuprash, D. V, Alimzhanov, M.B., Tumanov, A. V, et al. (1999) TNF and lymphotoxin beta cooperate in the maintenance of secondary lymphoid tissue microarchitecture but not in the development of lymph nodes. **Journal of immunology**, 163 (12): 6575–80

Kwanhian, W., Lenze, D., Alles, J., et al. (2012) MicroRNA-142 is mutated in about 20% of diffuse large B-cell lymphoma. **Cancer Medicine**, 1 (2): 141-155

Lagos-Quintana, M., Rauhut, R., Lendeckel, W., et al. (2001) Identification of novel genes coding for small expressed RNAs. **Science**, 294 (5543): 853–8

Lagos-Quintana, M., Rauhut, R., Meyer, J., et al. (2003) New microRNAs from mouse and human. **RNA**, 9: 175–9

Lal, A., Navarro, F., Maher, C.A., et al. (2009) miR-24 Inhibits cell proliferation by targeting E2F2, MYC, and other cell-cycle genes via binding to "seedless" 3'UTR microRNA recognition elements. **Molecular cell**, 35 (5): 610–25

Landgraf, P., Rusu, M., Sheridan, R., et al. (2007) A mammalian microRNA expression atlas based on small RNA library sequencing. **Cell**, 129 (7): 1401–14

Lane, P.J.L., Gaspal, F.M., McConnell, F.M., et al. (2012) Lymphoid tissue inducer cells: pivotal cells in the evolution of CD4 immunity and tolerance? **Frontiers in immunology**, 3 (February): 24

Lau, N.C., Lim, L.P., Weinstein, E.G., et al. (2001) An abundant class of tiny RNAs with probable regulatory roles in Caenorhabditis elegans. **Science**, 294 (5543): 858–62

Lawrie, C.H., Soneji, S., Marafioti, T., et al. (2007) MicroRNA expression distinguishes between germinal center B cell-like and activated B cell-like subtypes of diffuse large B cell lymphoma. **International journal of cancer. Journal international du cancer**, 121 (5): 1156–61

Lee, C., Das, B. and Lin, T. (2012) A rare fraction of drug resistant follicular lymphoma cancer stem cells interacts with follicular dendritic cells to maintain tumourigenic potential. **British journal of Haematology**, 158 (1): 79–90

Lee, C., Lin, W.-N., Lin, C., et al. (2006) Transcriptional regulation of VCAM-1 expression by tumor necrosis factor-alpha in human tracheal smooth muscle cells: involvement of MAPKs, NF-kappaB, p300, and histone acetylation. **Journal of cellular physiology**, 207 (1): 174–86

Lee, H.-M., Jin, H.-S., Park, J.-W., et al. (2003a) IL-4 augments anisomycin-induced p38 activation via Akt pathway in a follicular dendritic cell (FDC)-like line. **FEBS Letters**, 549 (1-3): 110–114

Lee, I.Y., Bae, Y.-D., Jeoung, D.-I., et al. (2007) Prostacyclin production is not controlled by prostacyclin synthase but by cyclooxygenase-2 in a human follicular dendritic cell line, HK. **Molecular immunology**, 44 (12): 3168–72

Lee, I.Y., Cho, W., Kim, J., et al. (2008) Human follicular dendritic cells interact with T cells via expression and regulation of cyclooxygenases and prostaglandin E and I synthases. **Journal of immunology**, 180 (3): 1390–7

Lee, I.Y., Ko, E., Kim, S., et al. (2005) Human follicular dendritic cells express prostacyclin synthase: a novel mechanism to control T cell numbers in the germinal center. **Journal of immunology**, 175 (3): 1658–64

Lee, R.C. and Ambros, V. (2001) An extensive class of small RNAs in Caenorhabditis elegans. **Science**, 294 (5543): 862–4

Lee, R.C., Feinbaum, R.L. and Ambros, V. (1993) The C. elegans heterochronic gene lin-4 encodes small RNAs with antisense complementarity to lin-14. **Cell**, 75 (5): 843–854

Lee, Y., Ahn, C., Han, J., et al. (2003b) The nuclear RNase III Drosha initiates microRNA processing. **Nature**, 425 (6956): 415–9

Lee, Y., Jeon, K., Lee, J.-T., et al. (2002) MicroRNA maturation: stepwise processing and subcellular localization. **The EMBO journal**, 21 (17): 4663–70

Lee, Y., Kim, M., Han, J., et al. (2004) MicroRNA genes are transcribed by RNA polymerase II. **the The European Molecular Biology Organization Journal**, 23 (20): 4051–4060

Leger-Ravet, M.B., Peuchmaur, M., Devergne, O., et al. (1991) Interleukin-6 gene expression in Castleman's disease. **Blood**, 78 (11): 2923–30

Legler, D.F., Loetscher, M., Roos, R.S., et al. (1998) B cell-attracting chemokine 1, a human CXC chemokine expressed in lymphoid tissues, selectively attracts B lymphocytes via BLR1/CXCR5. **The Journal of experimental medicine**, 187 (4): 655–60

Leite, K.R.M., Morais, D.R., Reis, S.T., et al. (2013) MicroRNA 100: a context dependent miRNA in prostate cancer. **Clinics (São Paulo, Brazil)**, 68 (6): 797–802

Leonhardt, F., Grundmann, S., Behe, M., et al. (2013) Inflammatory neovascularization during graft-versus-host disease is regulated by αv integrin and miR-100. **Blood**, 121 (17): 3307–18

Lewis, B.P., Shih, I., Jones-Rhoades, M.W., et al. (2003) Prediction of mammalian microRNA targets. **Cell**, 115 (7): 787–798

Lewis, M. a, Quint, E., Glazier, A.M., et al. (2009) An ENU-induced mutation of miR-96 associated with progressive hearing loss in mice. **Nature genetics**, 41 (5): 614–8

Li, J., Wan, Y., Ji, Q., et al. (2013) The role of microRNAs in B-cell development and function. **Cellular & molecular immunology**, 10 (2): 107–112

Li, L. and Choi, Y.S. (2002) Follicular dendritic cell-signaling molecules required for proliferation and differentiation of GC-B cells. **Seminars in Immunology**, 14 (4): 259–266

Libermann, T.A. and Baltimore, D. (1990) Activation of Interleukin-6 Gene Expression through the NF-KB Transcription Factor. **Molecular and cellular biology**, 10 (5): 2327–2334

Lim, L.P., Lau, N.C., Garrett-Engele, P., et al. (2005) Microarray analysis shows that some microRNAs downregulate large numbers of target mRNAs. **Nature**, 433 (7027): 769–73

Lin, J., Lwin, T., Zhao, J.-J., et al. (2011) Follicular dendritic cell-induced microRNA-mediated upregulation of PRDM1 and downregulation of BCL-6 in non-Hodgkin's B-cell lymphomas. **Leukemia**, 25 (1): 145–52

Lindhout, E. and Groot, C. de (1995) Follicular dendritic cells and apoptosis: life and death in the germinal centre. **The Histochemical Journal**, 183: 167–183

Liu, H., Yue, D., Chen, Y., et al. (2010) Improving performance of mammalian microRNA target prediction. **BMC bioinformatics**, 11 (1): 476

Liu, X., Wang, C., Chen, Z., et al. (2011) MicroRNA-138 suppresses epithelial-mesenchymal transition in squamous cell carcinoma cell lines. **The Biochemical journal**, 440 (1): 23–31

Loher, P. and Rigoutsos, I. (2012) Interactive exploration of RNA22 microRNA target predictions. **Bioinformatics (Oxford, England)**, 28 (24): 3322–3

Lu, L.F. and Liston, A. (2009) MicroRNA in the immune system, microRNA as an immune system. **Immunology**, 127: 291–8

Lu, T.-P., Lee, C.-Y., Tsai, M.-H., et al. (2012) miRSystem: An Integrated System for Characterizing Enriched Functions and Pathways of MicroRNA Targets. **PloS one**, 7 (8): e42390

Luo, Z., Ronai, D. and Scharff, M.D. (2004) The role of activation-induced cytidine deaminase in antibody diversification, immunodeficiency, and B-cell malignancies. **The Journal of allergy and clinical immunology**, 114 (4): 726–35

Luzina, I.G., Atamas, S.P., Storrer, C.E., et al. (2001) Spontaneous formation of germinal centers in autoimmune mice. **Journal of leukocyte biology**, 70 (4): 578–84

Lwin, T., Lin, J., Choi, Y.S., et al. (2010) Follicular dendritic cell-dependent drug resistance of non-Hodgkin lymphoma involves cell adhesion-mediated Bim down-regulation through induction of microRNA-181a. **Blood**, 116 (24): 5228–36

Mabbott, N., Kenneth Baillie, J., Kobayashi, A., et al. (2011) Expression of mesenchyme-specific gene signatures by follicular dendritic cells: insights from the meta-analysis of microarray data from multiple mouse cell populations. **Immunology**, 133 (4): 482–98

Mabbott, N.A., Farquhar, C.F., Brown, K.L., et al. (1998) Involvement of the immune system in TSE pathogenesis. **Immunology today**, 19 (5): 201–3

Mabbott, N.A., Mackay, F., Minns, F., et al. (2000) Temporary inactivation of follicular dendritic cells delays neuroinvasion of scrapie. **Nature medicine**, 6 (7): 719–20

Mabbott, N.A., McGovern, G., Jeffrey, M., et al. (2002) Temporary blockade of the tumor necrosis factor receptor signaling pathway impedes the spread of scrapie to the brain. **Journal of virology**, 76 (10): 5131–9

Mabbott, N.A., Young, J., McConnell, I., et al. (2003) Follicular Dendritic Cell Dedifferentiation by Treatment with an Inhibitor of the Lymphotoxin Pathway Dramatically Reduces Scrapie Susceptibility. **Journal of virology**, 77 (12): 6845–6854

Mackay, F. and Browning, J.L. (1998) Turning off follicular dendritic cells. **Nature**, 395 (6697): 26–7

MacLennan, I.C.M. (1994) Germinal Centers. **Annual Review of Immunology**, 12 (1): 117–139

Maeda, K., Matsuda, M. and Imai, Y. (1995) Follicular dendritic cells: structure as related to function. **Current topics in microbiology and immunology**, 201: 119–39

Magari, M., Nishikawa, Y., Fujii, Y., et al. (2011) IL-21-dependent B cell death driven by prostaglandin E2, a product secreted from follicular dendritic cells. **Journal of immunology**, 187 (8): 4210–8

Manolagas, S.C., Bellido, T. and Jilka, R.L. (1995) New insights into the cellular, biochemical, and molecular basis of postmenopausal and senile osteoporosis: roles of IL-6 and gp130. **International journal of immunopharmacology**, 17 (2): 109–16

Maragkakis, M., Reczko, M., Simossis, V. a, et al. (2009) DIANA-microT web server: elucidating microRNA functions through target prediction. **Nucleic acids research**, 37 (Web Server issue): W273–6

Marsico, A., Huska, M.R., Lasserre, J., et al. (2013) PROmiRNA: a new miRNA promoter recognition method uncovers the complex regulation of intronic miRNAs. **Genome Biology**, 14 (8): R84

Martinez-Sanchez, A. and Murphy, C. (2013) MicroRNA Target Identification—Experimental Approaches. **Biology**, 2 (1): 189–205

Matsumoto, M., Fu, Y.-X., Molina, H., et al. (1997) Lymphotoxin-α-deficient and TNF receptor-I-deficient mice define developmental and functional characteristics of germinal centers. **Immunological Reviews**, 156 (1): 137–144

Matsumoto, M., Iwamasa, K., Rennert, P.D., et al. (1999) Involvement of distinct cellular compartments in the abnormal lymphoid organogenesis in lymphotoxin-alpha-deficient mice and alymphoplasia (aly) mice defined by the chimeric analysis. **Journal of immunology**, 163 (3): 1584–91

McBride, P.A., Eikelenboom, P., Kraal, G., et al. (1992) PrP protein is associated with follicular dendritic cells of spleens and lymph nodes in uninfected and scrapie-infected mice. **The Journal of pathology**, 168 (4): 413–8

Mcculloch, L., Brown, K.L., Bradford, B.M., et al. (2011) Follicular Dendritic Cell-Specific Prion Protein (PrP c) Expression Alone Is Sufficient to Sustain Prion Infection in the Spleen. **PLoS Pathogens**, 7 (12)

McCulloch, L., Brown, K.L. and Mabbott, N. a (2013) Ablation of the cellular prion protein, PrPC, specifically on follicular dendritic cells has no effect on their maturation or function. **Immunology**, 138 (3): 246–57

Mebius, R.E., Streeter, P.R., Michie, S., et al. (1996) A developmental switch in lymphocyte homing receptor and endothelial vascular addressin expression regulates lymphocyte homing and permits CD4+ CD3- cells to colonize lymph nodes. **Proceedings of the National Academy of Sciences of the United States of America**, 93 (20): 11019–24

Mencía, A., Modamio-Høybjør, S., Redshaw, N., et al. (2009) Mutations in the seed region of human miR-96 are responsible for nonsyndromic progressive hearing loss. **Nature genetics**, 41 (5): 609–13

Miksa, M., Amin, D., Wu, R., et al. (2007) Fractalkine-induced MFG-E8 leads to enhanced apoptotic cell clearance by macrophages. **Molecular medicine**, 13 (11-12): 553–60

Milan, Z., Taylor, C., Duncan, B., et al. (2011) Statistical modeling of hemodynamic changes during orthotopic liver transplantation: predictive value for outcome and effect of marginal donors. **Transplantation proceedings**, 43 (5): 1711–5

Milićević, N.M., Milićević, Z. and Westermann, J.J. (2011) Lipopolysaccharide-Induced In Vivo Activation of Follicular Dendritic Cells is Tumor Necrosis Factor Receptor-1 Independent. **Anatomical record**, 000 (July): 1–4

Minajeva, a, Kulke, M., Fernandez, J.M., et al. (2001) Unfolding of titin domains explains the viscoelastic behavior of skeletal myofibrils. **Biophysical journal**, 80 (3): 1442–51

Miranda, K.C., Huynh, T., Tay, Y., et al. (2006) A pattern-based method for the identification of MicroRNA binding sites and their corresponding heteroduplexes. **Cell**, 126 (6): 1203–17

Mita, Y., Dobashi, K., Endou, K., et al. (2002) Toll-like receptor 4 surface expression on human monocytes and B cells is modulated by IL-2 and IL-4. **Immunology Letters**, 81 (1): 71–75

Mita, Y., Dobashi, K., Shimizu, Y., et al. (2001) Toll-like receptor 2 and 4 surface expressions on human monocytes are modulated by interferon-gamma and macrophage colony-stimulating factor. **Immunology letters**, 78 (2): 97–101

Mitchell, J. and Abbot, A. (1965) Ultrastructure of the antigen-retaining reticulum of lymph node follicles as shown by high-resolution autoradiography. **Nature**, 208 (5009): 500–2

Miyanishi, M., Segawa, K. and Nagata, S. (2012) Synergistic effect of Tim4 and MFG-E8 null mutations on the development of autoimmunity. **International immunology**, 24 (9): 551–559

Morse, L., Chen, D., Franklin, D., et al. (1997) Induction of cell cycle arrest and B cell terminal differentiation by CDK inhibitor p18(INK4c) and IL-6. **Immunity**, 6 (1): 47–56

Muñoz, L.E., Janko, C., Schulze, C., et al. (2010) Autoimmunity and chronic inflammation - two clearance-related steps in the etiopathogenesis of SLE. **Autoimmunity reviews**, 10 (1): 38–42

Munoz-Fernandez, R., Blanco, F.J., Frecha, C., et al. (2006) Follicular dendritic cells are related to bone marrow stromal cell progenitors and to myofibroblasts. **Journal of immunology**, 177 (1): 280–9

Murphy, M., Walter, B.N., Pike-Nobile, L., et al. (1998) Expression of the lymphotoxin beta receptor on follicular stromal cells in human lymphoid tissues. **Cell death and differentiation**, 5 (6): 497–505

Myers, R.C., King, R.G., Carter, R.H., et al. (2013) Lymphotoxin α1β2 expression on B cells is required for follicular dendritic cell activation during the germinal center response. **European journal of immunology**, 43 (2): 348–59

Navarro, F. and Lieberman, J. (2010) Small RNAs Guide Hematopoietic Cell Differentiation and Function. **J Immunol**, 184 (11): 5939–5947

Nawata, Y., Eugui, E.M., Lee, S.W., et al. (1989) IL-6 is the principal factor produced by synovia of patients with rheumatoid arthritis that induces B-lymphocytes to secrete immunoglobulins. **Annals of the New York Academy of Sciences**, 557: 230–8, discussion 239

Nelms, K., Keegan, a D., Zamorano, J., et al. (1999) The IL-4 receptor: signaling mechanisms and biologic functions. **Annual review of immunology**, 17: 701–38

Neyt, K., Perros, F., GeurtsvanKessel, C.H., et al. (2012) Tertiary lymphoid organs in infection and autoimmunity. **Trends in immunology**, 33 (6): 297–305

Ngo, Korner, H., Gunn, M.D., et al. (1999) Lymphotoxin alpha/beta and tumor necrosis factor are required for stromal cell expression of homing chemokines in B and T cell areas of the spleen. **The Journal of experimental medicine**, 189 (2): 403–12

Van Nierop, K. and De Groot, C. (2002) Human follicular dendritic cells: function, origin and development. **Seminars in Immunology**, 14 (4): 251–257

Van Nieuwerburgh, F., Soetaert, S., Podshivalova, K., et al. (2011) Quantitative bias in Illumina TruSeq and a novel post amplification barcoding strategy for multiplexed DNA and small RNA deep sequencing. Lightowlers, B. (ed.). **PloS one**, 6 (10): e26969

Nimmerjahn, F. and Ravetch, J. V (2008) Fcgamma receptors as regulators of immune responses. **Nature reviews. Immunology**, 8 (1): 34–47

Nishikawa, Y., Hikida, M., Magari, M., et al. (2006) Establishment of lymphotoxin beta receptor signaling-dependent cell lines with follicular dendritic cell phenotypes from mouse lymph nodes. **The Journal of Immunology**, 177 (8): 5204–5214

Nishimoto, N., Terao, K., Mima, T., et al. (2008) Mechanisms and pathologic significances in increase in serum interleukin-6 (IL-6) and soluble IL-6 receptor after administration of an anti-IL-6 receptor antibody, tocilizumab, in patients with rheumatoid arthritis and Castleman disease. **Blood**, 112 (10): 3959–64

Nossal, G.J., Abbot, A., Mitchell, J., et al. (1968) Antigens in immunity. XV. Ultrastructural features of antigen capture in primary and secondary lymphoid follicles. **The Journal of experimental medicine**, 127 (2): 277–90

Ooi, C.H., Oh, H.K., Wang, H.Z., et al. (2011) A densely interconnected genome-wide network of microRNAs and oncogenic pathways revealed using gene expression signatures. **PLoS genetics**, 7 (12): e1002415

Ozen, I., Boix, J. and Paul, G. (2012) Perivascular mesenchymal stem cells in the adult human brain: a future target for neuroregeneration? **Clinical and translational medicine**, 1 (1): 30

Pall, G.S. and Hamilton, A.J. (2008) Improved northern blot method for enhanced detection of small RNA. **Nature protocols**, 3 (6): 1077–84

Pålsson-McDermott, E.M. and O'Neill, L. a J. (2004) Signal transduction by the lipopolysaccharide receptor, Toll-like receptor-4. **Immunology**, 113 (2): 153–62

Park, C.-S. and Choi, Y.S. (2005) How do follicular dendritic cells interact intimately with B cells in the germinal centre? **Immunology**, 114 (1): 2–10

Park, C.-S., Yoon, S.-O., Armitage, R.J., et al. (2004) Follicular dendritic cells produce IL-15 that enhances germinal center B cell proliferation in membrane-bound form. **Journal of immunology**, 173 (11): 6676–83

Pasquinelli, a E., Reinhart, B.J., Slack, F., et al. (2000) Conservation of the sequence and temporal expression of let-7 heterochronic regulatory RNA. **Nature**, 408 (6808): 86–9

Pasquinelli, A.E. (2012) MicroRNAs and their targets: recognition, regulation and an emerging reciprocal relationship. **Nature reviews. Genetics**, 13 (4): 271–82

Van de Pavert, S. a, Olivier, B.J., Goverse, G., et al. (2009) Chemokine CXCL13 is essential for lymph node initiation and is induced by retinoic acid and neuronal stimulation. **Nature immunology**, 10 (11): 1193–9

Pena, J.T.G., Sohn-Lee, C., Rouhanifard, S.H., et al. (2009) miRNA in situ hybridization in formaldehyde and EDC-fixed tissues. **Nature methods**, 6 (2): 139–41

Petrelli, a, Perra, a, Schernhuber, K., et al. (2012) Sequential analysis of multistage hepatocarcinogenesis reveals that miR-100 and PLK1 dysregulation is an early event maintained along tumor progression. **Oncogene**, 31 (42): 4517–26

Pillai, R.S., Bhattacharyya, S.N. and Filipowicz, W. (2007) Repression of protein synthesis by miRNAs: how many mechanisms? **Trends in Cell Biology**, 17 (3): 118–126

Qin, D., Wu, J., Vora, K.A., et al. (2000) Fc gamma receptor IIB on follicular dendritic cells regulates the B cell recall response. **Journal of immunology**, 164 (12): 6268–75

Radoux, D., Heinen, E., Kinet-Denoël, C., et al. (1984) Precise localization of antigens on follicular dendritic cells. **Cell and tissue research**, 235 (2): 267–74

Rajwanshi, V., Håkansson, A., Sørensen, M., et al. (2000) The Eight Stereoisomers of LNA (Locked Nucleic Acid): A Remarkable Family of Strong RNA Binding Molecules We acknowledge the Danish Natural Science Research Council, the Danish Technical Research Council, and Exiqon A/S for financial support. Ms Britta M. **Angewandte Chemie (International ed. in English)**, 39 (9): 1656–1659

Ramiro, A.R. (2010) MicroRNAs and the Immune System Monticelli, S. (ed.). **Methods**, 667: 177–192

Ramkissoon, S.H., Mainwaring, L.A., Ogasawara, Y., et al. (2006) Hematopoietic-specific microRNA expression in human cells. **Leukemia Research**, 30 (5): 643–647

Rand, T. a, Petersen, S., Du, F., et al. (2005) Argonaute2 cleaves the anti-guide strand of siRNA during RISC activation. **Cell**, 123 (4): 621–9

Rao, D.S., O'Connell, R.M., Chaudhuri, A. a., et al. (2010) MicroRNA-34a perturbs B lymphocyte development by repressing the forkhead box transcription factor Foxp1. **Immunity**, 33 (1): 48–59

Raschke, W.C., Baird, S., Ralph, P., et al. (1978) Functional macrophage cell lines transformed by Abelson leukemia virus. **Cell**, 15 (1): 261–7

Raymond, C., Roberts, B. and Garrett-Engele, P. (2005) Simple, quantitative primer-extension PCR assay for direct monitoring of microRNAs and short-interfering RNAs. **Rna**, (2003): 1737–1744

Reinhart, B.J., Slack, F.J., Basson, M., et al. (2000) The 21-nucleotide let-7 RNA regulates developmental timing in Caenorhabditis elegans. **Nature**, 403 (6772): 901–6

Rennert, P., James, D. and Mackay, F. (1998) Lymph node genesis is induced by signaling through the lymphotoxin β receptor. **Immunity**, 9 (1): 71–79

Rennert, P.D., Browning, J.L., Mebius, R., et al. (1996) Surface lymphotoxin alpha/beta complex is required for the development of peripheral lymphoid organs. **The Journal of experimental medicine**, 184 (5): 1999–2006

Reynes, M., Aubert, J.P., Cohen, J.H., et al. (1985) Human follicular dendritic cells express CR1, CR2, and CR3 complement receptor antigens. **Journal of immunology**, 135 (4): 2687–94

Rezk, S. a, Nathwani, B.N., Zhao, X., et al. (2013) Follicular dendritic cells: origin, function, and different disease-associated patterns. **Human pathology**, 44 (6): 937–50

Richard, D.J., Bolderson, E., Cubeddu, L., et al. (2008) Single-stranded DNA-binding protein hSSB1 is critical for genomic stability. **Nature**, 453 (7195): 677–81

Ripley, B.J.M., Goncalves, B., Isenberg, D. a, et al. (2005) Raised levels of interleukin 6 in systemic lupus erythematosus correlate with anaemia. **Annals of the rheumatic diseases**, 64 (6): 849–53

Robinson, M.D., McCarthy, D.J. and Smyth, G.K. (2010) edgeR: a Bioconductor package for differential expression analysis of digital gene expression data. **Bioinformatics**, 26 (1): 139–40

Robinson, M.D. and Oshlack, A. (2010) A scaling normalization method for differential expression analysis of RNA-seq data. **Genome biology**, 11 (3): R25

Rodriguez, A., Vigorito, E., Clare, S., et al. (2007) Requirement of bic/microRNA-155 for normal immune function. **Science**, 316: 608–11

Roozendaal, R. and Mebius, R.E. (2011) Stromal cell-immune cell interactions. **Annual review of immunology**, 29: 23–43

Ruike, Y., Ichimura, A., Tsuchiya, S., et al. (2008) Global correlation analysis for micro-RNA and mRNA expression profiles in human cell lines. **Journal of human genetics**, 53 (6): 515–23

Rümenapp, U., Freichel-Blomquist, A., Wittinghofer, B., et al. (2002) A mammalian Rho-specific guanine-nucleotide exchange factor (p164-RhoGEF) without a pleckstrin homology domain. **The Biochemical journal**, 366 (Pt 3): 721–8

Sacedón, R., Díez, B., Nuñez, V., et al. (2005) Sonic hedgehog is produced by follicular dendritic cells and protects germinal center B cells from apoptosis. **Journal of immunology**, 174 (3): 1456–61

Saetrom, P., Heale, B.S.E., Snøve, O., et al. (2007) Distance constraints between microRNA target sites dictate efficacy and cooperativity. **Nucleic acids research**, 35 (7): 2333–42

Sánchez-Jiménez, C., Carrascoso, I., Barrero, J., et al. (2013) Identification of a set of miRNAs differentially expressed in transiently TIA-depleted HeLa cells by genome-wide profiling. **BMC molecular biology**, 14 ((1)): 4

Sato, F., Tsuchiya, S., Terasawa, K., et al. (2009) Intra-platform repeatability and inter-platform comparability of microRNA microarray technology. **PloS one**, 4 (5): e5540

Satoshi Obika, Daishu Nanbu, yoshiyuki Hari, Ken.ichiro Morio, Yasuko In, Toshimasa Ishida, and T.I.* (1997) Synthesis of 2'-O,4'-C-Methyleneuridine and -cytidine. Novel Bicyclic Nucleosides Having a Fixed C a ,-endo Sugar Puckering. **Tetrahedron**, 38 (50): 8735–8738

Schmedtje, J.F., Ji, Y.S., Liu, W.L., et al. (1997) Hypoxia induces cyclooxygenase-2 via the NF-kappaB p65 transcription factor in human vascular endothelial cells. **The Journal of biological chemistry**, 272 (1): 601–8

Schmittgen, T.D., Jiang, J., Liu, Q., et al. (2004) A high-throughput method to monitor the expression of microRNA precursors. **Nucleic acids research**, 32 (4): e43

Schmitz, J., Petrasch, S., Van Lunzen, J., et al. (1993) Optimizing follicular dendritic cell isolation by discontinuous gradient centrifugation and use of the magnetic cell sorter (MACS). **Journal of immunological methods**, 159 (1-2): 189–96

Schriever, F. and Freedman, A. (1989) Isolated human follicular dendritic cells display a unique antigenic phenotype. **The Journal of Experimental medicine**, 169 (June)

Schwarz, D.S., Hutvágner, G., Du, T., et al. (2003) Asymmetry in the assembly of the RNAi enzyme complex. **Cell**, 115 (2): 199–208

Selbach, M., Schwanhäusser, B., Thierfelder, N., et al. (2008) Widespread changes in protein synthesis induced by microRNAs. **Nature**, 455 (7209): 58–63

Sellheyer, K., Schwarting, R. and Stein, H. (1989) Isolation and antigenic profile of follicular dendritic cells. **Clinical and Experimental Immunology**, 78 (3): 431–436

Shaffer, a L., Lin, K.I., Kuo, T.C., et al. (2002) Blimp-1 orchestrates plasma cell differentiation by extinguishing the mature B cell gene expression program. **Immunity**, 17 (1): 51–62

El Shikh, M.E., El Sayed, R., Szakal, A.K., et al. (2006) Follicular dendritic cell (FDC)-FcgammaRIIB engagement via immune complexes induces the activated FDC phenotype associated with secondary follicle development. **European journal of immunology**, 36 (10): 2715–24

El Shikh, M.E., El Sayed, R.M., Tew, J.G., et al. (2007a) Follicular dendritic cells stimulated by collagen type I develop dendrites and networks in vitro. **Cell and tissue research**, 329 (1): 81–9

El Shikh, M.E.M. and Pitzalis, C. (2012) Follicular dendritic cells in health and disease. **Frontiers in immunology**, 3 (September): 292

El Shikh, M.E.M., El Sayed, R.M., Wu, Y., et al. (2007b) TLR4 on follicular dendritic cells: an activation pathway that promotes accessory activity. **Journal of immunology**, 179 (7): 4444–50

Shimamura, T., Imoto, S., Shimada, Y., et al. (2011) A novel network profiling analysis reveals system changes in epithelial-mesenchymal transition. **PloS one**, 6 (6): e20804

Shin, C., Nam, J.J.-W., Farh, K.K.K.-H., et al. (2010) Expanding the MicroRNA Targeting Code: Functional Sites with Centered Pairing. **Molecular Cell**, 38 (6): 789–802

Shirdel, E. a., Xie, W., Mak, T.W., et al. (2011) NAViGaTing the Micronome – Using Multiple MicroRNA Prediction Databases to Identify Signalling Pathway-Associated MicroRNAs Ballestar, E. (ed.). **PLoS ONE**, 6 (2): e17429

Singh, S., Singh, P.K., Bhadauriya, P., et al. (2012) Lafora disease E3 ubiquitin ligase malin is recruited to the processing bodies and regulates the microRNA-mediated gene silencing process via the decapping enzyme Dcp1a. **RNA biology**, 9 (12): 1–10

Smith, B.A., Gartner, S., Liu, Y., et al. (2001) Persistence of infectious HIV on follicular dendritic cells. **Journal of immunology**, 166 (1): 690–6

Smolen, J.S., Schoels, M.M., Nishimoto, N., et al. (2013) Consensus statement on blocking the effects of interleukin-6 and in particular by interleukin-6 receptor inhibition in rheumatoid arthritis and other inflammatory conditions. **Annals of the rheumatic diseases**, 72 (4): 482–92

Solly, K., Wang, X., Xu, X., et al. (2004) Application of real-time cell electronic sensing (RT-CES) technology to cell-based assays. **Assay and drug development technologies**, 2 (4): 363–72

Song, J., Duncan, M.J., Li, G., et al. (2007) A novel TLR4-mediated signaling pathway leading to IL-6 responses in human bladder epithelial cells. **PLoS pathogens**, 3 (4): e60

Sonkoly, E., Ståhle, M. and Pivarcsi, A. (2008) MicroRNAs and immunity: Novel players in the regulation of normal immune function and inflammation. **Seminars in Cancer Biology**, 18 (2): 131–140

Sood, P., Krek, A., Zavolan, M., et al. (2006) Cell-type-specific signatures of microRNAs on target mRNA expression. **Proceedings of the National Academy of Sciences of the United States of America**, 103 (8): 2746–51

Spierings, D.C., McGoldrick, D., Hamilton-Easton, A.M., et al. (2011) Ordered progression of stage-specific miRNA profiles in the mouse B2 B-cell lineage. **Blood**, 117 (20): 5340–9

Sprenger, R., Toellner, K.M., Schmetz, C., et al. (1995) Follicular dendritic cells productively infected with immunodeficiency viruses transmit infection to T cells. **Medical microbiology and immunology**, 184 (3): 129–34

Stark, A., Brennecke, J., Bushati, N., et al. (2005) Animal MicroRNAs confer robustness to gene expression and have a significant impact on 3'UTR evolution. **Cell**, 123 (6): 1133–46

Stark, A., Brennecke, J., Russell, R.B., et al. (2003) Identification of Drosophila MicroRNA targets. **PLoS biology**, 1 (3): E60

Sukumar, S., El Shikh, M.E., Tew, J.G., et al. (2008) Ultrastructural study of highly enriched follicular dendritic cells reveals their morphology and the periodicity of immune complex binding. **Cell and tissue research**, 332 (1): 89–99

Sukumar, S., Szakal, A.K. and Tew, J.G. (2006) Isolation of functionally active murine follicular dendritic cells. **Journal of immunological methods**, 313 (1-2): 81–95

Suzuki, K., Grigorova, I., Phan, T.G., et al. (2009) Visualizing B cell capture of cognate antigen from follicular dendritic cells. **J Exp Med**, 206: 1485–93

Suzuki, K., Maruya, M., Kawamoto, S., et al. (2010) The Sensing of Environmental Stimuli by Follicular Dendritic Cells Promotes Immunoglobulin A Generation in the Gut. **Immunity**, 33 (1): 71–83

Sylvain Gubian, Alain Sewer, P.S. (2010) **ExiMiR: R functions for the normalization of Exiqon miRNA array data.**

Szakal, A.K. and Hanna, M.G. (1968) The ultrastructure of antigen localization and viruslike particles in mouse spleen germinal centers. **Experimental and molecular pathology**, 8 (1): 75–89

Szakal, A.K., Kapasi, Z.F., Haley, S.T., et al. (1995) A theory of follicular dendritic cell origin. **Current Topics in Microbiology and Immunology**, 201: 1–13

Tackey, E., Lipsky, P. and Illei, G. (2004) Rationale for interleukin-6 blockade in systemic lupus erythematosus. **Lupus**, 13 (5): 339–343

Tak, P.P. and Firestein, G.S. (2001) NF- κ B in defense and disease NF-κB : a key role in inflammatory diseases. **NF-kB in defense and disease**, 107 (1): 7–11

Tang, L., Yang, J., Liu, W., et al. (2009) Liver sinusoidal endothelial cell lectin, LSECtin, negatively regulates hepatic T-cell immune response. **Gastroenterology**, 137 (4): 1498–508.e1–5

Taylor, P.R., Pickering, M.C., Kosco-Vilbois, M.H., et al. (2002) The follicular dendritic cell restricted epitope, FDC-M2, is complement C4; localization of immune complexes in mouse tissues. **European journal of immunology**, 32 (7): 1888–96

Teng, G., Hakimpour, P., Landgraf, P., et al. (2008) microRNA-155 is a negative regulator of Activation Induced Cytidine deaminase. **Immunity**, 28 (5): 621–629

Tew, J.G., Kosco, M.H., Burton, G.F., et al. (1990) Follicular dendritic cells as accessory cells. **Immunological reviews**, 117 (117): 185–211

Thai, T.-H., Calado, D.P., Casola, S., et al. (2007) Regulation of the germinal center response by microRNA-155. **Science**, 316 (5824): 604–8

Todaro, G. and Green, H. (1963) Quantitative studies of the growth of mouse embryo cells in culture and their development into established lines. **The Journal of cell biology**, (6): 299–313

De Togni, P., Goellner, J., Ruddle, N.H., et al. (1994) Abnormal development of peripheral lymphoid organs in mice deficient in lymphotoxin. **Science**, 264 (5159): 703–7

Tridon, V., May, M.J., Ghosh, S., et al. (2005) **NFjB activates in vivo the synthesis of inducible Cox-2 in the brain.**, pp. 1047–1059

Tsan, M. and Gao, B. (2004) Endogenous ligands of Toll-like receptors. **Journal of Leukocyte Biology**, 76 (Sept): 514–519

Tsang, J., Zhu, J. and Oudenaarden, A. van (2007) MicroRNA-mediated feedback and feedforward loops are recurrent network motifs in mammals. **Molecular cell**, 26 (5): 753–767

Tsang, J.S., Ebert, M.S. and Van Oudenaarden, A. (2010) Genome-wide dissection of microRNA functions and cotargeting networks using gene set signatures. **Molecular cell**, 38 (1): 140–53

Tseng, W.-P., Su, C.-M. and Tang, C.-H. (2010) FAK activation is required for TNF-alpha-induced IL-6 production in myoblasts. **Journal of cellular physiology**, 223 (2): 389–96

Uccelli, A., Moretta, L. and Pistoia, V. (2006) Immunoregulatory function of mesenchymal stem cells. **European journal of immunology**, 36 (10): 2566–73

Usui, K., Honda, S.-I., Yoshizawa, Y., et al. (2012) Isolation and characterization of naïve follicular dendritic cells. **Molecular immunology**, 50 (3): 172–6

Valencia-Sanchez, M.A., Liu, J., Hannon, G.J., et al. (2006) Control of translation and mRNA degradation by miRNAs and siRNAs. **Genes & development**, 20 (5): 515–24

Ventura, A., Young, A.G., Winslow, M.M., et al. (2008) Targeted deletion reveals essential and overlapping functions of the miR-17 through 92 family of miRNA clusters. **Cell**, 132 (5): 875–86

Vermeulen, A., Behlen, L., Reynolds, A., et al. (2005) The contributions of dsRNA structure to Dicer specificity and efficiency. **RNA**, 11 (5): 674–82

Victoratos, P., Lagnel, J., Tzima, S., et al. (2006) FDC-Specific Functions of p55TNFR and IKK2 in the Development of FDC Networks and of Antibody Responses. **Immunity**, 24 (1): 65–77

Vigorito, E., Perks, K.L., Abreu-Goodger, C., et al. (2007) microRNA-155 regulates the generation of immunoglobulin class-switched plasma cells. **Immunity**, 27 (6): 847–59

Vinuesa, C.G., Sanz, I. and Cook, M.C. (2009) Dysregulation of germinal centres in autoimmune disease. **Nat Rev Immunol**, 9 (12): 845–857

Vondenhoff, M.F.R., Desanti, G.E., Cupedo, T., et al. (2008) Separation of splenic red and white pulp occurs before birth in a LTalphabeta-independent manner. **Journal of leukocyte biology**, 84 (1): 152–61

Wahid, F., Shehzad, A., Khan, T., et al. (2010) MicroRNAs: synthesis, mechanism, function, and recent clinical trials. **Biochimica et biophysica acta**, 1803 (11): 1231–43

Wang, B., Yanez, A. and Novina, C.D. (2008a) MicroRNA-repressed mRNAs contain 40S but not 60S components. **Proceedings of the National Academy of Sciences of the United States of America**, 105 (14): 5343–8

Wang, G., Chen, L., Meng, J., et al. (2013) Overexpression of microRNA-100 predicts an unfavorable prognosis in renal cell carcinoma. **International urology and nephrology**, 45 (2): 373–9

Wang, X. (2008) miRDB: a microRNA target prediction and functional annotation database with a wiki interface. **RNA**, 14 (6): 1012–7

Wang, X., Cho, B., Suzuki, K., et al. (2011) Follicular dendritic cells help establish follicle identity and promote B cell retention in germinal centers. **Journal of Experimental Medicine**, 208 (12): 2497–510

Wang, Y., Baskerville, S., Shenoy, A., et al. (2008b) Embryonic stem cell-specific microRNAs regulate the G1-S transition and promote rapid proliferation. **Nature genetics**, 40 (12): 1478–83

Wang, Y., Huang, G., Wang, J., et al. (2000) Antigen persistence is required for somatic mutation and affinity maturation of immunoglobulin. **European Journal of Immunology**, 30 (8): 2226–2234

Wang, Zhang, J., Li, F., et al. (2005) MicroRNA identification based on sequence and structure alignment. **Bioinformatics**, 21 (18): 3610–4

Wang, Zhang, J.-S., Zheng, Q., et al. (2008c) The unique localization of ZFP185 at uropod of mouse T lymphocytes. **Scandinavian journal of immunology**, 67 (4): 340–4

Wang, Zheng, Q., Zhang, J.-S., et al. (2008d) Molecular cloning and characterization of a novel mouse actin-binding protein Zfp185. **Journal of molecular histology**, 39 (3): 295–302

Wilhelm, P., Riminton, D.S., Ritter, U., et al. (2002) Membrane lymphotoxin contributes to anti-leishmanial immunity by controlling structural integrity of lymphoid organs. **European journal of immunology**, 32 (7): 1993–2003

Withers, D.R., Kim, M.-Y., Bekiaris, V., et al. (2007) The role of lymphoid tissue inducer cells in splenic white pulp development. **European journal of immunology**, 37 (11): 3240–5

Witkos, T.M., Koscianska, E. and Krzyzosiak, W.J. (2011) Practical Aspects of microRNA Target Prediction. **Current molecular medicine**, 11 (2): 93–109

Worm, J., Stenvang, J., Petri, A., et al. (2009) Silencing of microRNA-155 in mice during acute inflammatory response leads to derepression of c/ebp Beta and down-regulation of G-CSF. **Nucleic acids research**, 37 (17): 5784–92

Wu, Y., El Shikh, M.E.M., El Sayed, R.M., et al. (2009) IL-6 produced by immune complex-activated follicular dendritic cells promotes germinal center reactions, IgG responses and somatic hypermutation. **International Immunology**, 21 (6): 745–756

Wu, Y., Sukumar, S., El Shikh, M.E., et al. (2008) Immune complex-bearing follicular dendritic cells deliver a late antigenic signal that promotes somatic hypermutation. **Journal of immunology**, 180 (1): 281–90

Xiao, C., Calado, D.P., Galler, G., et al. (2007) MiR-150 controls B cell differentiation by targeting the transcription factor c-Myb. **Cell**, 131: 146–59

Yagi, K., Yamamoto, K., Umeda, S., et al. (2013) Expression of multidrug resistance 1 gene in B-cell lymphomas: association with follicular dendritic cells. **Histopathology**, 62 (3): 414–20

Yamaguchi, H., Takagi, J., Miyamae, T., et al. (2008) Milk fat globule EGF factor 8 in the serum of human patients of systemic lupus erythematosus. **Journal of leukocyte biology**, 83 (5): 1300–7

Yamane, A., Resch, W., Kuo, N., et al. (2011) Deep-sequencing identification of the genomic targets of the cytidine deaminase AID and its cofactor RPA in B lymphocytes. **Nature immunology**, 12 (1): 62–9

Yan, Y., Wang, Y.-H. and Diamond, B. (2012) IL-6 contributes to an immune tolerance checkpoint in post germinal center B cells. **Journal of autoimmunity**, 38 (1): 1–9

Yan, Z. (2006) Regulation of TLR4 expression is a tale about tail. **Arteriosclerosis, thrombosis, and vascular biology**, 26 (12): 2582–4

Yang, J.-S., Phillips, M.D., Betel, D., et al. (2010) Widespread regulatory activity of vertebrate microRNA* species. **RNA**, 17 (2): 312–26

Yang, Z., Bian, C., Zhou, H., et al. (2011) MicroRNA hsa-miR-138 inhibits adipogenic differentiation of human adipose tissue-derived mesenchymal stem cells through adenovirus EID-1. **Stem cells and development**, 20 (2): 259–67

Yau, I.W., Cato, M.H., Jellusova, J., et al. (2013) Censoring of Self-Reactive B Cells by Follicular Dendritic Cell-Displayed Self-Antigen. **The Journal of Immunology**, 191 (3): 1082–1090

Yébenes, V. de (2013) Regulation of B-cell development and function by microRNAs. **Immunological reviews**, 253 (1): 25–39

Yekta, S., Shih, I.-H. and Bartel, D.P. (2004) MicroRNA-directed cleavage of HOXB8 mRNA. **Science**, 304 (5670): 594–6

Yi, R., Qin, Y., Macara, I.G., et al. (2003) **Exportin-5 mediates the nuclear export of pre-microRNAs and short hairpin RNAs**., pp. 3011–3016

Ying, S.-Y. and Lin, S.-L. (2006) Current perspectives in intronic micro RNAs (miRNAs). **Journal of biomedical science**, 13 (1): 5–15

Yoon, S.-O., Zhang, X., Berner, P., et al. (2009) Notch ligands expressed by follicular dendritic cells protect germinal center B cells from apoptosis. **Journal of immunology**, 183 (1): 352–8

Yoshida, K., Van den Berg, T.K., Dijkstra, C.D., et al. (1993) Two functionally different follicular dendritic cells in secondary lymphoid follicles of mouse spleen, as revealed by CR1/2 and FcR gamma II-mediated immune-complex trapping. **Immunology**, 80 (1): 34–39

Yoshida, K., Kaji, M., Takahashi, T., et al. (1995) Host origin of follicular dendritic cells induced in the spleen of SCID mice after transfer of allogeneic lymphocytes. **Immunology**, 84 (1): 117–126

Zamorano, J., Mora, a L., Boothby, M., et al. (2001) NF-kappa B activation plays an important role in the IL-4-induced protection from apoptosis. **International immunology**, 13 (12): 1479–87

Zekri, L., Huntzinger, E., Heimstädt, S., et al. (2009) The silencing domain of GW182 interacts with PABPC1 to promote translational repression and degradation of microRNA targets and is required for target release. **Molecular and cellular biology**, 29 (23): 6220–31

Zhang, C., Huys, A., Thibault, P. a, et al. (2012) Requirements for human Dicer and TRBP in microRNA-122 regulation of HCV translation and RNA abundance. **Virology**, 433 (2): 479–88

Zhang, J., Jima, D.D., Jacobs, C., et al. (2009) Patterns of microRNA expression characterize stages of human B-cell differentiation. **Blood**, 113 (19): 4586–4594

Zhang, J. and Perelson, A.S. (2013) Contribution of Follicular Dendritic Cells to Persistent HIV Viremia. **Journal of virology**, 87 (14): 7893–901

Zhang, X., Park, C.-S., Yoon, S.-O., et al. (2005) BAFF supports human B cell differentiation in the lymphoid follicles through distinct receptors. **Int. Immunol.**, 17 (6): 779–788

Zhang, Y. and Verbeek, F.J. (2010) Comparison and integration of target prediction algorithms for microRNA studies. **Journal of integrative bioinformatics**, 7 (3): 1–13

Zheng, H., Fu, R., Wang, J., et al. (2013) **Advances in the Techniques for the Prediction of microRNA Targets**., pp. 8179–8187

Zheng, Y.-S., Zhang, H., Zhang, X.-J., et al. (2012) MiR-100 regulates cell differentiation and survival by targeting RBSP3, a phosphatase-like tumor suppressor in acute myeloid leukemia. **Oncogene**, 31 (1): 80–92

Zhou, B., Wang, S., Mayr, C., et al. (2007) miR-150, a microRNA expressed in mature B and T cells, blocks early B cell development when expressed prematurely. **Proceedings of the National Academy of Sciences of the United States of America**, 104 (17): 7080–7085

Zinkernagel, R.M., Bachmann, M.F., Kündig, T.M., et al. (1996) On immunological memory. **Annual review of immunology**, 14: 333–67

Zinovyev, A., Morozova, N., Gorban, A.N., et al. (2008) Mathematical modeling of microRNA-mediated mechanisms of translation repression. Schmitz, U., Wolkenhauer, O. and Vera, J. (eds.). **Advances in experimental medicine and biology**, 774: 189–224

Zipori, D. (2006) The stem state: mesenchymal plasticity as a paradigm. **Current stem cell research & therapy**, 1 (1): 95–102

Appendix A

R scripts used for illumina miRNA sequencing analysis

```
# creating text files of updated data, deleting any rows that
dont have a mature mouse hit

# read the file
  dat <- read.delim("491_at1.txt")
# select only those rows with a mature mouse hit
  dat <- subset(dat, Best.human.mature.hit !="")
# write the new data to a file
  write.table(dat,file="at1.txt")

# make this into a general function

processrows <- function(filename){

  dat <- read.delim(filename)
  dat <- subset(dat, Best.human.mature.hit !="")
  return(dat)
}

  write.table(dat,file="___.txt")
```

```
# collapsing data (sum coverage values from same mature hits)


# Read data in
  x <- read.table("dt4.txt")
# select the subset you want
  x <- subset(x, select = c(Best.human.mature.hit,
Coverage.of.mature.hit))
<# write that to a file
  write.table(x, file="dt4S.txt")>
# sum the coverage values of the same micros
  y <- aggregate(x$Coverage.of.mature,
by=list(Best.human.mature.hit=x$Best.human.mature.hit), FUN=sum)
# write that to a file
  write.table (y, file="dt4Y.txt")

collapse <- function(filename) {
  # Read in data
  # Select the apt. cols
  # Sum the coverage values of the same micros

 dat <- read.delim(filename)
 dat <- subset(dat, select = c(Best.human.mature.hit,
Coverage.of.mature))
 dat <- aggregate(dat$Coverage.of.mature,
by=list(Best.human.mature.hit=dat$Best.human.mature.hit),
FUN=sum)
 names(dat)[3] <- "Coverage.of.mature"
 return(dat)
}
```

```
# merging miR data


zeroF <- read.table("at4Y.txt")
zeroM <- read.table("dt2Y.txt")
zero <- merge(zeroF, zeroM, by = "Best.human.mature.hit",
all=TRUE)
names(zero)[2] <- "zeroF"
names(zero)[3] <- "zeroM"

oneF <- read.table("at3Y.txt")
oneM <- read.table("dt1Y.txt")
one <- merge(oneF, oneM, by = "Best.human.mature.hit", all=TRUE)
names(one)[2] <- "oneF"
names(one)[3] <- "oneM"

threeF <- read.table("at2Y.txt")
threeM <- read.table("dt4Y.txt")
three <- merge(threeF, threeM, by = "Best.human.mature.hit",
all=TRUE)
names(three)[2] <- "threeF"
names(three)[3] <- "threeM"

fiveF <- read.table("at1Y.txt")
fiveM <- read.table("dt3Y.txt")
five <- merge(fiveF, fiveM, by = "Best.human.mature.hit",
all=TRUE)
names(five)[2] <- "fiveF"
names(five)[3] <- "fiveM"

fourteenF <- read.table("bt3Y.txt")
fourteenM <- read.table("ct1Y.txt")
fourteen <- merge(fourteenF, fourteenM, by =
"Best.human.mature.hit", all=TRUE)
names(fourteen)[2] <- "fourteenF"
names(fourteen)[3] <- "fourteenM"

twentyoneF <- read.table("bt2Y.txt")
twentyoneM <- read.table("ct4Y.txt")
twentyone <- merge(twentyoneF, twentyoneM, by =
"Best.human.mature.hit", all=TRUE)
names(twentyone)[2] <- "twentyoneF"
names(twentyone)[3] <- "twentyoneM"

twentyeightF <- read.table("bt1Y.txt")
twentyeightM <- read.table("ct3Y.txt")
twentyeight <- merge(twentyeightF, twentyeightM, by =
"Best.human.mature.hit", all=TRUE)
names(twentyeight)[2] <- "twentyeightF"
names(twentyeight)[3] <- "twentyeightM"

LTbF <- read.table("bt4Y.txt")
LTbM <- read.table("ct2Y.txt")
```

```
LTb <- merge(LTbF, LTbM, by = "Best.human.mature.hit", all=TRUE)
names(LTb)[2] <- "LTbF"
names(LTb)[3] <- "LTbM"

zeroone <- merge(zero, one, by = "Best.human.mature.hit",
all=TRUE)
threefive <- merge(three, five, by = "Best.human.mature.hit",
all=TRUE)
fourteentwentyone <- merge(fourteen, twentyone, by =
"Best.human.mature.hit", all=TRUE)
twentyeightLTb <- merge(twentyone, LTb, by =
"Best.human.mature.hit", all=TRUE)
all1 <- merge(zeroone, threefive, by = "Best.human.mature.hit",
all=TRUE)
all2 <- merge(fourteentwentyone, twentyeightLTb, by =
"Best.human.mature.hit", all=TRUE)
merge <- merge(all1, all2, by = "Best.human.mature.hit",
all=TRUE)
write.table(merge, file="merged.txt")
```

```
# Using edgeR package to calculate normalisation factors

# load edgeR
  library(edgeR)

# read in counts data
  D <- read.table("xlmerge.txt")

# Take off miR coloum and change into matrix
  D <- D[ ,-1]
  D <- as.matrix(D)

# Create a DGEList
  d <- DGEList(counts = D, group = substr(colnames(D), 1, 16))

# check samples output
  d$samples

# OUTPUT
     group lib.size norm.factors
X0f    X0f  2615192            1
X0m    X0m  2818664            1
X1f    X1f   915598            1
X1m    X1m   502000            1
X3f    X3f  3749696            1
X3m    X3m  1722589            1
X5f    X5f   991678            1
X5m    X5m  1224624            1
X14f  X14f   635175            1
X14m  X14m   921157            1
X21f  X21f  2741291            1
X21m  X21m  2291138            1
X28f  X28f   404405            1
X28m  X28m   873814            1
ltbf  ltbf  1844101            1
ltbm  ltbm  3247595            1

# calculate the normalization factors
  d <- calcNormFactors(d)

# check samples output
  d$samples

# OUTPUT
     group lib.size norm.factors
X0f    X0f  2615192    0.6124565
X0m    X0m  2818664    0.5152068
X1f    X1f   915598    1.9378149
X1m    X1m   502000    1.3194413
X3f    X3f  3749696    0.3662188
X3m    X3m  1722589    1.3499490
X5f    X5f   991678    1.4875536
X5m    X5m  1224624    1.6431315
X14f  X14f   635175    1.6615986
```

```
X14m  X14m   921157    1.3976537
X21f  X21f  2741291    0.5301450
X21m  X21m  2291138    0.6728704
X28f  X28f   404405    1.5800473
X28m  X28m   873814    2.0315369
ltbf  ltbf  1844101    0.7911965
ltbm  ltbm  3247595    0.4875362

#use cpm function to get counts per million from DGEList
counts <- cpm(d, normalized.lib.size=TRUE)
head(counts)
write.table (counts, file="TMM_norm_counts.txt")
```

```
# TMM normalisation of seq data with -142-3p deleted.

#load edgeR
 library(edgeR)

#read in data
 D <- read.delim("del.142-3p.txt")

#Take off miR coloum and change to matrix
 D <- D[ ,-1]
 D <- as.matrix(D)

#create DGElist
 d <- DGEList(counts = D, group = substr(colnames(D), 1, 16))

#check samples
 d$samples

#OUTPUT
 group lib.size norm.factors
X0f    X0f   822999            1
X0m    X0m   758462            1
X1f    X1f   880010            1
X1m    X1m   486996            1
X3f    X3f   692047            1
X3m    X3m   914581            1
X5f    X5f   957081            1
X5m    X5m  1170790            1
X14f  X14f   612302            1
X14m  X14m   887932            1
X21f  X21f   675716            1
X21m  X21m   611892            1
X28f  X28f   381622            1
X28m  X28m   836199            1
ltbf  ltbf   675328            1
ltbm  ltbm   737251            1


#calculate normalisation factors
 d <- calcNormFactors(d)

#check output
 d$samples

#OUTPUT
 group lib.size norm.factors
X0f    X0f   822999    1.1092514
X0m    X0m   758462    1.0368655
X1f    X1f   880010    1.0661379
X1m    X1m   486996    0.8187085
X3f    X3f   692047    1.0842188
X3m    X3m   914581    1.2498697
X5f    X5f   957081    0.7366625
X5m    X5m  1170790    0.8902237
```

X14f	X14f	612302	0.9729092
X14m	X14m	887932	0.5895419
X21f	X21f	675716	1.1095535
X21m	X21m	611892	1.2223025
X28f	X28f	381622	0.8840909
X28m	X28m	836199	0.9978496
ltbf	ltbf	675328	1.2911265
ltbm	ltbm	737251	1.2650591

```
# normalisation with data only from tag 1 and 3 time points

# read in the xlmerge file
  D <- read.delim("xlmerge.txt")
# delete coloums don't want
  D <- D[ ,-1]
  D <- D[ ,-2]
  D <- D[ ,-2]
  D <- D[ ,-4]
  D <- D[ ,-4]
  D <- D[ ,-8]
  D <- D[ ,-8]
  D <- D[ ,-10]
  D <- D[ ,-10]
# write file
  write.table(D, file="raw1&3.txt")
# load edgeR
  library(edgeR)
# Take off miR column and change into matrix
  D <- D[ ,-1]
  D <- as.matrix(D)
  is.matrix(D)
# Create a DGEList
  d <- DGEList(counts = D, group = substr(colnames(D), 1, 8))
# check samples output
  d$samples

# OUTPUT
     group lib.size norm.factors
X1f    X1f   915598            1
X1m    X1m   502000            1
X5f    X5f   991678            1
X5m    X5m  1224624            1
X14f  X14f   635175            1
X14m  X14m   921157            1
X28f  X28f   404405            1
X28m  X28m   873814            1

# calculate the normalisation factors
  d <- calcNormFactors(d)
# check samples output
  d$samples

# OUTPUT
     group lib.size norm.factors
X1f    X1f   915598    1.2957730
X1m    X1m   502000    0.8488325
X5f    X5f   991678    0.8626299
X5m    X5m  1224624    1.0344219
X14f  X14f   635175    1.1038309
X14m  X14m   921157    0.7842650
X28f  X28f   404405    0.9162668
X28m  X28m   873814    1.2845159
```

```
# REPEAT BUT TAKE OFF 142-3p...

# DGEList output
     group lib.size norm.factors
X1f    X1f   880010            1
X1m    X1m   486996            1
X5f    X5f   957081            1
X5m    X5m  1170790            1
X14f  X14f   612302            1
X14m  X14m   887932            1
X28f  X28f   381622            1
X28m  X28m   836199            1

# normfactors output
     group lib.size norm.factors
X1f    X1f   880010    1.3007873
X1m    X1m   486996    0.8441690
X5f    X5f   957081    0.8623671
X5m    X5m  1170790    1.0441264
X14f  X14f   612302    1.1065248
X14m  X14m   887932    0.7850813
X28f  X28f   381622    0.9347188
X28m  X28m   836199    1.2455533

# REPEAT FOR TAGs 2&4...

# output for DGEList
     group lib.size norm.factors
X0f    X0f  2615192            1
X0m    X0m  2818664            1
X3f    X3f  3749696            1
X3m    X3m  1722589            1
X21f  X21f  2741291            1
X21m  X21m  2291138            1
ltbf  ltbf  1844101            1
ltbm  ltbm  3247595            1

# output for calcNormFactors
     group lib.size norm.factors
X0f    X0f  2615192    1.0240848
X0m    X0m  2818664    0.8516186
X3f    X3f  3749696    0.6101051
X3m    X3m  1722589    1.9834753
X21f  X21f  2741291    0.8386001
X21m  X21m  2291138    0.9677108
ltbf  ltbf  1844101    1.3495629
ltbm  ltbm  3247595    0.8651549

# REPEAT but without 142-3p...

# output for DGEList
     group lib.size norm.factors
X0f    X0f   822999            1
X0m    X0m   758462            1
X3f    X3f   692047            1
X3m    X3m   914581            1
```

```
X21f  X21f   675716            1
X21m  X21m   611892            1
ltbf  ltbf   675328            1
ltbm  ltbm   737251            1

# output from calcNormFactors
  group lib.size norm.factors
X0f    X0f   822999    0.9445184
X0m    X0m   758462    0.9113083
X3f    X3f   692047    0.9231458
X3m    X3m   914581    1.0808624
X21f  X21f   675716    0.9854850
X21m  X21m   611892    1.0570229
ltbf  ltbf   675328    1.0359653
ltbm  ltbm   737251    1.0789563
```

Appendix B

R scripts used for the analysis of miRNA microarray data

```
# ExiMiR

# set working directory
setwd("M:/Array stuff/Raw data files")

# Install makecdfenv package
source("http://www.bioconductor.org/biocLite.R")
    biocLite("makecdfenv")

# Create array annotation environment
library(makecdfenv)
cdfenv <- make.cdf.env(cdf.path = "Affymetrix", filename =
"miRNA-2_0.cdf")

# load the CEL files into R
library(affy)
abatch <- ReadAffy(cdfname = 'cdfenv', celfile.path =
'Affymetrix')

# Can use RMA normalisation applied to abatch
eset.rma <-rma(abatch)

# Or can use spike-in probe-based approach in ExiMiR which may
give better results
# load ExiMiR package
source("http://www.bioconductor.org/biocLite.R")
biocLite("ExiMiR")
library(ExiMiR)
eset.spike <- NormiR(abatch)
# OUTPUT
# No Exiqon Spike Control probes, trying with Affy Spike Control
probes...
# Not enough common variance to guarantee good performance of
spike-in normalization (0.28 < 0.5).
# Using median normalization...

# Exiqon from text files to expressionsets
library(ExiMiR)

# create array annotation environment
galenv <- make.gal.env(gal.path = "Exiqon")

# read raw txt files into R
ebatch <- ReadExi(galname = 'galenv', txtfile.path = "Exiqon")

# load affy package and apply RMA normalisation
library(affy)
eset.rma <- rma(ebatch, background = FALSE)

# Or use spike-in dataset from ExiMiR
```

```
eset.spike <- NormiR(ebatch)

# ExiMiR doesn't seem to work for all datasets therefore will go
back to RMA
Aff.eset.rma <- rma(abatch)
Exi.eset.rma <- rma(ebatch)
a <- exprs(Aff.eset.rma)
e <- exprs(Exi.eset.rma)
write.table(a, file = "affy.rma.txt")
write.table(e, file = "exiq.rma.txt")

# Edit data files in excel as appropriate
# read the data back in
affy <- read.table("affy.rma.txt", header = TRUE)
exiq <- read.table("exiq.rma.txt", header = TRUE)
head(affy)
head(exiq)

# make into a matrix
affy <- as.matrix(affy)
exiq <- as.matrix(exiq)

# create a function to draw barplots from affy data
customBar <- function(dataname, rowname) {
  print(barplot(dataname[rowname, ], col=
c("lightblue1","lightblue1","skyblue2","skyblue2","mediumblue","m
ediumblue","blueviolet","blueviolet"), main = rowname, ylab =
"log2FC(intensity)"))
}
customBar(dat, "mmu-miR-491*")
```

Appendix C

Affymetrix miRNA microarray data

The RMA-normalised miRNA expression values and fold-change of the mean expression value for each of the time points are shown with the mean expression value of the Day 0 samples set as a baseline value of 1.00. The data shown is threshold filtered, with miRNAs that did not have an expression value of at least 10 for both duplicates from at least one time point excluded. The table is ordered with those miRNAs showing the most significant decrease in expression in the $LTb^{-/-}$ samples compared to the Day 0 samples first and those with the most significant increase last. Those miRNAs with a 2-fold or greater difference in expression between Day 0 and $LTb^{-/-}$ samples, with a change in the same direction at day 2 and day 14 were considered for further analysis and are highlighted in yellow. Before selection of miRNAs for further study similarity of the duplicates from each time point was also assessed, miRNAs that had a 2-fold difference or greater within any of the duplicates (in red) were excluded from further analysis.

	Expression values									Fold change from Day 0			
miRNA ID	0a	0b	2a	2b	14a	14b	LTa	LTb		Day 0-0	Day 2-0	Day 14-0	LTb-0
mmu-miR-708	77	71	61	54	72	23	17	12		1.00	0.78	0.64	0.20
mmu-miR-138	446	713	535	597	260	299	199	213		1.00	0.98	0.48	0.36
mmu-miR-138*	28	57	32	33	17	40	11	22		1.00	0.76	0.66	0.40
mmu-miR-2137	14440	8194	9958	9273	6505	6490	5349	4038		1.00	0.85	0.57	0.41
mmu-miR-124	22	15	10	8	6	5	7	9		1.00	0.48	0.28	0.42
mmu-miR-466d-3p	12	13	14	12	16	17	6	5		1.00	1.06	1.36	0.45
mmu-miR-187	298	374	363	259	161	185	156	152		1.00	0.93	0.52	0.46
mmu-miR-290-5p	19	14	7	10	7	14	8	7		1.00	0.52	0.64	0.47
mmu-miR-491	19	14	10	13	12	13	8	8		1.00	0.71	0.75	0.49
mmu-miR-466h	59	42	63	39	98	46	32	18		1.00	1.02	1.43	0.49
mmu-miR-1893	90	43	69	38	57	32	27	40		1.00	0.80	0.66	0.50
mmu-miR-671-3p	32	22	12	34	37	32	16	10		1.00	0.85	1.28	0.50

mmu-miR-762	1939	716	1229	796	1054	509	817	522		1.00	0.76	0.59	0.50
mmu-miR-100	569	745	502	520	446	502	306	345		1.00	0.78	0.72	0.50
mmu-miR-1937c	23	14	9	12	10	13	8	11		1.00	0.56	0.63	0.52
mmu-miR-1224	1084	947	476	785	576	661	576	524		1.00	0.62	0.61	0.54
mmu-miR-1937a	327	204	328	162	244	175	161	135		1.00	0.92	0.79	0.56
mmu-miR-297a*	9	13	16	11	9	8	7	6		1.00	1.19	0.77	0.56
mmu-miR-27a*	37	48	43	27	36	33	28	20		1.00	0.83	0.81	0.56
mmu-miR-139-3p	79	134	133	123	77	88	69	51		1.00	1.20	0.77	0.56
mmu-miR-1894-3p	220	107	120	95	129	99	106	82		1.00	0.66	0.69	0.57
mmu-miR-1937b	245	124	210	101	188	113	103	112		1.00	0.84	0.82	0.58
mmu-miR-711	29	15	23	15	21	12	10	15		1.00	0.88	0.77	0.59
mmu-miR-2133	1926	1155	1873	1170	982	967	825	1024		1.00	0.99	0.63	0.60
mmu-miR-151-3p	674	737	519	664	482	554	522	345		1.00	0.84	0.73	0.61
mmu-miR-193b	209	224	267	208	153	132	138	130		1.00	1.10	0.66	0.62
mmu-miR-335-5p	11	6	3	13	13	10	5	5		1.00	0.97	1.39	0.63
mmu-miR-467b	12	9	13	4	13	22	4	10		1.00	0.78	1.63	0.63
mmu-miR-1959	289	164	186	83	195	113	117	170		1.00	0.59	0.68	0.63
mmu-miR-542-5p	13	35	69	30	23	24	13	17		1.00	2.06	0.97	0.64
mmu-miR-296-5p	11	13	17	8	8	12	7	8		1.00	1.04	0.86	0.65
mmu-miR-698	25	19	6	16	15	22	15	14		1.00	0.51	0.84	0.65
mmu-miR-30a*	111	129	115	107	106	127	93	66		1.00	0.93	0.97	0.66
mmu-miR-184	9	29	21	15	12	20	10	16		1.00	0.94	0.83	0.66
mmu-miR-466f	129	91	140	125	159	89	93	53		1.00	1.20	1.12	0.66
mmu-miR-455	595	909	629	837	613	793	634	368		1.00	0.97	0.94	0.67
mmu-miR-19a	60	47	92	47	86	69	46	26		1.00	1.30	1.45	0.67

mmu-miR-669h-3p	22	50	15	67	36	45	36	13		1.00	1.15	1.13	0.67
mmu-miR-29b	62	33	58	30	49	50	30	34		1.00	0.93	1.05	0.68
mmu-miR-1940	72	82	43	61	65	66	64	41		1.00	0.68	0.85	0.69
mmu-miR-330*	67	97	80	78	57	84	58	54		1.00	0.96	0.86	0.69
mmu-miR-503	140	141	298	165	134	115	100	93		1.00	1.65	0.89	0.69
mmu-miR-212	53	55	70	58	54	44	39	36		1.00	1.18	0.90	0.69
mmu-miR-2141	447	247	400	200	340	231	264	217		1.00	0.86	0.82	0.69
mmu-miR-467a	284	348	351	379	374	362	227	210		1.00	1.16	1.17	0.69
mmu-miR-468	38	38	18	33	30	24	24	28		1.00	0.68	0.71	0.69
mmu-miR-296-3p	110	95	153	159	95	120	85	59		1.00	1.52	1.05	0.70
mmu-miR-674	1891	2442	2039	2425	1475	1769	1679	1409		1.00	1.03	0.75	0.71
mmu-miR-672	44	76	47	40	39	29	45	42		1.00	0.73	0.57	0.72
mmu-miR-301a	23	19	43	22	25	36	18	13		1.00	1.54	1.43	0.72
mmu-miR-669b	23	13	22	12	44	16	17	9		1.00	0.95	1.65	0.72
mmu-miR-3474	13	15	14	14	11	11	12	8		1.00	1.00	0.77	0.72
mmu-miR-669a	75	39	76	54	93	79	42	40		1.00	1.14	1.50	0.72
mmu-miR-297a	42	23	38	25	66	26	32	15		1.00	0.96	1.40	0.73
mmu-miR-467f	45	50	65	67	86	68	53	17		1.00	1.38	1.61	0.73
mmu-miR-669d	17	8	17	10	26	11	11	8		1.00	1.05	1.45	0.74
mmu-miR-712	58	28	65	39	46	29	29	35		1.00	1.20	0.86	0.74
mmu-miR-2135	2576	1879	2295	1735	1695	1596	1754	1561		1.00	0.90	0.74	0.74
mmu-miR-877	37	25	44	32	35	30	21	26		1.00	1.21	1.03	0.75
mmu-miR-500	698	977	812	845	569	731	637	624		1.00	0.99	0.78	0.75
mmu-miR-326	180	156	206	147	143	98	110	144		1.00	1.05	0.72	0.76
mmu-miR-351	425	603	552	690	419	503	404	374		1.00	1.21	0.90	0.76

mmu-miR-149	170	220	202	153	174	175	147	150		1.00	0.91	0.89	0.76
mmu-miR-712*	17	15	36	6	11	16	15	9		1.00	1.32	0.87	0.76
mmu-miR-151-5p	2931	3065	2626	2548	2145	2382	2295	2301		1.00	0.86	0.75	0.77
mmu-miR-3472	116	37	52	48	39	48	55	63		1.00	0.65	0.57	0.77
mmu-miR-1941-5p	55	85	64	64	53	58	52	56		1.00	0.92	0.80	0.77
mmu-miR-2145	4177	2368	4068	2415	2293	2049	2252	2814		1.00	0.99	0.66	0.77
mmu-miR-345-3p	53	56	49	63	53	47	47	38		1.00	1.02	0.92	0.77
mmu-miR-320	1180	1805	1296	1699	1136	1353	1221	1097		1.00	1.00	0.83	0.78
mmu-miR-541	49	39	57	55	46	43	31	38		1.00	1.27	1.00	0.78
mmu-miR-501-3p	164	202	197	156	135	147	134	155		1.00	0.96	0.77	0.79
mmu-miR-467a-1*	60	69	69	83	95	101	51	51		1.00	1.18	1.51	0.79
mmu-miR-30c-2*	64	96	85	52	71	58	62	66		1.00	0.86	0.80	0.80
mmu-miR-30a	779	779	924	774	733	732	602	638		1.00	1.09	0.94	0.80
mmu-miR-223	300	168	297	157	340	216	184	191		1.00	0.97	1.19	0.80
mmu-miR-188-5p	51	58	56	78	33	52	47	41		1.00	1.22	0.78	0.80
mmu-miR-1943	11	11	9	9	10	13	7	10		1.00	0.82	1.07	0.80
mmu-miR-1187	359	337	315	356	417	299	343	218		1.00	0.96	1.03	0.81
mmu-miR-125a-3p	74	60	64	74	46	53	54	56		1.00	1.03	0.74	0.82
mmu-miR-1196	1046	1245	847	1195	950	1015	1011	863		1.00	0.89	0.86	0.82
mmu-miR-1964	37	33	43	34	41	29	28	29		1.00	1.11	1.01	0.82
mmu-miR-34a	434	374	374	295	329	273	348	319		1.00	0.83	0.75	0.82
mmu-miR-214*	30	47	42	51	42	37	27	37		1.00	1.20	1.02	0.83
mmu-miR-1839-5p	862	799	602	670	659	724	727	657		1.00	0.77	0.83	0.83
mmu-miR-423-3p	857	955	844	859	788	777	778	745		1.00	0.94	0.86	0.84

mmu-miR-181d	240	260	356	299	293	383	204	219		1.00	1.31	1.35	0.85
mmu-miR-17*	1294	1698	1523	1605	1219	1357	1301	1235		1.00	1.05	0.86	0.85
mmu-miR-324-3p	119	164	152	156	127	157	109	132		1.00	1.09	1.00	0.85
mmu-miR-466j	73	71	103	92	122	71	73	49		1.00	1.35	1.34	0.85
mmu-miR-339-3p	63	69	62	55	57	67	52	60		1.00	0.89	0.94	0.85
mmu-miR-574-5p	455	550	385	560	453	424	440	419		1.00	0.94	0.87	0.85
mmu-miR-99b	1736	2799	2014	2644	1629	2099	1876	2006		1.00	1.03	0.82	0.86
mmu-miR-135a*	37	14	24	17	17	22	17	27		1.00	0.81	0.77	0.86
mmu-miR-207	56	45	59	51	63	37	45	42		1.00	1.08	0.99	0.86
mmu-miR-22	4753	4356	4115	4152	3886	3752	4193	3637		1.00	0.91	0.84	0.86
mmu-let-7e	3817	4709	4437	4331	3742	3862	3570	3764		1.00	1.03	0.89	0.86
mmu-miR-744*	12	16	11	5	15	11	11	13		1.00	0.58	0.92	0.86
mmu-miR-125b-3p	31	27	34	20	26	21	21	29		1.00	0.94	0.82	0.86
mmu-miR-125a-5p	3079	3342	3023	3181	2868	3163	2693	2870		1.00	0.97	0.94	0.87
mmu-miR-466b-3-3p	48	47	55	47	49	57	31	50		1.00	1.09	1.12	0.87
mmu-miR-680	8	16	10	11	9	8	10	10		1.00	0.85	0.73	0.87
mmu-miR-652	3220	3738	3253	3590	2539	2905	2991	3051		1.00	0.98	0.78	0.87
mmu-miR-674*	135	147	150	118	136	141	120	125		1.00	0.95	0.99	0.87
mmu-miR-466b-3p	61	36	57	61	63	70	38	46		1.00	1.22	1.38	0.87
mmu-let-7d*	83	97	97	98	99	126	89	68		1.00	1.09	1.25	0.87
mmu-miR-140	170	144	183	130	171	165	152	123		1.00	1.00	1.07	0.87
mmu-miR-346	167	252	133	270	155	265	174	192		1.00	0.96	1.00	0.87
mmu-miR-181a	5284	6842	7276	7164	5392	6216	5400	5213		1.00	1.19	0.96	0.88
mmu-miR-222	1774	2053	1566	1842	1686	1765	1726	1636		1.00	0.89	0.90	0.88

mmu-miR-143	7910	8512	8282	8669	7908	7638	7178	7250		1.00	1.03	0.95	0.88
mmu-miR-181b	1290	1744	1938	1874	1387	1389	1303	1387		1.00	1.26	0.91	0.89
mmu-miR-574-3p	583	888	702	900	614	756	673	632		1.00	1.09	0.93	0.89
mmu-miR-466c-5p	78	41	88	71	127	59	62	44		1.00	1.33	1.56	0.89
mmu-miR-665	16	10	13	7	22	6	11	12		1.00	0.75	1.10	0.89
mmu-miR-298	81	101	121	136	92	116	96	67		1.00	1.41	1.13	0.89
mmu-miR-194	840	856	790	805	774	796	761	754		1.00	0.94	0.93	0.89
mmu-miR-20b*	10	11	12	12	17	13	8	11		1.00	1.13	1.41	0.89
mmu-miR-362-5p	260	356	332	292	284	304	282	269		1.00	1.01	0.95	0.89
mmu-miR-669c	308	269	276	278	337	278	278	237		1.00	0.96	1.07	0.89
mmu-miR-24	14674	15832	15016	15422	14701	14121	14220	13094		1.00	1.00	0.94	0.90
mmu-miR-429	12	11	11	9	8	18	10	11		1.00	0.88	1.10	0.90
mmu-miR-667	22	6	16	15	9	11	14	11		1.00	1.08	0.70	0.90
mmu-miR-185	2580	2854	2675	2926	2576	2721	2558	2319		1.00	1.03	0.97	0.90
mmu-miR-455*	19	12	22	10	14	11	14	13		1.00	1.05	0.82	0.90
mmu-miR-130b	1033	1533	1635	1722	1255	1373	1194	1118		1.00	1.31	1.02	0.90
mmu-miR-497	325	425	401	350	390	401	305	372		1.00	1.00	1.05	0.90
mmu-miR-484	55	54	97	52	51	67	45	53		1.00	1.38	1.09	0.91
mmu-miR-345-5p	87	146	121	130	85	114	98	113		1.00	1.07	0.85	0.91
mmu-miR-93*	268	316	269	323	294	313	285	244		1.00	1.01	1.04	0.91
mmu-miR-466g	154	161	157	296	202	225	171	116		1.00	1.44	1.36	0.91
mmu-miR-339-5p	506	714	504	482	437	495	552	559		1.00	0.81	0.76	0.91
mmu-miR-195	3091	3071	2576	2902	2920	3324	2772	2852		1.00	0.89	1.01	0.91
mmu-miR-378	2663	3290	2969	3248	2713	2856	2809	2625		1.00	1.04	0.94	0.91
mmu-miR-203	86	57	96	60	91	96	54	76		1.00	1.09	1.31	0.91

mmu-miR-1981	218	315	261	262	234	240	265	222		1.00	0.98	0.89	0.91
mmu-miR-103	8620	10582	9383	9805	8676	9177	8931	8677		1.00	1.00	0.93	0.92
mmu-miR-1195	3452	2625	3998	3081	4089	2961	2846	2730		1.00	1.16	1.16	0.92
mmu-miR-193*	55	81	79	76	70	68	59	66		1.00	1.14	1.02	0.92
mmu-miR-466f-3p	534	802	445	1016	732	935	737	492		1.00	1.09	1.25	0.92
mmu-miR-27a	1989	1908	2589	2000	1759	1888	1764	1825		1.00	1.18	0.94	0.92
mmu-miR-582-3p	11	11	13	12	14	10	11	10		1.00	1.08	1.06	0.92
mmu-miR-2138	10151	7661	8197	8475	7301	6721	8421	8020		1.00	0.94	0.79	0.92
mmu-miR-2861	7411	5100	4267	5597	4231	4232	5889	5684		1.00	0.79	0.68	0.93
mmu-miR-328	185	189	214	156	183	170	170	175		1.00	0.99	0.94	0.93
mmu-miR-532-5p	1227	1784	1391	1615	1223	1409	1430	1362		1.00	1.00	0.87	0.93
mmu-miR-29b*	35	12	10	4	14	6	30	14		1.00	0.29	0.43	0.93
mmu-miR-199a-5p	524	607	695	497	585	585	513	540		1.00	1.05	1.03	0.93
mmu-miR-342-5p	788	1017	917	846	857	874	871	815		1.00	0.98	0.96	0.93
mmu-miR-214	690	1108	987	1023	772	963	820	862		1.00	1.12	0.97	0.94
mmu-miR-30c-1*	66	73	60	52	72	48	67	63		1.00	0.80	0.86	0.94
mmu-miR-145	14557	15451	14890	15121	14252	14974	13224	14918		1.00	1.00	0.97	0.94
mmu-miR-467c	64	52	64	63	95	78	48	60		1.00	1.10	1.50	0.94
mmu-miR-125b-5p	5140	5307	5230	4420	4648	4710	4403	5428		1.00	0.92	0.90	0.94
mmu-miR-1935	185	114	224	125	255	139	155	127		1.00	1.17	1.32	0.94
mmu-miR-3471	18	14	19	16	15	16	16	13		1.00	1.11	1.02	0.94
mmu-miR-485*	19	11	6	8	8	17	10	19		1.00	0.45	0.79	0.95
mmu-miR-192	227	240	271	237	275	294	237	205		1.00	1.09	1.22	0.95
mmu-miR-106b	4348	4636	4743	5230	4943	5047	4784	3747		1.00	1.11	1.11	0.95
mmu-miR-425*	264	352	321	311	287	285	290	295		1.00	1.03	0.93	0.95

mmu-miR-1894-5p	305	459	290	498	342	451	433	298		1.00	1.03	1.04	0.96
mmu-miR-15a*	47	42	35	87	40	45	37	48		1.00	1.36	0.95	0.96
mmu-miR-27b*	51	41	41	38	53	48	39	49		1.00	0.86	1.10	0.96
mmu-miR-139-5p	1794	2337	2132	2045	1779	1911	1976	1993		1.00	1.01	0.89	0.96
mmu-miR-466a-3p	43	45	64	51	66	76	33	51		1.00	1.30	1.61	0.96
mmu-miR-2132	24345	24522	33205	26835	25128	22997	23208	23822		1.00	1.23	0.98	0.96
mmu-let-7f*	10	15	13	32	7	19	12	12		1.00	1.82	1.05	0.96
mmu-miR-24-2*	443	495	469	455	467	442	455	451		1.00	0.98	0.97	0.97
mmu-miR-423-5p	318	536	473	442	392	443	411	414		1.00	1.07	0.98	0.97
mmu-miR-182	81	100	104	88	122	125	88	87		1.00	1.06	1.37	0.97
mmu-miR-466i	123	121	136	159	237	191	142	93		1.00	1.21	1.76	0.97
mmu-miR-20b	1666	1898	1987	2329	2060	2185	1879	1574		1.00	1.21	1.19	0.97
mmu-miR-191	16972	18510	17306	18766	17193	18713	17628	16749		1.00	1.02	1.01	0.97
mmu-miR-709	26840	28121	29089	28548	30301	27816	27036	26251		1.00	1.05	1.06	0.97
mmu-miR-23b	11968	13026	12737	13298	12490	12584	12141	12136		1.00	1.04	1.00	0.97
mmu-miR-30e	313	193	434	316	337	327	255	238		1.00	1.48	1.31	0.97
mmu-miR-221	1963	1869	1744	1682	1839	1763	1885	1843		1.00	0.89	0.94	0.97
mmu-miR-877*	20	17	15	19	18	21	16	20		1.00	0.92	1.04	0.97
mmu-miR-24-1*	15	12	15	9	13	20	12	15		1.00	0.87	1.23	0.98
mmu-miR-99b*	56	75	83	81	57	81	68	60		1.00	1.25	1.05	0.98
mmu-miR-31	188	218	238	198	275	221	228	170		1.00	1.07	1.22	0.98
mmu-miR-107	6991	8069	7550	7100	7111	6973	7452	7336		1.00	0.97	0.94	0.98
mmu-miR-714	198	87	154	119	128	106	121	159		1.00	0.96	0.82	0.98
mmu-miR-26a	20364	20264	20184	20373	20166	20405	20156	19818		1.00	1.00	1.00	0.98
mmu-let-7b	16073	18148	18220	17884	16173	16656	16232	17514		1.00	1.06	0.96	0.99

mmu-miR-669e	20	10	11	16	25	11	19	11		1.00	0.89	1.17	0.99
mmu-miR-152	825	931	909	933	778	856	879	865		1.00	1.05	0.93	0.99
mmu-miR-27b	1839	1819	1816	1936	2060	2019	1875	1761		1.00	1.03	1.12	0.99
mmu-miR-720	126	82	126	55	137	97	87	120		1.00	0.87	1.12	1.00
mmu-miR-297c*	9	7	6	8	23	11	9	7		1.00	0.83	2.09	1.00
mmu-miR-411	9	9	9	8	12	11	9	10		1.00	0.94	1.23	1.00
mmu-let-7i	8409	5875	7269	6141	7892	6826	7470	6829		1.00	0.94	1.03	1.00
mmu-miR-466f-5p	156	119	177	138	203	120	163	113		1.00	1.14	1.17	1.00
mmu-miR-361	2640	3152	2902	3133	2717	3198	2782	3028		1.00	1.04	1.02	1.00
mmu-miR-20a	4681	4570	5372	5479	5386	5383	5078	4210		1.00	1.17	1.16	1.00
mmu-miR-181c	109	223	148	247	186	156	195	138		1.00	1.19	1.03	1.00
mmu-miR-10b	63	64	64	66	63	71	62	66		1.00	1.03	1.06	1.01
mmu-miR-130a	453	463	598	439	484	453	437	487		1.00	1.13	1.02	1.01
mmu-miR-342-3p	10530	11724	11494	12143	11389	11442	11088	11367		1.00	1.06	1.03	1.01
mmu-miR-331-3p	69	57	78	42	56	59	56	71		1.00	0.96	0.92	1.01
mmu-miR-874	21	29	29	34	26	25	23	27		1.00	1.27	1.03	1.01
mmu-miR-743b-5p	18	20	22	18	21	23	20	18		1.00	1.08	1.16	1.01
mmu-miR-17	6819	7082	6964	7924	7464	7566	7554	6531		1.00	1.07	1.08	1.01
mmu-miR-466c-3p	50	43	50	57	60	73	50	45		1.00	1.15	1.43	1.01
mmu-miR-140*	3883	5335	4939	5135	3807	4333	4531	4855		1.00	1.09	0.88	1.02
mmu-miR-99a	650	784	688	665	648	625	636	825		1.00	0.94	0.89	1.02
mmu-let-7d	16056	14935	16016	14858	16258	15545	15831	15783		1.00	1.00	1.03	1.02
mmu-miR-340-5p	10	6	13	7	18	13	8	8		1.00	1.20	1.86	1.02
mmu-miR-93	5853	6609	6761	6882	6430	6816	6492	6266		1.00	1.09	1.06	1.02
mmu-miR-22*	35	22	37	18	34	29	27	31		1.00	0.98	1.12	1.03

mmu-miR-2146	4876	3317	4619	3283	3694	2933	4056	4387		1.00	0.96	0.81	1.03
mmu-miR-106a	2251	2501	2527	2876	2630	2692	2635	2261		1.00	1.14	1.12	1.03
mmu-miR-713	29	13	24	41	33	40	26	18		1.00	1.53	1.71	1.03
mmu-miR-16	17049	15502	15977	17486	19196	17672	17697	15960		1.00	1.03	1.13	1.03
mmu-let-7c	18632	17123	18076	16464	17672	16330	18087	19008		1.00	0.97	0.95	1.04
mmu-miR-30d	1564	1785	1703	1679	1768	1661	1736	1741		1.00	1.01	1.02	1.04
mmu-miR-1906	90	66	92	77	78	61	78	84		1.00	1.08	0.89	1.04
mmu-miR-18a	641	621	883	916	798	809	726	584		1.00	1.43	1.27	1.04
mmu-miR-678	14	12	12	13	13	11	15	11		1.00	0.99	0.92	1.04
mmu-miR-706	26	87	8	74	36	60	85	32		1.00	0.72	0.86	1.04
mmu-miR-29a	4659	4035	4106	3948	4795	4306	4629	4418		1.00	0.93	1.05	1.04
mmu-miR-128	173	149	176	153	194	184	147	188		1.00	1.02	1.17	1.04
mmu-miR-689	110	83	31	68	33	65	55	147		1.00	0.51	0.51	1.04
mmu-miR-363	30	40	50	33	57	48	29	44		1.00	1.19	1.52	1.05
mmu-miR-671-5p	98	108	107	116	68	81	104	111		1.00	1.09	0.73	1.05
mmu-miR-30b*	76	88	83	58	77	78	87	85		1.00	0.86	0.94	1.05
mmu-miR-126-3p	7692	7022	6907	6858	7121	7908	7775	7673		1.00	0.94	1.02	1.05
mmu-miR-666-5p	6	13	8	11	11	11	10	10		1.00	1.00	1.13	1.05
mmu-miR-92a	5564	5874	6593	5563	6569	5913	5829	6300		1.00	1.06	1.09	1.06
mmu-miR-1955	14	35	37	35	25	35	28	24		1.00	1.47	1.23	1.06
mmu-miR-19b	2616	2739	3182	3028	3484	3256	3122	2563		1.00	1.16	1.26	1.06
mmu-miR-23a	13298	13023	13200	12665	13566	13096	13517	14471		1.00	0.98	1.01	1.06
mmu-miR-700	110	145	148	174	143	144	143	130		1.00	1.26	1.12	1.07
mmu-miR-532-3p	217	350	304	335	292	376	299	308		1.00	1.13	1.18	1.07
mmu-miR-199a-3p	1591	1439	1394	1336	1602	1698	1685	1567		1.00	0.90	1.09	1.07

mmu-miR-18a*	41	37	40	32	42	57	37	46		1.00	0.93	1.28	1.07
mmu-miR-129-3p	11	12	13	11	11	11	14	11		1.00	1.01	0.94	1.08
mmu-let-7g	3199	2110	2624	2106	3162	2514	2921	2818		1.00	0.89	1.07	1.08
mmu-miR-2140	437	333	321	293	356	380	389	447		1.00	0.80	0.96	1.09
mmu-miR-15b	6275	6023	5697	5837	6982	7149	6312	7075		1.00	0.94	1.15	1.09
mmu-miR-338-5p	41	29	31	29	40	31	43	33		1.00	0.86	1.01	1.09
mmu-miR-30c	3826	3461	3788	3804	4261	4102	3722	4223		1.00	1.04	1.15	1.09
mmu-miR-7a	27	23	34	13	33	16	28	26		1.00	0.95	0.99	1.09
mmu-miR-425	3616	4542	3887	4469	3915	4346	4365	4545		1.00	1.02	1.01	1.09
mmu-miR-15a	817	644	817	810	930	872	844	754		1.00	1.11	1.23	1.09
mmu-miR-21	705	500	822	533	877	688	699	627		1.00	1.12	1.30	1.10
mmu-miR-467d*	71	57	77	88	100	92	81	60		1.00	1.28	1.50	1.10
mmu-miR-871	10	9	9	11	12	11	11	11		1.00	1.01	1.15	1.10
mmu-let-7a	10366	8263	9317	7662	10399	9684	10088	10474		1.00	0.91	1.08	1.10
mmu-miR-676	174	210	230	188	221	220	217	208		1.00	1.09	1.15	1.11
mmu-miR-322	63	60	95	54	78	86	70	66		1.00	1.21	1.33	1.11
mmu-miR-210	108	133	213	122	132	142	138	131		1.00	1.39	1.13	1.11
mmu-miR-1944	360	295	325	324	441	413	367	362		1.00	0.99	1.30	1.11
mmu-miR-26b	235	177	211	197	288	236	222	237		1.00	0.99	1.27	1.11
mmu-miR-324-5p	137	183	196	213	128	201	161	196		1.00	1.28	1.03	1.12
mmu-miR-434-3p	37	47	53	38	55	55	46	48		1.00	1.09	1.31	1.12
mmu-miR-760	12	7	17	6	8	8	10	11		1.00	1.22	0.83	1.12
mmu-miR-199b	1525	1411	1372	1373	1721	1683	1682	1629		1.00	0.93	1.16	1.13
mmu-miR-150*	386	514	492	554	473	494	486	532		1.00	1.16	1.07	1.13
mmu-miR-7a*	47	49	37	43	57	57	58	51		1.00	0.83	1.20	1.13
mmu-miR-378*	220	267	269	249	243	291	266	287		1.00	1.06	1.10	1.14

mmu-miR-132	374	354	382	370	375	375	380	450		1.00	1.03	1.03	1.14
mmu-miR-1895	179	221	140	262	211	263	276	184		1.00	1.00	1.18	1.15
mmu-miR-146a	6307	4157	4590	3837	5421	5331	5906	6150		1.00	0.81	1.03	1.15
mmu-miR-29c	53	36	58	27	78	58	44	59		1.00	0.95	1.51	1.15
mmu-miR-98	88	86	83	59	81	96	83	119		1.00	0.81	1.02	1.16
mmu-miR-101b	25	33	58	34	55	20	35	32		1.00	1.58	1.28	1.16
mmu-miR-744	566	734	760	800	667	804	782	733		1.00	1.20	1.13	1.17
mmu-miR-106b*	1066	1169	1033	1245	1259	1318	1316	1310		1.00	1.02	1.15	1.17
mmu-miR-3473	121	78	125	60	152	73	108	127		1.00	0.93	1.13	1.18
mmu-miR-1306	35	53	46	53	51	57	58	46		1.00	1.12	1.22	1.18
mmu-miR-92b	82	48	87	69	90	54	71	83		1.00	1.19	1.10	1.18
mmu-miR-127	95	149	182	195	124	129	134	154		1.00	1.55	1.04	1.19
mmu-miR-28	438	534	413	474	477	541	574	579		1.00	0.91	1.05	1.19
mmu-miR-486	5230	3610	3782	4961	6389	5718	5628	4895		1.00	0.99	1.37	1.19
mmu-miR-327	9	12	13	15	12	11	12	14		1.00	1.30	1.07	1.19
mmu-miR-148a	125	85	128	101	109	138	142	108		1.00	1.09	1.18	1.19
mmu-miR-1982*	49	39	39	29	36	28	49	56		1.00	0.78	0.73	1.20
mmu-miR-350	105	123	143	120	142	147	116	158		1.00	1.15	1.26	1.20
mmu-miR-467b*	56	48	60	123	103	92	75	51		1.00	1.75	1.87	1.20
mmu-miR-18b	11	8	16	10	21	11	10	12		1.00	1.43	1.69	1.21
mmu-miR-322*	65	69	110	74	79	80	79	82		1.00	1.38	1.19	1.21
mmu-miR-10a	237	189	239	158	216	214	239	277		1.00	0.93	1.01	1.21
mmu-let-7g*	7	9	17	12	7	11	8	11		1.00	1.76	1.17	1.21
mmu-miR-200c	607	871	754	811	747	878	893	907		1.00	1.06	1.10	1.22
mmu-miR-1198	350	434	349	353	395	452	482	478		1.00	0.89	1.08	1.22
mmu-miR-16*	45	60	44	113	50	47	83	45		1.00	1.50	0.93	1.22

mmu-miR-1966	14	5	10	15	12	8	9	14		1.00	1.31	1.09	1.23
mmu-miR-362-3p	26	11	29	16	22	27	19	25		1.00	1.24	1.35	1.23
mmu-miR-669n	92	72	97	100	144	100	121	82		1.00	1.20	1.49	1.23
mmu-let-7f	2133	1485	1993	1605	2242	1938	2175	2272		1.00	0.99	1.16	1.23
mmu-miR-379	29	43	70	52	49	50	41	49		1.00	1.68	1.36	1.23
mmu-miR-2134	5825	3541	5855	3876	3827	3660	5425	6146		1.00	1.04	0.80	1.24
mmu-miR-141*	10	17	17	13	16	20	17	16		1.00	1.16	1.36	1.24
mmu-miR-30b	1411	1293	1482	1238	1695	1591	1620	1768		1.00	1.01	1.21	1.25
mmu-miR-1951	12	19	14	22	13	14	21	18		1.00	1.17	0.87	1.25
mmu-miR-1892	268	179	213	227	288	191	315	247		1.00	0.98	1.07	1.26
mmu-miR-150	12664	13219	13664	13099	14851	15657	15236	17379		1.00	1.03	1.18	1.26
mmu-miR-3072*	229	217	137	274	182	235	331	238		1.00	0.92	0.94	1.28
mmu-miR-383	63	75	35	47	44	40	101	76		1.00	0.59	0.60	1.28
mmu-miR-2183	19	18	20	19	23	14	21	27		1.00	1.03	0.98	1.28
mmu-miR-25	2244	2038	2345	2161	2918	2620	2477	3012		1.00	1.05	1.29	1.28
mmu-miR-3475	9	10	11	11	10	12	10	14		1.00	1.19	1.21	1.30
mmu-miR-2182	14	11	25	31	33	22	20	13		1.00	2.23	2.20	1.30
mmu-miR-1896	37	31	21	44	32	44	40	50		1.00	0.94	1.11	1.31
mmu-miR-421	257	248	292	241	319	360	343	320		1.00	1.06	1.35	1.31
mmu-miR-28*	517	596	497	645	596	711	714	754		1.00	1.03	1.18	1.32
mmu-miR-146b	234	188	256	199	343	265	290	268		1.00	1.08	1.44	1.32
mmu-let-7b*	34	44	45	80	41	66	50	54		1.00	1.60	1.38	1.32
mmu-miR-291b-5p	13	31	22	60	21	35	31	27		1.00	1.86	1.27	1.32
mmu-miR-21*	9	7	11	8	13	14	8	14		1.00	1.18	1.62	1.33
mmu-miR-370	135	48	182	73	156	56	117	126		1.00	1.39	1.16	1.33

mmu-miR-1965	90	53	79	58	97	73	101	90		1.00	0.96	1.19	1.33
mmu-miR-337-5p	17	10	13	16	11	16	19	17		1.00	1.09	1.01	1.33
mmu-miR-705	781	590	562	665	715	582	980	919		1.00	0.89	0.95	1.39
mmu-miR-1907	48	15	53	30	53	38	48	40		1.00	1.33	1.45	1.39
mmu-miR-467e	17	9	26	15	31	28	21	16		1.00	1.63	2.30	1.40
mmu-miR-30e*	53	36	53	46	56	75	61	65		1.00	1.11	1.46	1.41
mmu-miR-199b*	16	14	57	20	22	21	20	23		1.00	2.56	1.41	1.44
mmu-miR-34c*	18	17	24	29	24	25	27	26		1.00	1.47	1.37	1.46
mmu-miR-691	47	18	33	26	46	19	46	49		1.00	0.91	1.00	1.48
mmu-miR-155	2042	1419	1815	1277	2087	2232	2232	2902		1.00	0.89	1.25	1.48
mmu-miR-466e-3p	47	18	50	47	51	68	53	44		1.00	1.49	1.85	1.51
mmu-miR-501-5p	39	21	35	38	38	51	34	58		1.00	1.20	1.47	1.52
mmu-miR-1949	265	285	324	280	313	350	359	480		1.00	1.10	1.21	1.53
mmu-miR-1931	43	44	51	38	54	31	55	78		1.00	1.03	0.98	1.54
mmu-miR-1946b	35	15	32	35	61	34	44	33		1.00	1.37	1.92	1.56
mmu-miR-142-5p	16	11	23	10	22	10	28	14		1.00	1.26	1.20	1.62
mmu-miR-200b	9	21	23	12	28	18	25	23		1.00	1.20	1.57	1.63
mmu-miR-432	11	7	5	13	6	17	15	14		1.00	1.03	1.32	1.65
mmu-miR-1971	506	661	489	679	541	487	896	1028		1.00	1.00	0.88	1.65
mmu-miR-148b	60	27	80	58	82	70	68	78		1.00	1.59	1.75	1.68
mmu-miR-92a*	13	6	20	8	18	12	19	12		1.00	1.50	1.60	1.68
mmu-miR-374	45	39	53	52	87	76	68	73		1.00	1.25	1.94	1.68
mmu-miR-1839-3p	55	45	56	26	56	68	56	113		1.00	0.82	1.24	1.69
mmu-miR-494	149	118	98	124	120	137	165	295		1.00	0.83	0.96	1.73
mmu-miR-690	4944	5006	5498	3500	3655	3804	6049	11270		1.00	0.90	0.75	1.74

mmu-miR-483	22	23	17	35	35	23	52	27		1.00	1.16	1.28	1.74
mmu-miR-1930	6	7	5	13	9	8	12	11		1.00	1.40	1.30	1.76
mmu-miR-451	899	453	732	654	1449	1039	1097	1436		1.00	1.02	1.84	1.87
mmu-miR-200a	12	9	34	23	20	32	24	15		1.00	2.72	2.51	1.88
mmu-miR-2136	9	7	18	11	16	6	13	16		1.00	1.84	1.41	1.89
mmu-miR-382	9	5	23	8	8	6	10	17		1.00	2.26	0.98	1.96
mmu-miR-770-3p	21	33	18	36	23	23	48	58		1.00	1.00	0.86	1.97
mmu-miR-669f	19	12	28	36	38	51	35	27		1.00	2.09	2.89	2.04
mmu-miR-1946a	54	24	65	50	88	48	87	73		1.00	1.47	1.75	2.05
mmu-miR-3099*	6	5	15	15	22	11	11	13		1.00	2.69	2.88	2.14
mmu-miR-181a-1*	11	24	32	27	39	27	38	39		1.00	1.70	1.89	2.21
mmu-miR-216b	11	11	16	7	16	21	41	11		1.00	1.04	1.64	2.27
mmu-miR-3470a	6	11	9	7	10	4	16	30		1.00	0.94	0.89	2.77
mmu-miR-872*	19	8	21	24	31	23	32	45		1.00	1.65	2.00	2.86
mmu-miR-3470b	4	11	17	12	7	13	25	104		1.00	1.99	1.36	8.94

Exiqon miRNA microarray data

Shown are the expression values and fold-change of the mean expression value for each of the time points with the mean expression value of the Day 0 samples set as a baseline value of 1.00. The data shown is threshold filtered, with miRNAs that did not have an expression value of at least 50 for both duplicates of at least one time point (to give similar numbers of miRNA as seen in the affymetrix data set). The table is ordered with those miRNAs showing the most significant decrease in expression in the $LTb^{-/-}$ samples compared to the Day 0 samples first and those with the most significant increase last. Those miRNAs with a 2-fold or greater difference in expression between Day 0 and $LTb^{-/-}$ samples, with a change in the same direction at day 2 and day 14 were considered for further analysis and are highlighted in yellow. Before selection of miRNAs for further study similarity of the duplicates from each time point was also assessed, miRNAs that had a 2-fold difference or greater within any of the duplicates (in red) were excluded from further analysis.

	Expression values									Fold-change from Day 0			
miRNA ID	Day 0 a	Day 0 b	Day 2 a	Day 2 b	Day 14 a	Day 14 b	LTb-/- a	LTb-/- b		Day 0/0	Day 2/0	Day 14/0	LTb/0
mmu-miR-100	69	105	63	79	59	59	28	19		1.00	0.82	0.68	0.27
mmu-miR-592*	151	68	96	48	71	52	41	22		1.00	0.66	0.56	0.29
mmu-miR-2137	833	464	725	454	385	413	259	181		1.00	0.91	0.62	0.34
mmu-miR-3102*	174	117	120	119	99	104	63	36		1.00	0.82	0.70	0.34
mmu-miR-335-5p	51	68	55	86	44	64	26	14		1.00	1.19	0.91	0.34
mmu-miR-762	333	163	194	161	145	177	105	68		1.00	0.72	0.65	0.35
mmu-miR-33	347	262	469	486	197	329	154	68		1.00	1.57	0.86	0.36
mmu-miR-138	95	134	99	122	66	68	47	40		1.00	0.97	0.59	0.38
mmu-miR-3090*	140	94	105	97	84	92	58	36		1.00	0.86	0.75	0.40
mmu-miR-487b	148	123	126	172	117	187	81	30		1.00	1.10	1.12	0.41
mmu-miR-138-2*	338	267	253	386	298	439	193	58		1.00	1.06	1.22	0.41
mmu-miR-2861	89	51	65	48	39	49	36	22		1.00	0.81	0.63	0.42
mmu-miR-1983	2477	1682	2611	2799	1306	2525	1126	656		1.00	1.30	0.92	0.43
mmu-miR-25*	317	170	185	149	157	158	110	103		1.00	0.69	0.65	0.44

mmu-miR-290-5p	503	361	473	436	286	389	220	165		1.00	1.05	0.78	0.45
mmu-miR-193	50	43	61	62	34	41	26	16		1.00	1.34	0.80	0.45
mmu-miR-32	435	442	499	536	385	435	266	138		1.00	1.18	0.93	0.46
mmu-miR-187	67	80	55	66	40	39	35	34		1.00	0.83	0.54	0.47
mmu-miR-99a	106	155	95	121	103	95	77	45		1.00	0.83	0.76	0.47
mmu-miR-10b	68	90	54	68	58	63	47	27		1.00	0.78	0.77	0.47
mmu-miR-101b	365	425	363	429	334	399	246	130		1.00	1.00	0.93	0.48
mmu-miR-301a	215	224	335	329	241	268	145	64		1.00	1.51	1.16	0.48
mmu-miR-711	89	66	77	68	58	60	44	31		1.00	0.94	0.76	0.48
mmu-miR-151-5p	220	269	167	215	193	180	161	87		1.00	0.78	0.76	0.51
mmu-miR-130a	695	818	823	921	631	650	471	305		1.00	1.15	0.85	0.51
mmu-miR-467b	120	168	137	191	178	167	96	54		1.00	1.14	1.20	0.52
mmu-miR-152	122	160	122	154	123	121	101	48		1.00	0.98	0.86	0.53
mmu-miR-30a	588	645	604	680	490	595	407	243		1.00	1.04	0.88	0.53
mmu-miR-145*	79	112	64	87	78	88	61	40		1.00	0.79	0.87	0.53
mmu-miR-497	98	125	99	133	95	118	73	45		1.00	1.04	0.96	0.53
mmu-miR-181d	173	227	220	263	197	192	139	77		1.00	1.21	0.98	0.54
mmu-miR-3072	96	96	100	107	105	108	73	31		1.00	1.08	1.10	0.54
mmu-miR-29c	881	909	695	815	635	767	599	371		1.00	0.84	0.78	0.54
mmu-miR-362-3p	118	162	163	172	127	146	93	60		1.00	1.20	0.97	0.54
mmu-miR-365	98	140	102	126	105	110	82	48		1.00	0.96	0.91	0.55
mmu-miR-361*	82	90	86	89	78	80	60	34		1.00	1.02	0.92	0.55
mmu-miR-29a*	166	207	147	194	186	171	142	63		1.00	0.91	0.96	0.55
mmu-miR-450a	80	87	102	114	97	99	61	32		1.00	1.29	1.17	0.56
mmu-miR-1839-5p	63	80	46	66	59	66	51	30		1.00	0.78	0.87	0.56
mmu-miR-338-3p	124	111	115	120	98	112	88	44		1.00	1.00	0.90	0.56

mmu-miR-101a	1336	1498	1428	1502	1096	1327	981	618		1.00	1.03	0.86	0.56
mmu-miR-199b*	218	264	241	272	221	244	171	102		1.00	1.06	0.96	0.57
mmu-miR-140	482	598	433	576	529	504	385	227		1.00	0.93	0.96	0.57
mmu-miR-199a-5p	399	517	465	555	454	445	316	203		1.00	1.11	0.98	0.57
mmu-miR-674	151	164	135	172	147	135	117	62		1.00	0.97	0.90	0.57
mmu-miR-19a	931	962	1269	1250	898	1145	682	395		1.00	1.33	1.08	0.57
mmu-miR-99b	93	131	92	116	109	96	79	49		1.00	0.92	0.91	0.57
mmu-miR-181b	96	128	125	137	112	115	79	49		1.00	1.16	1.01	0.57
mmu-miR-130b	165	200	202	220	206	187	138	71		1.00	1.16	1.08	0.57
mmu-miR-27b	780	843	703	814	665	764	566	372		1.00	0.93	0.88	0.58
mmu-miR-3104-3p	59	64	59	69	61	59	44	27		1.00	1.05	0.98	0.58
mmu-miR-141	41	49	60	60	40	48	34	19		1.00	1.33	0.98	0.59
mmu-miR-322	230	290	289	305	238	258	187	118		1.00	1.14	0.95	0.59
mmu-miR-142-5p	8466	8321	10645	9465	6869	9735	5763	4169		1.00	1.20	0.99	0.59
mmu-miR-1249	73	86	103	101	83	81	62	33		1.00	1.28	1.03	0.59
mmu-miR-10a	364	473	275	351	324	290	306	192		1.00	0.75	0.73	0.60
mmu-miR-221	212	244	176	210	210	199	167	106		1.00	0.85	0.90	0.60
mmu-miR-532-5p	48	60	37	50	52	54	42	23		1.00	0.80	0.98	0.60
mmu-miR-148b	173	218	169	203	199	195	156	80		1.00	0.95	1.01	0.60
mmu-miR-195	1141	1357	1136	1303	1043	1166	850	654		1.00	0.98	0.88	0.60
mmu-miR-144	1939	937	2177	1845	1367	1722	1098	638		1.00	1.40	1.07	0.60
mmu-miR-652	279	332	231	294	290	279	228	144		1.00	0.86	0.93	0.61
mmu-miR-1186b	1025	824	685	1025	969	1207	745	400		1.00	0.93	1.18	0.62
mmu-miR-320	147	178	136	185	166	156	130	71		1.00	0.99	0.99	0.62
mghv-miR-M1-2-3p	48	46	54	50	46	43	36	22		1.00	1.11	0.94	0.62
mmu-miR-378	422	489	352	466	491	446	366	202		1.00	0.90	1.03	0.62

mmu-miR-1961	149	181	127	176	146	166	129	77		1.00	0.92	0.95	0.62
mmu-miR-30e*	269	356	230	314	310	291	242	148		1.00	0.87	0.96	0.62
mmu-miR-222	219	242	186	227	230	207	178	110		1.00	0.90	0.95	0.62
mmu-miR-199a-3p	446	530	405	492	454	496	370	240		1.00	0.92	0.97	0.62
mmu-miR-1264-3p	317	236	302	384	254	352	198	150		1.00	1.24	1.10	0.63
mmu-miR-128	48	56	46	50	52	51	42	23		1.00	0.92	0.99	0.63
mmu-miR-181a	758	907	920	943	803	789	610	444		1.00	1.12	0.96	0.63
mmu-miR-296-5p	43	50	51	56	47	45	38	21		1.00	1.15	1.00	0.63
mmu-miR-107	361	407	300	376	329	347	298	189		1.00	0.88	0.88	0.63
mmu-miR-1195	40	49	27	48	51	48	35	22		1.00	0.85	1.12	0.63
mmu-miR-29b	3548	2851	3150	3229	1969	2854	2205	1867		1.00	1.00	0.75	0.64
mmu-miR-433*	393	293	276	364	336	442	271	168		1.00	0.93	1.13	0.64
mmu-miR-27a	679	675	692	721	557	671	509	356		1.00	1.04	0.91	0.64
mmu-miR-143	4206	6025	3777	5642	3773	3768	3251	3289		1.00	0.92	0.74	0.64
mmu-miR-24-2*	123	160	130	158	139	128	110	71		1.00	1.02	0.94	0.64
mmu-miR-21	1489	1519	1486	1286	1172	1290	1238	702		1.00	0.92	0.82	0.65
mmu-miR-339-5p	323	409	259	311	326	323	297	176		1.00	0.78	0.89	0.65
mmu-miR-194	89	110	87	118	100	98	80	50		1.00	1.03	0.99	0.65
mmu-miR-145	1099	1242	1096	1138	872	1007	771	754		1.00	0.95	0.80	0.65
mmu-miR-103	759	912	655	756	724	740	638	452		1.00	0.84	0.88	0.65
mmu-miR-5097	1360	966	1205	1235	1160	1486	1046	483		1.00	1.05	1.14	0.66
mmu-miR-20b	853	935	886	1051	925	995	734	452		1.00	1.08	1.07	0.66
mmu-miR-26a	714	865	634	739	625	711	600	450		1.00	0.87	0.85	0.67
mmu-miR-338-5p	71	75	46	65	74	83	56	41		1.00	0.76	1.07	0.67
mmu-miR-186	84	91	81	96	106	106	77	40		1.00	1.01	1.21	0.67
mmu-miR-3068	131	131	120	160	131	138	110	65		1.00	1.07	1.03	0.67

mmu-miR-30e	1973	1859	2335	2266	1540	1972	1515	1050		1.00	1.20	0.92	0.67
mmu-miR-340-5p	353	418	333	398	342	369	291	226		1.00	0.95	0.92	0.67
mmu-miR-30d	734	865	653	808	660	800	649	425		1.00	0.91	0.91	0.67
mmu-miR-350	268	349	268	349	313	296	260	155		1.00	1.00	0.99	0.67
mmu-miR-3069-5p	135	155	111	148	191	167	131	64		1.00	0.89	1.24	0.67
mmu-miR-92a	78	92	73	95	92	107	73	42		1.00	0.99	1.17	0.67
mmu-miR-484	48	52	51	56	52	58	43	24		1.00	1.07	1.10	0.67
mmu-miR-142-3p	34485	38001	38446	38368	32089	33804	27404	21621		1.00	1.06	0.91	0.68
mmu-miR-770-5p	66	72	47	59	74	78	65	32		1.00	0.77	1.10	0.70
mmu-miR-425	358	431	333	409	389	400	328	223		1.00	0.94	1.00	0.70
mmu-miR-126-5p	693	738	625	745	595	682	614	387		1.00	0.96	0.89	0.70
mmu-miR-29a	12894	13434	8981	12998	11428	11217	9664	8762		1.00	0.83	0.86	0.70
mmu-miR-125b-5p	2160	2623	2048	2176	1665	1605	1600	1758		1.00	0.88	0.68	0.70
mmu-miR-21*	173	135	188	111	110	100	109	108		1.00	0.97	0.68	0.70
mmu-miR-1843-5p	411	486	305	428	443	433	370	261		1.00	0.82	0.98	0.70
mmu-miR-340-3p	62	75	53	66	66	66	56	41		1.00	0.87	0.96	0.70
mmu-miR-423-3p	156	186	128	185	186	168	153	89		1.00	0.92	1.04	0.71
mmu-miR-675-5p	238	267	228	243	226	237	220	137		1.00	0.93	0.92	0.71
mghv-mir-M1-3*	63	62	58	70	65	75	48	41		1.00	1.02	1.11	0.71
mmu-miR-17*	171	186	161	188	185	178	145	109		1.00	0.98	1.02	0.71
mmu-miR-374	374	375	316	343	387	371	353	184		1.00	0.88	1.01	0.72
mmu-miR-677	112	111	112	130	137	144	110	51		1.00	1.08	1.26	0.72
mmu-miR-3096-5p	820	837	752	904	964	879	752	445		1.00	1.00	1.11	0.72
mmu-miR-326	82	85	72	87	79	80	69	52		1.00	0.95	0.95	0.72
mmu-miR-106a	1074	1121	1187	1228	1106	1205	990	605		1.00	1.10	1.05	0.73
mmu-miR-148a	105	95	85	87	70	99	105	41		1.00	0.86	0.85	0.73

mmu-miR-767	335	279	218	292	321	347	273	175		1.00	0.83	1.09	0.73
mmu-miR-378	585	658	530	640	667	597	519	388		1.00	0.94	1.02	0.73
mmu-miR-361	366	422	323	396	396	367	338	238		1.00	0.91	0.97	0.73
mmu-miR-3084*	882	885	701	913	995	990	804	488		1.00	0.91	1.12	0.73
mmu-miR-668	134	113	64	114	118	131	105	76		1.00	0.72	1.01	0.73
mmu-miR-744	163	189	184	204	191	164	157	102		1.00	1.10	1.01	0.73
mmu-miR-98	1320	1489	1220	1407	1129	1293	1225	867		1.00	0.94	0.86	0.74
mmu-miR-140*	774	921	744	890	889	803	737	536		1.00	0.96	1.00	0.75
mmu-miR-677*	352	344	284	310	384	367	319	205		1.00	0.85	1.08	0.75
mmu-miR-125a-5p	929	1129	781	958	892	827	777	772		1.00	0.84	0.84	0.75
mmu-miR-24-1*	208	234	209	247	215	207	181	154		1.00	1.03	0.96	0.76
mmu-miR-19b	1886	2128	2386	2354	1886	2450	1739	1317		1.00	1.18	1.08	0.76
mmu-miR-511-3p	109	107	87	94	98	87	115	49		1.00	0.84	0.85	0.76
mmu-miR-3103*	77	77	50	109	92	104	60	58		1.00	1.03	1.27	0.76
mmu-miR-23b	5175	6851	3586	5258	5060	4495	4409	4845		1.00	0.74	0.79	0.77
mmu-miR-712	71	61	58	53	80	75	66	35		1.00	0.84	1.17	0.77
mmu-miR-16	13598	15437	11964	14625	13807	14053	11368	11055		1.00	0.92	0.96	0.77
mmu-miR-374	654	682	610	605	735	617	644	392		1.00	0.91	1.01	0.78
mmu-miR-185	183	205	169	213	230	190	177	124		1.00	0.98	1.08	0.78
mmu-miR-3069-3p	355	364	264	385	443	422	334	227		1.00	0.90	1.20	0.78
mmu-miR-15a	3032	3282	3150	3583	3027	3063	2643	2294		1.00	1.07	0.96	0.78
mmu-miR-22*	99	123	104	110	111	101	101	73		1.00	0.97	0.95	0.78
mmu-miR-342-3p	1110	1126	995	1066	1019	1074	970	786		1.00	0.92	0.94	0.78
mmu-miR-17	1237	1397	1336	1504	1388	1385	1242	828		1.00	1.08	1.05	0.79
mmu-miR-466a-3p	113	142	126	164	146	145	102	99		1.00	1.14	1.14	0.79
mmu-miR-331-3p	62	71	52	74	67	67	60	45		1.00	0.95	1.01	0.79

mmu-miR-22	2221	2527	2204	2357	1744	1666	1963	1838		1.00	0.96	0.72	0.80
mmu-let-7c	2356	2779	2143	2572	2092	2231	2036	2119		1.00	0.92	0.84	0.81
mmu-miR-25	688	688	634	764	788	766	639	476		1.00	1.02	1.13	0.81
mmu-let-7f	1781	1904	1584	1648	1439	1811	1631	1360		1.00	0.88	0.88	0.81
mmu-miR-92b	97	105	91	94	101	113	96	68		1.00	0.92	1.06	0.81
mmu-miR-342-5p	55	67	48	62	70	64	55	44		1.00	0.90	1.09	0.81
mmu-let-7a	2161	2625	2082	2389	1755	2119	1921	1990		1.00	0.93	0.81	0.82
mmu-miR-709	24103	30069	22340	28564	28789	23924	21754	22534		1.00	0.94	0.97	0.82
mmu-miR-720	27189	26973	28217	26774	26433	27814	25164	19317		1.00	1.02	1.00	0.82
mmu-miR-155	529	587	433	530	582	568	528	400		1.00	0.86	1.03	0.83
mmu-miR-24	3275	3489	2836	3298	3106	3208	2990	2664		1.00	0.91	0.93	0.84
mmu-miR-200c	38	56	35	48	56	54	49	29		1.00	0.89	1.17	0.84
mmu-miR-337-3p	150	140	115	167	158	172	143	99		1.00	0.97	1.14	0.84
mmu-miR-328	111	130	103	124	124	112	110	92		1.00	0.94	0.98	0.84
mmu-miR-28*	45	57	46	51	62	52	50	36		1.00	0.96	1.12	0.84
mmu-miR-493*	379	282	247	382	390	421	338	220		1.00	0.95	1.23	0.84
mmu-let-7g	4032	4943	3342	4818	4132	4024	3767	3845		1.00	0.91	0.91	0.85
mmu-miR-93	1192	1323	1267	1469	1414	1317	1246	914		1.00	1.09	1.09	0.86
mmu-miR-7a	327	333	339	390	433	373	316	253		1.00	1.11	1.22	0.86
mmu-miR-200b	64	85	68	75	75	73	67	61		1.00	0.97	0.99	0.86
mmu-miR-30b	3241	3844	2832	3402	3303	3389	3134	2993		1.00	0.88	0.94	0.86
mmu-let-7b	1851	2224	1710	2092	1752	1747	1684	1845		1.00	0.93	0.86	0.87
mmu-miR-23a	2878	3218	2464	2781	2741	2626	2727	2567		1.00	0.86	0.88	0.87
mmu-miR-30c	3150	3639	2808	3422	3276	3372	2972	2935		1.00	0.92	0.98	0.87
mmu-let-7i	2741	2998	2717	3220	2767	2797	2650	2345		1.00	1.03	0.97	0.87
mmu-miR-126-3p	3052	3243	2744	3170	2810	2817	2971	2512		1.00	0.94	0.89	0.87

mmu-miR-691	6584	6164	4517	8519	6425	7875	4811	6309		1.00	1.02	1.12	0.87
mmu-let-7d	1990	2343	1854	2131	1816	1957	1893	1888		1.00	0.92	0.87	0.87
mmu-miR-503	157	124	167	129	113	114	116	129		1.00	1.05	0.81	0.87
mmu-miR-664	167	178	152	194	173	189	172	129		1.00	1.00	1.05	0.87
mmu-miR-1949	610	636	618	747	769	773	606	485		1.00	1.10	1.24	0.88
mmu-miR-20a	1815	2013	2249	2383	2026	2144	1791	1596		1.00	1.21	1.09	0.89
mmu-miR-26b	2684	3095	2471	2829	2649	2801	2683	2446		1.00	0.92	0.94	0.89
mmu-miR-1971	136	157	138	113	118	116	124	136		1.00	0.86	0.80	0.89
mmu-miR-138-1*	211	221	205	263	212	282	200	186		1.00	1.08	1.14	0.89
mmu-miR-1839-3p	404	444	373	527	500	481	406	352		1.00	1.06	1.16	0.90
mmu-miR-139-5p	305	371	262	308	325	292	328	280		1.00	0.84	0.91	0.90
mmu-miR-3096-3p	1629	1624	1648	1699	1853	1784	1614	1316		1.00	1.03	1.12	0.90
mmu-miR-106b*	86	100	86	111	127	112	96	73		1.00	1.06	1.29	0.91
mmu-miR-144*	123	86	77	118	188	191	131	63		1.00	0.93	1.81	0.92
mmu-miR-223	2094	2200	2235	1832	1613	1831	2009	1978		1.00	0.95	0.80	0.93
mmu-miR-34a	830	711	697	808	644	740	724	708		1.00	0.98	0.90	0.93
mmu-miR-15b	3404	3891	3025	3946	4044	3887	3412	3368		1.00	0.96	1.09	0.93
mmu-miR-106b	2364	2533	2408	2614	2606	2520	2399	2156		1.00	1.03	1.05	0.93
mmu-miR-191	1819	2406	1933	2145	1974	1923	1924	2024		1.00	0.97	0.92	0.93
mmu-miR-214	207	253	222	236	261	249	219	214		1.00	1.00	1.11	0.94
mmu-miR-1843-3p	945	1022	769	970	994	979	986	889		1.00	0.88	1.00	0.95
mmu-miR-500	143	182	143	168	153	137	143	167		1.00	0.96	0.89	0.95
mmu-miR-582-3p	309	268	318	354	283	360	274	279		1.00	1.16	1.11	0.96
mmu-miR-875-3p	2207	1868	2200	2313	1800	2470	1904	2025		1.00	1.11	1.05	0.96
mmu-miR-710	76	73	60	55	62	63	65	80		1.00	0.77	0.84	0.98
mmu-miR-3084	2030	1994	1945	2209	2543	2281	2152	1788		1.00	1.03	1.20	0.98

mmu-miR-3107	331	213	186	273	427	399	329	209		1.00	0.84	1.52	0.99
mmu-miR-423-5p	263	303	232	285	318	265	271	296		1.00	0.91	1.03	1.00
mmu-let-7e	1621	1673	1629	1819	1510	1853	1442	1860		1.00	1.05	1.02	1.00
mmu-miR-690	19189	20878	18811	17521	20786	19865	20154	20241		1.00	0.91	1.01	1.01
mmu-miR-146a	2216	2148	1780	1772	1804	1882	2301	2124		1.00	0.81	0.84	1.01
mmu-miR-1186	181	194	144	207	198	210	186	196		1.00	0.93	1.09	1.02
mmu-miR-207	2481	1725	2178	2290	1808	2532	2104	2189		1.00	1.06	1.03	1.02
mmu-miR-185*	122	147	131	98	113	107	125	150		1.00	0.85	0.82	1.02
mmu-miR-146b	1681	1651	1356	1465	1451	1562	1768	1660		1.00	0.85	0.90	1.03
mghv-miR-M1-8	803	742	631	778	790	855	778	816		1.00	0.91	1.07	1.03
mmu-miR-299*	268	210	219	184	196	208	221	278		1.00	0.84	0.85	1.04
mmu-miR-467d*	82	103	98	121	99	104	90	106		1.00	1.18	1.09	1.06
mmu-miR-665	170	128	143	124	117	119	200	117		1.00	0.90	0.79	1.07
mmu-miR-466d-3p	229	272	253	274	269	254	233	313		1.00	1.05	1.04	1.09
mmu-miR-1935	146	150	148	153	152	166	150	173		1.00	1.02	1.07	1.09
mmu-miR-700*	54	58	44	58	67	61	57	68		1.00	0.91	1.14	1.11
mmu-miR-34b-3p	298	260	222	264	269	309	290	332		1.00	0.87	1.04	1.11
mmu-miR-705	86	83	90	85	89	87	86	106		1.00	1.03	1.04	1.13
mmu-miR-34c	58	60	40	69	65	48	69	67		1.00	0.93	0.96	1.15
mmu-miR-3095-3p	71	59	63	49	56	57	59	91		1.00	0.86	0.87	1.16
mmu-miR-130b*	57	59	49	62	71	61	59	77		1.00	0.95	1.13	1.16
mghv-mir-M1-8*	481	480	598	505	461	491	482	635		1.00	1.15	0.99	1.16
mmu-miR-669a-5p	114	130	136	147	139	126	125	160		1.00	1.16	1.08	1.16
mmu-miR-1903	133	136	116	128	149	136	137	177		1.00	0.91	1.06	1.17
mmu-miR-466a-3p	272	320	331	339	317	313	292	409		1.00	1.13	1.06	1.18
mmu-miR-16-1*	49	45	56	57	54	53	50	62		1.00	1.19	1.13	1.18

mmu-miR-503*	1092	965	831	944	1008	1106	1073	1412		1.00	0.86	1.03	1.21
mmu-miR-872*	439	384	402	443	434	470	442	554		1.00	1.03	1.10	1.21
mmu-miR-297a	69	79	78	85	79	76	75	104		1.00	1.10	1.04	1.21
mmu-miR-1947*	529	369	475	319	402	368	434	671		1.00	0.88	0.86	1.23
mmu-miR-294*	140	132	132	129	116	119	143	192		1.00	0.96	0.86	1.23
mmu-miR-290-3p	124	80	129	88	92	73	104	150		1.00	1.07	0.81	1.24
mmu-miR-451	27215	19090	21394	23255	28430	27514	31970	25653		1.00	0.96	1.21	1.24
mmu-miR-150	3669	5017	2852	3995	5277	5421	5225	5662		1.00	0.79	1.23	1.25
mmu-miR-3068*	1608	1475	1459	1538	1422	1677	1603	2299		1.00	0.97	1.01	1.27
mmu-miR-574-3p	53	69	72	61	60	63	63	92		1.00	1.09	1.01	1.28
mmu-let-7d*	88	92	76	81	96	92	102	134		1.00	0.87	1.04	1.31
mmu-miR-669a-3p	472	511	570	549	505	527	483	813		1.00	1.14	1.05	1.32
mmu-miR-320*	108	113	110	112	133	122	131	163		1.00	1.00	1.16	1.33
mmu-miR-3103	426	440	411	437	493	425	451	718		1.00	0.98	1.06	1.35
mmu-miR-3076-3p	60	51	50	51	61	62	62	90		1.00	0.91	1.11	1.37
mmu-miR-155*	147	156	149	170	172	157	176	238		1.00	1.05	1.09	1.37
mmu-miR-485*	143	137	129	125	155	143	161	227		1.00	0.91	1.07	1.39
mmu-miR-467b*	90	109	113	120	110	109	117	162		1.00	1.17	1.10	1.40
mmu-miR-297c	87	97	106	96	106	90	106	153		1.00	1.10	1.07	1.41
mmu-miR-466j	165	176	189	185	174	164	189	293		1.00	1.10	0.99	1.41
mmu-miR-329	58	68	66	70	67	58	80	100		1.00	1.08	0.99	1.42
mghv-miR-M1-4	211	195	209	198	205	220	240	353		1.00	1.00	1.05	1.46
mmu-miR-466m-5p	158	170	184	180	170	157	179	300		1.00	1.11	1.00	1.46
mmu-miR-544-5p	51	53	46	60	54	65	64	89		1.00	1.01	1.14	1.47
mmu-miR-669m-3p	268	297	308	298	304	300	335	499		1.00	1.07	1.07	1.48

mmu-miR-467h	127	155	162	160	147	137	163	254		1.00	1.14	1.01	1.48
mghv-mir-M1-2-5p	66	72	75	84	82	72	78	127		1.00	1.15	1.11	1.48
mmu-miR-1941-3p	85	87	93	86	100	90	106	151		1.00	1.03	1.10	1.49
mmu-miR-1224*	156	149	158	148	155	148	196	263		1.00	1.00	0.99	1.50
mmu-miR-3473	556	536	653	468	503	527	658	1013		1.00	1.03	0.94	1.53
mmu-miR-466f-5p	140	160	175	163	161	140	176	290		1.00	1.12	1.00	1.55
mmu-miR-467a*	350	393	426	397	390	385	419	734		1.00	1.11	1.04	1.55
mmu-miR-882	189	195	210	175	175	172	216	387		1.00	1.00	0.90	1.57
mmu-miR-204*	101	97	104	90	101	92	125	186		1.00	0.98	0.98	1.58
mmu-miR-669f-3p	690	803	840	792	718	734	776	1584		1.00	1.09	0.97	1.58
mmu-miR-669o-5p	463	495	538	507	505	475	518	999		1.00	1.09	1.02	1.58
mmu-miR-877	55	50	54	48	50	48	64	103		1.00	0.98	0.94	1.59
mmu-miR-291a-5p	37	37	42	24	32	26	51	67		1.00	0.89	0.79	1.60
mmu-miR-467e	104	125	128	135	138	138	144	222		1.00	1.15	1.21	1.60
mmu-miR-1900	472	379	498	341	384	349	611	751		1.00	0.99	0.86	1.60
mmu-miR-466i-3p	238	277	296	266	287	272	316	509		1.00	1.09	1.09	1.60
mmu-miR-669i	35	49	41	36	43	40	55	79		1.00	0.93	1.00	1.61
mmu-miR-465b-5p	68	65	59	72	61	71	85	130		1.00	0.98	0.99	1.62
mmu-miR-1943*	117	122	142	132	138	127	157	230		1.00	1.15	1.11	1.62
mmu-miR-466e-5p	242	263	315	265	282	249	309	511		1.00	1.15	1.05	1.63
mmu-miR-466n-5p	178	202	223	203	211	177	226	395		1.00	1.12	1.02	1.63
mmu-miR-669l	368	391	410	385	396	378	420	821		1.00	1.05	1.02	1.64
mmu-miR-1895	44	45	48	46	43	41	59	86		1.00	1.06	0.95	1.64
mmu-miR-466a-5p	225	238	264	242	260	215	283	476		1.00	1.09	1.02	1.64
mmu-miR-669e*	125	152	167	157	139	141	174	280		1.00	1.17	1.01	1.64
mmu-miR-1187	295	348	368	333	347	297	377	678		1.00	1.09	1.00	1.64

mmu-miR-335-3p	896	761	1002	815	738	846	961	1775		1.00	1.10	0.96	1.65
mmu-miR-665*	305	315	325	316	355	306	374	661		1.00	1.03	1.06	1.67
mmu-miR-466b-5p	318	326	368	334	337	306	374	706		1.00	1.09	1.00	1.68
mmu-miR-466c-5p	348	371	401	367	370	327	406	802		1.00	1.07	0.97	1.68
mmu-miR-669e	235	286	269	281	279	236	321	557		1.00	1.06	0.99	1.68
mmu-miR-881*	70	72	84	76	74	68	97	146		1.00	1.12	1.00	1.71
mmu-miR-883a-5p	593	538	689	577	550	638	697	1237		1.00	1.12	1.05	1.71
mmu-miR-667	379	316	401	313	319	365	444	756		1.00	1.03	0.98	1.73
mmu-miR-3077	60	62	68	66	65	65	85	125		1.00	1.11	1.07	1.73
mmu-miR-468	101	112	126	129	124	108	137	234		1.00	1.20	1.09	1.74
mmu-miR-669a-3-3p	696	772	867	771	726	725	808	1758		1.00	1.12	0.99	1.75
mmu-miR-669d-2*	67	87	99	82	79	87	84	184		1.00	1.18	1.08	1.75
mmu-miR-2183	56	62	87	60	62	57	82	125		1.00	1.25	1.01	1.76
mmu-miR-467f	349	382	420	364	384	366	446	842		1.00	1.07	1.03	1.76
mmu-miR-669d*	374	400	499	408	405	416	465	899		1.00	1.17	1.06	1.76
mmu-miR-669b*	414	496	526	473	483	462	532	1073		1.00	1.10	1.04	1.76
mmu-miR-574-5p	473	500	555	514	522	464	566	1171		1.00	1.10	1.01	1.79
mmu-miR-467c*	122	148	165	141	143	150	178	313		1.00	1.13	1.09	1.82
mmu-miR-669l*	354	397	456	374	394	389	474	897		1.00	1.11	1.04	1.83
mmu-miR-883b-5p	42	38	39	28	34	35	53	92		1.00	0.84	0.87	1.83
mmu-miR-466a-5p	414	431	485	448	456	419	503	1048		1.00	1.10	1.04	1.84
mmu-miR-505-5p	47	55	63	57	55	50	72	116		1.00	1.19	1.04	1.85
mmu-miR-297a*	286	353	397	322	346	328	406	789		1.00	1.12	1.05	1.87
mmu-miR-678	41	53	52	44	46	43	68	108		1.00	1.02	0.94	1.87
mmu-miR-351	223	166	255	150	153	167	265	465		1.00	1.04	0.82	1.88

mmu-miR-467g	486	559	619	524	552	508	647	1353		1.00	1.09	1.01	1.92
mmu-miR-669d	476	492	575	516	507	499	583	1288		1.00	1.13	1.04	1.93
mmu-miR-466d-5p	449	468	566	500	495	447	558	1228		1.00	1.16	1.03	1.95
mghv-miR-M1-3	65	77	79	83	77	79	108	169		1.00	1.15	1.10	1.96
mmu-miR-669f-5p	492	542	643	546	549	505	681	1342		1.00	1.15	1.02	1.96
mmu-miR-669c*	680	737	884	735	754	715	884	1972		1.00	1.14	1.04	2.02
mmu-miR-881	39	41	44	38	45	39	58	105		1.00	1.01	1.04	2.02
mmu-miR-669p*	674	719	840	672	731	719	899	1939		1.00	1.09	1.04	2.04
mmu-miR-490-3p	34	35	40	36	36	41	55	89		1.00	1.09	1.11	2.07
mmu-miR-1192	493	550	660	543	550	542	709	1456		1.00	1.15	1.05	2.08
mmu-miR-693-5p	72	75	99	81	85	83	120	195		1.00	1.21	1.13	2.13
mmu-miR-1957	61	47	80	76	83	88	105	124		1.00	1.46	1.59	2.13
mmu-miR-669k*	468	511	555	503	529	473	607	1489		1.00	1.08	1.02	2.14
mmu-miR-1196	759	634	764	620	745	779	961	2039		1.00	0.99	1.09	2.15
mmu-miR-467e*	759	846	1119	811	825	798	1100	2374		1.00	1.20	1.01	2.16
mmu-miR-466f-3p	544	593	688	577	582	580	742	1720		1.00	1.11	1.02	2.17
mmu-miR-758*	46	49	59	44	51	46	72	141		1.00	1.08	1.01	2.24
mmu-miR-466f	691	711	922	751	721	682	942	2260		1.00	1.19	1.00	2.28
mmu-miR-3470b	57	61	82	58	63	62	98	171		1.00	1.19	1.06	2.29
mmu-miR-325	238	223	293	227	257	266	391	697		1.00	1.13	1.13	2.36
mmu-miR-30b*	79	86	107	87	90	85	133	264		1.00	1.17	1.05	2.39
mmu-miR-669c	926	989	1273	953	975	895	1354	3244		1.00	1.16	0.98	2.40
mmu-miR-1929	72	85	105	78	86	86	135	244		1.00	1.16	1.10	2.41
mmu-miR-1958	57	57	57	48	58	56	94	184		1.00	0.93	1.00	2.45
mmu-miR-32*	555	589	727	582	596	576	801	2022		1.00	1.15	1.03	2.47
mmu-miR-669n	605	634	776	641	624	606	854	2218		1.00	1.14	0.99	2.48

mmu-miR-1897-5p	731	756	1056	774	699	790	1108	2585		1.00	1.23	1.00	2.48
mmu-miR-3082-5p	807	883	1162	866	933	794	1250	2993		1.00	1.20	1.02	2.51
mmu-miR-1934	33	22	38	18	22	21	58	82		1.00	1.01	0.76	2.53
mmu-miR-302a	139	124	163	107	122	121	252	426		1.00	1.03	0.92	2.58
mmu-miR-466i-5p	1127	1160	1524	1071	1181	1092	1563	4472		1.00	1.13	0.99	2.64
mmu-miR-3098-3p	151	150	179	132	171	162	287	530		1.00	1.04	1.11	2.72
mmu-miR-495*	51	54	82	54	58	52	100	188		1.00	1.30	1.05	2.76
mmu-miR-1981*	35	34	53	26	36	36	79	148		1.00	1.13	1.04	3.26
mmu-miR-300*	280	299	391	261	269	263	618	1315		1.00	1.12	0.92	3.34
mghv-miR-M1-6*	273	202	379	180	203	184	451	1145		1.00	1.18	0.81	3.36
mmu-miR-3474	131	90	180	86	83	77	318	441		1.00	1.20	0.72	3.43
mmu-miR-1907	19	23	28	12	18	18	52	90		1.00	0.97	0.88	3.46
mmu-let-7a-2*	40	35	69	30	39	38	98	189		1.00	1.32	1.03	3.84
mmu-miR-1952	255	215	506	197	225	222	575	1279		1.00	1.49	0.95	3.94
mmu-miR-1954	29	29	48	31	31	31	77	171		1.00	1.36	1.08	4.29
mmu-miR-491*	6440	4270	17480	4270	4468	5893	19475	40274		1.00	2.03	0.97	5.58
mmu-miR-763	19	11	32	7	9	12	99	89		1.00	1.34	0.71	6.41
mmu-miR-706	310	333	679	298	373	330	1106	3442		1.00	1.52	1.09	7.08
mmu-miR-3100-3p	138	114	297	76	112	87	445	1401		1.00	1.48	0.79	7.33

Appendix D

Table showing genes from ToppFun: biological processes in which predicted target genes for miR-100-5p, miR-138-5p and miR-2137 are enriched for.

Go: Biological Process	P-value	Hit	Total	Genes
chromatin modification	3.06E-06	24	435	JMJD1C, RBM14, SUV420H1, SIRT1, TP53, KMT2E, DNMT3A, PKN1, CHD9, CHD6, ZMYND11, EZH2, KMT2C, RSF1, CHD5, IL1B, SMARCA5, BAZ2A, MECP2, CECR2, KDM4A, DOT1L, SIN3A, L3MBTL3
response to decreased oxygen levels	6.71E-06	17	252	CHAT,NPPC,KCNMA1,CHRNB2,SIRT1,TP53,OXTR,SMAD3,MTOR,IL1B,NPEPPS,MECP2,SCNN1G,PMAIP1,RHOC,BBC3,NKX3-1
response to oxygen levels	1.43E-05	17	267	CHAT, NPPC, KCNMA1, CHRNB2, SIRT1, TP53, OXTR, SMAD3, MTOR, IL1B, NPEPPS, MECP2, SCNN1G, PMAIP1, RHOC, BBC3, NKX3-1
neural nucleus development	1.68E-05	5	18	CHRNB2, PHOX2B, HOXA1, KIRREL3, CDK5R1
axon guidance	1.89E-05	20	360	ST8SIA2, DCX, NTN3, EPHB3, HOXA1, NCK2, CDK5R1, ANK1, SEMA6A, ANK3, SEMA5A, UNC5D, RELN, COL4A2, EPHA8, RHOC, LAMC1, PLCG1, TRIO, EFNB3
chromatin silencing	2.21E-05	6	31	SIRT1, DNMT3A, SMARCA5, BAZ2A, MECP2, SIN3A
response to hypoxia	2.29E-05	16	249	CHAT, NPPC, KCNMA1, CHRNB2, SIRT1, TP53, SMAD3, MTOR, IL1B, NPEPPS, MECP2, SCNN1G, PMAIP1, RHOC, BBC3, NKX3-1
regulation of synapse organization	2.36E-05	7	46	CHRNB2, OXTR, EPHB3, MECP2, CBLN1, RELN, NEUROD2
chromatin organization	3.01E-05	25	532	JMJD1C, RBM14, SUV420H1, SIRT1,TP53, KMT2E,DNMT3A,PKN1, CHD9,CHD6,ZMYND11,EZH2, KMT2C, RSF1,CHD5, IL1B,SMARCA5, BAZ2A,MECP2,CECR2,H3F3B,KDM4A, DOT1L,SIN3A, L3MBTL3
negative regulation of gene expression, epigenetic	4.57E-05	6	35	SIRT1,DNMT3A,SMARCA5,BAZ2A,MECP2,SIN3A

locomotion	5.02E-05	44	1253	ST8SIA2, DCX, ACE, NTN3,DYNC2H1, PPARD,TNFAIP1,FOXC1,MYO18A, PHOX2B,EPHB3,HOXA1,PKN1,KIRREL3, NCK2,FMNL1,HAND2,CDK5R1,ANK1, SEMA6A,SMAD3,IL1B,ANK3,DVL2, SEMA5A,PRPF40A,KRIT1,UNC5D, HBEGF,RELN,COL4A2,SCNN1G, EPHA8,TTN,RHOC,LAMC1,NFATC2, PLCG1,CXCL3,ABHD2,TRIO, VCAN,EFNB3,OVOL2
regulation of synapse structure and activity	5.36E-05	7	52	CHRNB2,OXTR,EPHB3,MECP2,CBLN1,RELN, NEUROD2
positive regulation of signaling	7.75E-05	33	851	TGM2,ATR, FGF21,PPARD, CHRNB2,CDKN1C,BID, SIRT1,TP53,OXTR,ITSN1, NOX4,PKN1,HAND2,SMAD3, PTGIR,MTOR,IL1B,DVL2,MECP2,HBEGF, RELN,EPHA8,PMAIP1,NEUROD2,RHOC, BBC3,NKX3-1,MAP3K11,TMOD2, GRIA4, CD44,CSNK1D
positive regulation of cell communication	8.29E-05	33	854	TGM2,ATR,FGF21,PPARD,CHRNB2,CDKN1C,BID, SIRT1,TP53,OXTR,ITSN1,NOX4,PKN1,HAND2, SMAD3,PTGIR,MTOR,IL1B,DVL2,MECP2,HBEGF, RELN,EPHA8,PMAIP1,NEUROD2,RHOC,BBC3, NKX3-1,MAP3K11,TMOD2,GRIA4,CD44,CSNK1D
positive regulation of neuron apoptotic process	1.15E-04	6	41	TP53,CDK5R1,PMAIP1,RHOC,BBC3,MAP3K11
neuron development	1.31E-04	31	800	ST8SIA2,CHAT,DCX, NTN3,CLIC5,CHRNB2,CDKN1C, PHOX2B,EPHB3,HOXA1,NCK2,HAND2,CDK5R1, STRN,ANK1,SEMA6A,ANK3,SEMA5A,MECP2, UNC5D,RELN,COL4A2,ATCAY,EPHA8,NEUROD2, RHOC,LAMC1,PLCG1,TRIO,VCAN,EFNB3
positive regulation of neuron death	1.32E-04	6	42	TP53,CDK5R1,PMAIP1,RHOC,BBC3,MAP3K11

regulation of cell proliferation	1.39E-04	41	1189	TGM2,NPPC,FGF21,PPARD,CHRNB2,CD274,RARA,CDKN1C,BID,SIRT1,TP53,PHOX2B,TCF7,GPAM, NOX4,ICMT,NCK2,ING1,EZH2,HAND2,STRN, SMAD3,PTGIR,MTOR,IL1B,DVL2,KRIT1,MECP2 HBEGF,PTGES,KLF11,ARG1,DPT,PMAIP1,LAMC1, NFATC2,NKX3-1,PTPN14,CDC6,OSR1,OVOL2
histone methylation	1.51E-04	7	61	SUV420H1,KMT2E,EZH2,KMT2C,BAZ2A,MECP2, DOT1L
cell migration	1.62E-04	32	847	DCX,ACE,PPARD,TNFAIP1,FOXC1,MYO18A, PHOX2B,EPHB3,PKN1,KIRREL3,NCK2,FMNL1, HAND2,CDK5R1,SEMA6A,SMAD3,IL1B,DVL2, PRPF40A,KRIT1,HBEGF,RELN,SCNN1G,EPHA8, RHOC,LAMC1,NFATC2,PLCG1,CXCL3,ABHD2, VCAN,OVOL2
chromosome organization	1.71E-04	28	701	JMJD1C,RBM14,SUV420H1,SIRT1,TP53,KMT2E, DNMT3A,PKN1,CHD9,CHD6,ZMYND11,EZH2, KMT2C,RSF1,CHD5,IL1B,SMARCA5,BAZ2A,MECP2,CECR2,H3F3B,TNKS1BP1,TTN,SMC1B,KDM4A, DOT1L,SIN3A,L3MBTL3
protein alkylation	1.77E-04	8	83	SUV420H1,KMT2E,ICMT,EZH2,KMT2C,BAZ2A, MECP2,DOT1L
protein methylation	1.77E-04	8	83	SUV420H1,KMT2E,ICMT,EZH2,KMT2C,BAZ2A, MECP2,DOT1L
axonogenesis	1.89E-04	23	527	ST8SIA2,DCX,NTN3,CHRNB2,PHOX2B,EPHB3, HOXA1,NCK2,CDK5R1,ANK1,SEMA6A,ANK3, SEMA5A,UNC5D,RELN,COL4A2,EPHA8,RHOC, LAMC1,PLCG1,TRIO,VCAN,EFNB3
regulation of mitochondrial membrane permeability	1.94E-04	4	16	BID,TP53,PMAIP1,BBC3
positive regulation of protein oligomerization	1.94E-04	4	16	BID,TP53,PMAIP1,BBC3
positive regulation of intrinsic apoptotic signaling pathway	1.94E-04	4	16	TP53,PMAIP1,BBC3,NKX3-1
regulation of synapse assembly	2.31E-04	5	30	CHRNB2,OXTR,EPHB3,MECP2,CBLN1